MODELLING THE BENTHIC IMPACT OF COASTAL DISCHARGES

David R. Marlow

Submitted to Heriot-Watt University in partial
fulfilment of the requirements of the degree of
DOCTOR of PHILOSOPHY

Centre For Environmental Resource Management/IOE
Department of Civil and Offshore Engineering
Heriot-Watt University

April 1999

Table of Contents

List of Tables

List of Figures

Acknowledgements

My thanks go to the following:

To my Supervisor, Dr Steve Wallis, for his support and kind assistance throughout my research.

To Professor Roy Halliwell for his efforts in obtaining funding, supervisory role in the initial part of my research, and guidance throughout all my studies at Heriot-Watt.

To Professor Paul Jowitt (Head of Civil & Offshore Engineering) and Heriot-Watt University for continued financial support.

To the Staff of IOE for their invaluable help at various times.

To Anton Edwards and others at SEPA, Chris Cromey (SAMS), Dr Tom Pearson (SEAS), and Dr Paul Kingston (Heriot-Watt) for fruitful discussions and the supply of data.

Finally, to Terri Clements for her unflinching patience and encouragement throughout my research.

Abstract

The discharge of effluent into coastal waters can lead to environmental degradation, and proactive management of this practice is therefore desirable. This requires a capacity to predict environmental impacts. Benthic impacts can be detected in the redox state of the upper part of the sediment column. A mechanistic model has therefore been developed that describes vertical gradients of sedimentary redox intensity (Eh).

The model is essentially a one dimensional multi-component reaction-transport model. Bioturbation is represented using a simple Fickian analogue, and irrigation is modelled as a non-local exchange process. Degradation of organic matter is characterised as six sequential metabolic reactions. Monod formulations combined with an inhibition scheme are used to model the utilisation of electron acceptors. Various other reactions are also included. The model equations are discretised using finite differences, and solved for both steady state and transient cases. The redox intensity is calculated from the predicted distribution of oxidants and reductants using a simple Nerstian approach. Consequently, only a limited interpretation can be placed on the calculated Eh profile.

A theoretical investigation of the model response demonstrates that both high data requirements and uncertainty in parameter values impedes the predictive application of the redox model. Hence, whilst the model can describe the development of vertical redox gradients, and therefore has some diagnostic capacity, it does not represent a viable tool that would aid in the proactive management of coastal resources. An alternative modelling approach is, however, suggested that would use predicted carbon fluxes to give a qualitative expression of benthic impact.

Glossary of Main Symbols

x	Vertical distance (cm)
t	Time (years)
C	Concentration (nmole/cm^3)
i,n	Integer indices
ω	Burial rate of solids (cm/yr)
ω_f	Asymptotic burial rate of solids (cm/yr)
v	Burial rate of porewater (cm/yr)
v_f	Asymptotic burial rate of porewater (cm/yr)
φ	Porosity
ξ	(1-φ) for solid components; φ for porewater components
φ_f	Asymptotic porosity
ξ_f	Asymptotic solids content, that is (ξ_f=1-φ_f)
D_{free}	Molecular/ionic diffusion coefficient (cm^2/yr)
D_{sed}	Tortuosity corrected molecular/ionic diffusion coefficient (cm^2/yr)
θ	Tortuosity
D_b	Bioturbation coefficient (cm^2/yr)
D_i	Diffusion coefficient for irrigation (cm^2/yr)
α	Irrigation coefficient (/yr)
V_{ox}	Rate constant for primary redox reaction (/yr) (the subscript 'ox' denotes the oxidant being used)
k_1 (or k)	G-type rate constant (/yr)
K_{ox}	Half saturation constant (nmole/cm^3) (the subscript 'ox' denotes the oxidant being used)
G	Concentration of organic matter (nmole/cm^3)
J_{org}	Net flux of organic carbon to the SWI (nmole/cm^2)
K_{in}	Inhibition constant (nmole/cm^3)
k_{ch4}	Rate constant for methanogenesis (/yr)
K_{sp}	Apparent solubility constant (nmole/cm^3)^2

Introduction

As humankind's global 'footprint' grows there is an increasing need to integrate environmental considerations into all aspects of society. Consequently, the need to harmonise human activity with 'nature' is becoming less a dream of the idealist and more a demand of the realist. However, this does not mean that economic activity should cease, but that we need to find ways of minimising the overall impact of this activity -- we need to manage effectively all environmental resources, including those associated with coastal waters. The protection and proactive management of the environment, including coastal resources, is now recognised as an issue of global importance.

Of the various factors associated with the degradation of the coastal resource, perhaps the greatest threat is that posed by marine pollution. Marine pollution is produced by a diverse number of activities, can arise from both point and diffuse sources, and may be either chronic or acute in nature. However, this work focuses solely on chronic point-source discharges of organically rich effluents. This source of pollution arises because the discharge of effluent into coastal waters is a cost-effective disposal strategy. However, environmental degradation related to effluent disposal via unsatisfactory means is a very real concern, and proactive management of such wastes is therefore desirable.

The proactive management of effluent disposal involves a number of interconnected steps, including:

1. The proposal for a new or modified effluent-generating activity.
2. The characterisation of the effluent (discharge quantity, composition, etc.).
3. The classification of potential problems associated with the discharge (for example, resource conflicts, economic constraints).
4. The identification of alternative disposal strategies (for example, treatment levels, outfall design and siting, etc.).

5. The technical, economic, and environmental evaluation of each alternative and the associated impacts.
6. The selection and implementation of the best disposal option.
7. The subsequent monitoring of actual impacts arising from the discharge.

Point 5, the appraisal of each alternative, requires some capacity to predict the environmental impact associated with the discharge. Modelling tools provide this predictive capacity. The general aims of the research have therefore been to:

1. investigate the environmental impact of organically rich effluents discharged to the marine environment.
2. assess the currently available modelling tools and/or approaches for modelling of this impact.
3. develop and evaluate additional tools and/or modelling approaches.

Many types of model can be used to predict environmental impact. These include various empirical (that is, statistically based) approaches and optimisation-type models. Conceptual and verbal models are also widely used to convey ideas and evaluate impacts qualitatively. In engineering, however, there is a long tradition of using mechanistic models that, by definition, give an explicit mathematical description of processes occurring in the system of interest. Such models abound in the literature but are mostly concerned with the prediction of water quality. Modelling impact on the benthic environment has received less attention.

A specific focus of this work has therefore been to investigate the mechanistic modelling of benthic impacts associated with the discharge of organically rich effluents. The scope of the research has been limited to the consideration of anthropogenic enrichment alone. Toxic impacts outwith those associated with the enrichment are not considered explicitly.

Anthropogenic enrichment results from the deposition of effluent-related particulates. Any model of this impact must therefore consider three factors:

1. The composition of the effluent and associated particulate matter.
2. The interaction of the effluent with ambient currents and subsequent patterns of deposition.
3. The impact of the increased organic carbon load.

The composition of the effluent can be assessed by considering the source of the raw effluent and the proposed levels of treatment. The interaction of the effluent with the receiving water can be modelled using a number of existing approaches (e.g. Cromey *et al.*, 1998; Farley, 1990). The third factor, the prediction of benthic impact, has received less attention and is the focus of the modelling work presented herein.

A recent work that considers the modelling of benthic impact is a suit of models produced under the auspices of UKWIR called Benoss (Biological Effects and Organic Solids Sedimentation). Benoss models the dispersion, resuspension, and consolidation of effluent-related particulates and thereby predicts the net flux of particulate organic matter (POM) to the seabed. This flux is used as an input to a semi-empirical model from which the impact on the benthos is calculated. The impact is expressed in terms of changes to macrofaunal community structure.

Benoss is a generic modelling tool that was developed to support management decisions related to the marine disposal of effluent. However, one criticism of Benoss is that it fails to take into consideration the heterogeneity of the sedimentary environment. Consequently, Benoss predicts that a given flux of carbon produces the same impact at all sites, irrespective of the physical and chemical conditions in the overlying water column and/or within the sediment itself. Furthermore, the relationship between benthic impact and carbon flux used in Benoss was based on the results of physical process modelling of various sites.

With these limitations in mind, the modelling of sedimentary processes and associated impacts have been investigated. This research can therefore be considered as an independent extension of the work carried out by the developers of Benoss. It must be noted, however, that a report that preceded the development of Benoss (SNIFFER, 1994) stated that sedimentary processes should be taken into consideration. The absence of such processes from the Benoss suit of models perhaps highlights the difficulty involved in their inclusion.

As noted above, Benoss expresses benthic impact in terms of the macrofaunal community. This approach has its foundation in the post-implementation monitoring of a discharge, which often focuses on changes in the structure of this assemblage. However, the fact that the macrofauna are suitable for use in monitoring studies does not mean they should necessarily serve as the basis for a model. The impact of anthropogenic enrichment can also be detected in the microbiological characteristics of the benthos. A 'natural' parameter that reflects these characteristics is the redox intensity or Eh.

A mechanistic model has therefore been developed that describes the redox state of the sediment. Given an estimate of the net carbon flux, the model allows vertical gradients in sedimentary redox intensity to be calculated. The predictive assessment of a horizontal gradient of impact would therefore require the model to be applied at discrete locations around the effluent discharge.

The redox model presented is an improved version of three other sedimentary redox models described in the literature. It is essentially a model of early diagenesis and has therefore been developed with extensive reference to the early diagenetic modelling literature. (Diagenesis is the study of processes that bring about biogeochemical changes in a sediment column after particle deposition.) The model has been implemented as a number of computer programs written in FORTRAN 77. Both steady state and transient versions of the model have been developed and tested.

The model equations are general and are made site specific through the process of parameterisation. However, from an early stage it was recognised that the parameterisation and, consequently, the practical application of the redox model would be problematic. Nevertheless, it was considered that the model would still allow a meaningful and useful theoretical investigation of the problem. Since no fieldwork has been undertaken in this research, it is this theoretical investigation that is presented herein.

It is demonstrated that a mechanistic model can be developed that describes the benthic impact of a discharge, expressed in terms of redox intensity. However, the practical application of the model, at least in a management context, is problematic due to a limited understanding of important ecological processes and uncertainty in parameter values. One of the main sources of uncertainty is estimating how organic enrichment would effect the various parameters associated with the macrofaunal assemblage. Therefore, modelling the redox state of the sediment does not circumvent the problems associated with explicit modelling of the macrofaunal community, as was intended.

The potential for the practical application of any explicit benthic impact model is inferred from the theoretical treatment of the redox model. It is asserted that the modelling approach is questionable because any predictive capacity would, in practice, be swamped by uncertainty. In any case, any benthic impact model must rely on other physical process models to estimate the carbon flux. The subsequent modelling of benthic impact would therefore compound any uncertainty in the predictions of these models. Hence, an approach is suggested that would be based solely on the modelling of physical processes.

Since much of the model uncertainty stems from the limited mechanistic understanding of key ecological interactions, the question arises as to why any attempt has been made to model benthic impact generically. Specific reference is made to the development of Benoss, and it is noted that a range of factors can influence the model development cycle. In particular,

institutional pressures mean that there is a tendency to interpret model output more rigorously than is justified by the degree of mechanistic understanding or the quality of input data. The availability of computing power also means that the production of seemingly convincing models is now much easier than in the past.

Whilst the overall conclusions drawn from the modelling study are negative, this research still makes a contribution to the modelling of environmental impact in general and benthic impact in particular. Original contributions include:

1. An investigation into the mechanistic modelling of benthic impact.
2. The development and analysis of an improved sedimentary redox model.
3. The generic consideration of modelling techniques applied to the prediction of benthic impact.

The overall treatment of effluent disposal, benthic impact, redox intensity, and modelling work represents a relatively comprehensive and original synthesis of work drawn from a number of disciplines.

The main body of the thesis is divided in to nine Chapters. The first three Chapters discuss various concepts that underlie the subsequent modelling work. Chapter 4 delineates a conceptual model from which a mathematical model is subsequently developed. Chapters 5 to 7 consider various aspects of the model implementation and application. Chapter 8 gives a critique of the overall modelling approach. Finally, Chapter 9 gives the conclusions and recommendations for further work. A more detailed description of each Chapter is given below:

- Chapter 1 introduces a number of concepts that are central to the study of environmental impacts in coastal waters. The definitions of marine pollution and environmental impact adopted in this work are discussed. A brief deliberation of relevant social and ethical issues is also given.

- Chapter 2 considers the specific source of pollution and environmental impacts of concern herein; the discharge of organically rich effluents to the marine environment. The sources and generic characteristics of these effluents are discussed. The traditional methods of effluent treatment and disposal are also briefly described. Finally, a simple economic argument is outlined to show that high levels of treatment are not necessarily synonymous with good environmental practice.

- Chapter 3 considers approaches to the modelling of environmental impacts associated with the discharge of organically rich effluents. The various forms of benthic impact are discussed in some detail because these must be the focus of any benthic impact model. A review of two published benthic impact models is also given. It is shown that the models have various limitations that justify the investigation of an alternative approach based on redox concepts.

- Chapter 4 gives a more detailed treatment of redox intensity and sedimentary redox conditions. The processes associated with the formation of vertical redox gradients within sediments are discussed. An outline of problems associated with the measurement and interpretation of redox potentials is also given. The use of redox intensity as an operational parameter for characterising sedimentary environments is then considered. Finally, examples are given to illustrate that horizontal gradients in sediment redox conditions are indicative of benthic impact.

- Chapter 5 describes the sedimentary redox model developed to investigate if redox concepts provide a practical approach to the modelling of benthic impact. A review of three sedimentary redox models already presented in the literature is given. The mathematical basis and physical interpretation of the model are then described in some detail. The techniques used to solve the model equations are also outlined.

- Chapter 6 describes the techniques used in the verification and analysis of the redox model. An account is given of the model internal checks and the methods used to verify the implementation of the model equations. A sensitivity analysis using a simple parameter perturbation technique is also described. Empirical relationships given in the literature are then used to model the redox state of a range of idealised depositional environments. The Chapter ends by considering the modelling of transient systems. It is shown that steady state solutions can be related to the yearly averaged profiles of an equivalent transient case.

- Chapter 7 describes a modelling exercise in which the redox model is calibrated using a real data set (taken from the literature). The calibrated model is used to generate Eh and concentration profiles for the modelled site. The exercise provides a means of demonstrating the data requirements of a site-specific modelling study. Finally, the practical application of the redox model to the assessment of benthic impact is considered.

- Chapter 8 gives a critique of the overall modelling approach taken in the research. The limited interpretation that can be placed on the model Eh values is discussed. The deterministic nature of the model is then briefly considered and it is indicated that a stochastic model would be more appropriate. A general critique of benthic impact modelling is then given, and it is noted that various uncertainties mean that explicit benthic impact models are unlikely to provide any real capacity for recommending action. Factors that influence the model development cycle are also considered. Finally, a qualitative approach to benthic impact modelling is suggested that would be based solely on the output of physical process models.

- Conclusions and recommendations are given in Chapter 9.

Chapter 1

1. POLLUTION & ENVIRONMENTAL IMPACT

1.1 Introduction

This chapter introduces a number of concepts that are central to the study of environmental impacts in coastal waters. A brief introduction to the coastal resource and its exploitation is given first. The definitions of marine pollution and environmental impact adopted in this work are then discussed. Finally, the 'significance' of an environmental impact is considered, including a brief deliberation of relevant social and ethical issues. This Chapter therefore lays the conceptual foundations from which subsequent arguments are developed.

1.2 The Coastal Resource and its Exploitation

The marine environment covers approximately seventy-one per cent of the Earth's surface. The uses of this resource are manifold and include recreation and tourism, fisheries, mineral extraction, transport, and waste disposal. However, except for fishing and transport, human activity is generally restricted to the relatively shallow (<200m) coastal fringes. Coastal waters account for only twelve per cent of the total marine area (Hughes & Goodall, 1992). Hence, although the size of the oceans is great, the directly accessible resource is comparatively scarce. In addition, there is limited exchange between the open oceans and coastal waters. The coastal environment therefore acts as an accumulator of wastes and pollutants -- as much as ninety per cent of the contaminants entering the world's oceans remain in coastal waters (IUCN, 1991).

The potential for degrading the utility of coastal resources is therefore high. At the same time, the demands placed on the resources are huge and growing. For example, the UN Commission on Environment and Development (UNCED, 1992) estimated that more than half of the world's human population lived within 60 km of the coast. It was also estimated that this proportion could rise to over three-quarters by the year 2020. This distribution of human population

imposes a great load on the coastal environment. Furthermore, the rapid expansion of the near-coast population increases the potential for conflicts between users of individual coastal resources.

In the absence of controls, specific coastal resources are unpriced and widely accessible, and the market fails to reveal social values or restrain use (NRC, 1993). Consequently, over exploitation, environmental degradation, and conflicts between various activities are likely to occur. Such problems can only be resolved by the adoption of a coherent management policy that allows effective allocation of resources. Historically, coastal management has tended to be either absent or reactive in approach. However, the increasing demands placed on the environment, coupled with growing public awareness of environmental issues, means a more proactive resource management strategy is today required.

Greater proactivity in environmental matters has been emphasised at an international level by various agencies. In 1987, the Brundtland Commission's report "Our Common Future" brought the term 'sustainable development' into common usage. The report defined sustainable development as "meeting the needs of the present generation without compromising the needs of future generations". This view emphasises the need for environmental protection coupled with continuing economic and social development. Sustainable development defined in this way has been strongly endorsed by international organisations such as the World Bank (The World Bank, 1992; pg. 8). Sustainable development and environmental protection are also emphasised in Agenda 21 of the Rio Earth Summit (UNCED, 1992), which contains a complete chapter on coastal management. The protection and proactive management of the environment as a whole, and the coastal resource in particular, is thus recognised as an issue of global importance.

1.3 Marine Pollution

Of the various factors associated with the degradation of the coastal resource, perhaps the greatest threat is that posed by marine pollution. Marine pollution is produced by a diverse number of activities and can arise from both point and diffuse sources, and can be either chronic or acute in nature (Clark, 1992). However, the term 'pollution' is vague, and thus requires some definition.

In common usage, 'marine pollution' is synonymous with the introduction or discharge of substances such as oil and sewage into the sea. However, the marine environment has various processes that disperse and neutralise such inputs to render them harmless (Hughes & Goodall, 1992). We can therefore speak of the 'assimilative capacity' of the receiving water; that is, the capacity to absorb a given input without measurable harm. The assimilative capacity depends upon many physical and ecological factors, which vary in both time and space. Hence, the same pollutant load can fall well within the assimilative capacity of one area, but produce severe environmental degradation at another.

A more formal definition is given by the United Nations Group of Experts on the Scientific Aspects of Marine Pollution (e.g. GESAMP, 1990), who defined marine pollution as:

> "*The introduction by (people), directly or indirectly, of substances or energy into the marine environment resulting in such deleterious effects as harm to living resources, hazards to human health, hindrance to marine activities, including fishing, impairment of quality of use of sea-water and reduction of amenities*"

Pollution is therefore judged in terms of environmental impact, rather than the discharge of a specific substance. If there is no observable degradation the environment is not polluted, but can be said to be contaminated. The GESAMP definitions of pollution and contamination have been adopted through out this work. Furthermore, the terms 'pollutant' and 'contaminant' are used interchangeably to imply a substance or effluent that has the potential to cause pollution.

1.4 Environmental Impact

The term 'environmental impact' also requires some consideration since it has a wide range of connotations. 'Environment' can be taken to mean either the natural environment and its various components or can refer to the environment of humans. 'Impact' implies a change in the state of the environment. For the purposes of this work, however, an environmental impact (or simply impact) is defined as an adverse change in the natural environment that occurs as a direct result of the disposal of an organically rich effluent (discussed in Chapter 2).

An impact defined in this way is judged in terms of a deviation from a baseline condition; that is, the environmental condition that would be expected if the discharge was not present. This concept is illustrated schematically in Figure 1, which shows the departure of some measure of environmental quality away from the baseline condition. It should be noted that neither the baseline nor impact is constant in time.

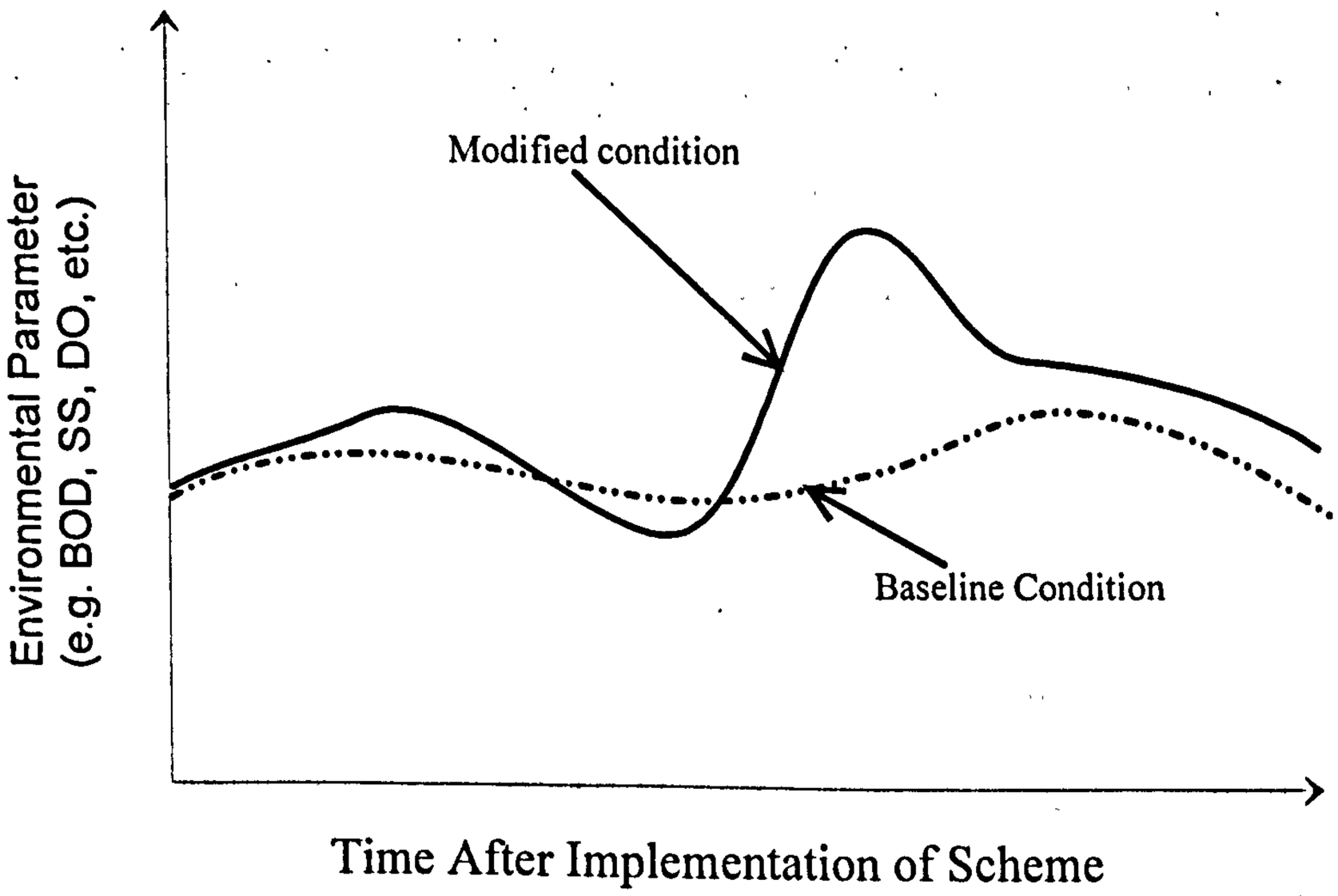

Figure 1 *Graphical Representation of Environmental Impact*

The definition of an environmental baseline is in itself problematic due to the variability of natural systems. However, all discharges produce some departure from a baseline condition at some scale, and could therefore be said to produce an impact. The real question is then one of significance -- whether or not an impact has crossed some threshold, however defined, and is deemed unacceptable.

The characterisation of an impact as 'unacceptable' is subjective and depends upon an observer's personal viewpoint and beliefs. Assessing 'significance' is then, essentially, a question of environmental ethics. The dominant ethic for judging significance in today's Western society is anthropocentric; that is, relating to human activity and welfare. Therefore, whilst 'impact' is considered in terms of the natural environment and can be assessed by scientific means, 'significance' is judged in terms of human interests and is inherently socio-political.

Anthropocentrism is also evident in the approaches adopted to mitigate environmental impacts. The Western world's current economic paradigm of a free market, growth orientated economy requires the application of science and technology to mitigate impacts. This is in part because the underlying technocentric ideology is inherently anthropocentric. The adoption of alternative ideologies, such as ecocentrism, which demands a more sympathetic relationship between human activity and nature, would require a huge paradigm shift.

A conventional ethical stance has been adopted throughout this work, which is both anthropocentric and technocentric. The health of the environment is not explicitly considered as an end in itself, and only traditional effluent disposal strategies are examined. Although such a stance can be criticised, it has been adopted simply because the significance of an impact is ultimately assessed with reference to some regulatory framework. Such frameworks arise from the ethical values that prevail in society and are therefore almost exclusively

anthropocentric. It should be noted, however, that even when seeking to protect the environment for human's benefit, protection is still afforded the environment as a whole.

Given the anthropocentric stance adopted, one final point has to be considered when defining 'significance' -- the influence of public opinion. Whilst science is used as a tool to provide technical assessment of an impact, the wider public are involved in determining the actions to be taken on the basis of the scientific evidence (Fairweather, 1993). On occasion, the scientific assessment of significance can differ widely from the public perception. This poses a problem for regulators/dischargers because whilst they might consider that a particular disposal option is adequate, the public may oppose its implementation. People's concerns can of course be addressed through a consultation process. However, such activities do not take place in an ethical 'vacuum', and a public consultation brings together many people and organisations with a wide range of values.

Unfortunately, when a problem is perceived in terms of competing values, consensus is philosophically intolerable (Miller & Kirk, 1992). The consultation process then tends to become one of conflict rather than constructive debate, and the arguments for and against a proposed scheme could become polarised by the competing value systems. This is especially true when domestic sewage is considered because the objectionable nature of the waste and associated health implications mean that its disposal is viewed as 'dirty' and inherently polluting. Public opinion is therefore often aggressive to any suggestion that a lower level of treatment can be justified on scientific grounds. Such feelings are exploited by environmental pressure groups that have a tendency to use emotive arguments that are perhaps more compelling than dry scientific 'fact'.

This has been recently shown in the case of Sunderland Council and CASSS (Campaign Against Sewage in the Sea at Sunderland). CASSS is an organisation formed to contest the proposal by Northumbrian Water Ltd to provide only primary treatment for the sewage of

Sunderland (UK). A quotation from the CASSS World Wide Web home page (CASSS, 1997) serves to highlight the emotive nature of their arguments:

> *"The proposed scheme allows the maximum possible contamination of the North Sea which is already seriously damaged by sewage and other waste discharges. Already fish stocks are massively depleted, spawning grounds devastated, diseased and poisoned fish found in growing numbers. Other sea life, seals and birds, is also badly affected."*

The use of such emotive language is likely to influence anyone with even a passing interest in the environment and thereby intensify the opposition to the proposed scheme.

Any debate is further clouded by the variability of natural systems and, consequently, the degree of uncertainty inherent in the assessment of impact. Obtaining an objective definition of 'significance' then becomes even more problematic. Direct involvement of the public in the decision making process can overcome such problems, as was shown by the Flyde Forum (discussed in Tuppen, 1996). Nevertheless, the case made by CASSS serves to illustrate the socio-political dimension of defining 'significance'.

1.5 Summary

The coastal resource is central to many human activities and the potential for degrading the utility of the resource is high. Greater proactivity is therefore required in the management of the resource. This is especially true of the management of marine pollution because it has a direct impact on most other resource users.

A formal definition of marine pollution has been adopted herein that requires the occurrence of an environmental impact. Environmental impact is taken to mean an adverse impact on the natural environment and associated living resources. However, the significance of the impact is still assessed in terms of human interests. Assessing 'significance' is therefore a question of environmental ethics, which is inherently socio-political. A conventional ethical stance has been adopted throughout this work, which is both anthropocentric and technocentric. The

health of the environment is not explicitly considered as an end in itself, and only traditional effluent disposal strategies are examined.

Chapter 2

2. ORGANICALLY RICH EFFLUENTS

2.1 Introduction

The preceding Chapter defined and discussed the terms 'pollution' and 'environmental impact', as they are applied throughout this work. This Chapter considers the particular source of pollution and environmental impacts of concern herein; the discharge of organically rich effluents.

The Chapter begins with a brief overview of effluent management. The sources and generic characteristics of organically rich effluents are then discussed. This is followed by a brief description of traditional methods of effluent treatment and disposal. Finally, a simple economic argument is outlined to show that high levels of treatment are not necessarily synonymous with good environmental practice.

2.2 Effluent Management

The discharge of effluent into coastal waters is a cost-effective disposal strategy. Consequently, large volumes of aqueous wastes are ultimately disposed of in this way. However, the quality and hence utility of the water near a discharge depend upon the quality of the effluent and the manner in which it is released (Wood *et al.*, 1993). Environmental degradation related to effluent disposal via unsatisfactory means is a very real concern, and effective management of such wastes is thus desirable.

Direct management of aqueous wastes can be achieved in three ways:

1. *Source Control*: The reduction at source of effluent volume and contaminant loads by processes that are more efficient and wastewater recycling.

2. *Final Treatment*: Treatment carried out before disposal to improve the quality of the final effluent.
3. *Ultimate Disposal Strategy*: The design and siting of an outfall to maximise dispersion and dilution so as to protect sensitive areas such as bathing waters and shellfish fisheries.

Other less 'visible' components such as educational and research activities are also important.

Source control strategies are compatible with the concept of sustainable development and from this perspective are the most desirable option. However, the consideration of such strategies is beyond the scope of this work. In any case, at any given time the scope for implementing source control is limited by practical and economic constraints. For example, the high asset value of conventional (water based) sewerage systems means that they will continue to be widely used. Furthermore, effluents such as domestic sewage are not particularly amenable to source control since production levels are related to the living habits of the human population. Hence, large volumes of effluent will continue to be produced and have to be disposed of in some way. Much of this effluent has a significant organic component and can therefore be termed 'organically rich'.

2.3 Organically Rich Effluents

For the purposes of this work, an organically rich effluent is defined as an effluent having a significant organic fraction that is susceptible to natural processes of decomposition. Examples of such effluents include:

1. Domestic sewage.
2. Effluents from food processing activities: for example, distilleries, creameries, breweries, and canneries.
3. Effluent from pulp and paper producing industries.
4. Effluents from oil production and processing industries.
5. Sewage sludge (including sludge dumping activities).

6. Fish farm effluents.

Sludge dumping and fish farming activities produce environmental impacts that are qualitatively similar to those produced by the discharge of effluents via an outfall (e.g. Pearson & Rosenberg, 1978; Gowen & Bradbury, 1987; Pearson, 1987; Brown *et al.*, 1987; Weston, 1990). These activities are referred to herein since they offer particularly clear examples of pertinent impacts. However, management issues connected with these operations warrant separate treatment, which is not given herein. The following discussion therefore focuses on effluents discharged via an outfall.

2.3.1 Generic Characteristics of Organically Rich Effluents

Many effluents are complex mixtures and exact composition depends upon the source. However, such effluents can be characterised by the following generic components:

2.3.1.1 Water Content

Organically rich effluents have a high water content and effluent density therefore approaches that of fresh water.

2.3.1.2 Solids

The solid fraction in effluents consists of both organic and inorganic substances. The term solid applies equally to particulate, colloidal, and dissolved material. Hence, the solid content of the effluent can be measured in various ways. Suspended solids (SS) are solids that can be removed by settling processes (Metcalf & Eddy, 1991). Effluents also contain colloidal and dissolved solids that can not be removed by settling. Total solids (TS) are defined as all the matter that remains as residue after evaporation of the water. Examples of the solids content of some effluents are given in Table 1 (data from Grace, 1978; Metcalf & Eddy, 1991).

Effluent Source	*TS (mg/L)*	*SS (mg/L)*
Weak Sewage	350	100
Medium Sewage	710	210
Strong Sewage	1200	350
Milk processing wastewater	1600	300
Meat packing wastewater	3300	1000

Table 1 *Typical Solid Contents of Effluents*

2.3.1.3 Organic Matter

The organic fraction of the effluents, which can be either biological or synthetic in origin, consists of both particulate organic matter (POM) and dissolved organic matter (DOM). Material of biological origin contains carbohydrates, proteins, and fats in various proportions. For example, the organic matter in domestic sewage consists of approximately 40-60% proteins, 25-50% carbohydrates, and 10% fats and oils (Metcalf & Eddy, 1991). Synthetic organics include substances such as surfactants, phenols, and some pesticides.

The organic content of the effluent can be measured as Biological Oxygen Demand (BOD) and/or Chemical Oxygen Demand (COD), (e.g. Sawyer *et al.*, 1994). BOD gives a measure of the organic fraction that decomposes over a specific time-scale, normally three or five days (indicated by BOD_3 and BOD_5 respectively). Some organic matter is refractory (that is, does not decompose) over this short time-scale and the BOD test does not give an assessment of this fraction. COD is measured by mixing the effluent with a strong oxidant such as potassium dichromate, which oxidises all the organic matter (e.g. Sawyer *et al.*, op. cit.). The COD test does not differentiate between biologically reactive or inert substances and thus gives an overestimate of the degradable organic matter. BOD and COD levels found in some typical effluents are given in Table 2 (data from Metcalf & Eddy, 1991).

Effluent Source	*BOD_5 (mg/L)*	*COD (mg/L)*
Weak Sewage	110	250
Medium Sewage	220	500
Strong Sewage	400	1000

Table 2 *Typical BOD & COD Contents of Sewage*

2.3.1.4 Nutrients

Organically rich effluents contain significant concentrations of biolimiting nutrients such as compounds of nitrogen and phosphorous. The nutrients can be in both organic and inorganic forms. Inorganic forms are immediately available to primary producers, whereas nutrients fixed within organic compounds only become available during decomposition.

2.3.1.5 Biological Components

Effluents contain various types of micro-organisms such as bacteria, fungi, algae, protozoa and viruses, some of which can be pathogenic; that is, they cause communicable disease. For example, over 100 pathogenic agents have been identified in domestic sewage (NRC, 1993).

2.3.1.6 Problem Contaminants

Many final effluents consist of a complex mix of chemicals. For example, sewage is often a mixture of industrial and domestic wastewater. Therefore, final effluents can be contaminated with a wide range of chemical compounds. Some of these contaminants are toxic and/or do not break down in the environment; that is, they are conservative. Examples of such compounds include dioxins, DDT, polychlorinated biphenyls (PCBs), and heavy metals such as mercury and cadmium.

Even when present in the effluent at undetectable levels, some contaminants can be subsequently concentrated in organisms and further concentrated in the food chain (O'Sullivan, 1971). This 'bio-accumulation' and 'bio-magnification' can give rise to significant and even lethal concentrations, especially in top carnivores such as sea mammals, fish, and sea birds.

For example, DDT concentrations in seawater are normally in the ng/L range, and in the mussel *Mytilus* spp. levels are generally below 20 ng/g. However, some predatory fish have up to 1900 ng/g of DDT in their liver oils (Gay *et al.* 1991). Law *et al.* (1989) also observed mean levels of DDT in the subcutaneous fats of seals of 3000 ng/g. Management of such pollutants can only be achieved through source control, rather than by utilising the assimilative capacity of the receiving water. Consequently, effluents contaminated with this type of substance are outwith the scope of this research.

2.4 Marine Disposal of Organically Rich Effluent

In the past, it was assumed that the enormous volume of the oceans meant that the marine environment had an almost infinite capacity to assimilate waste material (O'Sullivan, 1971). However, this assumption has proved untrue and effluent discharges can, and do, produce undesirable environmental impacts, especially on a local scale. Nevertheless, an environmentally benign method of disposal can be achieved through a combination of treatment and final disposal options, as outlined below.

2.4.1 Traditional Treatment Options

The purpose of treatment is to reduce the 'strength' of the effluent (in terms of BOD, SS, pathogenic contamination, etc.) so that significant environmental impact is not incurred. Traditional methods of treatment rely on a combination of physical and biological processes to achieve this reduction.

The lowest level of treatment, other than pre-treatment processes such as grit removal, is termed primary treatment. Primary treatment is a physical process in which particulate matter in the effluent is allowed to settle out in sedimentation tanks. Settling may be enhanced by the addition of certain chemicals that encourage flocculation. Primary treatment removes at least fifty per cent of the SS and reduces BOD by approximately twenty per cent.

The quality of the primary treated effluent can be improved by secondary treatment. During secondary treatment micro-organisms mineralise the organic matter and convert it into biomass, which is subsequently removed through settling. Secondary treatment is therefore analogous to natural processes of decomposition and results in an effluent with a much-reduced BOD and SS content. Additional treatment processes are available, termed tertiary treatments, which reduce specific contaminants such as nutrient content (See Metcalf & Eddy inc., 1991; & WRc, 1995 for a full description of treatment options).

2.4.2 Final Disposal

The treated or untreated effluent is ultimately discharged into the marine environment via some form of outfall. In its simplest form, this can be an open-ended pipe discharging at or above the waterline. Such outfalls are cheap to construct but provide poor environmental performance and give little scope for encouraging the dilution and dispersion of the effluent.

A better, if more expensive, option is to extend the outfall so it discharges into deeper water. The density difference between the waste and ambient waters then causes the effluent to rise as a buoyant plume. Ambient water is entrained at the plume periphery during the rise, which dilutes the effluent. This buoyant rise continues until either the surface is reached or the density of the effluent becomes equal to that of the ambient waters. This process, termed 'initial dilution', results in a lowering of concentrations and a concurrent reduction in the potential for immediate environmental impact. Incorporating a diffuser section into the design of the outfall can enhance initial dilution. (See WRc, 1990 and Wood *et al.*, 1993 for a comprehensive discussion of outfall design.)

After the buoyant rise, currents in the receiving waters disperse the effluent. It is therefore desirable to site the outfall some distance from shore in an area of dynamic currents. The effluent is then quickly mixed with the ambient waters and the potential for impact further

reduced. In addition, careful site selection can take advantage of currents that transport the effluent away from sensitive areas such as bathing waters and shellfish fisheries.

The design and siting of the outfall can be very effective in mitigating the potential for environmental impact. For example, even with relatively low levels of initial dilution (100:1), a discharge of raw sewage to marine waters produces a more effective dispersion of the organic matter than is achieved by secondary treatment and discharge to rivers (Paul & Midmer, 1989). In acknowledgement of this fact, the disposal of untreated effluent through a well-designed long sea outfall is sometimes termed 'marine treatment'.

In marine treatment schemes, environmental impacts are prevented solely by the design and prudent siting of the outfall (Paul & Midmer, 1989; Mackay & Haig, 1989). The 'treatment' is achieved by taking advantage of natural processes that disperse and decompose the waste. However, the discharge of raw effluent to the sea is repugnant to many people, and marine treatment schemes have therefore tended to be controversial. In any case, legislation has recently been adopted within the European Community that prevents the implementation of such schemes, at least for the disposal of urban wastewater (see the Urban Waste Water Treatment Directive, DIR 91/271 EEC, for details).

2.4.3 The Economics of Disposal Options

Treatment of effluent before disposal and the design and siting of an outfall are carried out to promote improvements in the quality of the receiving water. However, there are a number of costs associated with these improvements. For example, the construction of a treatment plant requires both an initial capital outlay and ongoing expenditure on maintenance and running costs. The construction of an outfall is similarly capital intensive. In addition, treatment processes themselves have environmental impacts associated with them. For instance, treatment plants reduce the amenity of surrounding land and produce pollutants such as sewage

sludge and objectionable smells. Treatment also requires power, so impacts associated with the power generation must also be considered.

If ever-higher levels of treatment are implemented there is a danger of incurring costs that are excessive compared to the environmental improvement realised. Furthermore, the pollutant load could simply be transferred from the receiving water to other components of the environment, that is, the air and land. Finally, the amount of funding available for environmental improvements at any one time is finite. Requiring implementation of 'excessive' levels of treatment could therefore divert funds from other more urgent work. For example, some concern has been expressed that the requirements of the Urban Waste Water Treatment Directive are at present diverting funds away from essential in-land projects (see UK Government, 1998 -- paragraph 203).

A balance must therefore be struck between alleviating the immediate environmental impacts associated with a discharge and the other 'costs' associated with the disposal scheme. This concept is illustrated graphically in the idealised cost/benefit curve shown in Figure 2 (after Kerr & Side, 1994). An efficient level of environmental improvement/protection is achieved when the marginal cost equals the marginal benefit; that is, point Q-P on the graph. The immediate impact of the discharge could be alleviated further, but the benefits realised would be outweighed by the additional costs. This is essentially a statement of the law of diminishing returns applied to effluent disposal.

This simple analysis presupposes that all the costs and benefits associated with a proposed scheme can be quantified in some meaningful way. The most obvious way of achieving this is to assess the cost/benefits in monetary terms, applying an appropriate discount rate. The capital required to construct and maintain the disposal scheme can be costed by conventional means. However, placing a monetary value on natural systems is subjective and depends upon such complex factors as ethics, personal wealth, and vested interest. Hence, it is notoriously difficult

to assess quantitatively the value of the environment or the cost of any impact. In addition, the environment is highly complex and variable, in both space and time. Therefore, quantifying all impacts associated with the discharge/treatment would be difficult, if not impossible, and would incur prohibitive costs associated with data collection.

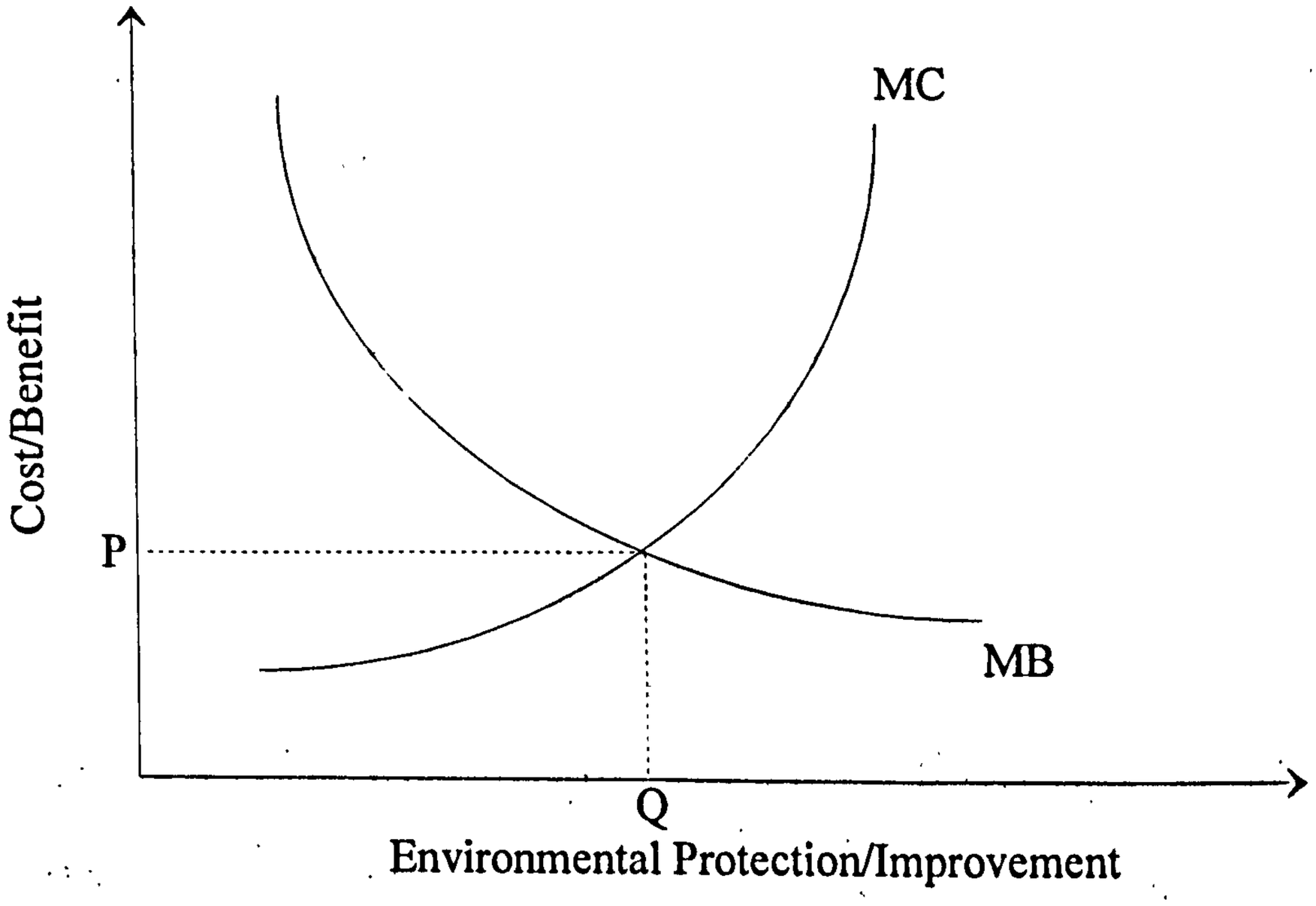

MB: *Marginal Benefit; the additional benefit accrued from providing one additional unit of environmental improvement.*

MC: *Marginal Cost; the additional cost of providing one additional unit of environmental improvement.*

Figure 2 *An Idealised Cost/Benefit Curve for Effluent Disposal*

Therefore, in practice it would be difficult to produce the curve illustrated in Figure 2. Nevertheless, the Figure still highlights the fact that environmental 'efficiency' is not necessarily synonymous with ever-higher levels of treatment. The utility of the coastal resource should be protected, but both economic and environmental constraints dictate that the quality of the effluent should be matched to the assimilative capacity of the receiving waters. It should be stressed, however, that such arguments do not apply to effluents that are significantly contaminated with conservative pollutants, especially those that have a tendency to bioaccumulate/biomagnify.

It has already been noted that the definition of an environmental baseline is problematic due to the variability of natural systems, in both time and space. Demonstrating that a receiving water is capable of assimilating a given waste load without significant impact is therefore likely to be even more problematic. In the face of this uncertainty, it could be argued that we should err on the side of over-treatment. In effect, this is the precautionary principle, which has been adopted at a regional and international level. For example, the principle is in Article 130R of the Maastricht Treaty (McEldowney & McEldowney, 1996), and Article 15 of the Rio Declaration (UNCED, 1992) states that:

> "*Where there are threats of serious or irreversible damage, lack of full scientific certainty should not be used as a reason for postponing cost-effective measures to prevent environmental degradation*"

However, the Marine Pollution Monitoring Management Group (MPMMG, 1994) state that the effects of organic discharges are reversed after cessation. Furthermore, if a discharge is within the assimilative capacity of the receiving water there is, by definition, no environmental degradation. Finally, it has already been noted that there are various environmental impacts associated with treatment. Hence, over-treatment of uncontaminated organically rich effluents is actually contrary to the spirit of the precautionary principle because it would increase the overall environmental impact. Nevertheless, compromising the utility of the resource through badly conceived engineering solutions is unacceptable. We therefore return to the desire to match the load imposed on the receiving water to its assimilative capacity. This requires the application of predictive modelling techniques, which are considered in the next Chapter.

It should be stressed that these arguments only apply if the effluent is relatively uncontaminated. It could then be argued, however, that such an effluent is a resource that should be recycled. In fact, Agenda 21 (UNCED, 1992) makes a commitment to the re-use of organic wastes in order to enhance society's ecological sustainability. It should be remembered, however, that the recycling of organic wastes is viable because the organic material and associated nutrients increase productivity. This beneficial effect can be obtained in both terrestrial and marine ecosystems. It can, therefore, be argued that marine disposal of

organically rich effluents is analogous to the application of fertiliser to land (e.g. Segar, 1985). Deciding which disposal or recycling route is the best option can only be truly resolved by the application of environmental life cycle analysis techniques. These techniques determine the best option for a particular scenario, which might well turn out to be a marine-based option; that is, a conventional disposal scheme.

2.5 Summary

The type of effluents considered in this work can be characterised as being organically rich. The discharge of organically rich effluents to coastal waters is cost effective, but management is required if the utility of the coastal resource is to be maximised. Whilst accepting that source control is the most desirable environmental option, an important part of any overall effluent management strategy is the way in which the effluent is ultimately disposed of. This involves a combination of treatment and the design and siting of a suitable outfall.

The ultimate disposal strategy is intended to bring about a reduction in the potential for immediate environmental impact. However, various costs are associated with both treatment and outfall construction. An environmentally benign disposal strategy is therefore not necessarily synonymous with ever-higher levels of treatment. Consequently, effluent quality should be matched to the assimilative capacity of the receiving waters.

Chapter 3

3. MODELLING BENTHIC IMPACTS

3.1 Introduction

This Chapter considers approaches to the modelling of environmental impacts associated with the discharge of organically rich effluents. The Chapter begins with a brief overview of why, in the context of effluent disposal, some form of predictive capacity is required. A modelling approach that is commonly taken is the modelling of water quality, but the focus of this research has been the modelling of benthic impact. The various forms of benthic impact are therefore discussed in some detail because they must be the focus of any impact model. A review of two published benthic impact models is then given. It is shown that these models have conceptual limitations that justify the investigation of an alternative approach based on redox concepts.

3.2 The Need for Predictive Models

Various environmental impacts are associated with the marine disposal of organically rich effluents (see Section 3.4). However, the extent of any impact depends upon a number of complex factors, including:

1. The characteristics of the discharge; the contaminant load (mass emission rate), effluent volume, peak loads, and variability in time.
2. The method of effluent release (for example, outfall design and siting).
3. The hydrodynamic characteristics of the receiving water; that is, stratification, dominant currents, flushing rates, etc.
4. The background water quality.
5. The environmental quality objectives of the area.

The potential for impact is therefore dependent upon both the contaminant load and the characteristics of the receiving water (e.g. Dempsey & Lack, 1989). Contaminant loads can be reduced through effluent treatment. However, as discussed in the previous Chapter, an efficient level of environmental improvement/protection is not necessarily synonymous with high levels of treatment. This fact, coupled with the wide range of environmental conditions encountered in coastal waters, means that a single 'efficient' disposal strategy can not be specified. Disposal strategies must therefore be tailored to the specific characteristics of the receiving water (NRC, 1993).

The design of an effluent disposal scheme therefore depends upon the evaluation of a number of site specific factors. Hence, some means of predictively assessing site suitability and comparing options is needed purely for design considerations. In addition, given the premise that a proactive management strategy is desirable, some predictive capacity is required to examine the environmental performance of a disposal scheme before its implementation. Deleterious effects can then be anticipated and appropriate action taken. Finally, various legislative requirements impose the need to predict the level of impact. (For example, see Article 6 of the Urban Waste Water Treatment Directive, DIR 91/271 EEC.) Therefore, the design of a particular disposal scheme, the management of coastal resources, and legislative requirements all demand some capacity for predicting impact. This capacity is provided through the use of modelling tools.

3.3 Approaches to Modelling

Two approaches can be taken to model the environmental impact of a discharge; the modelling of water quality and the modelling of benthic impact.

3.3.1 Water Quality Models

Water quality models are used to determine if a given discharge could cause water quality to fall below specified standards and thereby compromise resource utility by harming biota, imposing a risk to human health, or by producing direct economic damage such as the

contamination of fisheries. Water quality models abound in the literature and are not considered further herein.

3.3.2 Benthic Impact Models

Modelling the impact on the benthic environment has received less attention than water quality modelling. However, the need to predict benthic impact can be justified from a number of perspectives, for example:

1. The benthos are linked, both directly and indirectly, to exploitable resources.
2. The benthic ecosystem underpins many processes of ecological importance (for examples, nutrient cycles).
3. The health of the benthos is known to reflect directly the performance and suitability of a disposal scheme, especially with respect to the impact of suspended solids.
4. All ecological components can be considered to have some intrinsic (that is, wilderness) value.
5. Regulators can require that all impacts associated with a discharge be assessed.

Before discussing the tools available for modelling benthic impact, it is desirable to have a clear understanding of the impacts involved. The next section therefore considers these impacts in some detail.

3.4 The Benthic Impact of Organically Rich Effluents

Benthic impact can be produced by either the deposition of particulate matter or toxic effects associated with contaminants in the effluent. However, for the purposes of this work the environmental impact associated with toxics contamination is assumed to be of secondary importance. The 'reasonableness' of this assumption can be shown by reference to a report produced by the Ministry of Agriculture, Fisheries and Food (MAFF, 1993). The report considered monitoring practices for UK sewage sludge dumping grounds and stated:

> *"The biological effects of potentially toxic contaminants associated with the sewage sludge, e.g. certain trace metals, are considered to be secondary in importance at the concentrations generally encountered within the sediments"*

Toxic contaminants associate strongly with particulate matter (e.g. Cooper & Lack, 1987; NRC, 1993). Hence, elevated concentrations would be expected both in the sewage sludge and in the sediments of the dumping grounds. However, the MAFF report indicated that the impacts associated with this elevated contamination were still of secondary importance. Nevertheless, even at low levels of contamination, sensitive species can still be excluded by sub-lethal toxic effects (Spies, 1984). Consequently, if toxic contaminants are present in the effluent the separation of impacts is still somewhat artificial.

The benthic impacts of concern in this work result from the deposition of particulates and associated organic matter. The level of deposition, and therefore impact, depends upon a number of factors, as discussed below.

3.4.1 Increased Particle Deposition

In Section 2.4.2 it was noted that effluents discharged via a submarine outfall rise buoyantly. However, suspended solids have a higher density than seawater and therefore ultimately settle out on to the sediment. The settling velocity of the particles depend upon a number of factors, including particle size, excess density (over ambient), viscosity, and particle geometry (e.g. SNIFFER, 1994 and references therein).

Metcalf & Eddy (1991) give typical settling velocities of sewage related particles, observed in settling column tests, as $<10^{-4}$ cm/s. Pearson (1975) found that the average settling velocity of fibres from a pulp-mill effluent was 0.17 cm/s. Rates of settling therefore depend upon the source of the effluent. Furthermore, the level of treatment implemented modifies the settling characteristics of effluent-related particles.

Various processes in the marine environment affect the rate of settling. For example, the discharge of a low salinity effluent into marine waters leads to flocculation of effluent related particles (Gerlach, 1981). Differential settling rates, brownian motion, and current shear can also cause both natural and effluent related particles to collide and aggregate (e.g. Ferraro *et al.* 1991; Hendricks, 1992; Ernest *et al.*, 1995). These mechanisms increase the size of the particles and thereby enhance the settling rate of the suspended matter near the outfall. Dynamic currents and turbulence, on the other hand, tend to inhibit sedimentation.

Whilst settling, the suspended solids are transported by the ambient currents. The area over which sedimentation occurs therefore depends upon the velocity and direction of these currents. Once deposited the material can be resuspended by current and/or wave action and subsequently redeposited at some other location. Patterns of net deposition are therefore complex and vary from site to site. However, for illustrative purposes it is useful to consider a 'typical' pattern of deposition, as shown in Figure 3. Deposition rates are at a maximum in areas close to the outfall, then fall with distance until background levels are attained.

Since the effluents of concern herein are organically rich, much of the particulate matter deposited around an outfall is organic. The gradient of deposition shown in Figure 3 is therefore paralleled by a gradient in the quantity of particulate organic matter (POM) delivered to the sediment. The continual deposition of POM provides a reliable source of food that, to a point, artificially enhances the carrying capacity of the habitat, and is termed 'organic enrichment' or simply 'enrichment'. Moderate levels of organic enrichment can thus be beneficial to the benthic ecosystem. However, high levels of enrichment produce deleterious environmental impacts related to the decomposition of the organic matter, as described in the next section. (Note: Eutrophication associated with the discharge of organically rich effluents can also result in an increased deposition of organic matter; an impact not considered explicitly herein.)

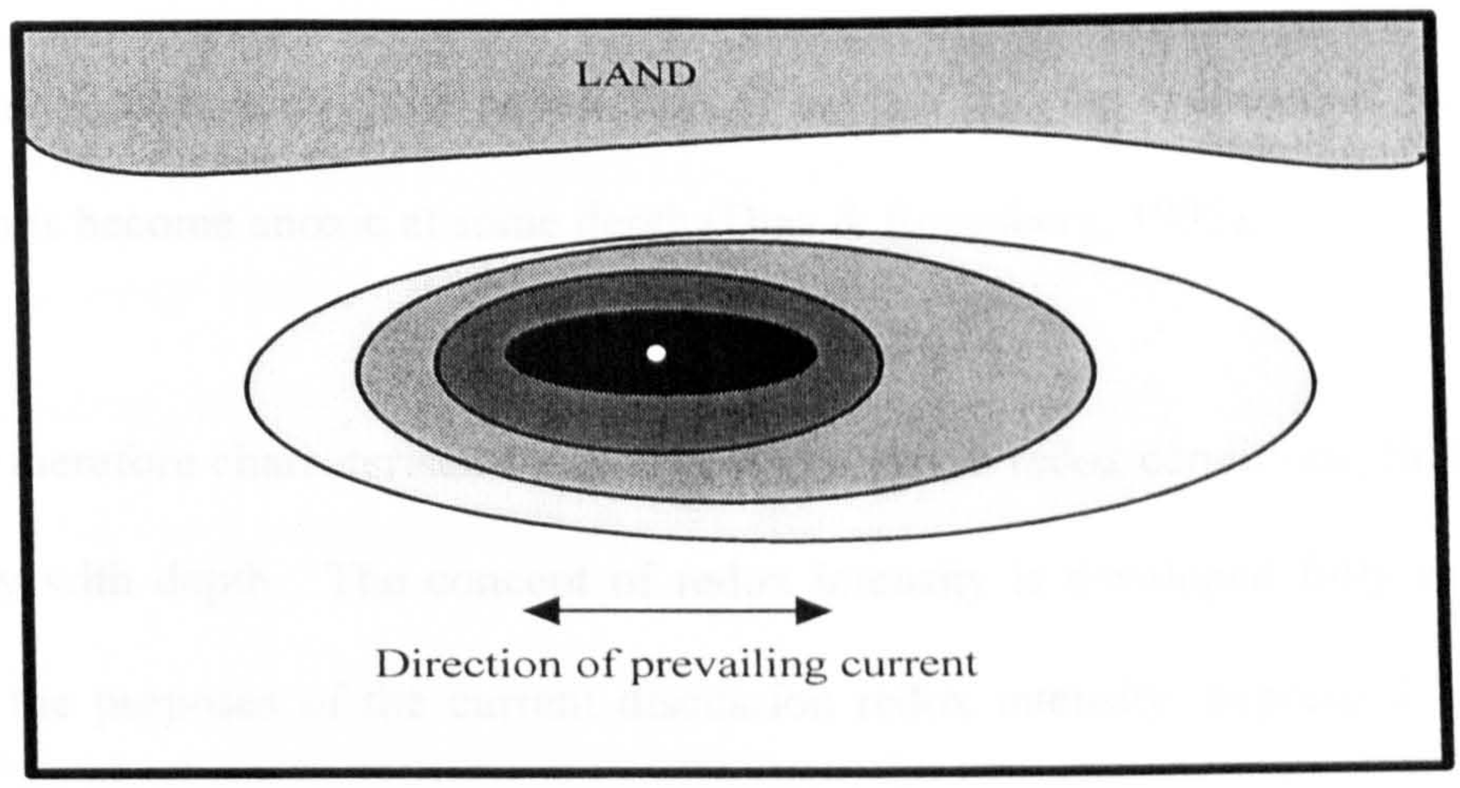

Upper Figure: A 'typical' pattern of deposition around an outfall; deposition is highest around the outfall (black zone) and falls to background level (white zone) at some distance away. Note the prevailing currents can make the pattern of deposition asymmetric about the outfall.

Lower Figure: The patterns of deposition around an outfall are characterised by gradients in the rate of deposition, as well as the flux of POM and organic enrichment (see text).

Figure 3 *Patterns of Deposition Around an Outfall*

3.4.2 Changes in Sediment Chemistry

Organic matter entering the sediment is decomposed via a number of metabolic pathways. However, aerobic respiration predominates wherever oxygen is available (see Section 4.3.1), and this metabolic pathway can be represented as:

$$Organic\ Matter + Oxygen \xrightarrow{organism} energy + CO_2 + water$$

The oxygen consumed in this reaction is replaced by a flux across the sediment-water interface (SWI). However, the oxygen content of water is normally less than 0.001 per cent, compared to an average of twenty per cent in the atmosphere at sea level (Ray, 1995). Consequently, the availability of dissolved oxygen in any aquatic environment is limited. Furthermore, the mineral matrix of the sediment acts as a barrier to the free exchange of water, ions, and

dissolved gases. Consequently, the penetration of oxygen into the sediment is restricted and marine sediments become anoxic at some depth (Diaz & Rosenberg, 1995).

Sediments are therefore characterised by a vertical gradient in redox conditions; that is, a fall in redox intensity with depth. The concept of redox intensity is developed fully in Chapter 4. However, for the purposes of the current discussion redox intensity, expressed herein as Eh (units of volts), can be considered as the tendency of the sediment to oxidise or reduce substances. Aerobic sediments are oxidising and characterised by a positive Eh of approximately +450 mV, whereas anaerobic sediments are reducing and have a negative Eh of down to about -250 mV (Fenchel & Finlay, 1995). The aerobic zone can often be distinguished by its light-brown colour, whereas the sediment of the anaerobic zone tends to be black due to the presence of sulphidic compounds. Often there is a layer between the aerobic and anaerobic zones where the Eh of the sediment falls rapidly. This layer is termed the redox potential discontinuity layer (RPDL), (Fenchel & Riedl, 1970).

The depth of the RPDL depends upon the balance between the supply and utilisation of oxygen (Rhoads, 1974). The additional input of organic matter associated with enrichment modifies this oxygen balance. Where input levels are high, oxygen is rapidly consumed and anaerobic decomposition dominates. A large portion of the sediment oxygen is then used in the re-oxidation of metabolic end products, rather than in aerobic respiration (e.g. Hansen & Blackburn, 1991), and the RPDL (that is, transition to reducing conditions) migrates towards the sediment-water interface (SWI). The depth of the RPDL can therefore be related to the level of organic enrichment. Consequently, a gradient in enrichment is also paralleled by a horizontal gradient in the redox state of the upper portion of the sediment column (e.g. Pearson & Stanley, 1979; Grizzle & Penniman, 1991).

The level of enrichment, however, is not simply related to the amount of organic matter delivered to the sediment, but also depends upon the quality of the organic substrates. This was

demonstrated by Harvey & Phillips (1995), who loaded experimental sediment systems with organic matter from various sources. The authors found that inputs of labile substrates such as fish-feed and primary settled sewage sludge produced significant changes in sediment chemistry. In contrast, inputs such as digested sludge had little effect because most of the labile organic material had been metabolised during treatment.

A fall in redox intensity is ecologically significant because it indicates a decline in the availability of dissolved oxygen. When the concentration of dissolved oxygen falls below 4-5 mg/L, detrimental effects are produced in many aerobic organisms, although the precise threshold varies from species to species (Gray, 1981). For example, many marine invertebrates are not significantly affected until concentrations drop below 2.8 mg/L (Diaz & Rosenberg, 1995).

Reducing conditions are also associated with elevated concentrations of metabolic products such as hydrogen sulphide (H_2S) and ammonia (NH_3). These products are toxic to many organisms. For example, H_2S inhibits the electron transport chain of aerobic respiration (Vismann, 1991; Diaz & Rosenberg, 1995). Spies (1984) notes that amphipods, fish, and other aquatic life have a low tolerance to H_2S and NH_3; a 96 hour LC_{50} (a measure of lethal concentration) of less than 1 part per million being common.

Stresses associated with hypoxia and the toxicity of metabolic products are dependent upon both concentrations and exposure time (Diaz & Rosenberg, 1995). An intensification of reducing conditions along a gradient of enrichment therefore decreases the volume of sediment suitable for habitation by many aerobic organisms. This contributes to the modification of community structures, as discussed in the next Section.

The changes in redox condition that occur along a gradient of enrichment can be seen in Plates 1 to 3. The photographs were taken using a REMOTS® system (Remote Ecological Monitoring

of the Seafloor; e.g. Rhoads & Germano, 1982; 1986) deployed at various stations at the Garroch Head sewage sludge dumping ground (plates from O'Conner *et al.*, 1989).

Plate 1 shows the state of the sediment outwith the area influenced by the dumping. The sediment is light brown (oxidised) near the SWI and there is only a gradual transition to a darker colour. Plate 2 shows the sediment at a station where an intermediate level of enrichment has been produced. The sediment exhibits a well-defined transition from brown to black sediment, which can be taken to be the depth of the RPDL. Hence, there is a clear vertical gradient in redox chemistry at this station. As the depth of the transition varies considerably over the small section of sediment shown, this frame also serves to highlight the heterogeneity of the sedimentary environment.

Finally, Plate 3 was taken in the central part of the dumping ground and shows the effect of high levels of enrichment. The physical and chemical composition of the sediment is obviously altered, when compared to that at the other stations. The sediment colour indicates reducing conditions up to the SWI and capitellid polychaetes and nematodes can be seen, which are characteristic biota of organically enriched sediments (see next Section).

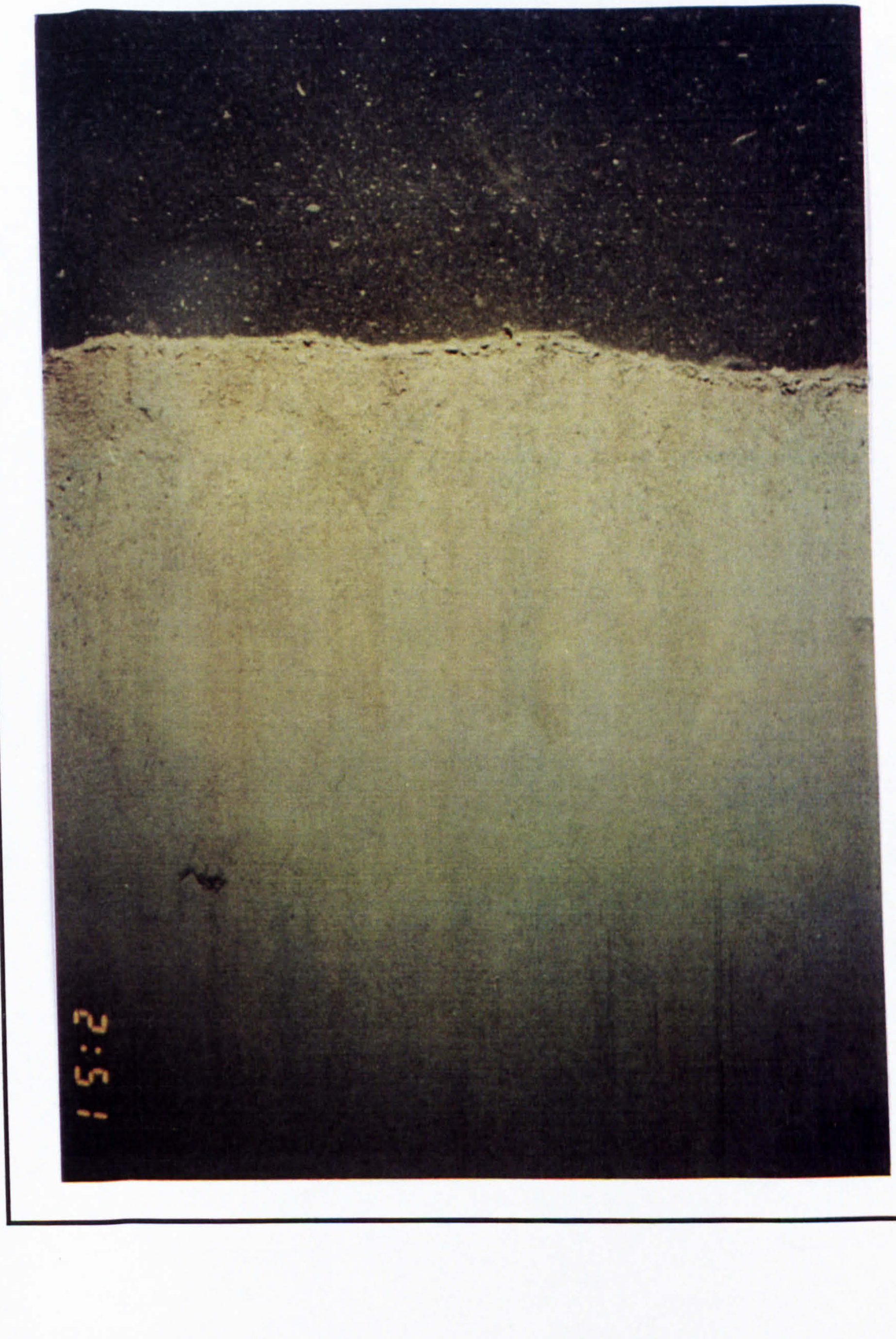

Plate 1: *Normal Sediment; note the gradual transition from light brown (oxidised) to darker (reduced) sediment.*

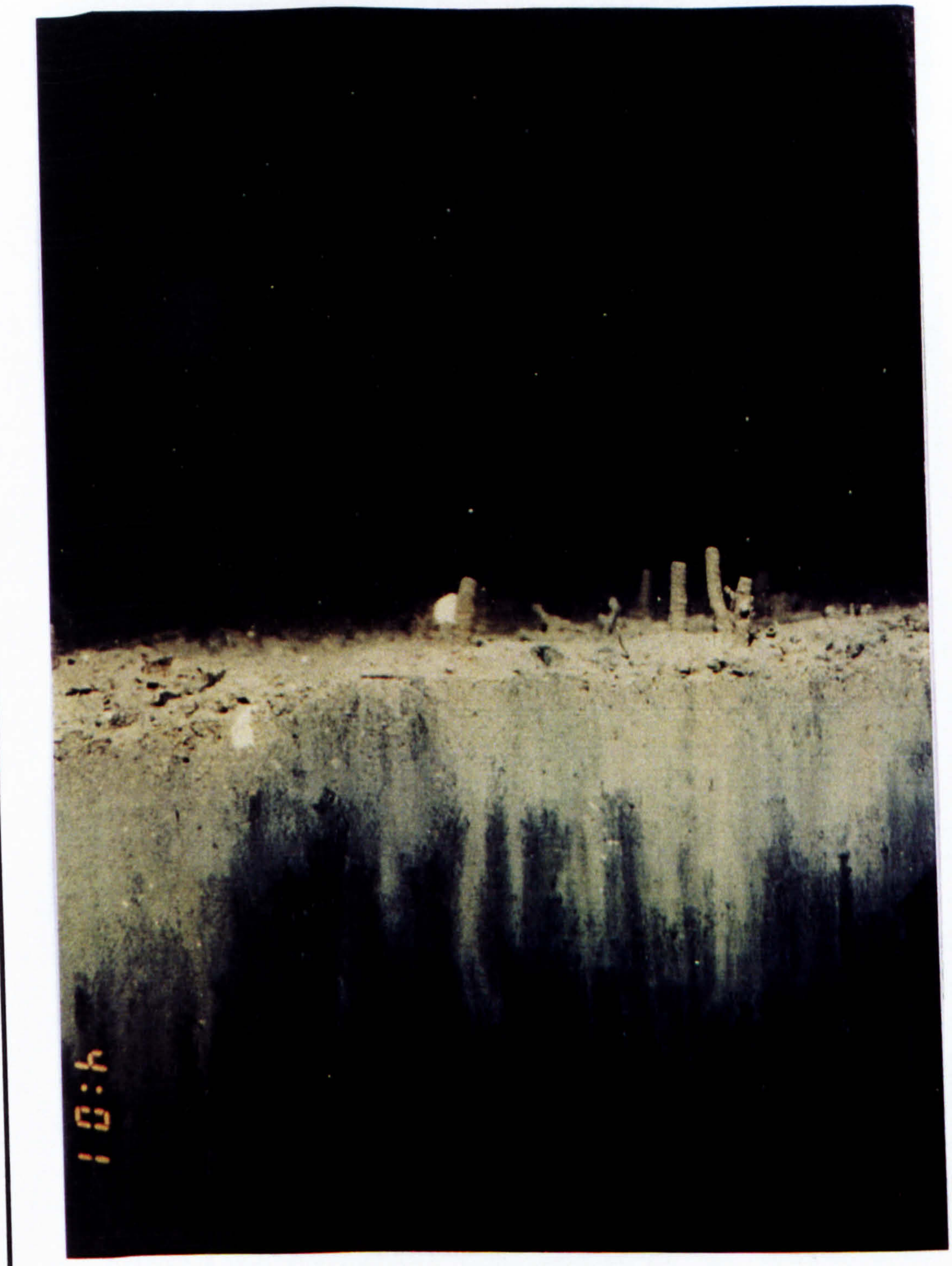

Plate 2: *Intermediate Level of Enrichment; note the clear transition from light brown to black sediment close to the SWI.*

Plate 3: *High Level of Enrichment; the physical and chemical composition of the sediment is obviously altered, compared to that at the other stations, and the dark sediment indicates anoxic conditions up to the SWI.*

3.4.3 Impacts on the Metazoa

As discussed above, the deposition of organic material around an outfall can lead to the deterioration of the sedimentary environment. Metazoa respond to this deterioration in various ways, ranging from small changes in physiological activity and productivity to the elimination of individuals and species. Species can be classified according to their response (after Tulkki, 1968). Species that are not able to tolerate the polluted conditions, and are thus excluded from the discharge area, are termed 'regressive'. Species that are able to capitalise on the new conditions, and thus colonise the polluted region, are termed 'transgressive'. Finally, species that are unaffected by the pollution are termed 'indifferent'.

Responses are however related to the degree of pollution. For example, where severe organic enrichment results in an emergent RPDL (that is, severely reducing conditions extending to above the SWI), all higher animals exhibit a regressive response. Hence, this classification is subjective and only meaningful when comparing responses of different species under a constrained set of conditions.

The biota of the marine environment can be grouped into a number of distinct ecological assemblages or communities. In a normal community, organisms are distributed according to the complex interaction of a wide range of both abiotic and biotic factors, which vary both spatially and temporally. However, the imposition of an overriding pollution-induced stress simplifies these interactions (Pearson, 1975). Over time, the integrated effect of this stress results in a restructuring of the community. Regressive species become excluded from the impacted area and transgressive species flourish. Consequently, the community structure represents a time integrated biological response to the stress imposed upon the system.

As noted in the preceding Section, the level of organic enrichment, and therefore environmental degradation, decreases with distance from the effluent source. Hence, in areas adjacent to the discharge the level of enrichment could impose an overriding stress. Nevertheless, at some

distance from the outfall the stress would still return to background levels. The community structure mirrors this gradient of environmental stress. Hence, in a 'typical' polluted area a spatial gradient can be defined along which the community gradually changes from one dominated by transgressive species to a normal community in areas that are unaffected by the discharge. It should, however, be noted that many natural variables modify community structure, and in areas where the pollution is not overriding, it is not always easy to separate natural variation from anthropogenic impact (Warwick, 1988).

The metazoa of the benthos are operationally grouped into two size-classes; the macrofauna and the meiofauna. The macrofauna are defined as those members of the benthos that are retained on a 0.5 mm or 1 mm meshed sieve. The meiofauna are defined as those members of the benthos that pass through a 0.5/1 mm mesh but are retained on a 63 μm meshed sieve (Warwick, 1988). The responses of these assemblages to organic enrichment are discussed in turn below. However, more emphasis is given to the macrofauna since this assemblage has more relevance to the modelling work detailed herein.

3.4.3.1 Impact on the Macrofauna

The classic macrofaunal community of excessively enriched sediment is dominated by transgressive deposit feeders such as the polychaetes *Capitella capitata and Malacoceros fuliginosa.* The presence of these opportunistic species in large abundance can therefore be used as an indicator of organic enrichment (Harvey & Phillips, 1995). Such organisms tolerate the adverse environmental conditions associated with the enrichment, and are able to capitalise on the disturbed conditions and exploit the elevated supply of food.

As noted above, however, characteristic patterns of deposition around an outfall produce horizontal gradients of enrichment. These gradients induce a succession in the macrofaunal community, as illustrated in Figure 4 (after Pearson & Rosenberg, 1978), rather than yielding just this 'classic' deposit feeding assemblage. The exact mechanisms responsible for the

ecological succession are not well understood (Grizzle & Penniman, 1991). Pearson & Rosenberg (1978) suggest that changes in trophic structure, interspecific interactions, increased environmental stress, and reduction in niche-space all contribute to the restructuring. Gray (1979) asserts that much of the change is driven by physical disturbances that favour r-strategists; that is, biota with early age of first reproduction, large reproductive effort, short generation time, and numerous off-spring (e.g. Valiela, 1995).

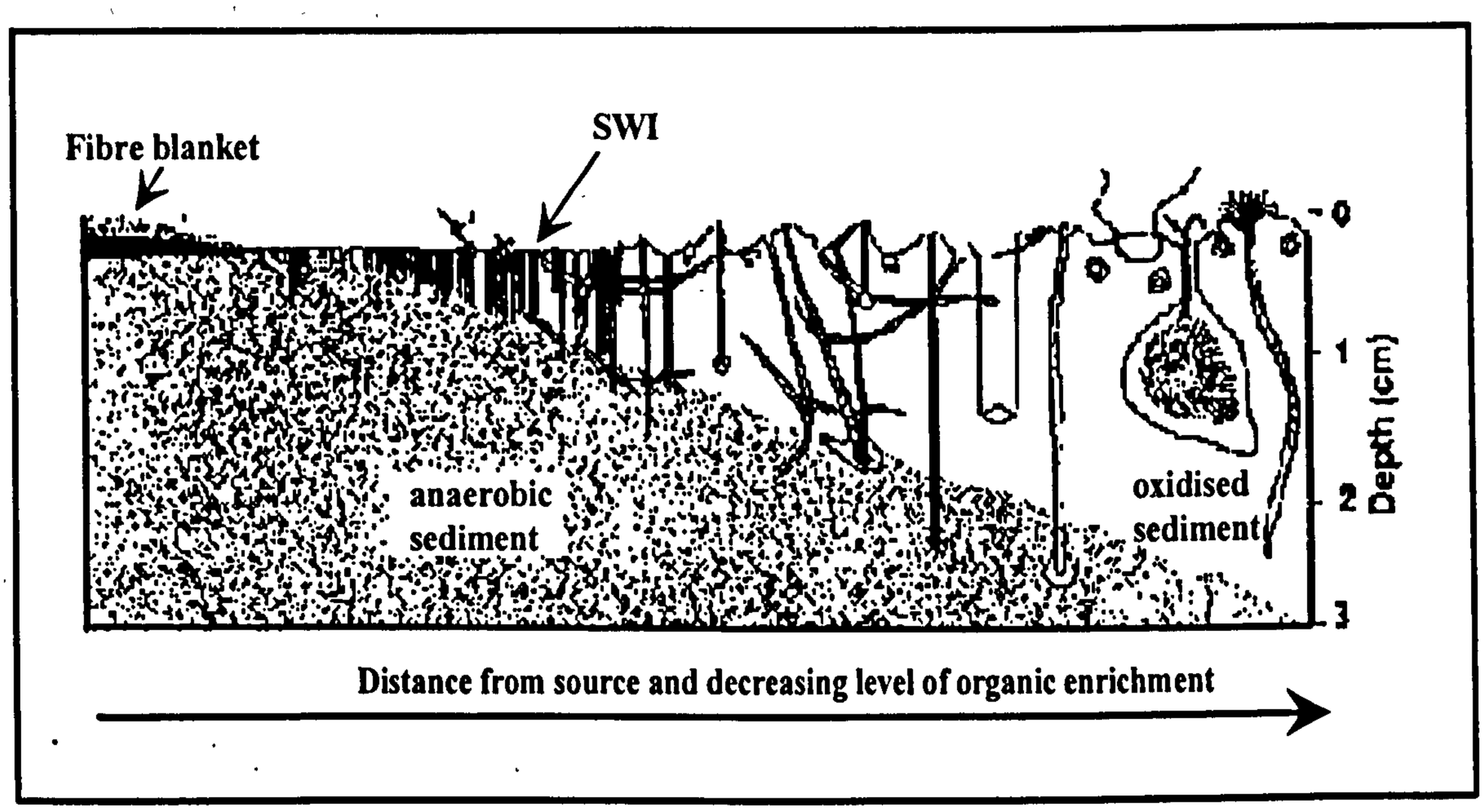

The gradient in enrichment induces a horizontal gradient in redox conditions, as shown by the changing depth of the oxidised sediment, and a change in macrofaunal community structure. In the grossly polluted area there are no macrofauna and a fibre blanket of bacteria (e.g. Beggiatoa spp.; see text below) can form. At some distance from the discharge (that is, the right hand side of the Figure), the community and redox conditions return too normal. At intermediate points, there is a succession in the macrofauna community structure. Pearson (1987) notes that this succession suggests a highly evolved response to carbon utilisation -- at the community level the adaptation is a progressive species replacement to maximise the utilisation of the available carbon.

Figure 4 *Succession Along a Gradient of Enrichment*

Four successional zones can be identified along the gradient of enrichment:

A grossly polluted zone: The deposition of organic matter is so high that anoxic conditions occur at or above the SWI. The sediment is characterised by high concentrations of substances associated with anaerobic decomposition, for example, H_2S. All macrofauna are excluded and bacteria such as *Beggiatoa* spp., which are able

to utilise the H_2S as an energy source, can form white mats covering the sediment of this zone (that is, the fibre blanket indicated in Figure 4).

A polluted zone: Inputs of organic matter are sufficient to degrade the environment. The sediment is characterised by low levels of dissolved oxygen and elevated levels of metabolic products; the RPDL approaches the SWI. The 'classic' macrofaunal community of excessively enriched sediment occurs in this zone, which is dominated by a few opportunistic species. Individuals of such species tend to be small (low biomass per individual) but can occur in huge abundance.

An enriched zone: The sediments are enriched but excessive degradation does not occur; a wide range of fauna can tolerate the conditions. Enhancement of food supply is sufficient to increase the carrying capacity of the habitat and a large biomass and species richness develops. However, the macrofaunal community structure is still modified because some of the most sensitive species associated with the 'normal' community of the area are excluded.

Normal Zone: the input of organic matter is at background levels. Hence, the macrofaunal community structure is 'normal' for the area.

Although this description implies that the zones are distinct, in reality the succession is continuous, and the separation into discrete zones is somewhat arbitrary.

Pearson & Rosenberg (1978) proposed a graphical model that illustrates this ecological succession. Heip (1995) discusses the model in detail and notes that it is still the basic reference for the literature on the benthic impacts associated with organic enrichment. The model, shown in Figure 5 (after Pearson & Rosenberg, 1978), is based on three indicators of community structure: species number (S), total abundance (A) and biomass (B). The model is

strongly biased towards communities of fine-grained sediments, but major qualitative features of the response are observed in disturbed communities of sand-dwelling fauna (Rhoads & Germano, 1982; Vetter, 1996). Pearson & Rosenberg (1978) note that the exact form of the model is modified by many environmental factors. However, the general response has been found to be applicable to many discharges (see Pearson & Rosenberg, 1978, and references therein).

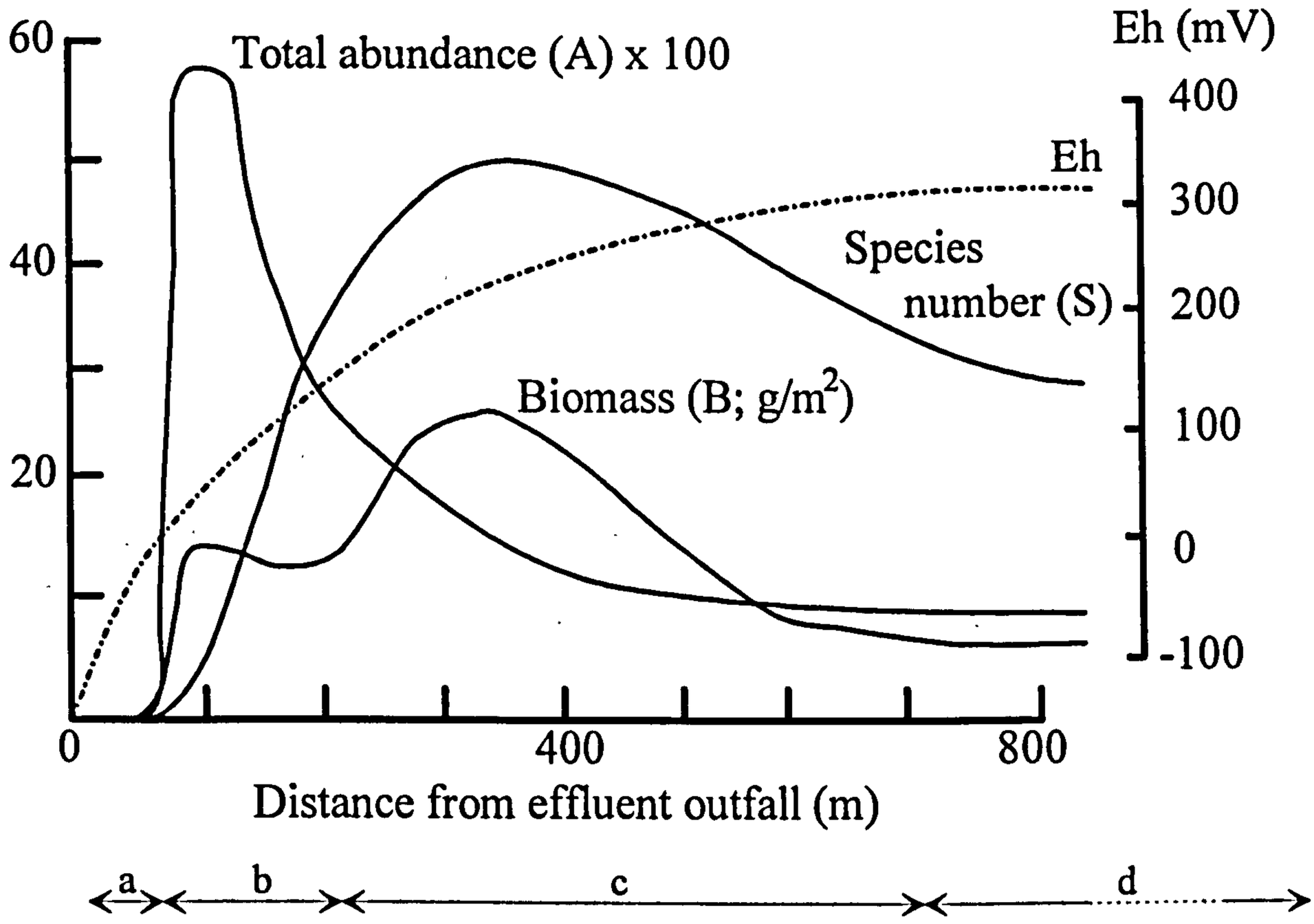

The arrows indicate the zonation discussed in the text: (a) indicates the grossly polluted zone; (b) the polluted zone; (c) the enriched zone; (d) the normal zone. The extent of each zone has been arbitrarily selected and is for illustrative purposes only.

Figure 5 *A Model of Benthic Succession*

The Pearson-Rosenberg model indicates that at moderately high levels of disturbance (distance of between 50 to 200 m in Figure 5; that is, zone 'b') the macrofaunal community is dominated by a small number of species, occurring in large abundance, with a relatively low total biomass. This type of community is therefore characterised by a low biomass to abundance ratio (B/A, the average biomass of each individual, termed the size ratio) and a high abundance to species number ratio (that is, A/S, the average number of individuals per species, termed the abundance

ratio). These ratios therefore provide one means of assessing change in macrofaunal community structure along a gradient of enrichment (e.g. MPMMG, 1994).

By way of illustration, consider an area of undisturbed sediment with homogeneous gross physical characteristics, for example, similar inputs of POM and the same silt/clay content. Since there is no disturbance, the macrofaunal community is stable and characterised by high species diversity (high S). The average number of individuals per species is low (low A/S ratio) but biomass per individual tends to be high (high B/A ratio). The precise composition of such a community still varies according to factors such as recruitment success. However, the community structure is relatively stable in that various life strategies are represented consistently. For instance, deposit feeders would represent a consistent fraction of the community, but the actual species present would vary over space and time (P.F. Kingston, personal communication). Nevertheless, if the macrofauna were sampled along a transect it would be expected that no clear gradient in A/S and B/A ratios would be observed.

Now consider the same system but with a gradient of enrichment imposed. Outwith the area of disturbance the community structure, expressed as A/S and B/A, would still approximate the baseline condition. However, the community would become progressively disturbed along the gradient of enrichment, and this would be observed in a change in the derived community structure indicators; that is, the A/S and B/A ratios.

This illustrates the BACI (before, after and control, impact) approach to sampling and monitoring; that is, the level of environmental impact can be determined by comparing the community before and after implementation of a disposal scheme and/or between a control and an impacted station. In practice, variations in abiotic factors in space and fluctuations in populations in space and time make the BACI approach more problematic than this simple treatment would suggest (e.g. Ferraro *et al.* 1991; Underwood, 1992).

A severe gradient of enrichment is implicit in the Pearson & Rosenberg model and such gradients would be indicative of a disposal scheme that gives poor environmental performance. If the volume of effluent discharged and/or physical conditions result in only moderate levels of enrichment, however, the response of the macrofauna is less predictable. For instance, the addition of fine material can reduce the stability of the sediment and make it more prone to resuspension during storm events. Consequently, particle deposition augments benthic productivity but can also impose perturbations that reduce the stability of communities. For example, Zmarzley *et al.* (1994) found that communities within the footprint of an outfall (that is, the area of impact) were much less persistent over time than those beyond.

Moderate levels of organic enrichment do not necessarily result in an increase in macrofaunal abundance and biomass. For example, Davies & Wade (1985) examined the benthic impact of a steelworks discharge in the Usk estuary (UK). The effluent was a complex mix of neutralised pickling liquor, rolling and cutting oils, boiler effluents, as well as some sewage. The amount of organic matter discharged was significant and was estimated as being equivalent to ten per cent of natural inputs. However, near to the outfall the macrofaunal community was found to be relatively impoverished, as shown by a lack of the polychaete *Neries diversicolor*. The authors suggested that other toxic and/or physical impacts had counteracted the enriching effect of additional organic material. This example therefore serves to illustrate that toxic/physical impacts can be more significant than the effect of organic enrichment (compare with Section 3.4).

The community structure of the macrofauna is correlated with many factors such as the median grain size, silt content, and bottom shear stress (e.g. Heip & Craeymeersch, 1995). Gradients in these factors, which are often associated with changes in depth, are therefore paralleled by changes in the macrofauna community. Furthermore, the community structure, even on a local scale, can be influenced by differing levels of natural disturbance (e.g. Valiela, 1995). Consequently, a gradient in macrofaunal community structure does not necessarily indicate

pollution. For example, Perkins (1979) describes results from a study of an effluent disposal scheme in the Solway Firth. The benthic community exhibited a lowering of diversity and abundance in areas immediately adjacent to the outfall, thereby suggesting an impact attributable to the discharge. However, subsequent investigations showed that this view was erroneous and that the impoverishment of the community was produced by wave action and concurrent sediment instability.

3.4.3.2 Impact on the Meiofauna

As with the macrofauna, the meiofauna are affected by the physical and chemical changes associated with enrichment. In addition, the deposition of fine effluent-related particulates can reduce porosity, which has a negative effect on the space-limited meiofaunal communities (e.g. Sandulli & de Nicola, 1991).

Organic enrichment can induce a decrease in meiofaunal species diversity and an increase in abundance (e.g. Gee *et al.*, 1985). At high levels of pollution a decrease in both abundance and diversity and a corresponding increase in species dominance can be observed (e.g. Gee *et al.*, 1985; Keller, 1985). A meiofaunal abundance close to zero has also been noted in severely enriched areas (e.g. Sandulli & de Nicola, 1991). The response of the meiofauna to enrichment is therefore somewhat analogous to that of the macrofauna.

However, there are a number of differences. For example, in enriched areas there is a tendency towards smaller sized species of macrofauna but a shift towards larger sized species of meiofauna (e.g. Heip *et al.*, 1988). Furthermore, the abundance and biomass of the meiofauna do not give a consistent measure of impact, although measures of diversity are more reliable (Coull & Chandler, 1992; Duplissa & Hargrave, 1996). Consequently, the meiofauna exhibit a less predictable response to enrichment than do the macrofauna (Duplissa & Hargrave, op. cit.).

The various components of the meiofaunal community respond differently to organic enrichment. Raffaelli & Mason (1981) found that copepods are more sensitive to environmental stress than nematodes. As levels of enrichment increase the ratio of nematodes to copepods (N/C) would therefore be expected to rise. However, a number of studies have demonstrated that this is not always the case. For example, Gee *et al.* (1985) found that the N/C ratio was inversely correlated with enrichment. The authors suggested that the differential response of the nematode and copepod assemblages was a better indicator of disturbance. However, the use of the N/C ratio was modified by Raffaelli (1987) to include the effect of habitat requirements and the different responses of copepod species. Coull & Chandler (1992) note that with these refinements the N/C ratio is a reasonable approach to pollution assessment. Hence, all other environmental factors being equal, gradients in enrichment should be paralleled by changes in the nematode/copepod ratio.

Recent work by Schratzberger & Warwick (1998) has studied the effect of organic enrichment on nematodes. The authors found that enrichment lead to an altered community, as measured by a variety of community structure indicators. However, the degree of change depended upon the size and frequency of the dosing events. Since these characteristics would change along a gradient of enrichment, it can be inferred that the impact on the meiofaunal community structure would also change along this same gradient. Furthermore, it was found that the degree of impact depended upon the natural tolerance of the nematodes to organic enrichment. This last point is noteworthy since it suggests that communities from organically rich sediments are more tolerant to additional enrichment than communities from organically poor sediments.

3.5 Approaches to the Modelling of Benthic Impact

As discussed above, benthic impact can be manifested in a number of ways. Management of effluent disposal is therefore required if these effects are to be minimised. This management should ideally be based on the best available scientific information. Monitoring programs provide the necessary information once a disposal scheme is in operation. However, as already

discussed, some predictive capacity is required at the planning stage or when a change in the operation of an existing scheme is proposed.

In the context of the current discussion, this means that some form of benthic impact model is required. To be meaningful such a model must relate effluent load to one or all of the impacts outlined in previous sections. Furthermore, it is desirable that the model should be generic and be able to discriminate between alternative design options such as different treatment levels and discharge locations. Two models have been presented in the literature that attempt to predict benthic impact, as discussed below.

3.5.1 Mass Emission Rates & Benthic Impact

A strong positive correlation between the amount of solids discharged and the impact on the macrofauna was found in studies of outfalls discharging into the coastal waters off Southern California (see Bascom, 1982 for a review of these studies). Mearns & Word (1982) subsequently developed empirical models by assuming that this correlation indicated a cause and effect relationship. Four equations were produced by regression analysis of log transformed data:

$$S_e = (1.77 J_e .10^{-3})^{1.75}$$

$$A_e = (4.11 J_e .10^{-4})^{0.96}$$

$$A_{i30} = (2.11 J_e .10^{-5})^{2.55}$$

$$A_{i60} = (8.42 J_e .10^{-5})^{2.16}$$

Equations 3-1 to 3-4

where S_e is the total excess standing crop of benthic infauna (metric tonnes wet weight), A_e is the size of area occupied by the total standing excess crop (km^2), A_{i30} is the area in which subsurface deposit feeders are the dominant infauna (km^2), A_{i60} is the area where surface and subsurface deposit feeders predominate (km^2), and J_e is the mass emission rate of suspended solids (metric tonnes/year).

These empirical models have the advantage that they are simple and allow the level of benthic impact to be calculated for any mass emission rate. The model output is also expressed in a way that facilitates the comparison of alternative schemes. This can be readily seen in Table 3, which shows the predicted impact associated with a range of discharges (after MPMMG, 1994). It can be seen that the level of benthic impact (that is, the magnitude of S_e, A_e, A_{i30}, and A_{i60}) is proportional to the size of the discharge (indicated as population equivalents, pe). The Table also shows that the impact can be reduced by implementing higher levels of treatment. Such predictions would therefore allow regulatory agencies and dischargers to easily compare the environmental impact of various disposal options.

	Untreated		*Primary*		*Secondary*	
	10,000 pe	*150,000 pe*	*10,000 pe*	*150,000 pe*	*10,000 pe*	*150,000 pe*
S_e (T)	0.12	13.16	0.03	3.91	0.003	0.306
A_e (km^2)	0.08	1.01	0.04	0.52	0.01	0.129
A_{i30} (m^2)	1	532	0.1	90.8	0.002	2.22
A_{i60} (m^2)	97	33461	21.6	7478.2	0.94	322.85

NB: pe indicates population equivalent; untreated, primary and secondary indicate the level of treatment

Table 3 *Predicted Impact for Various Discharges*

It has been noted previously, however, that a single 'efficient' effluent disposal strategy can not be specified due to the heterogeneity of the coastal environment. It is therefore highly unlikely that a universally applicable empirical model could be produced that linked discharge characteristics to benthic impact. Furthermore, the model equations (3-1 to 3-4) were developed from data taken in areas with similar characteristics, for example:

1. The discharges were all in deep water (20-60m) via large outfalls.
2. Each area had similar hydrographic and faunal regimes.
3. All the discharge areas had predominantly longshore currents with similar energy spectra.

Application of the equations to areas with different characteristics would therefore be questionable. (This point is also discussed in MPMMG (1994) with respect to the applicability of the model equations to UK waters.)

Hence, whilst the empirical models serve as a basis for management decisions made in the study area (that is, the coastal waters off Southern California), it is doubtful that they would apply to discharges made under different conditions. This supposition is supported by two studies carried out by the Forth River Purification Board (FRPB 1994a; 1994b) in which observed benthic impacts were compared with predictions made using the empirical models. In both cases, the empirical models grossly overestimated the impact. For example, Table 4 shows the predicted and observed biological effect for a discharge in the Firth of Forth, Scotland (FRPB, 1994a).

Parameter	*Predicted*	*Observed*
S_e	105 T	0
A_e	3.2 km^2	0
A_{i30}	0.011 km^2	< 0.01 km^2
A_{i60}	0.43 km^2	< 0.01 km^2

Table 4 *Predicted Versus Observed Biological Impact*

It is possible that the model equations could be tailored to other sites if sufficient data was available. However, the equations were developed for an area subjected to prolonged and intensive studies. Hence, it must be assumed that similar levels of data availability would be required to modify the models. The modelling approach could therefore only be applied, with any confidence, if a substantial amount of historical field data was available. In any case, the data requirements imply that the approach is suitable for managing existing outfalls, rather than predicting the impact of proposed discharges. The generic application of the modelling approach is therefore questionable.

3.5.2 Benoss

The empirical approach taken by Words & Mearns (op. cit.) is highly desirable since it allows complex environmental interactions to be expressed simply, whilst retaining a physical significance. However, since the approach is not generic it is of limited value to the predictive assessment of benthic impact. A more general approach is taken in Benoss, a suit of models produced under the auspices of UKWIR (UKWIR, 1996; Cromey *et al.* 1998).

Benoss models the physical processes in the receiving water using well-developed techniques, including a Eulerian approach to tidal currents and Lagrangian (random walk) approach to effluent dispersion and advection. The model also allows the characteristics of the effluent to be specified. When suitably parameterised, the model predicts the carbon deposition rate at discrete locations throughout the discharge area. This deposition rate (that is, carbon flux) is then used as an input to another model that estimates the macrofaunal community structure at each node. The community structure is expressed as the infaunal trophic index (ITI) of Word (1979, see also WRc, 1992). The overall benthic impact is therefore indicated by gradients of ITI values.

One criticism that can be made of Benoss is that it fails to take into consideration the heterogeneity of the sediment environment. A given carbon flux predicted by the model always produces the same impact, irrespective of the physical and chemical nature of the sediment or overlying water. In addition, Cromey *et al.* (1998) note that the 'semi-empirical' relationship used to calculate ITI values was generated using field observations of macrofaunal abundance at different sites, in conjunction with deposition rates predicted via the same physical process models used in Benoss. Hence, the derived relationship between benthic impact and carbon flux depends upon the quality of this physical process modelling. Consequently, the 'semi-empirical' approach used to calculate the benthic impact (that is, the ITI value) is somewhat questionable.

3.5.3 Other Modelling Approaches

Other models have been developed that involve an implicit consideration of benthic impact. For example, Omori *et al.* (1994) developed a model that considered the oxygen balance of the coastal system when exposed to anthropogenic enrichment. Similarly, models have been developed for quantifying the oxygen demand imposed by the sediment on the overlying water column (e.g. Di Toro *et al.*, 1990; Chapra, 1997). All the models, however, use a limited mathematical description of sedimentary processes.

3.5.4 An Alternative Modelling Approach

It has already been noted that an explicit model of benthic impact should ideally be generic and must reflect the environmental impact in some meaningful way. As discussed above, an empirical association between discharge characteristics and benthic impact is not considered generic. In contrast, the physical models used by Cromey *et al.* (1998) can be tailored to a wide range of scenarios. However, the overall modelling approach would be improved if the method for quantifying benthic impact were derived independently of the physically based models. Furthermore, the ultimate expression of impact would be more meaningful if the heterogeneity of the benthic environment was reflected in some way.

Two approaches could be taken to achieve these improvements. Firstly, the carbon deposition and level of benthic impact could be linked empirically. Secondly, a mechanistic model could be developed that assesses the benthic impact associated with the carbon flux. The first approach would require a substantial amount of experimental and/or fieldwork and has therefore not been investigated, although it is considered further in Chapter 8. The second approach, which can be investigated theoretically, requires that some relevant measure of benthic impact be selected as the focus of the modelling effort.

The models of Mearns & Word (1982) and Cromey *et al.* (1998) both express the benthic impact in terms of changes in the macrofaunal community structure. This approach has its

foundation in the monitoring of a discharge, which generally includes sampling of the macrofauna. The macrofaunal assemblage is monitored for a number of reasons, for example:

1. The macrofauna can be sampled quantitatively with comparative ease using coring or grab sampling techniques.
2. The macrofauna can be identified to species level.
3. The response of the macrofauna to enrichment is well documented and impact can often be recognised by considering gross indicators of community structure and associated ratios (see Section 3.4.3.1).

However, the fact that the macrofauna are sampled in monitoring programs does not mean they are a suitable focus for a mechanistic benthic impact model. For instance, the variability and heterogeneity of the macrofaunal community and complexity of the ecological interactions are factors that would be difficult to incorporate into a generic model. Similar restrictions apply to the modelling of the meiofaunal assemblage. Using the metazoa as a focus of modelling effort is therefore problematic.

It has already been noted that benthic impact can also be detected in the redox intensity of the sediment. As discussed in the next Chapter, vertical gradients in redox intensity reflect the distribution of oxidants used in the decomposition of organic material. By inference, therefore, these gradients also reflect the distribution of bacteria and other micro-organisms that utilise these oxidants (Scott & Morgan, 1990). The microbiology of the sediment can be directly linked to the chemical and physical properties of the sediment and the ecological health of the overall system (Findlay & Watling, 1997b). Redox concepts therefore provide a potential focus for a benthic impact model. The redox state of sedimentary systems is discussed more fully in the next Chapter. The development and analysis of a redox model are then described in Chapters 5 and 6.

3.6 Summary

A single approach to the disposal of organically rich effluents can not be specified due to the heterogeneity of the coastal system. Some predictive capacity is therefore required to assess the suitability of a proposed scheme or the impact of a change in operation of an existing scheme. This predictive capacity is in part provided by mathematical models.

Benthic impacts can result from toxics contamination or organic enrichment, but only organic enrichment is considered herein. The effect of organic enrichment can be observed in a number of ways, for example, elevated deposition of organic carbon, changes in sediment chemistry (expressed as Eh), and impacts on the metazoa. A benthic impact model must therefore relate one or all of these impacts to the characteristics of the effluent discharge.

Two models of benthic impact have been presented in the literature that predict changes in macrofaunal community structure. However, the complexity and heterogeneity of the metazoan assemblages are factors that would be difficult to incorporate into a generic mechanistic model. Redox concepts provide an alternative focus for the modelling effort, and the potential for this approach is investigated in subsequent Chapters.

Chapter 4

4. Sediment Redox Intensity

4.1 Introduction

As noted in Chapter 3, the redox state of the sediment is a potential focus for a benthic impact model. As such, a more detailed consideration of redox intensity is deemed appropriate. Hence, this Chapter discusses various concepts associated with redox intensity, and gives particular emphasis to the redox state of sedimentary systems.

The Chapter begins with a brief introduction to redox potential as a thermodynamically valid variable. Various factors associated with the formation of vertical redox gradients within sediments are then discussed. This is followed by an outline of problems associated with the interpretation of redox potentials measured in natural systems. The use of redox intensity as an operational variable for characterising sedimentary environments is then considered. Finally, examples are given that illustrate the application of redox concepts to the detection of benthic impact. This Chapter therefore forms a conceptual model from which the mathematical model discussed in Chapter 5 can be developed.

4.2 The Redox Intensity of Natural Systems

An oxidation-reduction, or redox, reaction involves the transfer of electrons between products and reactants. The redox state of a system can be characterised using an extensive property, termed 'poise', or an intensive property (e.g. Grundl, 1995), referred to in this work as 'redox intensity', 'redox potential', or simply as 'Eh'. It is this intensive property that is of interest herein.

The redox intensity of a system is related to the activities of all the redox sensitive species present. In a closed system at equilibrium these activities are constant and the Eh is well

defined. The whole system can then be characterised by a single redox potential. This potential can be calculated from the activities of any redox couple present via the Nernst equation (named for the German physicist who proposed it, Walter H. Nernst 1864-1941). For example, consider a redox reaction between a generalised redox couple (RED/OX) and the H^+/H_2 couple:

$$dRED + 2bH^+(aq) \rightarrow cOX + bH_2(g)$$

where the lower case letters indicate stoichiometric coefficients. The corresponding half reactions can be written:

$$dRED \rightarrow cOX + ne^-$$

$$2bH^+ + ne^- \rightarrow bH_2(g)$$

with $2b=n$. If the activity of the hydrogen ion and gas are unity (that is, the second half reaction is the Standard Hydrogen Electrode) then the Nernst equation can be expressed as:

$$Eh = E^o + \frac{RT}{nF} \ln \frac{\{a_{ox}\}^c}{\{a_{red}\}^d} \qquad \textbf{Equation 4-1}$$

NB: *The activities of RED and OX must be known (see Section 5.9.1). However, the activities of the hydrogen ion (H^+) and hydrogen gas (H_2) are unity and therefore would not effect this calculation.*

where:

Eh is the redox potential.

E^o is the standard electrode potential

R is the gas constant

T is the absolute temperature

F is the Faraday constant

n is the number of electrons taking part in the redox reaction

a_{red}, a_{ox} are the activities of RED/OX (see Section 5.9.1)

In natural systems, however, new materials are constantly being added and the redox chemistry is therefore in a state of flux. True equilibrium is not attained and the simple theory of Nernstian potentials is therefore not adequate for describing the overall redox state of such systems (Grundl, 1995). For practical purposes, however, the application of the Nernst

equation can be extended to media in metastable or partial equilibrium. The Eh is then defined only with respect to those couples that are reactive enough to approach mutual equilibrium (Billen, 1978).

A number of authors have indicated that a state of partial equilibrium is approached in the sub-system of mineral redox couples involved in the metabolisms of micro-organisms (e.g. Thorstenson, 1970; Berner, 1971; Billen, 1978). Billen (1978) asserted that the redox intensity of natural systems is best defined with respect to this subsystem, which consists of the following species:

$$H_2O/O_2,\ Mn^{2+}/MnO_2,\ NH_4^+/NO_3^-,\ FeCO_3/Fe(OH)_3,\ HS^-/SO_4^{2-},\ NH_4^+/N_2,\ CH_4/CO_2$$

A redox potential defined in this way characterises the distribution of oxidants and associated reduced products, but does not take into account the presence of reduced organic matter.

4.3 Redox Gradients in Sedimentary Systems

Gradients of redox intensity develop in physically stable environments when the net-addition or removal of a redox sensitive component is faster than the homogenisation by mixing processes (Tebo *et al.*, 1984). Hence, a gradient in redox intensity develops wherever the rate of supply of oxidants is exceeded by utilisation in both biotic and abiotic redox reactions.

As noted earlier, vertical redox gradients are always present in sediments because of the characteristic patterns of oxygen supply and utilisation. The exact form of this vertical gradient, however, depends upon the complex interaction of a number of physical, chemical, and biological processes. These are dominated by the transport and utilisation of organic substrates and oxidants, but the physical structure of the sediment and the characteristics of the overlying water also have a significant influence. The vertical gradient in redox intensity can therefore be considered as an integrative measure of a number of biotic and abiotic characteristics of the sedimentary environment (Davis *et al.*, 1998). The various factors that influence the form of the redox profile are considered in turn below.

4.3.1 The Role of Microbial Metabolisms

In most marine sediments organic carbon is the only reducing agent that enters the sediment column (Ruddy, 1997). Hence, the oxidation of this reductant is central to the development of vertical redox gradients. The oxidation of sedimentary organic matter is mediated by both the metazoa, such as deposit-feeders, and saprophytic micro-organisms (bacteria and fungi). However, it is decomposition carried out by micro-organisms that dominates the turnover and transformation of chemical compounds (Berner, 1980). Hence, the microbial assemblage has the greatest influence on the redox state of the sediment, and the metabolic activities of the metazoa are thus not considered explicitly herein.

Many micro-organisms degrade, or mineralise, organic matter via respiratory metabolisms; that is, they oxidise organic substrates through the reduction of a mineral oxidant (e.g. Fenchel & Finlay, 1995). Other microbes use only fermentative reactions that do not require an oxidant; part of the organic substrate is instead oxidised at the expense of another part, which is reduced. Fermentation forms a critical link in the microbial ecology of anaerobic environments since it provides the main mechanism by which macromolecules are broken down into low molecular weight components. These components are subsequently mineralised via respiratory metabolisms (Fenchel & Finlay, 1995). However, fermentation does not in itself result in a change in the redox state of the environment. Hence, it is the respiratory metabolisms that are of direct concern here.

The main oxidants used as terminal electron acceptors in respiratory metabolisms are oxygen, nitrate, Mn-oxides, Fe-oxides, sulphate, and carbonate. Compounds of intermediate oxidation level (e.g. N_2O, NO_2^-, $S_2O_3^-$ & S^0) are also used (e.g. Berner, 1980; Fenchel & Finlay, 1995; Stumm & Morgan, 1996) but are not considered in this work. Thermodynamic calculations for the various metabolic processes show that each of the oxidants yields a different amount of energy, as shown in Table 5 (after Berner, 1980).

Metabolic Pathway	ΔG° (kj/mol of CH_2O)
Oxic Respiration	-475
Denitrification	-448
Mn-Oxide Reduction	-349
Fe-Oxide reduction	-114
Sulphate reduction	-77
Methanogenesis	-58

NB: CH_2O represents an idealised carbohydrate unit

Table 5 *The Free Energy Change of Metabolic Processes*

As indicated in the Table, oxic respiration yields the most energy, followed by denitrification, metal-oxide reduction (Mn-oxides first followed by Fe-oxides), sulphate reduction and finally methanogenesis. Methanogenesis (also called carbonate reduction) yields the least energy because it does not result in a complete mineralisation of the organic substrate -- energy rich methane is produced as an end-product.

Micro-organisms utilising all these metabolic processes do not occur together. Instead, different assemblages of microbes succeed one another roughly in the order of the free energy yield of their metabolisms (e.g. Berner, 1980; Froelich *et al.*, 1979; Stumm & Morgan; 1996). This succession is in part due to competitive exclusion; that is, micro-organisms that utilise metabolisms that are more efficient out compete organisms using less efficient ones. Such competition is thought to exist between sulphate reducers and methanogenic micro-organisms. Hence, sulphate reducers out compete methanogens for their mutual substrates' acetate and H_2. Consequently, the presence of sulphate effectively inhibits methanogenesis (Fenchel & Finlay, 1995).

Physiological considerations are also central to the succession. For example, Jørgensen (1983) notes that the presence of nitrate inhibits the capacity of some microbes to reduce Fe-oxide (that is, ferric iron). Hence, ferric iron is only utilised where nitrate is exhausted. Oxygen is toxic to many anaerobic micro-organisms and these obligate anaerobes are therefore excluded

from aerobic zones (Fenchel & Finlay, 1995). Finally, some bacterial strains can utilise a number of electron acceptors, but less energetically favourable pathways are repressed in the presence of a more 'efficient' oxidant (e.g. Myers & Nealson, 1988).

4.3.1.1 Diagenetic Zonation

The succession of metabolisms, coupled with patterns of oxidant supply and utilisation, allows sediments to be divided into diagenetic zones according to the dominant metabolic pathways used. The reactions associated with each zone involve a combination of chemical species, as shown in Table 6 (Modified from Meadows & Campbell, 1993). As the Table indicates, the metabolic activity consumes both reduced organic substrates and oxidants.

Diagenetic Zone	*Species Liberated*	*Species Consumed*[1]
Aerobic zone	CO_2, NH_3, H_3PO_4	O_2 + Organic Matter
Nitrate reduction	CO_2, HCO_3^-, NH_4^+, N_2, HPO_4^{2-}	NO_3 + Organic Matter
Mn reduction	HCO_3^-, NH_4^+, HPO_4^{2-},Mn^{2+}	MnO_2 + Organic Matter
Fe reduction	HCO_3^-, NH_4^+, HPO_4^{2-},Fe^{2+}	$Fe(OH)_3$ + Organic Matter
Sulphate reduction	CO_2, HCO_3^-, NH_4^+, HPO_4^{2-},HS^-	SO_4^{2-} + Organic Matter
Methanogenesis	CO_2, HCO_3^-, CH_4, NH_4^+, HPO_4^{2-}	Organic Matter

Note 1: Dissolved species of carbon consumed are not detailed

Table 6 *Diagenetic Sediment Zones and Chemical Species Liberated/Consumed*

In the simplest of treatments, the diagenetic zonation is assumed to occur only in the vertical, as illustrated schematically in Figure 6a. As the Figure illustrates, oxic respiration occurs in the surface layer. However, oxygen becomes exhausted at some depth, and nitrate reduction then becomes the dominant metabolic process. Likewise, the nitrate concentration tends to zero at some characteristic depth, and metal-oxide reduction then begins. If sufficient organic substrates are available a similar transition occurs from metal-oxide reduction to sulphate reduction, and finally from sulphate reduction to methanogenesis.

As noted previously, the redox intensity characterises the availability of oxidants. (In effect, a higher Eh is found when a given oxidant is present than when it is absent.) Hence, this

progressive oxidant exhaustion is paralleled by a decrease in the sediment redox intensity and a transition to more reducing conditions. Furthermore, the gradient in redox intensity, and therefore the depth of each diagenetic zone, must reflect the distribution of bacteria and other micro-organisms that utilise the oxidants.

A one-dimensional (that is, vertical) diagenetic zonation is, however, highly idealised because the presence of macrofaunal burrows produces an inherently three-dimensional structure (e.g. Aller, 1982; Forster, 1996), as illustrated in Figure 6b. Furthermore, local concentrations of microbial metabolisms can occur within detrital particles that are significantly different to those in the surrounding sediment. For example, Jørgensen (1977a) calculated that a 2 mm diameter detrital particle was large enough to be anoxic at the centre, even when surrounded by aerobic sediment. Canfield (1993) also notes that a strict diagenetic sequence is not absolutely adhered to since there can be a considerable overlap between the various zones.

Conceptualising the diagenetic zonation as unidirectional might therefore seem inappropriate. However, if sediment samples taken from a given depth interval are laterally homogenised, any horizontally heterogeneity is 'averaged out' (Berner, 1980). This leaves only vertical gradients, which gives a closer approximation to the idealised 1-D diagenetic zonation. Furthermore, the simplified zonation lends itself to the 1-D modelling approach taken herein (discussed fully in Chapter 5).

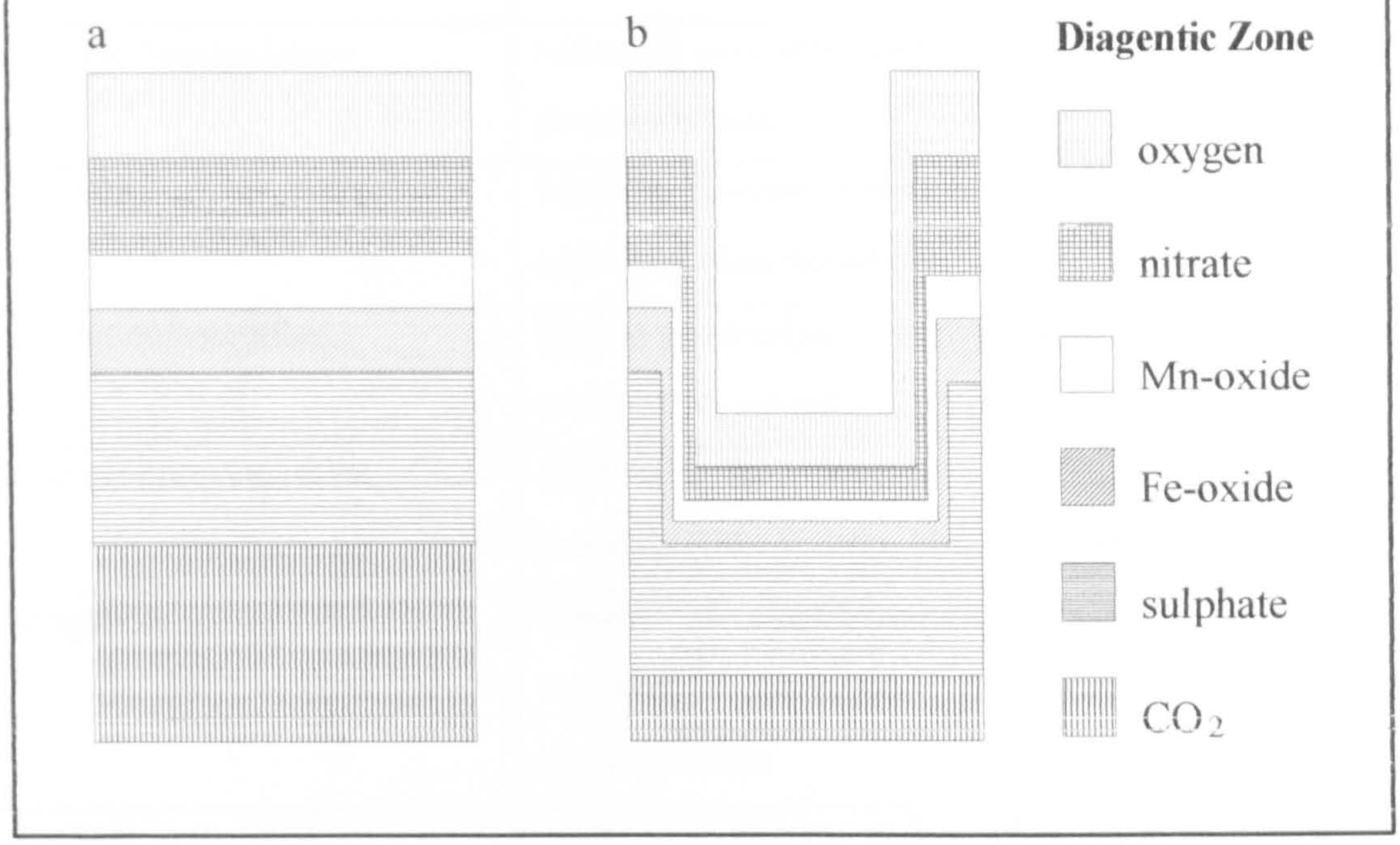

The successional utilisation of oxidants allows the sediment to be divided into vertical zones according to the dominant electron acceptor used within (a). However, macrofaunal burrows and micro-niches (not shown) create a 3d structure, which complicates the zonation (b).

Figure 6 *Vertical Zonation of Sediment by Dominant Electron Acceptor*

4.3.2 The Influence of the Macrofauna

Whilst the metabolic activities of the macrofauna are not considered explicitly herein, various other activities of these animals affect the degradation of sedimentary organic matter, as summarised in Table 7 (after Aller, 1994a).

Perhaps the most significant effects are those that modify the transport regime within the sediment. For example, mobile deposit-feeders move laterally and vertically within the sediment, which mixes both particles and solutes. This mixing increases the flux of various oxidants within the sediment and between the sediment and overlying water (Rhoads, 1974; Aller, 1982). In addition, the mixing of particles influences the distribution of sedimentary POM. In fact, Rice & Rhoads (1989) note that the standing crop and vertical distribution of metabolizable organic matter are fundamentally inter-linked with the biomass, species composition and feeding depths of the deposit-feeding community.

Macrofaunal Activity	*Effect*
Particle Manipulation	Substrate exposure, surface area increase, increase in decomposition
Grazing	Microbe consumption, bacterial growth stimulation, increased mineralisation
Excretion/secretion	Mucus production, nutrient release, bacterial growth stimulation, increased mineralisation
Construction/secretion	Synthesis of refractory or inhibitory structural products (tube linings, body structural products)
Irrigation	Supply of soluble oxidants, metabolite build-up lowered, increased re-oxidation, increased mineralisation
Particle Transport	Transport between major redox zones, increased re-oxidation, redox oscillations

Table 7 *Macrofaunal Activity and Degradation*

Since the redox intensity is related to both the degradation of organic matter and the availability of oxidants, the macrofauna can have a profound affect on the redox profile of the sediment. For example, when organic inputs are low macrofaunal activity constantly homogenises and aerates the surface layer of sediment, which forces the RPDL to move away from the SWI.

In contrast, in areas with a high input of organic material the macrofauna have less effect, since there is a migration of the RPDL towards the sediment surface. Pearson & Rosenberg (1978) speculated that this upward migration was related to the elimination of deep burrowing macrofaunal species. However, opportunistic polychaetes such as *Capitella* and *Malacoceros* spp. can penetrate many centimetres below the SWI of highly enriched sediments. Therefore, the reducing conditions do not preclude the deep burrowing of these species (Pearson, 1982 and references therein).

This was illustrated by Pearson (1987) who describes an investigation into the depth distribution of fauna at the Garrock Head sewage sludge dumping ground (Firth of Clyde, Scotland). The level of enrichment, the total number of macrofauna, the percentage of animals found at depth, and the maximum depth of penetration were all found to increase markedly toward the centre of the dumpsite. For example, at the edge of the dumpsite less than one per cent of the macrofauna were found below 12 cm. At the centre, where the sediment was highly enriched and abundant opportunistic species dominated the macrofaunal assemblage, this proportion was greater than five per cent. The presence of these deep dwelling opportunists, however, did not extend the depth of the aerated zone, which remained confined to a thin surface layer. Consequently, the influence of the macrofauna on vertical redox gradients depends, in part, upon the level of organic enrichment.

4.3.3 The Influence of Sediment Structure

The nature and structure of marine sediments are determined largely by the hydrographic conditions in the overlying water and the amount and type of sedimentary material available. However, once deposited, the grain-size distribution, grain shape, and spatial segregation of particles are modified by the biota (e.g. Rhoads, 1974). Deposit feeding can also result in an unconsolidated and pellatized upper layer that is easily resuspended.

The physical structure of the sediment influences the diffusion of solutes and gasses across the SWI and therefore modifies the form of the redox gradients. For example, an increase in the clay/silt content of the sediment reduces pore-space, which inhibits diffusive fluxes. This has the effect of sharpening the gradients in redox intensity and raising the RPDL towards the sediment surface (Fenchel & Riedl, 1970). Conversely, an increase of mean grain size and sorting increases the permeability of the sediment. This reduces the 'resistance' to transport within the sediment, which causes the RPDL to migrate away from the SWI.

Figure 7 (after Fenchel & Finlay, 1995) shows characteristic redox profiles of two types of sediment. The upper profile is characteristic of sandy sediment with a low flux of organic matter and a high permeability. As shown, the Eh of such sediments remains positive over a relatively large depth. The lower profile is more characteristic of a muddy sediment with a high organic load. Only the very top of the sediment is oxidising, with a negative Eh being observed just below the sediment surface.

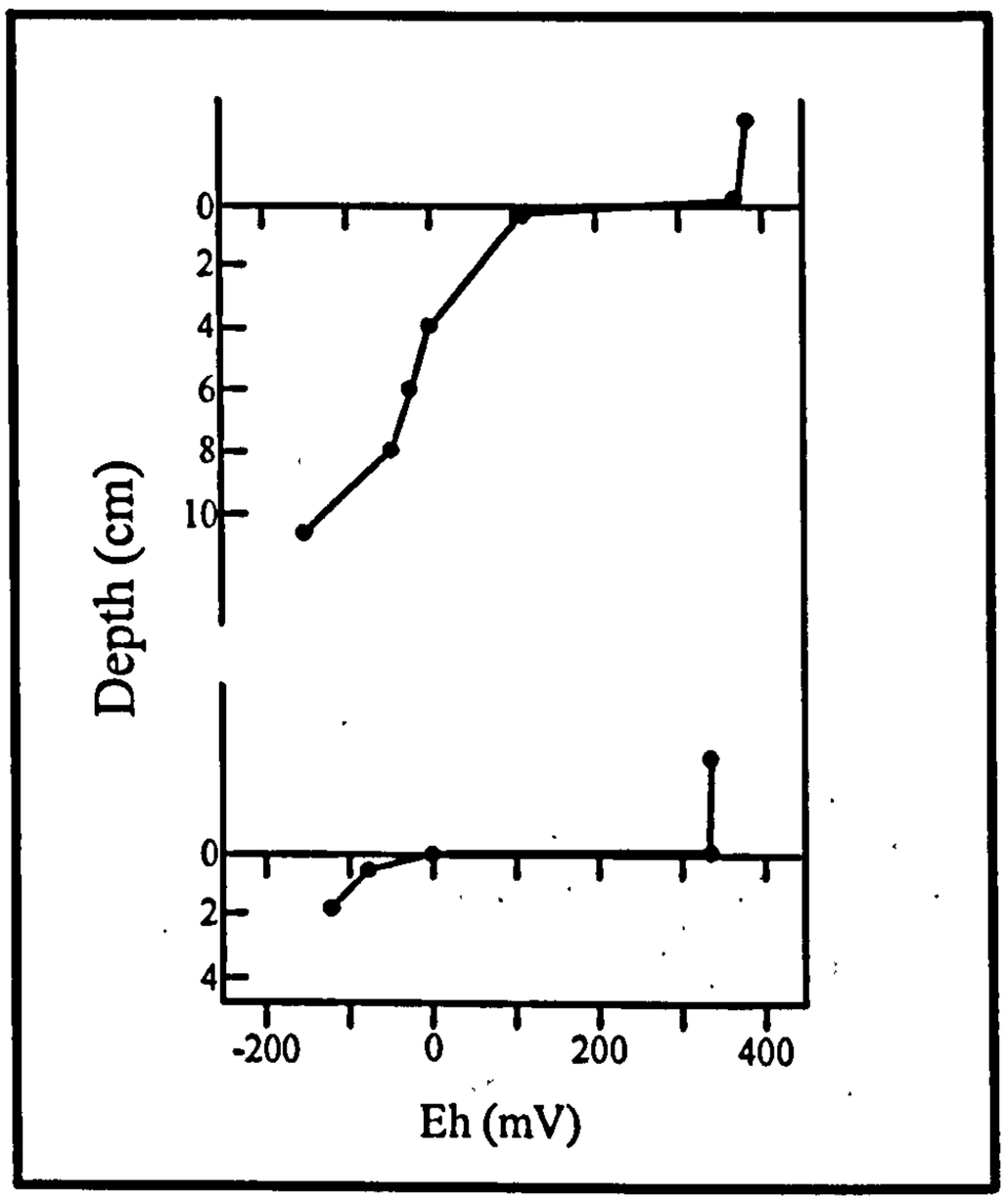

Figure 7 *Characteristic Vertical Redox Profiles of Sediments*

4.3.4 The Influence of the Overlying Water

As noted above, the physical structure of the sediment is influenced by the hydrodynamic characteristics of the overlying waters: muds are deposited in relatively quiescent waters, whereas sands are deposited in areas that are more dynamic. Relatively quiescent waters also allow low density organic detritus to settle out, and once deposited the detritus is less likely to be resuspended and removed by currents. Muds therefore tend to receive a higher load of organic matter. This high loading intensifies the vertical redox gradients of such sediments.

The chemical composition of the overlying water also influences the redox chemistry of the sediments. For example, in areas where dissolved oxygen levels of bottom waters are depressed the RPDL migrates towards the sediment surface. In addition, a diffusive sub-layer can form at the SWI that modifies the transport of dissolved oxygen and other oxidants into the sediment (Jorgensen & Revsbech, 1985). The sediment structure and redox chemistry are consequently both intimately linked with the characteristics of the overlying water.

4.4 Measurement of Eh in Natural Systems

Whilst the focus of this work is the use of redox intensity as a model variable, the model output should ideally be compared to intensities measured in sedimentary systems. Such measurements can be made either indirectly, through the total analysis of all redox couples present in a sample, or directly using an electrode.

The redox state of the sediment can best be determined by the first method; that is, the total analysis of all redox couples (Hostettler, 1984). However, this approach requires considerably more effort than direct measurements taken with an electrode, and no data of this type was available for use in this work. In contrast, a large number of data sets were obtained that included electrode measurements of Eh. Unfortunately, the interpretation of these measurements is difficult, and the use of electrode potentials in model verification/calibration is therefore problematic. To support this assertion a brief review of the problems associated with the measurement and interpretation of electrode potentials is given below.

4.4.1 Electro-active Couples and Measured Potentials

The redox intensity of a system can be measured simply by immersing a suitable electrode (e.g. platinum) in the solution under study. However, a thermodynamically valid interpretation of this potential can only be made if reversible reactions are taking place at the electrode surface. Unfortunately, many important redox couples present in natural systems are irreversible and these species do not influence the potential adopted by the electrode.

Peiffer *et al.* (1992) designate redox couples that exchange electrons at the electrode surface at a significant rate as sensor effective redox couples (SERCs), and those which do not as sensor ineffective redox couples (SIRCs). Hence, the potential adopted by the electrode is determined only by SERCs. Inorganic SERCs are limited to Fe^{3+}/Fe^{2+}; S^0/S^{2-}; Mn^{4+}/Mn^{2+}; O_2/H_2O_2, and organic SERCs are largely limited to quinone/hydroquinone (Peiffer *et al.*, 1992; Grundl, 1995).

If a system is in a state of internal equilibrium all redox couples present are, by definition, at the same redox potential. The fact that only SERCs determine the electrode potential is therefore irrelevant. However, many redox reactions occurring in natural systems do not couple strongly with one another. It is therefore possible to have several redox couples at the same locale at different apparent redox intensities (Stumm, 1965). The potential adopted by an electrode then depends upon the combined effect of all of the SERCs present (Peiffer *et al.*, 1992), with each SERC exchanging electrons independently.

When this situation occurs the apparent equilibrium condition of net zero exchange current (that is, a steady potential) is produced by a balance between the anodic and cathodic exchange currents of the uncoupled redox reactions (Stumm & Morgan, 1996). The resulting electrode potential is termed a 'mixed potential' because it is not directly related to the redox intensity of any particular couple. The relevance of this is simply that the electrode potentials measured in natural systems are normally mixed and, therefore, can not be interpreted quantitatively (e.g. Lindberg & Runnels, 1984).

4.4.2 Electrode Poisoning

An electrode used to measure Eh should ideally be inert and act only as a site for electron exchange without influencing the reactions taken place at the solution/electrode interface. However, Whitfield (1974) found that in both highly oxidising and reducing environments the commonly used platinum electrode is 'attacked'; that is, oxides and sulphides form on the

electrode surface. This modifies the reactions taking place at the electrode surface, which alters the exchange currents. The potential adopted by the electrode is then no longer simply a characteristic of the system under study, and the electrode is said to be 'poisoned'. Whitfield (1974) concluded that a platinum electrode is only inert over a limited range of redox intensities encountered in the environment.

4.4.3 Accuracy and Repeatability of Redox Measurements

Zobell (1946) states that with a suitable analytical technique redox potentials measured in simple, well-poised systems can be reproduced to the nearest mV. However, in natural systems, which are complex and poorly poised, a continuous drift in measured Eh is observed. Reproducibility is at best ±10-20 mV and possibly as poor as ±50 mV.

The accuracy of redox potentials measured in natural systems is therefore not high. However, as the span of potentials measured in marine sediments is around 700 mV, even the lowest level of 'precision'(that is, ±50 mV) represents a relatively small fraction of the total range. Whitfield (1969) suggested that a reproducibility of 25 mV is sufficient for the use of Eh as an operational parameter for characterising the redox state of sediments (see below).

4.4.4 Redox Potential as an Operational Parameter

Long equilibrium times and large discrepancies between electrode potentials and actual solution composition have led to considerable scepticism over the use of electrodes for making Eh measurements in natural systems (Houston-Kempton *et al.* 1990). However, measured electrode potentials can be linked empirically to observed chemical or biological characteristics of a particular system (Whitfield 1969). This is because anaerobic sediments tend to transfer electrons to the electrode, thereby producing a negative electrode potential. Conversely, aerobic or oxidised sediments tend to remove electrons from the electrode, thereby yielding a positive potential.

Hence, whilst it must be accepted that quantitative interpretation of a measured potential is not usually possible, electrodes do give a qualitative indication of the degree of stagnation of the environment. A number of authors have therefore argued that electrode potentials can be useful as an operational parameter for characterising natural sediments (e.g. Zobell, 1946; Whitfield, 1969; Pearson & Stanley, 1979). As Zobell (1946) noted:

> "*While the Eh values obtained for the sediment are more descriptive than physicochemically exact, such values may prove to be a useful means of characterising sediments, since so many chemical and biological processes which affect the diagenesis of sediments are influenced by the redox potential*".

The redox potential of sediment cores therefore enables comparative assessments to be made of the dominant redox conditions (e.g. Pearson & Stanley, 1979). However, even when electrode potentials are used in this operational way a number of difficulties are encountered. For example, the insertion of the electrode disturbs the environment and can lead to releases of gases or introduction of air, which can influence the potential established (Whitfield, 1969). Furthermore, as noted previously, the sedimentary environment is heterogeneous and contains micro-niches in which the redox conditions differ considerably from those prevalent in the surrounding environment. Any diffusion of reduced species from the micro-niche into the surrounding sediment could then give an erroneous indication of redox conditions (Morris & Stumm, 1967).

4.5 Redox Potential as an Indicator of Benthic Impact

Whilst accepting all the practical and conceptual limitations associated with electrode potentials, Eh data can still be produced with sufficient quality to allow sediments to be characterised in terms of varying redox conditions. This technique has found application in the assessment of benthic impact.

Pearson & Stanley (1979) studied the impact of a paper mill effluent on the sediment of a Scottish Loch. Their studies included the analysis of sedimentary chemistry and benthic community structure in the field, and experimental studies of sediments in a laboratory setting.

Both the experimental and fieldwork showed that changes in the sediment redox state were correlated with variations in organic load -- an increase in the input of organic matter produced a corresponding intensification of reducing conditions. The authors also found a correlation between the variation in sediment redox conditions and changes in benthic community structure. For example, the total number of macrofaunal species declined as the sediment became more reducing, but the proportion of annelid species rose.

Recent work by Davis *et al.* (1998) supports this empirical link between Eh and the condition of the benthic community. The authors studied the recovery of the New York Bight 12-Mile sewage sludge disposal site. It was again found that sediment redox potential was correlated with the number of species. The correlation exhibited an exponential form that ranged between five to six species for Eh of -0.15 Volts at a depth of 0.5 cm, to fifty-one species when the Eh at 0.5 cm had risen to 0.30 Volts. The increase in the number of species (and by inference change in Eh) was also found to be correlated with a reduction in the labile organic matter and physical sediment erosion; that is, winnowing of fine particulate material that had accumulated during the dump site operation. This again illustrates the connection between redox conditions and other physical characteristics of the sediment and depositional regime.

Monitoring of the Garrock Head sewage sludge dump site (Firth of Clyde, Scotland) has for many years involved measurements of redox potential (e.g. Pearson, 1987). The site is designated as being of the accumulating type; that is, dumped material is not widely dispersed (UK Department of the Environment, 1979). Very strong gradients of enrichment are therefore observed.

Figure 8 shows a number of redox profiles measured on an East-West transect across the dumping ground (data from Seas Ltd, 1997). Point P7 (see legend, Figure 8) is at the centre of the dumping ground, P4 is a station 3 km to the West, and P10 a station 3 km to the East of the centre. The redox profile at a control site 10 km away is also shown for comparison. It can be

seen that the sediment at the control is oxidised (Eh >0) to the maximum depth shown (10 cm). Sediments at the other stations are more reducing. This change in the vertical profiles of redox potential indicates that there is a horizontal gradient of sedimentary redox conditions across the dumping ground. (It is noteworthy that the most reducing conditions are found at the Eastern edge of the dumpsite, not the centre.)

In themselves, these redox profiles do not categorically demonstrate benthic impact since it is possible that other changes could account for this horizontal gradient in redox conditions. However, Figure 9 shows the change in macrofaunal biomass measured in 1993 and 1996 (data from Seas Ltd, 1994 & 1997) along a hypothetical gradient out from the centre of the dumping ground. (The gradient is hypothetical because not all the stations are actually on the same transect.) The seventeen-year mean is also shown for comparative purposes. It can be seen that the biomass increases towards the centre of the dumpsite indicating an enriched community.

The enrichment is even more apparent if other gross indicators of community structure are considered. Table 8 details the abundance to species number ratio (A/S) and the biomass to abundance ratio (B/A) along the hypothetical gradient. The high abundance ratio (that is, A/S) at the centre of the dumping ground indicates a community dominated by a small number of species. The low size ratio (that is, B/A) at the centre indicates that the total biomass is composed of numerous small animals. By definition, the control station at 10 km represents typical non-impacted sediment of the area. The difference between the control and other stations is therefore a measure of impact. At the centre of the dumping ground the community structure indicators reflect the proliferation of opportunistic species, which shows sediment conditions are characterised by moderately high levels of organic enrichment (see Chapter 3).

The depth averaged Eh values across the hypothetical gradient are shown in Figure 10, again for 1993 and 1996. (Whilst depth averaging of Eh has no specific chemical interpretation, it is a useful means of summarising vertical redox profiles, which allows horizontal gradients in

redox conditions to be seen more clearly.) The depth averaged Eh is low at the centre of the dumping ground, which indicates the prevalence of more reducing conditions. Furthermore, comparison of Figures 9 and 10 indicate that the biomass and depth averaged Eh are negatively correlated with one another (correlation coefficients: -0.86 for 1996 & -0.81 for 1993). The gradient of impact observed in the benthic macrofaunal community is therefore paralleled by a change in sediment Eh. Hence, the horizontal gradient in redox conditions is indicative of benthic impact.

Distance (km)	A/S (96)	B/A (96)	A/S (93)	B/A (93)
0	2492	2	1297	13
1.2	224	4	300	7
1.5	683	4	230	7
1.7	167	5	209	13
2	11	27	10	53
2.6	4	81	5	52
3	6	47	5	130
10 (Control)	2	82	1	86

A/S: Abundance:Species ratio -- abundance ratio
B/A: Biomass:Abundance ratio -- size ratio

Table 8 *Indicators of Community Structure at Garroch Head*

The same qualitative impact has been observed at the site for many years (e.g. Pearson, 1987), although quantitative measures of impact have fluctuated. This can be seen in the plot of biomass shown in Figure 9. In both years shown the peak in biomass occurs at the centre of the site. However, in 1993 the biomass at this station was ninety-six per cent higher than in 1996 and sixty-three per cent higher than the long-term mean. This further emphasises the temporal dimension of environmental impact. Finally, it is noteworthy that the variation in biomass at the centre of the dumping ground is much greater than that observed at the control station. As noted previously, this is to be expected since communities in enriched sediments tend to be less stable than communities in non-impacted sediments.

Similar qualitative correlations between horizontal gradients in sediment redox state and other measures of impact have been observed in many data sets relating to effluent discharges. For example, a horizontal gradient in Eh was detected in sediments in Largo Bay, on the Fife coast (Scotland) that was attributed to a discharge of sewage (FRPB, 1987). Stations within 500 m of the discharge were impacted, and sediments near to the outfall were anaerobic at the surface. The horizontal gradient in redox conditions was again shown to parallel changes in community structure. This case is of particular note since it was shown that the change in redox conditions along the gradient was not attributable to other factors. For example, a range of sediment types were observed in the area, but the most reducing conditions occurred in sediments that were characterised as coarse grained (compare with Section 4.3.3).

A similar, if more extreme impact, was detected in Inverkeithing Bay, in the Firth of Forth. Effluent discharged from a paper mill introduced extremely high levels of cellulose into a bay with restricted water exchange. Consequently, the benthos was found to be highly impoverished, and the sediment noted to be black, strongly smelling, with an emergent RPDL (FRPB, 1984).

The benthic impact of a steelworks discharge in the Usk estuary was mentioned in Chapter 3. It was noted that for this discharge toxic and/or physical impacts prevented the macrofauna from capitalising on the organic enrichment. Nevertheless, the authors (Davies & Wade, 1985) still detected an area of low redox potential extending 200m from the outfall. This implies that the redox potential gave a qualitative measure of the impact although organic enrichment was not the over-riding concern.

Figures 11 and 12 illustrate the benthic impact of a fish farm in Loch Spelve (data from SEPA, 1996). The Figures show the depth averaged redox potential and the abundance to species number ratio (A/S ratio) along a transect out from the fish farm, which is positioned at 0 km. It can be seen that the sediment redox conditions are more reducing close to the fish farm. High

A/S values were also observed close to the farm indicating enriched conditions. However, at a station immediately adjacent to the farm the benthic community was extremely impoverished with only four individuals present in the sample taken there, indicating severely degraded conditions. When these two Figures are considered together they again show that a horizontal gradient of redox conditions is indicative of the overall benthic impact.

Similar impacts have been detected at many fish farm sites. For example, at a fish farm in Loch Sween redox conditions in the top portion of the sediment were reducing within 25 m of the cages (CRPB, 1991a). Conditions rapidly deteriorated closer to the cages and beneath the cage were characterised as azoic. Sediment conditions were, however, oxidising at distances greater than 25 m, indicating the localised extent of the impact. Similar results were found in Loch Fyne (CRPB, 1991b), the Sound of Mull (CRPB, 1990) and many other sites (e.g. Brown *et al.*, 1987; Gowen & Bradbury, 1987; Hargrave *et al.*, 1993; Weston, 1990; Findlay & Watling, 1997a and references therein).

Not all inputs of organic matter produce a disturbance that is observable in the macrofaunal community. Redox conditions at such sites can, however, still be used to give a qualitative comparison of sedimentary conditions, but must then be interpreted with more care. For example, Figure 13 shows the Eh profiles at a marine outfall discharging primary treated sewage in the Firth of Forth (data from FRPB, 1994a). All profiles were taken along a transect out from the outfall diffuser section. Station 3 (st. 3, in legend of Figure 13) was within 50 m of the diffuser line, Station 6 (st. 6) and Station 10 (st. 10) were at distances of approximately 750m and 2 km respectively.

It can be seen that all stations exhibit an oxidised surface layer. However, the most reducing sediment conditions were observed at the station closest to the discharge point (Station 3). Other measures of impact were also highest at this station including the number of tomato pips, which is a good indicator of sewage deposition. The report (FRPB, 1994a) notes that

associated settlement of larger solids could explain the lower redox potentials recorded at the station. However, little impact was observed in the benthic community of the site, although the report did indicate that at distances less than 50 m some disturbance to the community could occur. (The sampling program was not designed to detect this.)

It is noteworthy that at station 23, which is the furthest distance from the diffuser at over 4 km, redox conditions are only slightly less reducing than at station 3. However, given the lack of impact at the stations in between, this is unlikely to be due to enrichment associated with the outfall. This further emphasises that Eh is determined by a combination of factors and that the horizontal gradients of redox state must be interpreted with care when the impact is not overriding.

FRPB (1994a) also provide a summary of redox conditions measured at 4 cm for the period 1981-1993. The plots of Eh values for station 3, 6 and 10 are shown in Figure 14. It can be seen that the sediment redox conditions exhibit a significant variation over this period, and the Eh at station 3 was not always the lowest. This again emphasises that where there is no overriding gradient of enrichment redox measurements must be interpreted with caution.

The examples given above show that a horizontal gradient in the redox state of the upper portion of the sediment can be indicative of benthic impact. This therefore supports the assertion that redox concepts represent a possible approach to the modelling of this impact. The theoretical foundations for such a redox model, its analysis and application are considered in Chapters 5 to 7. However, it should be stressed that the qualitative nature of redox potentials prevents their use in model calibration and verification.

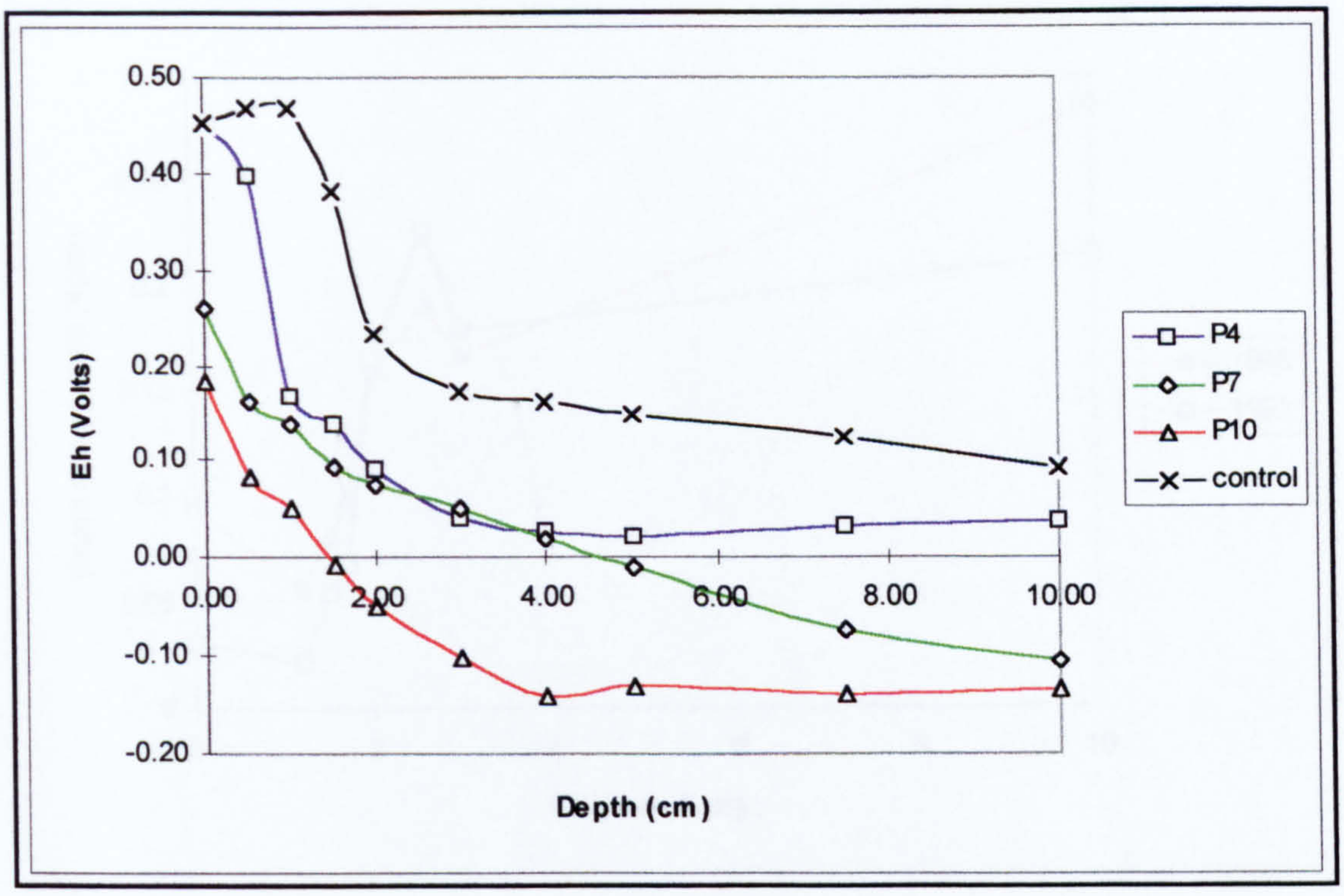

NB: P7 is at the centre of the dumping grounds; P4 is 3 km to the West; P10 is 3 km to the East; the control is 10 km away from the centre.

Figure 8 *Redox Profiles at Garroch Head (1996)*

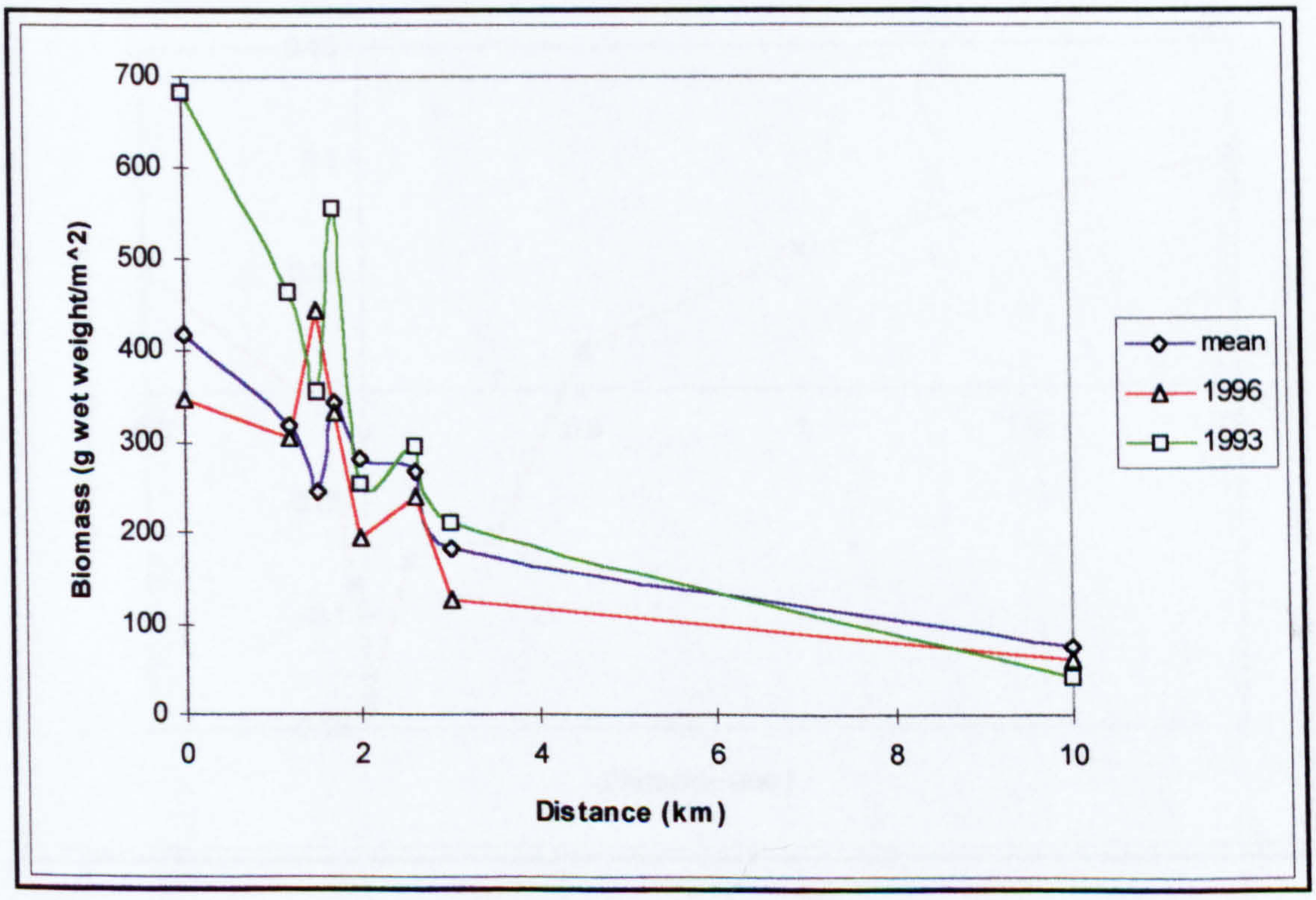

Figure 9 *Biomass at Garroch Head*

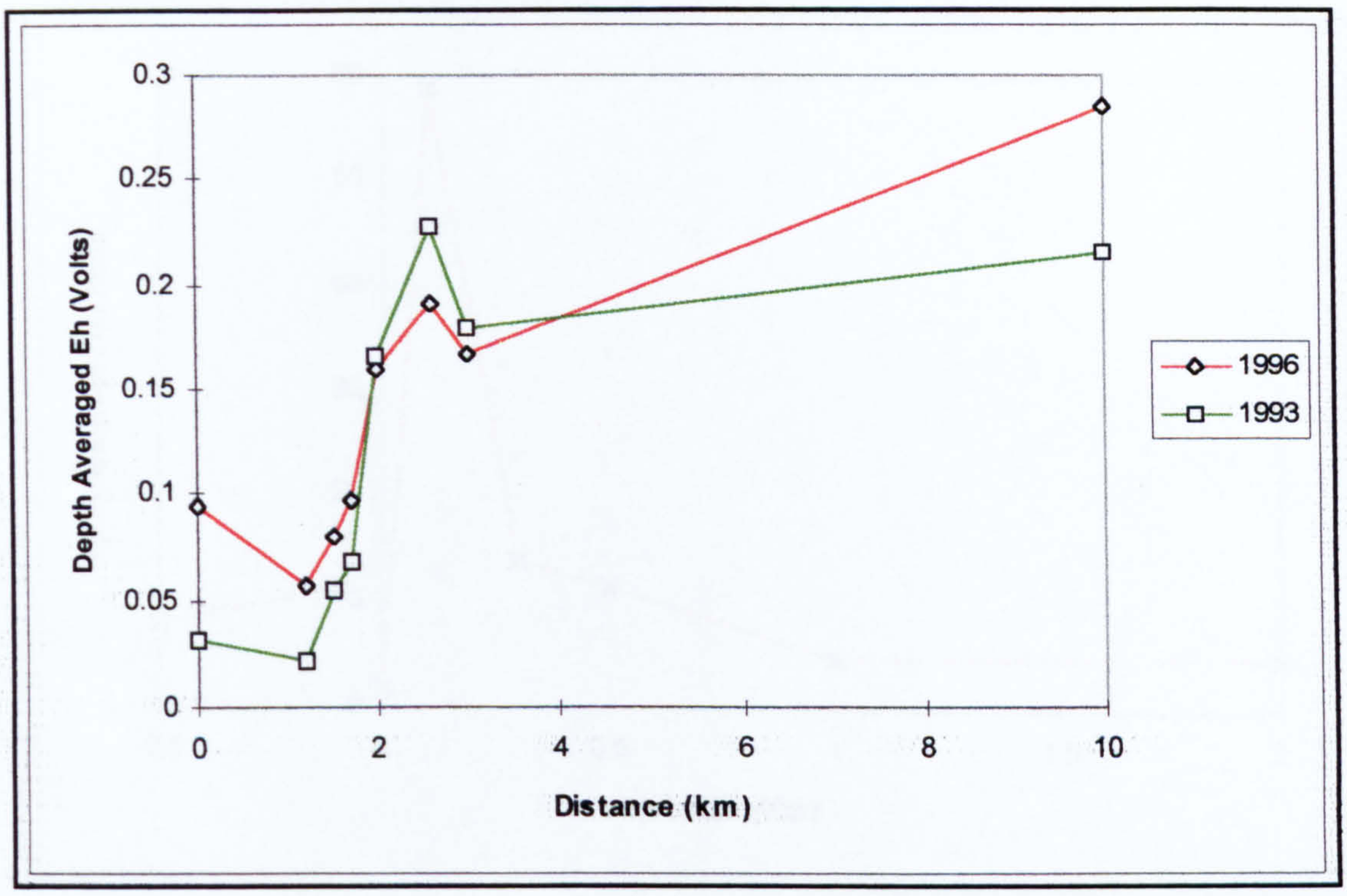

Figure 10 *Depth Averaged Eh at Garroch Head (1993 & 1996)*

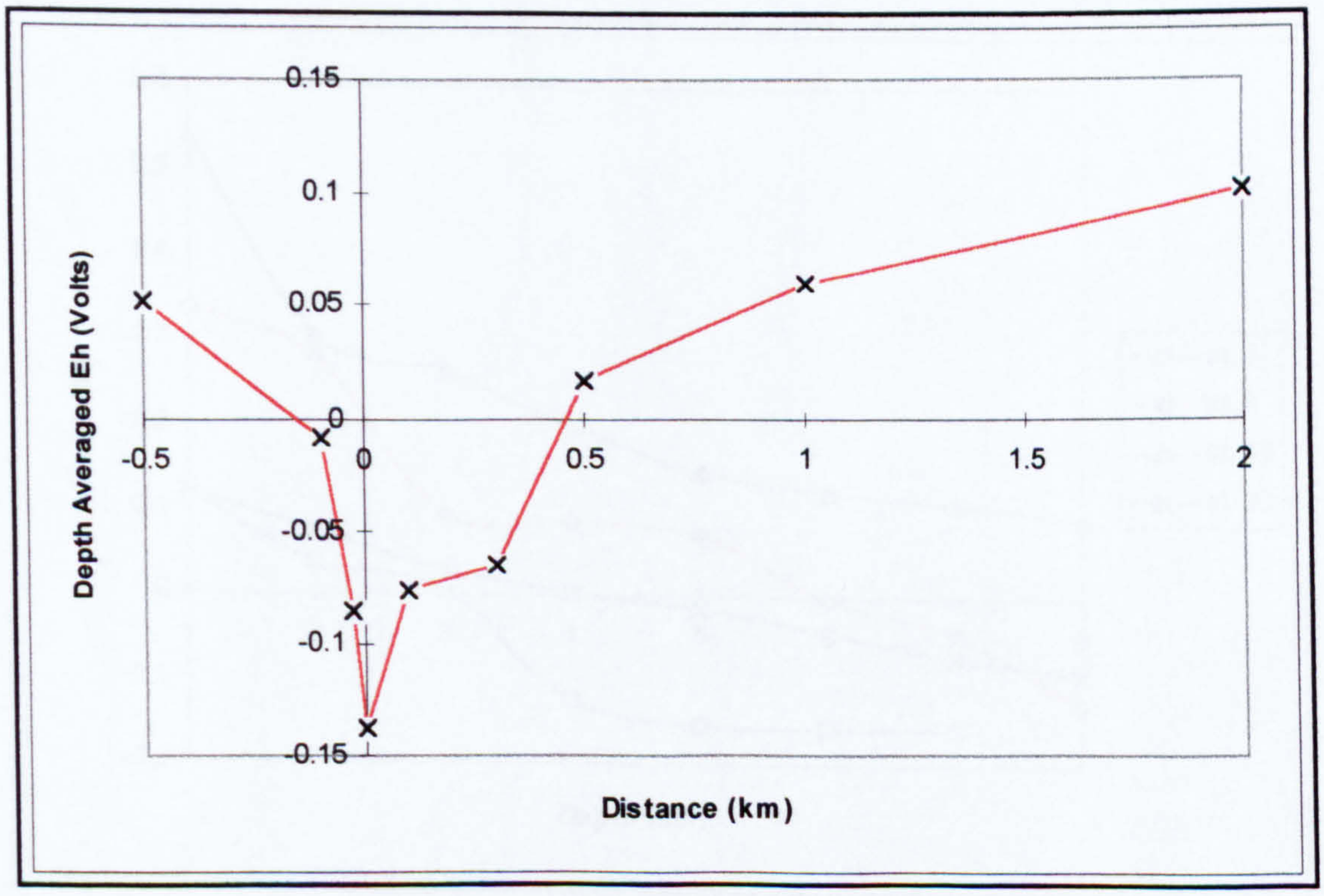

Figure 11 *Depth Averaged Eh at A Fish Farm Site*

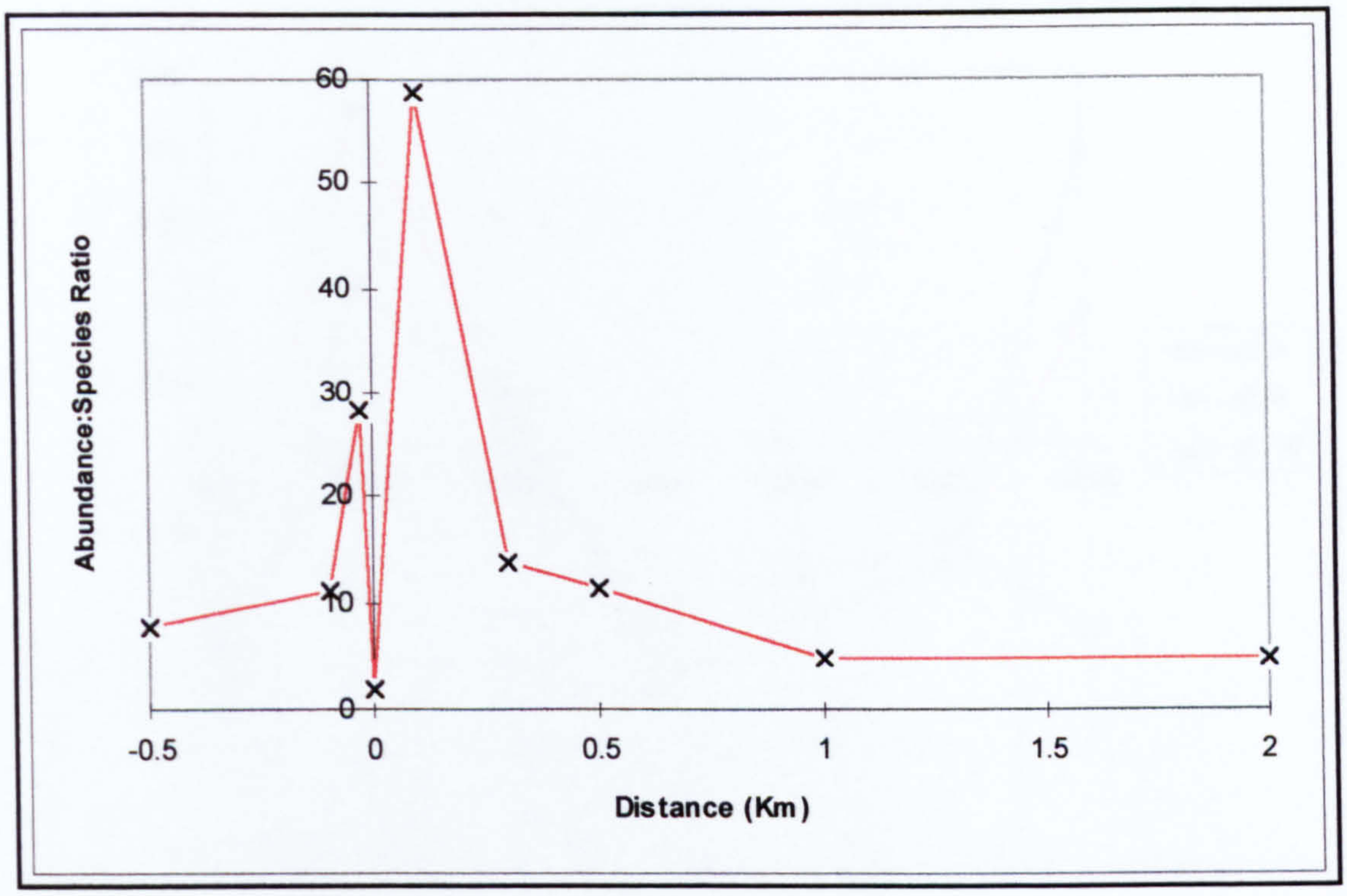

Figure 12 *The A/S Ratio at a Fish Farm Site*

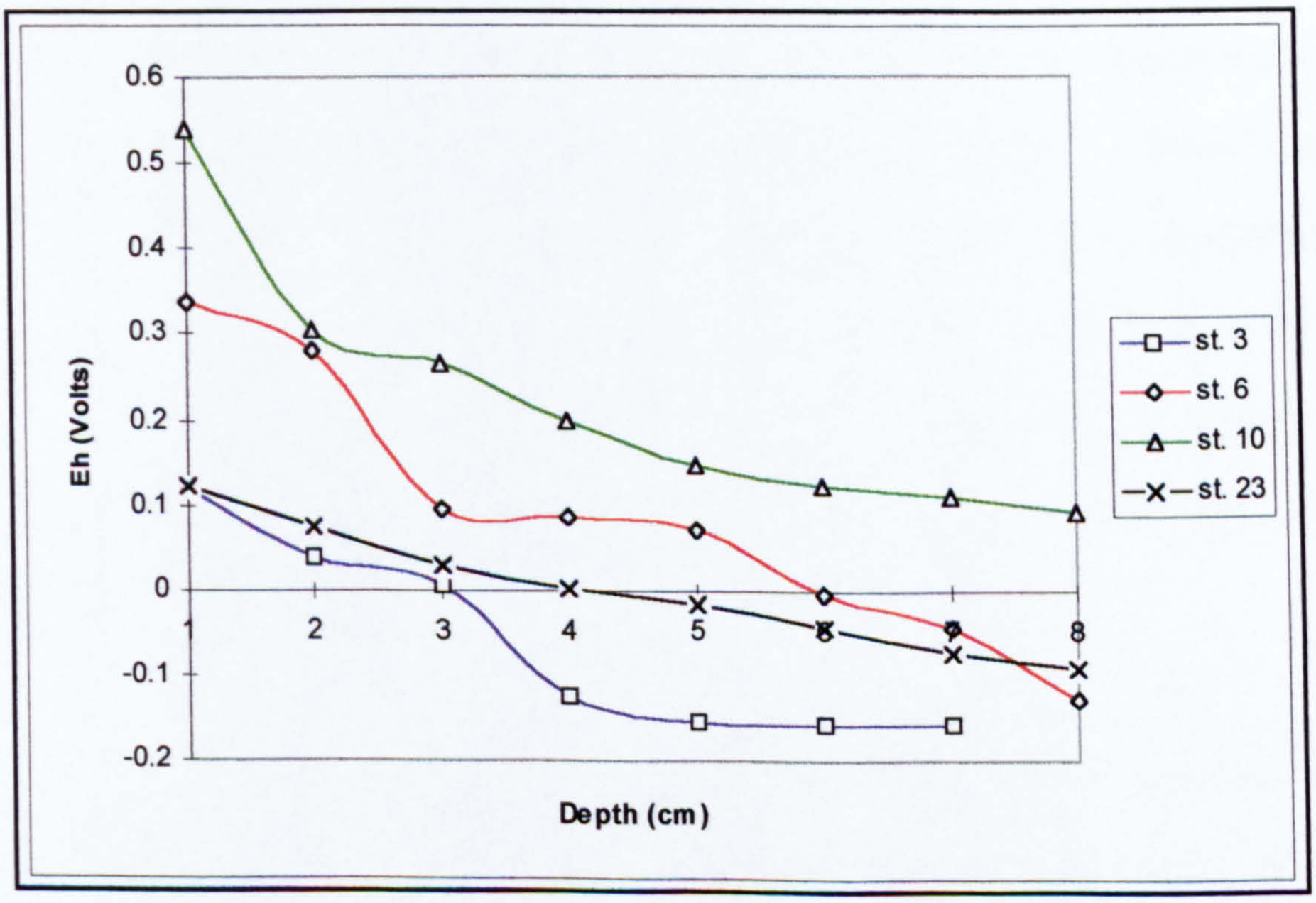

NB: st. 3 (that is, station 3) is positioned at approximately 50m from the diffuser; st. 6 at 750 m; st. 10 at 2 km; and st. 23 at 4 km.

Figure 13 *Redox Profiles at Seafield (1994)*

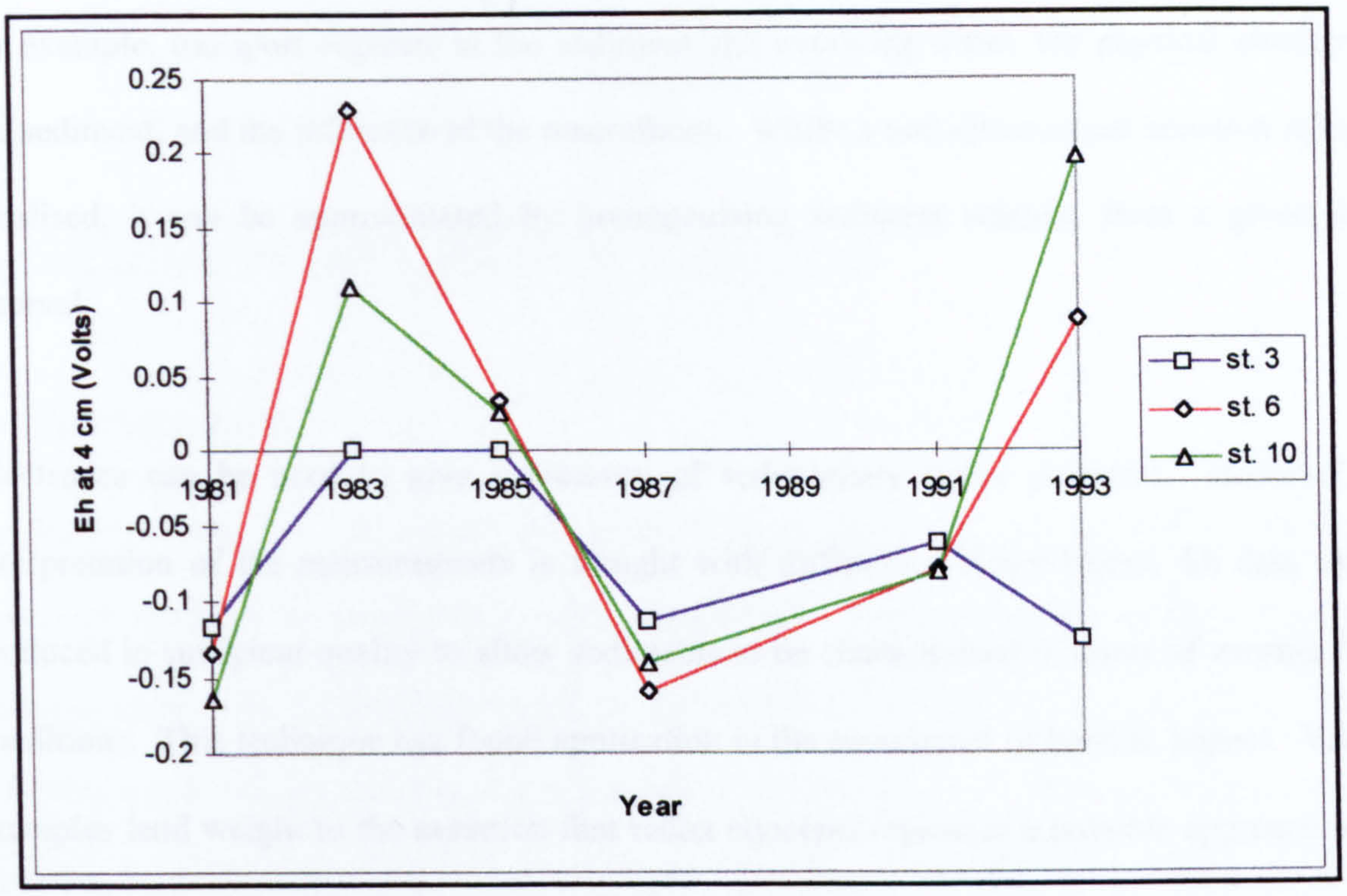

Figure 14 *Temporal Variation of Redox Profiles at Seafield*

4.6 Summary

Redox intensity, or Eh, is a variable that characterises the redox state of an aqueous system. In closed systems at equilibrium the redox potential is well defined. However, in natural systems new materials are being constantly added, which maintains an overall state of disequilibrium. The redox potential of such systems is best defined with respect to those couples that are reactive enough to approach mutual equilibrium; for example, the sub-system of mineral redox couples involved in metabolisms. The redox potential of stable and metastable systems can be calculated using the Nernst equation.

Vertical redox gradients develop in all sediments because the supply of oxidants is inhibited by the mineral matrix. The gradients result from decompositional processes that involve the break down of sedimentary organic matter and the consumption of oxidants. Various ecological interactions between microbial assemblages lead to a characteristic pattern of oxidant exhaustion, which can be represented as a 1-D diagenetic zonation. The extent of each diagenetic zone, and thus the form of the vertical redox gradient, is modified by various factors,

for example, transport regimes in the sediment and overlying water, the physical structure of the sediment, and the influence of the macrofauna. Whilst a one-dimensional zonation is highly idealised, it can be approximated by homogenising sediment samples from a given depth interval.

Electrodes can be used to give a measure of sedimentary redox potential. However, the interpretation of the measurements is fraught with difficulty. Nevertheless, Eh data can be produced in sufficient quality to allow sediments to be characterised in terms of varying redox conditions. This technique has found application in the assessment of benthic impact. Various examples lend weight to the assertion that redox concepts represent a possible approach to the modelling of benthic impact.

Chapter 5

5. SEDIMENTARY REDOX MODELS

5.1 Introduction

In Chapters 3 and 4, it was shown that a discharge of organically rich effluent can produce a horizontal gradient in sedimentary redox conditions. It was therefore asserted that redox concepts provide a potential approach to the modelling of benthic impact. This Chapter describes a sedimentary redox model developed to test this premise. The model allows vertical gradients in sedimentary redox chemistry to be calculated. The predictive assessment of a horizontal gradient in redox conditions would therefore require the model to be applied at discrete locations around the effluent discharge.

The redox model is relatively complex and includes many of the processes that influence the redox state of the sediment. Consequently, the model involves a large number of parameters. Hence, from an early stage in the model development it was anticipated that the practical application of the model would be problematic. Whilst accepting this limitation, it was considered that the redox model would still allow a theoretical investigation of the proposed modelling approach. Furthermore, a theoretical analysis can identify the most critical parameters and thereby guide any subsequent model simplification deemed appropriate.

This Chapter starts with a review of three sedimentary redox models already presented in the literature. The mathematical principles underlying the current redox model are then examined, and this is followed by a description of the model itself. The methods used to solve the model equations are then outlined. Since this work is not specifically aimed at marine geochemists or diagenetic modellers, the treatment given below is relatively thorough. Furthermore, some descriptions of relevant sedimentary processes have been included to help clarify the

interpretation of the model. A summary of the model and model assumptions can be found at the end of the Chapter.

5.2 Published Sedimentary Redox Models

Three models of sediment redox intensity have been published in the literature. The first two models (Billen & Verbeustel, 1979; Billen, 1982) were developed to describe the vertical distribution of microbial metabolisms within the sediment. The third model (Park & Jaffe, 1996) was developed to allow an assessment of post-depositional metal mobility. All three models are based on the diagenetic equation popularised by Berner (e.g. Berner, 1980) and are therefore essentially models of early diagenesis.

Diagenesis is the study of processes that bring about biogeochemical changes in sediments after particle deposition. Early diagenetic models therefore describe mathematically the distribution of materials in the top layer of the sediment and hence the formation of biogeochemical gradients. These gradients reflect changes in the redox state of the sediment and can therefore be used to derive a measure of the redox intensity of the system. This concept forms the basis of the published redox models outlined below and the approach that has been taken in this work.

5.2.1 The Redox Model of Billen & Verbeustel (1979)

The main assumption underlying the redox model detailed in Billen & Verbeustel (1979) is that an internal equilibrium is reached by the subsystem of mineral redox couples involved in the metabolism of micro-organisms. As indicated in Section 4.2, in reality such an equilibrium is approached but is not actually reached. Other assumptions include:

1. A one-dimensional modelling approach is taken; horizontal heterogeneity in the sediment is ignored.
2. Organotrophic activity (that is, decomposition by microbes) is assumed to decrease exponentially with depth.

3. Transport mechanisms within the sediment are assumed Fickian (that is, related to local concentration gradients, see Section 5.6.1.2 below). A single apparent dispersion coefficient is used for all species; that is, solutes and particulates are subject to the same degree of mixing.
4. Advection due to deposition at the sediment water interface (SWI) is ignored.
5. The sedimentary system is assumed to be at steady state.

Given these assumptions, an ordinary differential equation (ODE) can be written that, with appropriate boundary conditions, allows the depth distribution of a function F(z) to be calculated. F(z) is defined as the weighted-sum of all the oxidants used in metabolic activity. From the depth distribution of F(z), and given the assumption of internal equilibrium, an implicit relationship between the Eh and depth can be derived. The model is solved for the concentration profile of the redox couples and the Eh profile of the sediment. Billen & Verbeustel (1979) note that:

> *"(The) model is not intended to simulate accurately the whole complexity of the intricate bacterial metabolisms occurring in the sediments, but only to show that very simple assumptions can indeed explain the general trends of the distribution of redox processes in the sedimentary column"*

5.2.2 The Redox Model of Billen (1982)

The model described by Billen (1982) is essentially an improved version of that presented in Billen & Verbeustel (1979). The main difference is that nitrate is not assumed to be at equilibrium with the other oxidants. Its distribution is instead calculated from a separate diagenetic model. In addition, separate diffusion coefficients are used for the solid and interstitial (porewater) phases. Finally, the model includes the precipitation and dissolution of three authigenic solids that exert a control over the interstitial concentrations of redox sensitive species. The model is again solved for the concentration profiles of the redox couples and the Eh profile of the sediment.

5.2.3 The Redox Model of Park & Jaffe (1996)

Both of the models described above were solved analytically by the respective authors. However, such analytical models do not capture the complex dynamics of sedimentary systems (Wang & Van Cappellen, 1995). Over recent years a number of multi-component early diagenetic models have been published (e.g. Boudreau, 1996; Dhaker & Burdige, 1996; Van Cappellen & Wang, 1996; Soetaert *et al.*, 1996a). This type of model gives a more complete mathematical description of the sedimentary system but requires the implementation of numerical methods.

The redox model of Park & Jaffe (1996) is based on an early diagenetic model of this type and can be summarised thus:

1. A 1-D modelling approach is taken.
2. The vertical distributions of eleven species are modelled; these are the organic matter, oxidants, and reduced species involved in heterotrophic activity.
3. A sequential use of oxidants in the order of decreasing free energy yield is assumed. The inhibition of less 'efficient' metabolisms is implemented using logical switches (switches that are set to one or zero depending upon the predicted conditions).
4. A separate rate constant is applied to each of the metabolic processes. An approach similar to that taken by Tromp *et al.* (1995) but different to that taken in many other diagenetic models.
5. Irrigation is modelled as a Fickian process.
6. Precipitation and dissolution are included as first order reactions.
7. The model is written for steady state conditions.

The model consists of a system of coupled ODEs (eleven in all: one for each species modelled) that are discretised using central differences. The algebraic system of equations that results is solved using an iterative numerical method described by Rabouille & Gaillard (1991a; see also

1991b). The redox intensities are calculated from the depth distribution of chemical species output by the diagenetic part of the model.

As noted above, the modelling approach taken by Park & Jaffe (op. cit.) is similar to that of other multi-component early diagenetic models. However, a number of criticisms can be made of their overall implementation:

1. The ODEs are discretised using a central difference formulation; as discussed in Section 5.12.1.1, the use of a blended scheme is more appropriate, at least for the solid phases.
2. The model does not include the evolution of CO_2.
3. The steady state formulation means that the effect of seasonal fluctuations in sedimentary conditions can not be examined.
4. Authigenic solid phases are not included explicitly within the model, although the effect of the precipitation and dissolution of these phases on solute concentrations are included as first order reactions. Explicit inclusion of authigenic species allows an improved formulation for these reactions to be used.
5. Irrigation is an inherently non-local process and the use of a diffusion analogue to account for its effect is therefore somewhat questionable.
6. The metabolic succession is implemented via switches. This results in a unidirectional diagenetic zonation with no overlap. As discussed below, this representation is not suitable for modelling coastal environments.

In addition, the authors presented only a limited analysis of their model and did not consider its practical application. An alternative redox model has been developed as part of this research that addresses these issues and is therefore considered an improvement on the model described in Park & Jaffe (1996). It should be noted, however, that the model is still essentially a multi-component diagenetic model and has therefore been developed with extensive reference to the early diagenetic modelling literature.

5.3 The Mathematical Basis of Diagenetic Models

As noted previously, the distribution of materials within the sediment can be described mathematically by the diagenetic equation (e.g. Berner, 1980). The general diagenetic equation is based on the differential form of the mass conservation law and can be written:

$$\frac{\partial \hat{C}}{\partial t} = -\nabla \sum \hat{F} + \sum \hat{S} + \sum \hat{R} \qquad \textbf{Equation 5-1}$$

where the 'hat' indicates that each term is written per unit volume of total sediment (porewater + solid phase) and:

t	indicates time.
$\hat{C}$	is the analytical concentration of the component species.
$\nabla \sum \hat{F}$	is the divergence of all the local transport fluxes.
$\sum \hat{S}$	represents all source and sink terms.
$\sum \hat{R}$	represents the rate of all reaction terms.

As indicated above, the diagenetic equation is expressed in terms of the analytical concentration. For example, the analytical concentration of sulphate represents the concentration of all sulphate containing species; that is, (after Berner, 1980):

$$C_{SO_4^{2-}} = C_{free\,SO_4^{2-}} + C_{NaSO_4^{2-}} + C_{KSO_4^{2-}} + C_{MgSO_4^{2-}} + C_{CaSO_4^{2-}} + \sum C_{organic\,SO_4^{2-}}$$

In an ideal model the terms on the right hand side of Equation 5-1 would therefore represent all processes that influence the distribution of the component species in question.

The differential form of the diagenetic equation results from the assumption that the sediment-porewater system can be described as a continuum; that is, a system within which the physical properties vary continuously. This assumption, the so called 'continuum hypothesis', is used in many scientific fields. For example, the properties of fluids are described using variables such as velocity and density. These variables are assumed continuous but are actually macroscopic manifestations of microscopic properties. The continuous variables 'express' the average effect of many molecules and the 'continuity' is therefore idealised. However, fluids do appear

continuous for most practical purposes. In contrast, sediments are discontinuous even at the relatively large scale of individual grains. Hence, Litchtner (1996, p.2) notes that:

> "*The continuum hypothesis (applied to porous media) requires a major leap of faith that can not be justified a posteriori*"

However, the continuum hypothesis has for many years been applied successfully to the mathematical modelling of sedimentary systems and other porous media.

The continuum description of sediments requires that the microscopic properties be averaged in some way. This averaging process must smooth out microscopic variations without eliminating the gradients in macroscopic properties that are the focus of the modelling work. The dimensions of the averaging volume must consequently be large compared to the grain size but small compared to the characteristic length scale over which macroscopic quantities change (Litchtner, 1996). In addition, if a 1-D modelling approach is adopted (see below) the horizontal length scale of the averaging volume should also integrate any lateral heterogeneity (Van Cappellen & Gaillard, 1996). This horizontal length scale is, therefore, the mathematical equivalent of homogenising sediment samples from a given depth interval.

5.3.1 The 1-D Approximation

Sedimentary environments exhibit predominantly vertical gradients in the biological and chemical properties of the system. In addition, most data sets for sediments are in the form of depth profiles (Van Cappellen & Wang, 1995). It is therefore natural to use a 1-D model to describe early diagenesis. The 1-D diagenetic equation is derived in Boudreau (1997, p. 30-32) and in its general form can be written:

$$\frac{\partial \hat{C}}{\partial t} = -\frac{\partial \sum \hat{F}}{\partial x} + \sum \hat{S} + \sum \hat{R} \qquad \textbf{Equation 5-2}$$

where x indicates the vertical dimension.

5.4 Concentration and Porosity

The concentration ($\hat{C}$) in the diagenetic equation (Equation 5-2) is defined in terms of the bulk sediment; that is, mass per volume of total sediment (solids + porewater). However, concentrations can also be expressed in terms of either the volume of solids or porewater. The relationship between these two expressions of concentration is given by:

$$\hat{C} = \xi C \qquad \textbf{Equation 5-3}$$

where C is the concentration in terms of unit volume of solid or porewater, as appropriate. Xi (ξ) is related to the sediment porosity (φ), which is defined as:

$$\varphi = \frac{\text{Volume of Porewater}}{\text{Volume of Total Sediment}} \qquad \textbf{Equation 5-4}$$

Xi is then:

for solid species: $\xi = 1 - \varphi$

for porewater species: $\xi = \varphi$ **Equation 5-5**

The porosity depends upon the physical structure of the sediment. In coarse grained well sorted sandy sediments particles pack together according to their geometry and produce a porosity in the range of 0.36 to 0.46 (Berner, 1980). For the purposes of early diagenetic models, the porosity of these sediments can be considered constant with depth; no compaction occurs.

In contrast, fine-grained sediments are influenced by surface electrostatic effects that initially cause them to pack together in an open 'house of cards' structure of high initial water content (porosity 0.7 to 0.9). As more material accumulates, however, the weight of the overlying sediment overcomes the electrostatic effects and grains are forced together, thereby reducing the porosity (Berner, 1980). Fine-grained sediments therefore undergo compaction and are characterised by gradients in porosity. Van Cappellen & Gaillard (1996) note that a porosity decrease of ten per cent is commonly observed over the top few centimetres of such sediments.

At greater depths, the porosity decrease is much slower; that is, the depth profile of porosity is asymptotic.

5.5 Component Species

Marine sediments are highly complex environments that contain a wide range of chemical substances. However, a mathematical model can only give an idealised representation of reality. The redox model must therefore represent the sedimentary system in a simplified manner, whilst retaining sufficient chemical complexity to capture the major redox transformations of interest herein. This is achieved by simultaneously modelling the distribution of a number of component species.

The inclusion of every component species found within marine sediments would, however, be impracticable. Fortunately, components that do not react or accumulate on the time-scale of interest need not be considered (Van Cappellen & Gaillard, 1996). Both highly reactive and unreactive component species are therefore not modelled. Furthermore, given the aims of this study, those components that do not influence the major redox transformations can also be ignored. These include phosphates and some chemical species that control the sediment pH.

Sedimentary environments exhibit vertical gradients of pH that are related to heterotrophic activity. However, the pH of marine sediments is less variable than Eh and rarely exceeds the limits pH 7.0 to 8.2 (e.g. Ben-Yaakov, 1973). Consequently, pH provides less scope for characterising sedimentary environments (Berner, 1981). Therefore, the redox model does not explicitly consider acid-base chemistry and a constant value of pH is specified throughout the model domain.

The component species included within the redox model are listed in Table 9. The organic carbon is an idealised representation of the bioavailable particulate organic matter. Oxygen, nitrate, the metal-oxides (MnO_2 & $Fe(OH)_3$), and sulphate are the main oxidants used by

heterotrophic micro-organisms, as discussed previously in Chapter 4. The iron and manganese oxides represent the idealised bioavailable fraction of the total metal-oxide concentrations. Ammonia, total dissolved sulphides (TS), total dissolved carbonates (TC), Mn^{2+}, Fe^{2+} and methane are reduced products of degradation. The component TS actually consists of two species: HS^- and H_2S. Likewise, the component TC represents the sum of the three main mineral forms of dissolved carbon found in the porewater; that is, $\sum CO_2$. Both TS and TC can be divided into their constituent species using an assumption of local equilibrium (see Section 5.6.3). The three authigenic solids FeS, $MnCO_3$ and $FeCO_3$ are included because they modify the distribution of other redox sensitive species (Mn^{2+}, Fe^{2+}, HS^-) through precipitation and dissolution reactions (e.g. Balzer, 1982).

Solid Component Species	*Chemical Symbol*
Organic Carbon (G)	CH_2O
Manganese Oxide	MnO_2
Iron Oxide	$Fe(OH)_3$
Manganese Carbonate (e.g. Rhodochrosite)	$MnCO_3$
Ferrous Carbonate (e.g. Siderite)	$FeCO_3$
Iron Mono-sulphide (a generic AVS)	FeS

Porewater Component Species	*Chemical Symbol*
Oxygen	O_2
Nitrate	NO_3^-
Reduced Manganese	Mn^{2+}
Reduced Iron	Fe^{2+}
Sulphate	SO_4^{2-}
Ammonia Nitrogen	NH_4^+
Methane	CH_4
Total Dissolved Carbonate (TC)	$CO_2+CO_3^{2-}+HCO_3^-$
Total Dissolved Sulphides (TS)	H_2S+HS^-

Table 9 *Model Component Species*

These three authigenic solids are the same as those considered in the models of Billen (1982) and Van Cappellen & Wang (1996). Pure rhodochrosite ($MnCO_3$) is assumed to be the dominant solid phase controlling the porewater Mn^{2+} concentrations, although mixed Mn, Ca and Mg carbonates may also be important (e.g. Burdige, 1993). Sulphides (TS) produced during sulphate reduction react rapidly with iron rich particles to form the acid volatile sulphides (AVSs) mackinawite and greigite (e.g. Berner, 1971; Berner, 1984). These labile sulphides are transient intermediaries that commonly convert to pyrite (FeS_2). However, the labile sulphides control the dissolved iron concentration in sulphide-rich sediments. Hence, the model considers only a generic iron mono-sulphide (FeS), rather than the thermodynamically stable pyrite (Boudreau & Canfield, 1988). The porewater Fe^{2+} concentration is also influenced by the formation of iron carbonates (e.g. Burdige, 1993), again assumed to be a pure phase $FeCO_3$. Finally, explicit modelling of the adsorped Mn^{2+} and Fe^{2+} has not been implemented. In effect, these interfacial species are included within the authigenic Mn and Fe phases.

5.6 Constitutive Equations

A diagenetic equation (Equation 5-2) is written for each of the components listed in Table 9. This set of fifteen equations therefore forms the basis of the redox model. However, the model can not be solved until appropriate constitutive equations have been selected; that is, until the mathematical forms of the fluxes, reactions, and source-sink terms in the diagenetic equation have been specified. The mathematical representations of these terms are discussed below.

It was noted earlier that in an ideal model the terms on the right hand side of the diagenetic equation would represent all processes that influence the distribution of the component species. However, given the complexity of sedimentary systems, inclusion of all processes would be impractical, especially for a generic model such as that developed herein. The redox model therefore only considers processes that are commonly included in early diagenetic models. Sedimentary processes that are not modelled include physical processes like impressed flow

and biological activity such as head-down deposit feeding. The mathematical forms used to represent these processes can be found in Boudreau (1997) and references therein.

5.6.1 Local Transport Fluxes ($\sum$ F terms)

Local transport within the sediment can be separated into advective and diffusional fluxes, each of which are discussed in turn below:

5.6.1.1 Advective Fluxes: The Deposition of Sedimentary Materials

If the SWI is taken as a reference, the accumulation of sedimentary material can be considered as an advection of both solids and porewaters away from the SWI (Berner, 1980). The magnitude of this advection is related to the burial rate, that is, the rate at which new material is accreting. Advective fluxes due to the deposition of material (F_{adv}) are described mathematically as:

for solid phases:	$F_{adv} = \xi \omega C$	
for interstitial phases:	$F_{adv} = \xi \nu C$	**Equation 5-6**

where ω is the rate of advection for the solid phase, and ν the advection rate for the interstitial water, both having units of cm/yr.

In coarse-grained, non-compacting, sediments both the solid phase and interstitial water are advected at the same rate. Conversely, in fine-grained, compacting, sediments the solid and porewater phases are advected away from the SWI at different velocities. This is because interstitial waters are 'squeezed' from the pores as the grains compact. Hence, compaction slows the rate of advection of porewater components relative to that of the solid phase (see Berner, 1980; Boudreau, 1997 for a more detailed description).

A detailed mathematical treatment of compaction is beyond the scope of this work. However, following the example of a number of authors (e.g. Berner, 1980; Boudreau, 1996; 1997),

compaction has been assumed to be at steady state. With this assumption the following relationships hold:

for solid phases:	$\xi\omega = \xi_f \omega_f$	
for interstitial phases:	$\xi\nu = \varphi_f \nu_f$	**Equation 5-7**

where φ_f is the asymptotic value of porosity, ω_f is the asymptotic value of solids advection (that is, burial rate), v_f is the asymptotic value of porewater advection, and $\xi_f = 1 - \varphi_f$.

Hence, if the asymptotic values (φ_f, ω_f, v_f) and the depth profile of porosity are known, the assumption of steady state compaction allows the values of ω and v to be calculated at any depth. Furthermore, by definition the asymptotic velocities (ω_f, v_f) occur where porosity gradients approach zero and compaction is no longer significant; that is, where the solids and porewater are advected at the same rate. This means that for the interstitial phase Equation 5-7 can be written as:

$\xi\nu = \varphi_f \omega_f$	**Equation 5-8**

Hence, the assumption of steady state compaction allows Equations 5-6 to be rewritten as:

for solid phases	$F_{adv} = \xi_f \omega_f C$	
for interstitial phases	$F_{adv} = \varphi_f \omega_f C$	**Equation 5-9**

5.6.1.2 Diffusional Fluxes

Diffusional fluxes within the sediment result from a number of distinct processes, each of which is described in turn below. However, the flux resulting from each process is modelled in the same way, using the formalism of Fick's first law. Fick's first law can be considered as a deterministic expression of random motions occurring at the microscopic scale. The result of these random motions is that there is a net transport of molecules from regions of high

concentration to regions of low concentration. Hence, diffusion tends to smooth out concentration gradients (e.g. Crank, 1975).

According to Fick's first law, the diffusional fluxes (F_{dif}) occurring in the sediment can be represented mathematically as:

$$F_{dif} = -D\frac{\partial C}{\partial x} \qquad \textbf{Equation 5-10}$$

Hence, the diffusional flux is dependent upon the magnitude of the local gradients of concentration and a diffusion coefficient (D). The diffusion coefficient reflects the intensity of the random motions. The minus sign indicates that the net flux is from a high concentration to a low concentration, that is, opposite to the direction of the gradient.

Molecular and Ionic Diffusion

Molecular and ionic diffusion are produced by the random (thermal) motion of individual molecules. This type of diffusion can occur within and between the various phases, but the most significant mode of transport occurs within the interstitial waters. Diffusion within particulate matter and on the surface of solids can normally be neglected (Berner, 1980).

Diffusion in dilute solutions has been studied extensively and a number of theoretical and empirical models have been developed (see Berner, 1980; Boudreau, 1997 for a review). However, the interstitial waters of marine sediments are not dilute, but are moderately concentrated multi-component solutions. The diffusion of interstitial species is therefore modified by solute-solute interactions.

A strict treatment of this multi-component diffusion would make the task of modelling the diffusional flux more complex (see Van Cappellen & Gaillard, 1996). Fortunately, diffusion in the porewaters of marine sediments is sufficiently like diffusion in dilute solutions that the additional complexity can be ignored (Van Cappellen & Gaillard, 1996; Boudreau, 1997).

Boudreau (1997) notes that the exception is situations where the major ions chlorine and sodium are important. Since these species are not included within the present model, a simplified Fickian treatment of molecular/ionic diffusion can be used.

Modelling molecular/ionic diffusion as a Fickian process requires that a diffusion coefficient be calculated for each interstitial species. This calculation has been implemented in the redox model using a public domain subroutine (Boudreau, 1996; 1997). The subroutine calculates the relevant molecular/ionic diffusion coefficients in solution (D_{free}), and corrects for the influence of temperature, salinity, and pressure. However, following the example of Van Cappellen & Wang (1995; 1996), the diffusion coefficient for total sulphides (TS) and total carbonates (TC) are calculated as the weighted-sum of the diffusion coefficients of the constituent species.

The mineral matrix prevents the 'free' diffusion of solutes in sediments; that is, diffusing species must follow a tortuous path. Hence, the diffusion coefficients calculated via Boudreau's subroutine (D_{free}) must be corrected for tortuosity (θ), which is defined mathematically as:

$$\theta = \frac{dl}{dx} \qquad \textbf{Equation 5-11}$$

where dl is the actual distance travelled per unit length dx. The diffusion coefficient corrected for the tortuosity (D_{sed}) is given by:

$$D_{sed} = \frac{D_{free}}{\theta^2} \qquad \textbf{Equation 5-12}$$

A number of simple models have been presented in the literature that express the square of the tortuosity in terms of the porosity (see Boudreau, 1997 p. 129 for a compilation). The model adopted herein is a form of Archie's law, which can be written as:

$$\theta^2 = \varphi^{1-a} \qquad \textbf{Equation 5-13}$$

where a is a fitting parameter, which for unconsolidated muds is 2.7 ± 0.3 (Van Cappellen & Gaillard, 1996). Following the example of Van Cappellen & Wang (1995; see also Ullman & Aller, 1982), the form of the tortuosity corrected diffusion coefficient used herein is:

$$D_{sed} = \left(\varphi^{2}\right) D_{free} \qquad \textbf{Equation 5-14}$$

which is equivalent to specifying a=3 in Archie's Law.

Bioturbation

The burrowing and feeding activities of the macrofauna produce mixing-like processes in the upper layer of sediments, termed 'bioturbation'. (See Matisoff 1982 & 1995 for a review of bioturbation and its effects on sediment chemistry.) Bioturbation dominates the transport of particulates in the top 5-20 cm of most sedimentary systems (Van Cappellen & Gaillard, 1996). Exceptions include sediments that animals can not colonise, and high-energy environments where wave/current induced mixing of particulates can dominate. Bioturbation also mixes the porewaters, but is usually not the dominant transport mechanism of this phase.

Bioturbation is actually a generic term used to describe the aggregate effect of a number of distinct processes occurring at various scales in both time and space. The exact mathematical treatment of the individual processes would be difficult. Hence, the usual approach is to consider all the processes together and model the overall effect as a random, Fickian like diffusion process. Matisoff (1982) notes that:

> "*Solid particles are clearly not diffusing, but the random transport of particulates on a macroscopic scale caused by the action of organisms may be described by such a mechanism in the appropriate spatial and temporal context*".

Wheatcroft *et al.* (1990) used a random walk model to show that the Fickian diffusion analogue gives a poor representation of the actual mechanisms of vertical mixing. Boudreau (1986) also considered theoretical aspects of the diffusional representation of bioturbation in detail. Boudreau concluded that in many cases transport of particulate matter is a non-local process. It should, however, be noted that the vast majority of diagenetic modelling studies use the Fickian

model to account for the effects of bioturbation, and this practice has been followed herein. Furthermore, whilst accepting the limitations of the Fickian analogue, it is noteworthy that both Soetaert *et al.* (1996b) and Boon & Duineveld (1998) have compared the use of the simple diffusive model of bioturbation with more sophisticated non-local exchange models. In both cases it was found that for the majority of the sites studied the diffusive model gave the better fit to the depth profiles of tracers. Nevertheless, Dauwe *et al.* (1998) note that diffusive mixing is mainly associated with mobile subsurface deposit-feeding or burrowing species and free living predators. Strictly speaking, therefore, the use of the Fickian representation of bioturbation is restricted to sediments dominated by such biota.

As with all Fickian processes, the bioturbation flux is dependent upon local gradients and a diffusion coefficient, which is termed the bioturbation coefficient (D_b). The flux (F_{bio}) of a solid or interstitial species due to bioturbation can be written as:

$$F_{bio} = -D_b \, \xi \frac{\partial C}{\partial x} \qquad \textbf{Equation 5-15}$$

This formulation is termed intraphase mixing by Boudreau (1997). Pure intraphase mixing does not smooth out porosity gradients (Muslow *et al.*, 1998). This formulation is therefore consistent with the use of porosity as a driving variable; that is, porosity gradients are imposed rather than modelled (see Section 5.8).

The bioturbation coefficient parameterises the activities of the macrofauna. The magnitude of the coefficient is therefore related to the macrofaunal species present, the number of individuals, and the level of their activity. All these factors vary widely in time and space. Consequently, the level of bioturbation varies considerably throughout the marine environment. For example, Van Cappellen *et al.* (1993) note that the bioturbation coefficients determined in diagenetic studies vary over four orders of magnitude. The coefficient tends to be highest in sediments that are rapidly accreting because such sediments receive a large flux of organic matter and can therefore sustain elevated levels of macrofaunal activity.

The macrofauna require oxygen to live and must therefore maintain intermittent or constant contact with the overlying oxygenated water, a task that becomes more difficult as the burrowing depth increases. In addition, the depth limit for feeding activities represents an energetic trade-off between the amount of energy obtained from the reactive POM at depth and the metabolic expenditure in foraging and processing of the material (paraphrased from Rice & Rhoads, 1989). The macrofauna are therefore concentrated in the top part of the sediment and do not often penetrate below a certain depth, which is a characteristic of the sedimentary environment and/or the species in question. Intuitively, the bioturbation coefficient should exhibit a depth dependency that reflects this depth distribution of the macrofauna.

The simplest approach for representing the depth distribution of bioturbation is to assume a two-layer sediment structure. The bioturbation coefficient is then constant down to the mixing depth (x_1) and zero below, that is:

$$D_b(x) = D_b\big|_{swi} \qquad 0 < x < x_1$$

$$D_b(x) = 0 \qquad x_1 < x \qquad \textbf{Equation 5-16}$$

Penetration of fauna below the mixing depth x_1 occurs but the influence on sediment properties is assumed negligible. Another common approach is to assume that the depth dependence can be represented by some rational function such as the decaying exponential used by Christensen (1982).

Other Diffusional Processes

One additional diffusional flux with coefficient D_i has been included in the redox model. This flux can be used to represent hydrodynamic dispersion (e.g. Boudreau, 1997) or to account for the irrigational activities of the macrofauna. As discussed below, representing irrigation as a Fickian process is somewhat questionable. However, if this approach is taken then D_i (the diffusion coefficient for irrigation) can be calculated as an enhanced molecular diffusion coefficient. The 'enhancement factor' is determined by measuring the flux of a solute across

the SWI. Since these flux measurements are relatively easy to make, Soetaert *et al.* (1996a) assert that representing irrigation in this way is a pragmatic modelling approach.

5.6.1.3 Mathematical Representation of the Flux Term

Substituting the mathematical representations of the fluxes described above into the diagenetic equation (Equation 5-2) gives the total flux ($\sum F$) for solids as:

$$\sum F = -D_b \xi \frac{\partial C}{\partial x} + \xi_f \omega_f C \qquad \textbf{Equation 5-17}$$

whereas, for porewater species the total flux is given by:

$$\sum F = -(D_b + D_{sed} + D_i) \xi \frac{\partial C}{\partial x} + \varphi_f \omega_f C \qquad \textbf{Equation 5-18}$$

It should be noted that the diagenetic equation is written in terms of the divergence of these fluxes; that is, the first derivative of the flux with respect to the space variable '*x*'.

5.6.2 Source & Sink Terms ($\sum$S terms)

The $\sum$S term in the diagenetic equation represents non-local processes that influence the distribution of both solutes and particulate matter. However, only one process of this type is included in the redox model; that is, irrigation.

5.6.2.1 Irrigation

Many species of the macrofauna build permanent and/or impermanent burrows that they actively irrigate; that is, flush with water. Irrigation is carried out as part of the animal's respiration (that is, to provide oxygen), and can prevent the build up of metabolic products such as ammonia and hydrogen sulphide. This later point is especially significant in organically rich sediments where high levels of anaerobic respiration can occur.

Irrigational activities are capable of maintaining water in burrows at a composition similar to that of the overlying seawater. Hence, irrigation increases the surface area available for solute

exchange between the interstitial water of the sediment and the bottom water; that is, exchange also occurs across the burrow wall (e.g. Aller, 1982; Boudreau & Marinelli, 1994). Irrigation can also influence the pathways of degradation and the rates of redox reactions in marine sediments (e.g. Aller & Aller, 1998). Irrigational activities can therefore have a significant effect on the distribution of solutes in the sediment, and consequently, the form of the redox gradients. The exact influence, however, depends upon the size and spacing of organisms, the periodicity of the irrigational activity and the species of animal present (e.g. Aller, 1980a; Boudreau & Marinelli, 1994; Forster & Graff, 1995; Marinelli & Boudreau, 1996), as well as the level of organic enrichment (see Section 4.3.2)

As noted above, a Fickian diffusion analogue can be used to model irrigation (e.g. Berner, 1980; Aller, 1980a; Park & Jaffe, 1996, Soetaert *et al.*, 1996a). However, since animals actively draw water from the SWI to flush out their burrows, irrigation does not depend upon local gradients in porewater concentration and is therefore inherently non-local. Consequently, a Fickian diffusion analogue does not give a realistic representation of the process.

A number of models have been proposed as an alternative to the Fickian approach. For example, Aller (1980a, 1980c) presented a 2-D radial diffusion model in which the geometry of the burrow was considered explicitly. This model gives a conceptually superior representation of irrigation but can not be incorporated into a 1-D model. Hence, the model of irrigation used herein is a simple non-local exchange function, which has been implemented in a number of other 1-D diagenetic models (e.g. Emerson *et al.*, 1984; Aller & Yingst, 1985; Boudreau, 1996; Van Cappellen & Wang, 1996).

In this model of irrigation, the net extraction/delivery of a solute is assumed proportional to the difference between the concentrations in the burrow water and surrounding porewater. If the composition of the burrow water is assumed the same as that of the overlying water, the function can be written:

$$S(x) = \alpha(x)\{C(0) - C(x)\} \qquad \textbf{Equation 5-19}$$

where $\alpha(x)$ is the non-local exchange coefficient of irrigation (/yr), C(0) is the solute concentration at the upper boundary (that is, the SWI), and C(x) is the concentration at depth x. The irrigation coefficient (α) indicates how frequently a certain volume of porewater is exchanged with the overlying water.

Since the irrigation coefficient is associated with the activities of the infauna, the intensity of irrigation should be related to the distribution of fauna within the sediments. This can be shown with reference to Boudreau (1984), who demonstrated the non-local exchange model of irrigation could be related to Aller's 2-D radial diffusion model by:

$$\alpha(x) = \frac{D_{sed}\, r_1}{(r_2^2 - r_1^2)(\bar{r} - r_1)} \qquad \textbf{Equation 5-20}$$

where D_{sed} is the tortuosity corrected molecular diffusion coefficient, r_1 is the inner radius of the micro-environment, r_2 is the effective outer radius of the solid region, and $\bar{r}$ is the radius where the concentration of the diffusing solute is equal to the laterally averaged concentration; that is, $r_1 < \bar{r} < r_2$.

In effect, r_1 is the burrow radius and r_2 depends upon the population abundance of the macrofauna. For any given macrofaunal species, r_1 is approximately constant. Furthermore, $\bar{r}$ is a function of the overall transport regime in the sediment. Hence, the main variable in Equation 5-20 is r_2, which is related to the macrofaunal abundance. The non-local exchange coefficient is therefore proportional to the abundance and, by inference, the biomass of the infauna.

The presence of the diffusion coefficient in Equation 5-20 indicates that the non-local exchange function is solute specific. This can be readily incorporated into the model by using the ratios of different molecular diffusion coefficients (e.g. Aller & Yingst, 1985). However, this

additional complexity is not considered in this work and a 'system wide' irrigation coefficient has been adopted.

Intuitively, the intensity of irrigation should also be related to the depth distribution of fauna within the sediments, that is, the exchange coefficient should exhibit a depth dependence (e.g. Martin & Banta, 1992). This depth dependence can be represented in a variety of ways. For instance, an exponentially decaying exchange coefficient was used successfully by Wang & Van Cappellen (1996) to describe solute profiles at two study sites. A number of authors have also used a two-layer model analogous to Equation 5-16 to describe the depth distribution of irrigation (e.g. Boudreau, 1996; Van Cappellen & Wang, 1996).

5.6.3 Reaction Terms ($\sum R$ terms)

The $\sum R$ term in the diagenetic equation represents the rates of the biogeochemical reactions that influence the distribution of the component species. Three types of reaction are included in the redox model. First, the primary redox reactions; that is, the metabolic reactions associated with the mineralisation of the sedimentary particulate organic matter (POM), which drive the formation of redox gradients. Second, the secondary redox reactions; that is, reactions that do not involve the mineralisation of POM directly, but can have a significant influence on the distribution of redox sensitive species. Finally, the model includes precipitation and dissolution reactions, which control the porewater concentration of some components.

The rates of these reactions are sufficiently slow that kinetic formulations must be used, as discussed below. However, this kinetic approach is not required for reactions between the constituent species that comprise the total carbonate (TC) and the total sulphide (TS) concentration. Instead, these reactions are assumed so rapid that chemical equilibrium is maintained in the face of transport processes; that is, local equilibrium is maintained. With this assumption, the proportion of each constituent species can be calculated from equilibrium

relationships. (see Van Cappellen & Wang 1995, 1996 and references therein for the equilibrium relationships used in this work.)

5.6.3.1 Primary Redox Reactions

As discussed in Chapter 4, mineralisation of organic matter is carried out via a number of metabolic pathways. In reality, each pathway consists of a succession of complex reactions. However, detailed metabolic reaction schemes are not normally used in environmental or geochemical models (Boudreau, 1992). Instead, the metabolic processes are represented as 'bulk' reactions that only consider the initial reactants (reduced organic substrates and the main mineral oxidants) and final products. No attempt is made to model the highly complex biochemistry of the cell, and the micro-organism can be considered simply as a catalyst of the bulk reaction. Boudreau (1992) notes that whilst such models are a simplification they need not be considered overly simplistic

In this study, the degradation of organic matter is modelled as a sequence of six primary redox reactions. This is the same approach as that taken by Park & Jaffe (1996) and similar to that taken by Tromp *et al.* (1995). Each reaction is assumed to occur according to the stoichiometric relationship detailed in Table 10 (after Van Cappellen & Wang, 1995). Except for methanogenesis, monod rate laws are used to represent the rate of each reaction (e.g. Boudreau & Westrich, 1984). Methanogenesis does not involve an oxidant and is therefore represented simply as a first order reaction. The monod rate law can be written as:

$$\frac{dG}{dt} = -V_{ox} G \left(\frac{C_{ox}}{K_{ox} + C_{ox}} \right) \qquad \textbf{Equation 5-21}$$

where G represents the concentration of degradable organic matter, K_{ox} is the half saturation constant, C_{ox} is the concentration of the oxidant, and V_{ox} is a rate constant. K_{ox} is termed the half saturation constant because when C_{ox} equals K_{ox} the reaction rate is exactly half that observed when the oxidant concentration is saturating.

Primary Redox Reactions
$POM + (x+2y)\,O_2 + (y+2z)\,HCO_3^- \xrightarrow{R_{O_2}} (x+y+2z)\,CO_2 + yNO_3^- + zHPO_4^{2-} + (x+2y+2z)\,H_2O$
$POM + \left(\frac{4x+3y}{5}\right)NO_3^- \xrightarrow{R_{NO_3}} \left(\frac{2x+4y}{5}\right)N_2 + \left(\frac{x-3y+10z}{5}\right)CO_2 + \left(\frac{4x+3y-10z}{5}\right)HCO_3^- + zHPO_4^{2-} + \left(\frac{3x+6y+10z}{5}\right)H_2O$
$POM + 2xMnO_2 + (3x+y-2z)\,CO_2 + (x+y-2z)H_2O \xrightarrow{R_{MnO_2}} 2xMn^{2+} + (4x+y-2z)HCO_3^- + yNH_4^+ + zHPO_4^{2-}$
$POM + 4xFe(OH)_3 + (7x+y-2z)\,CO_2 \xrightarrow{R_{Fe\,III}} 4xFe^{2+} + (8x+y-2z)HCO_3^- + yNH_4^+ + zHPO_4^{2-} + (3x-y+2z)H_2O$
$POM + \frac{x}{2}SO_4^{2-} + (y-2z)CO_2 + (y-2z)H_2O \xrightarrow{R_{SO_4}} \frac{x}{2}H_2S + (x+y-2z)HCO_3^- + yNH_4^+ + zHPO_4^{2-}$
$POM + (y-2z)H_2O \xrightarrow{R_{CH_4}} \frac{x}{2}CH_4 + \left(\frac{x-2y+4z}{2}\right)CO_2 + (y-2z)HCO_3^- + yNH_4^+ + zHPO_4^{2-}$

with POM = $(CH_2O)_x(NH_3)_y(H_3PO_4)_z$, where x, y, z is the C:N:P ratio of the organic matter

NB: As noted in Chapter 4, methanogenesis is sometimes termed carbonate reduction, which implies that an oxidant is used. This is because methanogenesis actually proceeds via two steps (from Berner, 1980):

$$2CH_2O + 2H_2O \rightarrow 2CO_2 + 8(H) \quad followed\ by \quad 8(H) + CO_2 \rightarrow CH_4 + 2H_2O$$

Where (H) is a generalised reducing agent Hence, the second step does involve the reduction of CO_2 to CH_4. However, the general reducing agent (H) is derived from organic matter. Hence, when only initial reactants and final products are considered the overall process of methanogenesis is the sum of these two reactions; that is, the disproportionation of organic matter to carbon dioxide and methane (Berner, 1980).

Table 10 *Stoichiometries of Degradation*

Referring to Equation 5-21, it can be seen that when oxidant concentration is saturating ($C_{ox} >> K_{ox}$), the quotient in the Equation is approximately unity. The reaction rate is then approximately equal to $V_{ox}G$; that is, the monod rate law reduces to a first order reaction. However, at low concentrations of the oxidant, the quotient becomes less than unity and the reaction rate falls. Hence, the overall effect of the monod rate law is that the reaction rate is first order in G when the oxidant concentration is saturating ($C_{ox} >> K_{ox}$), but is hyperbolic in the oxidant concentration when oxidant availability is low ($C_{ox} < K_{ox}$). The monod scheme therefore accounts for the effect of both oxidant and organic substrate availability on the rate of mineralisation.

As discussed in Chapter 4, different assemblages of microbes succeed one another roughly in the order of the free energy yield of their metabolisms. Hence, the six primary redox reactions do not occur together. A variety of physiological and ecological factors induces this metabolic succession, but for the purposes of a model, no distinction has to be made between the various mechanisms. It is sufficient to recognise that the presence of a more energetically favourable oxidant tends to inhibit a less efficient metabolic pathway.

Various formulations could be used to represent this inhibition (e.g. Rabouille & Gaillard, 1991b; Van Cappellen & Wang, 1995; Boudreau, 1996). The form adopted herein follows the scheme suggested by Van Cappellen & Gaillard (1996), in which inhibition is represent by:

$$I = \frac{K_{in}^{ox}}{C_{ox} + K_{in}^{ox}} \qquad \textbf{Equation 5-22}$$

where I is the inhibition factor, K_{in}^{ox} is the inhibition constant for the oxidant in question, and C_{ox} is the concentration of the inhibiting oxidant.

The inhibition factor is applied to each metabolic reaction yielding less energy than the oxidant in question (C_{ox}). Hence, the inhibited reaction rate (R_{inhib}) can be written as:

$$R_{inhib} = I R_{full} \qquad \textbf{Equation 5-23}$$

where R_{full} is the rate of the reaction in the absence of inhibition. From Equations 5-22 and 5-23 it can be seen that when the concentration of the inhibiting oxidant (C_{ox}) is much greater than the inhibition constant (K_{in}), the inhibition factor (I) approaches zero, and the reaction (R_{inhib}) is fully inhibited. However, as C_{ox} falls, the inhibition factor tends towards unity and the reaction rate approaches R_{full}. When C_{ox} equals zero the reaction is no longer inhibited.

This inhibition scheme therefore results in a smooth transition between the diagenetic zones. Furthermore, the depth of each zone is not imposed but arises naturally from the specified conditions. This in turn means that the calculated redox profiles vary according to the

characteristics of the sediment being modelled; a prerequisite if the model is to be generic. Finally, the inhibition scheme allows some overlap between the diagenetic zones. Wang & Van Cappellen (1996) note that this vertical overlap is equivalent to the integration of horizontal heterogeneity at a given depth; that is, the overlap is the 1-D representation of the 3-D diagenetic zonation commonly observed in coastal sediments.

Van Cappellen & Gaillard (1996) note that a set of inhibition constants for use in this scheme has not been determined. However, the authors suggest that the half saturation constants for each metabolic pathway can be used as guide values. The justification for this is that less efficient reactions are only inhibited in the presence of high concentrations of 'preferred' oxidants. The half saturation constant is by definition a concentration at which the availability of an oxidant is limiting. The values for the half saturation constants used in this work were taken from Van Cappellen & Wang (1995).

Combining all the factors discussed above leads to the kinetic representation of degradation detailed in Table 11. At any depth in the sediment, the total rate of mineralisation is then:

$$R_{org} = R_{O_2} + R_{NO_3} + R_{MnO_2} + R_{Fe_{III}} + R_{SO_4} + R_{CH_4} \qquad \textbf{Equation 5-24}$$

Some or all of the reactions on the right hand side of Equation 5-24 will be zero, depending upon the concentrations of oxidants and the availability of labile organic matter.

Studies of degradation show that many organic compounds are rapidly oxidised under both oxic and anoxic conditions (e.g. Henrichs & Reeburgh, 1987). However, easily degraded organic fractions tend to be utilised in the aerobic zone. This preferential degradation of labile substrates means that there is an increasing amount of refractory organic matter with depth. Material in anaerobic diagenetic zones therefore tends to be more refractory than in oxic zones, and oxidation rates are correspondingly reduced (e.g. Van Cappellen *et al.*, 1993 and references therein).

Process	*Kinetic Formulation (Rate Law)*
Oxic Respiration	$\frac{dG}{dt} = -\frac{V_{O_2} G C_{O_2}}{(K_{O_2} + C_{O_2})} = -R_{O_2}$
Denitrification	$\frac{dG}{dt} = -\frac{V_{NO_3} G C_{NO_3}}{(K_{NO_3} + C_{NO_3})} \cdot \frac{K_{in}^{O_2}}{C_{O_2} + K_{in}^{O_2}} = -R_{NO_3}$
Mn-Oxide Reduction	$\frac{dG}{dt} = -\frac{V_{Mn} G C_{Mn}}{(K_{Mn} + C_{Mn})} \cdot \frac{K_{in}^{O_2}}{C_{O_2} + K_{in}^{O_2}} \cdot \frac{K_{in}^{NO_3}}{C_{NO_3} + K_{in}^{NO_3}} = -R_{MnO_2}$
Fe-Oxide reduction	$\frac{dG}{dt} = -\frac{V_{Fe} G C_{Fe}}{(K_{Fe} + C_{Fe})} \cdot \frac{K_{in}^{O_2}}{C_{O_2} + K_{in}^{O_2}} \cdot \frac{K_{in}^{NO_3}}{C_{NO_3} + K_{in}^{NO_3}} \cdot \frac{K_{in}^{Mn}}{C_{Mn} + K_{in}^{Mn}} = -R_{Fe_{III}}$
Sulphate Reduction	$\frac{dG}{dt} = -\frac{V_{SO_4} G C_{SO_4}}{(K_{SO_4} + C_{SO_4})} \cdot \frac{K_{in}^{O_2}}{C_{O_2} + K_{in}^{O_2}} \cdot \frac{K_{in}^{NO_3}}{C_{NO_3} + K_{in}^{NO_3}} \cdot \frac{K_{in}^{Mn}}{C_{Mn} + K_{in}^{Mn}}$ $\cdot \frac{K_{in}^{Fe}}{C_{Fe} + K_{in}^{Fe}} = -R_{SO_4}$
Methanogenesis	$\frac{dG}{dt} = -k_{CH_4} G \cdot \frac{K_{in}^{O_2}}{C_{O_2} + K_{in}^{O_2}} \cdot \frac{K_{in}^{NO_3}}{C_{NO_3} + K_{in}^{NO_3}} \cdot \frac{K_{in}^{Mn}}{C_{Mn} + K_{in}^{Mn}}$ $\cdot \frac{K_{in}^{Fe}}{C_{Fe} + K_{in}^{Fe}} \cdot \frac{K_{in}^{SO_4}}{C_{SO_4} + K_{in}^{SO_4}} = -R_{CH_4}$

Table 11 *Kinetic Scheme for Degradation*

As indicated in Table 11, each of the six primary redox reactions has a rate constant associated with it (that is, V_{o2}, V_{no3}, V_{mn}, V_{fe}, V_{so4}, and k_{ch4} in the Table). The magnitude of these rate constants must reflect the average reactivity of the organic material within each diagenetic zone. Hence, the change in the lability of organic matter with depth can be represented simply by setting the rate constants to successively lower values; that is, V_{o2}, $\geq V_{no3}$, $\geq V_{mn}$, $\geq V_{fe}$, $\geq V_{so4}$, $\geq k_{ch4}$. Furthermore, if each rate constant is set to the same value the model reverts to a 1-G formulation; that is, degradation is independent of oxidant concentrations and is modelled as a first order reaction in 'G'. This kinetic scheme was therefore considered more flexible than the pure G-model approach used in many diagenetic studies (see Berner, 1964; Jørgensen, 1979; Berner, 1980).

Various other models have been presented in the literature that describe the variable lability of sedimentary organic matter. For example, Boudreau & Ruddick (1991) used a continuum of reactivities to represent degradation. Middelberg (1989) proposed a model in which the rate constant was expressed as a continually decreasing function of time. These models provide a conceptually superior description of decomposition. However, their application has been limited. Parameterising these formulations generically was therefore considered problematic. Furthermore, it is not clear how these models could be incorporated into a multi-component diagenetic model of the type described herein. Finally, it is the effect of degradation on solute distribution that is of interest, rather than the process of degradation itself. Consequently, these alternative models were not used.

5.6.3.2 Secondary Redox Reactions

The secondary redox reactions included in the redox model have been previously used in a number of early diagenetic models described in the literature (e.g. Boudreau, 1996; Van Cappellen & Wang, 1996). The stoichiometries used to characterise the reactions were taken from Van Cappellen & Wang (1995, 1996), and are detailed in Table 12. The reactions shown in the Table involve at least one product of a primary redox reaction and can be abiotic or enzymatically mediated.

The rate laws used to represent the secondary reactions have been taken without modification from the work of Van Cappellen & Wang (1995, 1996). These authors reviewed the literature and presented a comprehensive set of rate laws and rate constants for the main reactions involving the principle redox elements carbon, oxygen, nitrogen, sulphur, iron, and manganese. Their reaction scheme, which was subsequently included in Boudreau's monograph on diagenetic modelling (Boudreau, 1997), is summarised in Table 13.

Secondary Redox Reactions
$Mn^{2+} + \frac{1}{2}O_2 + 2HCO_3^- \xrightarrow{R7} MnO_2 + 2CO_2 + H_2O$
$Fe^{2+} + \frac{1}{4}O_2 + 2HCO_3^- + \frac{1}{2}H_2O \xrightarrow{R8} Fe(OH)_3 + 2CO_2$
$2Fe^{2+} + MnO_2 + 2HCO_3^- + 2H_2O \xrightarrow{R9} 2Fe(OH)_3 + MN^{2+} + 2CO_2$
$NH_4^+ + 2O_2 + 2HCO_3^- \xrightarrow{R10} NO_3^- + 2CO_2 + 3H_2O$
$H_2S + 2O_2 + 2HCO_3^- \xrightarrow{R11} SO_4^{2-} + 2CO_2 + 2H_2O$
$H_2S + 2CO_2 + MnO_2 \xrightarrow{R12} MN^{2+} + S^0 + 2HCO_3^-$
$H_2S + 4CO_2 + 2Fe(OH)_3 \xrightarrow{R13} 2Fe^{2+} + S^0 + 4HCO_3^- + 2H_2O$
$FeS + 2O_2 \xrightarrow{R14} Fe^{2+} + SO_4^{2-}$
$CH_4 + 2O_2 \xrightarrow{R15} CO_2 + 2H_2O$
$CH_4 + CO_2 + SO_4^{2-} \xrightarrow{R16} 2HCO_3^- + H_2S$

Table 12 *Stoichiometries of Secondary Reactions*

Kinetic Formulation (Rate Law)
$R_7 = k_7[Mn^{2+}][O_2]$
$R_8 = k_8[Fe^{2+}][O_2]$
$R_9 = k_9[Fe^{2+}][MnO_2]$
$R_{10} = k_{10}[NH_4^+][O_2]$
$R_{11} = k_{11}[O_2][TS]$
$R_{12} = k_{12}[MnO_2][TS]$
$R_{13} = k_{13}[Fe(OH)_3][TS]$
$R_{14} = k_{14}[FeS][O_2]$
$R_{15} = k_{15}[CH_4][O_2]$
$R_{16} = k_{16}[CH_4][SO_4^{2-}]$

Table 13 *Rate Laws for Secondary Reactions*

As indicated in Table 13, the rates of homogenous secondary redox reactions (reactions between solutes) are modelled as second order, or bimolecular, reactions; that is, they have the form:

$$R = k[\mathrm{Ox}][\mathrm{Red}] \qquad \textbf{Equation 5-25}$$

where k represents a rate constant, [Ox] is the concentration of the oxidant, and [Red] the concentration of the reductant involved in the reaction.

Several of the reactions detailed in Table 13 are heterogeneous; that is, reactions between solids and solutes. Such reactions should ideally be described through boundary conditions. However, this approach is impractical in diagenetic modelling studies and heterogeneous reactions are therefore modelled as pseudo-homogenous (Boudreau, 1997). This approach is based on the assumption that the reacting solid is evenly distributed throughout the averaging volume (see Section 5.3). It then 'appears' that the reaction is occurring continuously through the volume, although it is actually only taking place at the solid-solute interface. With this assumption, heterogeneous reactions can be modelled with the same rate laws used to represent homogeneous reactions (e.g. Equation 5-25).

The adoption of the simple bimolecular rate law given by Equation 5-25 can be justified for many of the reactions listed in Table 13 (Van Cappellen & Wang, 1995; 1996). For example, the kinetics of the abiotic oxidation of Fe^{2+} and Mn^{2+} has been shown experimentally to follow a bimolecular rate law. However, Van Cappellen & Wang (1995) note that the bimolecular form has been adopted for nitrification (R_{10}) and methane oxidation (R_{15}) in the absence of detailed kinetic information. The rate law does, however, satisfy qualitative requirements that the rate should be related to the concentration of the reactants and should be zero if either reactant is absent.

5.6.3.3 Precipitation - Dissolution Reactions

The stoichiometries used to characterise the precipitation-dissolution reactions were again taken from Van Cappellen & Wang (1995, 1996), and are detailed in Table 14. The reactions are expressed as linear rate laws, as shown in Table 15 (after Van Cappellen & Wang, 1996).

Precipitation - Dissolution Reactions
$Mn^{2+} + 2HCO_3^- \xleftrightarrow{R19,R18} MnCO_3 + CO_2 + H_2O$
$Fe^{2+} + 2HCO_3^- \xleftrightarrow{R21,R20} FeCO_3 + CO_2 + H_2O$
$Fe^{2+} + 2HCO_3^- + H_2S \xleftrightarrow{R23,R22} FeS + 2CO_2 + 2H_2O$

Table 14 *Stoichiometries of Precipitation-Dissolution Reactions*

Kinetic Formulation (Rate Law)
$R_{18} = k_{18}\delta_{18}\left\{\frac{[Mn^{2+}][CO_3^{2-}]}{K'_{spMnCO_3}} - 1\right\}$
$R_{19} = k_{19}\delta_{19}[MnCO_3]\left\{1 - \frac{[Mn^{2+}][CO_3^{2-}]}{K'_{spMnCO_3}}\right\}$
$R_{20} = k_{20}\delta_{20}\left\{\frac{[Fe^{2+}][CO_3^{2-}]}{K'_{spFeCO_3}} - 1\right\}$
$R_{21} = k_{21}\delta_{21}[FeCO_3]\left\{1 - \frac{[Fe^{2+}][CO_3^{2-}]}{K'_{spFeCO_3}}\right\}$
$R_{22} = k_{22}\delta_{22}\left\{\frac{[Fe^{2+}][HS^-]}{a_{H^+}K'_{spFeS}} - 1\right\}$
$R_{23} = k_{23}\delta_{23}[FeS]\left\{1 - \frac{[Fe^{2+}][HS^-]}{a_{H^+}K'_{spFeS}}\right\}$

where the square brackets denote concentrations, a_{H+} is the hydrogen ion activity and:

$\delta_{18}; \delta_{20}; \delta_{22} = 0$ for $IAP \leq K'_{sp}$ $\quad$ $\delta_{19}; \delta_{21}; \delta_{23} = 1$ for $IAP \leq K'_{sp}$

$\delta_{18}; \delta_{20}; \delta_{22} = 1$ for $IAP \geq K'_{sp}$ $\quad$ $\delta_{19}; \delta_{21}; \delta_{23} = 0$ for $IAP \geq K'_{sp}$

Table 15 *Rate Laws for Precipitation-Dissolution Reactions*

The rates of the precipitation and dissolution reactions are dependent upon the saturation state of the porewater (that is, the Ion Activity Product; IAP) with respect to the apparent solubility constant (K_{sp}) of the solid in question. The rates observed in real sediments also depend upon the reactive mineral area. In addition, the saturation state of porewater with respect to a given phase depends upon the individual activities of the ions in solution, accounting for ion pairing and non-specific interactions. Both these effects are ignored to allow the simplified formulation given in Table 15 to be used (Van Cappellen & Wang, 1995).

5.6.3.4 Adsorption

The distribution of cations such as ammonia and reduced forms of both Mn and Fe are modified by adsorption/desorption processes (e.g. Berner, 1980; Canfield *et al.*, 1993b; Aller, 1994b). However, interfacial Mn and Fe species are not considered explicitly herein. Instead, the adsorped phases are 'lumped' together with the authigenic phases. Such an approach is not possible for ammonia because both of the nitrogenous species included within the model are solutes. The adsorption of ammonia is therefore modelled explicitly using a simple linear isotherm (e.g. Berner, 1980; Boudreau, 1997), which takes the form:

$$\overline{C} = k_{NH4} C \qquad \textbf{Equation 5-26}$$

where $\overline{C}$ is the concentration of adsorped phase, C is the concentration in solution, and k_{NH4} is an adsorption constant.

5.7 The Model Equations

The mathematical representations of the various fluxes and non-local processes given above are substituted into the general diagenetic equation (Equation 5-2) to form the equations of the redox model. For each solid component species the model equation is then:

$$\frac{\partial \xi C}{\partial t} = -\frac{\partial}{\partial x}\left(-D_b\ \xi \frac{\partial C}{\partial x} + \xi_f \omega_f C\right) + \xi \sum \hat{R} \qquad \textbf{Equation 5-27}$$

Note because compaction is modelled as steady state:

$$\frac{\partial \xi C}{\partial t} = \xi \frac{\partial C}{\partial t}$$ **Equation 5-28**

For each of the dissolved component species, except for ammonia, the model equation takes the form:

$$\frac{\partial \xi C}{\partial t} = -\frac{\partial}{\partial x}\left(-(D_b + D_i + D_{sed})\,\xi \frac{\partial C}{\partial x} + \varphi_f \omega_f C\right) + \alpha(x)\,\xi\,\{C(0) - C(x)\} + \xi \sum \hat{R}$$ **Equation 5-29**

As discussed in Section 5.6.3.4, the diagenetic equation for ammonia is modified to account for the effect of adsorption. Following the derivation detailed in Berner (1980), assuming the average solids density is approximately constant and the adsorption can be represented by a linear isotherm (Equation 5-26), the model equation for ammonia can be expressed as:

$$A\frac{\partial C}{\partial t} = -\frac{1}{\varphi}\frac{\partial}{\partial x}\left(-[D_t \varphi + D_b(1-\varphi)k_{NH4}]\frac{\partial C}{\partial x} + (\varphi_f \omega_f C + \xi_f \omega_f C k_{NH4})\right) + \frac{\alpha(x)\varphi\{C(0) - C(x)\}}{\varphi} + \frac{\xi}{\varphi}\sum \hat{R}$$ **Equation 5-30**

where $A = \left\{1 + \frac{k_{NH4}(1-\varphi)}{\varphi}\right\}$; $D_t = D_b + D_{sed} + D_i$

The reaction terms (that is, the $\sum \hat{R}$ terms in Equations 5-27, 5-28, and 5-29) for each of the component species are detailed in Table 16. It should be noted that the reactions produce a significant amount of coupling between the model equations. (NB: the governing Equations for each component species are detailed explicitly in Appendix I.)

Species	*Reaction Scheme*
CH_2O	$\sum \hat{R} = -R_{O_2} - R_{NO_3} - R_{MnO_2} - R_{Fe_{III}} - R_{SO_4} - R_{CH_4}$
O_2	$\sum \hat{R} = -\left(\frac{x+2y}{x}\right) R_{O_2} - \frac{1}{2} R_7 - \frac{1}{4} R_8 - 2(R_{10} + R_{11} + R_{14} + R_{15})$
NO_3^-	$\sum \hat{R} = \left(\frac{y}{x}\right) R_{O_2} - \left(\frac{4x+3y}{5x}\right) R_{NO_3} + R_{10}$
MnO_2	$\sum \hat{R} = -2R_{MnO_2} + R_7 - R_9 - R_{12}$
$Fe(OH)_3$	$\sum \hat{R} = -4R_{Fe_{III}} + R_8 + 2R_9 - 2R_{13}$
SO_4^{2-}	$\sum \hat{R} = -\frac{1}{2} R_{SO_4} + R_{11} + R_{14} - R_{16}$
CH_4	$\sum \hat{R} = -\frac{1}{2} R_{CH_4} - R_{15} - R_{16}$
NH_4^+	$\sum \hat{R} = \frac{y}{x}(R_{MnO_2} + R_{Fe_{III}} + R_{SO_4} + R_{CH_4}) - R_{10}$
TC	$\sum \hat{R} = R_{O_2} + R_{NO_3} + R_{MnO_2} + R_{Fe_{III}} + R_{SO_4} + \frac{1}{2} R_{CH_4} + R_{15} + R_{16} - R_{18} + R_{19} - R_{20} + R_{21}$
Mn^{2+}	$\sum \hat{R} = 2R_{MnO_2} - R_7 + R_9 + R_{12} - R_{18} + R_{19}$
Fe^{2+}	$\sum \hat{R} = 4R_{Fe_{III}} - R_8 - 2R_9 + 2R_{13} + R_{14} - R_{20} + R_{21} - R_{22} + R_{23}$
TS	$\sum \hat{R} = \frac{1}{2} R_{SO_4} - R_{11} - R_{12} - R_{13} + R_{16} - R_{22} + R_{23}$
$MnCO_3$	$\sum \hat{R} = R_{18} - R_{19}$
$FeCO_3$	$\sum \hat{R} = R_{20} - R_{21}$
FeS	$\sum \hat{R} = R_{22} - R_{14} - R_{23}$

Note, the multiplying factors applied to the rate laws correspond to the assumed stoichiometries of the reactions, as detailed in Table 12 and 14, and x:y is the C:N ratio of the POM (see Table 10)

Table 16 *Full Reaction Scheme*

5.8 The Depth Dependence of Parameters

The diffusion coefficients, porosity, and irrigation coefficient can all vary with depth. The representation of this depth dependence in a generic model is, however, somewhat arbitrary. Nevertheless, it is desirable to examine the effect of the dependency on the redox profiles generated by the model. To this end, depth dependencies have been incorporated into the redox model using a number of functions that have been implemented in other diagenetic models.

The depth profile of porosity is assumed to take the following form (e.g. Boudreau, 1997):

$$\varphi(x) = \varphi_f + (\varphi_{swi} - \varphi_f) \exp(-\beta\ x) \qquad \textbf{Equation 5-31}$$

where $\varphi(x)$ is the porosity at depth x, φ_{swi} is the initial porosity at the SWI, φ_f is the asymptotic value of porosity, and β is a decay constant. The porosity is therefore modelled as an exponential function that falls from a maximum value at the SWI to an asymptotic value φ_f at depth. Zero porosity gradients can be implemented simply by setting the initial and final values of porosity to the same value. The model then reverts to the case of no compaction.

The depth dependence of the diffusion coefficients D_i and D_b have been implemented as a decaying exponential of the form:

$$A(x) = A(0)\exp\left(-x^2 / 2x_b^2\right) \qquad \textbf{Equation 5-32}$$

where A represents D_i or D_b as appropriate and x_b is a decay constant.

The depth dependence of the irrigation coefficient has been implemented as:

$$\alpha(x) = \alpha(0)\exp\left(-\alpha_1\ x\right) \qquad \textbf{Equation 5-33}$$

where α is the irrigation coefficient and α_1 is a decay constant.

The depth dependence of the irrigation and diffusion coefficients D_i and D_b have also been implemented as functions that are constant to a given depth (x_1) then decrease linearly over some depth range (x_1 to x_2) and are zero thereafter; that is:

$$A(x) = A(0) \qquad 0 < x < x_1$$

$$A(x) = A(0) - A(0)\left(\frac{x - x_1}{x_2 - x_1}\right) \qquad x_1 < x < x_2$$

$$A(x) = 0 \qquad x \geq x_2 \qquad \textbf{Equation 5-34}$$

where A represents α, D_i or D_b as appropriate. The depth dependence of the molecular diffusion coefficient (D_{sed}) results from the gradient in porosity and therefore requires no additional treatment.

The model equations (5-27, 5-29, and 5-30) involve the spatial derivatives of porosity and the diffusion coefficients. These derivatives can be calculated analytically from the functions given above. Hence, when the depth profiles of the diffusion coefficients (D_i and D_b -- again represented as A in Equation 5-35 to 5-37) are expressed as decaying exponentials, the spatial derivatives are given by:

$$\frac{d}{dx}A(x) = -\frac{x}{x_b^2}A(0)\exp\left(-x^2/2x_b^2\right) \qquad \textbf{Equation 5-35}$$

When linearly decreasing functions are used, the gradient is then:

$$\frac{d}{dx}A(x) = -\frac{A(0)}{(x_1 - x_2)} \qquad \textbf{Equation 5-36}$$

for $x_1 < x < x_2$ (zero otherwise). In the case of the bioturbation coefficient when x_1 is set equal to x_2 the gradient is then given as:

$$\frac{d}{dx}D_b(x) = -\frac{D_b(0)}{\Delta x} \qquad \textbf{Equation 5-37}$$

for $x = x_2$ (zero otherwise). This is equivalent to assuming D_b falls to zero over one spatial step (that is, Δx). The spatial derivative of porosity is given by:

$$\frac{d}{dx}\varphi\ (x) = -\beta(\varphi_{swi} - \varphi_f)\exp(-\beta x) \qquad \textbf{Equation 5-38}$$

The spatial derivative of solid contents (1-φ) is therefore:

$$\frac{d}{dx}(1 - \varphi\ (x)) = \beta(\varphi_{swi} - \varphi_f)\exp(-\beta x) \qquad \textbf{Equation 5-39}$$

As noted previously, the molecular diffusion coefficient D_{free} is corrected for the tortuosity to give D_{sed}. Noting that D_{free} is not depth dependent, the spatial derivative of the tortuosity corrected diffusion coefficient is given by:

$$\frac{d}{dx}D_{sed}(x) = \frac{d}{dx}\left(\varphi^2\right)D_{free} = -2\beta\varphi D_{free}\left(\varphi_{swi} - \varphi_f\right)\exp(-\beta x) \qquad \textbf{Equation 5-40}$$

5.9 Calculating The Redox Intensity

The model equations detailed above describe mathematically the concentrations of oxidants and reductants in the top portion of the sediment. Gradients in these concentrations therefore reflect changes in redox state. Hence, the distribution of the components can be used to derive a vertical profile of redox intensity. However, since the model is a kinetic formulation the calculated concentration profiles do not necessarily conform to a state of internal equilibrium. Hence, at any given depth the various redox couples of interest could be at different apparent redox potentials.

Morel & Hering (1993) note that in such systems the activities (see Section 5.9.1 below) of the dominant redox couple can be used to characterise the redox state of the whole system. In this study, the dominant couple is assumed to correspond to the metabolic process that predominates at any given depth (see Grundl, 1995). The model redox potentials are therefore calculated from one of the redox couples, detailed in Table 17 (Billen, 1982; Stumm & Morgan, 1996), in combination with the Nernst equation (Equation 4-1). (The thermodynamic data used to calculate the standard electrode potential E° for each couple are given in Appendix II.)

This approach is essentially the same as that taken by Park & Jaffe (1996). However, as noted previously, Park & Jaffe (op. cit.) used an inhibition scheme that allows only one metabolic pathway to occur at any given depth. In contrast, the inhibition scheme adopted herein allows an overlap between the various diagenetic zones. Therefore, at depths where more than one oxidant is being reduced some method is required to select the dominant redox couple.

Couple	*Half reaction*
O_2/ H_2O	$O_2(g) + 4H^+ + 4e^- \rightarrow 2H_2O$
NO_3^-/N_2	$NO_3^- + 6H^+ + 5e^- \rightarrow \frac{1}{2} N_2(g) + 3H_2O$
MnO_2/MN^{2+}	$MnO_2 + 4H^+ + 2e^- \rightarrow Mn^{2+} + 2H_2O$
$Fe(OH)_3/Fe^{2+}$	$Fe(OH)_3 + 3H^+ + 1e^- \rightarrow Fe^{2+} + 3H_2O$
SO_4^{2-}/HS^-	$SO_4^{2-} + 9H^+ + 8e^- \rightarrow HS^- + 4H_2O$
HCO_3^-/CH_4	$HCO_3^- + 9H^+ + 8e^- \rightarrow CH_4(g) + 3H_2O$

Table 17 *Mineral Redox Couples and Half Reactions*

It has therefore been assumed that the dominant couple at any given depth is that of the most energetically favourable oxidant which is still inhibiting other metabolisms, or the HCO_3^-/CH_4 couple if all other oxidants are exhausted. Hence, the sedimentary redox intensity is calculated from the O_2/H_2O couple until the following condition is met:

$$I_{NO3} > I_t$$

where I_{NO3} is the inhibition factor for nitrate (see Equation 5-22) and I_t is a user defined constant ($0 < I_t < 1$). When I_{NO3} becomes greater than I_t, oxygen is effectively exhausted and the O_2/H_2O couple is no longer considered dominant. The redox intensity is then calculated from the NO_3^-/N_2 couple. This couple is again used until the oxidant (that is, nitrate) concentration falls to a level where the reduction of the next oxidant (Mn-oxide in this case) is no longer significantly inhibited.

The value of I_t therefore has a strong bearing on the redox profile generated and a standard value must be adopted to allow meaningful comparisons of different profiles be made. In the modelling work that follows (in Chapters 6 & 7), a value of 0.95 has been used throughout. This is equivalent to assuming oxidant exhaustion occurs when the concentration of the inhibiting oxidant falls below five per cent of its inhibition constant (that is, K_{in}^{ox}).

5.9.1 Activities of Redox Couples

The model equations are written in terms of the analytical or total concentration of the component species. The Nernst equation, however, involves the activities of the redox couples (see Equation 4-1, p. 67). The relationship between activity (a) and concentration (C) is given by:

$$a = \gamma C$$

where γ is an activity coefficient. For the purposes of diagenetic studies the activities (a) of solid species and water can be assumed to be one (e.g. Berner, 1971; Berner, 1980). However, at the ionic strength of seawater (that is, approximately 0.7 M) the activities of porewater species are less than calculated from concentrations due to solute-solute interactions; that is, the activity coefficients of porewater species are less than one. It is therefore conceptually more satisfying to make some estimate of the activity coefficients of these components.

A number of empirical and theoretical models have been developed that allow the activity coefficients of ionic species to be estimated. However, the simple models are restricted to aqueous environments of low ionic strength. For example, one commonly used model, the Davies formula, is only applicable to ionic strengths less than 0.5 M (Stumm & Morgan, 1996). However, Morel & Hering (1993, p 77) note:

> *"In aquatic systems the ionic strength rarely exceeds 0.7M and the inaccuracies introduced by using the Davies equation are usually smaller than other sources of errors and uncertainties"*

This is certainly the case in the current study where the aim is to provide an assessment of sedimentary conditions rather than accurately model ionic interactions. Hence, it is assumed that the Davies formula gives a sufficiently accurate estimate of the activity coefficients. It is further assumed that the activity coefficients so calculated can be applied to the concentrations of the component species without having to consider speciation explicitly. Therefore, the calculated values are assumed to be the total activity coefficient (e.g. Berner, 1980; Berner, 1971) of each ionic component.

The Davies formula can be written as (Morel & Hering, 1993; Stumm & Morgan, 1996):

$$\log(\gamma_i) = -AZ_i^2\left[\frac{I^{1/2}}{1+I^{1/2}} - 0.3I\right] \qquad \textbf{Equation 5-41}$$

where γ_i is the activity coefficient of the ith species, I is the ionic strength and Z_i is the charge on the ion in question. Assuming the relative permitivity (dielectric constant) for water is 78, A is defined as:

$$A = 1.82 \times 10^6 (78T)^{-3/2} \qquad \textbf{Equation 5-42}$$

where T is the absolute temperature.

The activities of dissolved gases are normally taken to be equivalent to their partial pressures, which can be calculated from Henry's law (e.g. Stumm & Morgan, 1996). For example, oxygen gas in equilibrium with an aqueous solution can be represented by the reaction:

$$O_2\,(gas) \leftrightarrow O_2\,(aq)$$

Assuming pressure is low enough so that partial pressure is approximately equal to fugacity, the equilibrium constant for this reaction can be written:

$$K_H = \frac{\gamma C_{O2}}{P_{O2}} \qquad \textbf{Equation 5-43}$$

The equilibrium constant K_H is termed Henry's constant, which, like all equilibrium constants, is temperature dependent. The temperature dependency of any equilibrium constant can be derived from the relationship between free energy and enthalpy, which can be written as:

$$\frac{\partial \ln K}{\partial T} = \frac{\Delta H^o}{RT^2} \qquad \textbf{Equation 5-44}$$

Over the limited temperature range of interest in this work ΔH^o can be assumed constant and the integrated form of Equation 5-44 can be used (Sawyer *et al.*, 1994), that is:

$$\log\frac{K_{T2}}{K_{T1}} = \frac{-\Delta H^o}{2.3R}\left(\frac{T_1 - T_2}{T_1 T_2}\right) \qquad \textbf{Equation 5-45}$$

The values of Henry's constant at 25°C (K_{T1}) are given in Table 18 (from Stumm & Morgan, 1996). Values at other temperatures are calculated from Equation 5-45, used in conjunction with the thermodynamic data given in Appendix II. (Equation 5-45 can also be used to calculate the standard electrode potential at any given temperature, again using data given in Appendix II.)

Gas	*K_H (M/atm)*
O_2	1.26×10^{-3}
CH_4	1.29×10^{-3}

Table 18 *Henry's Coefficients at 25 ℃*

Solubility of gasses tends to decrease with increasing ionic strength, an effect known as 'salting out'. This effect can be accounted for by estimating the activity coefficient of neutral species (γ in Equation 5-43), which can be estimated via the following empirical formulation (Berner, 1971):

$$\log(\gamma_i) \approx k_m I \qquad \textbf{Equation 5-46}$$

where k_m is the salting coefficient, which can be taken to be 0.1 (Morel & Hering, 1993). This treatment is not exact, but allows the influences of varying ionic strength to be incorporated into the model in a manner that is both tractable and consistent. Finally, it should be noted that the evolution of N_2 is not modelled explicitly and the partial pressure of nitrogen is assumed to be 0.78 atmospheres.

Once the activity coefficients of each component species are determined, the activity of each porewater component can be calculated simply by multiplying the concentrations by the activity coefficients. The activities of the components associated with the dominant metabolic pathway at each depth are then substituted into the Nernst Equation (Equation 4-1) and the redox potential calculated (Appendix I includes more details concerning the calculation of Eh).

5.10 The Model Domain

The fifteen model equations describe the distribution of the component species throughout the model domain. The extent of the domain is defined as:

$$0 \leq x \leq L$$

$$0 \leq t \leq \infty$$

where L is the maximum depth of sediment considered, measured vertically down from the SWI (at $x = 0$), and t is time. The model domain in time is therefore semi-infinite.

5.11 Auxiliary Conditions

The model equations described in Section 5.7 involve indeterminacies that can only be removed by specifying appropriate boundary and initial conditions. In the redox model, the upper boundary condition for organic carbon (J_{org}) is specified as a known flux (Robins or type 3 boundary condition), implemented as:

$$J_{org} = -\xi_{swi} D_b(0) \left(\frac{\partial G}{\partial x} \right)\Bigg|_{x=0} + \xi_{swi}\, \omega(0) G(0) \qquad \textbf{Equation 5-47}$$

The known flux (J_{org}) is assumed to be the net flux of carbon that is available for incorporation into the sediment. Hence, post-depositional redistribution of organic carbon via processes such as resuspension and lateral advection are assumed implicit in the specified carbon flux.

A no-flux (Neumann or type 2) condition is specified at the upper boundary for the three authigenic species (FeS, $FeCO_3$, and $MnCO_3$). This no-flux condition is implemented using a formula analogous to Equation 5-47 but with the known value as zero.

Known concentrations (Dirichlet or type 1 boundary conditions) are used at the upper boundary of all the other species; that is:

$$C(0) = \textit{known value} \qquad \textbf{Equation 5-48}$$

Hence, no account is taken of the diffusive sub-layer that can influence diffusive fluxes at the SWI under some hydrodynamic regimes (e.g. Jørgensen & Revsbech, 1985, Boudreau, 1996).

The lower boundary condition for all species is specified as a zero gradient (Neumann or type 2), which therefore forces the gradients at the lower boundary to be zero; that is:

$$\left.\frac{\partial C}{\partial x}\right|_{x=L} = 0 \qquad \textbf{Equation 5-49}$$

The initial concentrations of each component species throughout the model domain are also required. Steady state problems (see below) are relatively insensitive to the initial conditions specified, and any reasonable function can be used. For example, exponential functions are used to approximate the initial depth distribution of organic carbon and oxygen. For unsteady problems the initial conditions are more important, as discussed in Chapter 6 (Section 6.9.2).

5.12 Solution Techniques

The set of fifteen equations with auxiliary conditions make up a fully specified problem that can be solved. However, the equations include non-linear terms and are extensively coupled through the rate laws (see Table 16). The complexity of the model means that an analytical solution can not be obtained and numerical methods must therefore be used.

Finite differences have therefore been used to discretise the model equations. Hence, the continuous model domain is replaced with a discrete analogue defined as:

$$0 \le i\Delta x \le L \quad (0 < i < N)$$

$$0 \le n\Delta t \le \infty \quad (0 < n < \infty)$$

where i and n are integer indices in space and time respectively and N is the number of nodes. Concentrations are therefore calculated at discrete points, rather than continuously, and the numerical solution consists of a set of fifteen vectors that simultaneously satisfy the model equations and auxiliary conditions throughout the model domain.

Two numerical solution techniques have been implemented. The first uses a full differencing approach, which is suitable for obtaining the numerical solution for steady state conditions. The second technique uses the numerical method of lines, which can be used to solve the model under transient conditions. Both methods are discussed in more detail below.

5.12.1 Steady State Solution

A steady state system is by definition time invariant and the time derivative in the model equations can therefore be set to zero. However, in the solution technique outlined below, the time derivative has been retained and discretised using finite differences. This allowed large 'time steps' to be specified, which accelerated the convergence of the scheme. Furthermore, this solution technique could be extended to satisfy transient conditions. However, the numerical techniques required to solve transient problems are complex, and it is more sensible to use a peer reviewed integrator, as discussed in Section 5.12.2 below.

5.12.1.1 Discretisation Scheme

Finite difference approximations are used to represent each of the derivative terms in the model equations. In the case of interstitial species, the derivatives are discretised using a standard finite difference scheme. Similar schemes have been used to solve a number of diagenetic models detailed in the literature (e.g. Rabouille & Gaillard, 1991a; 1991b; Van Cappellen & Wang, 1995; Van Cappellen & Wang, 1996). The time derivative is replaced with a first order finite difference approximation:

$$\frac{\partial C}{\partial t} = \frac{C_i^{n+1} - C_i^n}{\Delta t} \qquad \textbf{Equation 5-50}$$

where Δt is the time step, 'n' is the index in time and 'i' the index in space. The first and second derivatives in space are replaced with central difference (second order accurate) approximations; that is:

$$\frac{\partial C}{\partial x} = \theta\left(\frac{C_{i+1}^{n+1} - C_{i-1}^{n+1}}{2\Delta x}\right) + (1-\theta)\left(\frac{C_{i+1}^{n} - C_{i-1}^{n}}{2\Delta x}\right) \qquad \textbf{Equation 5-51}$$

and

$$\frac{\partial^2 C}{\partial x^2} = \theta\left(\frac{C_{i+1}^{n+1} - 2C_i^{n+1} + C_{i-1}^{n+1}}{\Delta x^2}\right) + (1-\theta)\left(\frac{C_{i+1}^{n} - 2C_i^{n} + C_{i-1}^{n}}{\Delta x^2}\right) \qquad \textbf{Equation 5-52}$$

where Δx represents the constant spacing between each node. Theta (θ) is a weighting coefficient that specifies the time step (actually iteration step for a steady state solution, see below) from which the concentrations are taken. Theta can be set to any value between zero and one. If theta equals one the scheme is fully implicit; concentrations are taken at the new time step (n+1). If theta equals zero then the scheme is fully explicit; all information comes from the previous time step (n).

A popular choice for theta is 0.5, which gives the Crank-Nicolson scheme. This scheme is second order accurate in both time and space due to the cancellation of error terms. However, under steady state conditions the model solution is time invariant and accuracy in time is therefore meaningless. Hence, a steady state solution can be obtained using a fully implicit scheme (that is, with theta set to one), which has the advantage of being unconditionally stable. This then allows large 'time steps' to be specified to accelerate convergence, without affecting the accuracy.

The model equations for solid species are discretised using essentially the same scheme described above. However, a central difference approximation of the first derivative in space can give rise to spurious oscillations when used to model transport that is advection dominated (e.g. Abbott & Basco, 1989; Boudreau, 1997). Unfortunately, transport of solids is always advection dominated below the bioturbation zone. Hence, a central difference formulation could give rise to numerical problems in this region of the model domain. Following the example of Boudreau (1996), a blended finite difference scheme has therefore been used to represent the first derivative in space (see also Fiadeiro & Veronis, 1977). This scheme can be written:

$$\frac{\partial C}{\partial x} = \left(\frac{(1-\sigma)C_{i+1} + 2\sigma C_i - (1+\sigma)C_{i-1}}{2\Delta x}\right) \qquad \textbf{Equation 5-53}$$

Note, for clarity the weighting coefficient and time indices are not shown.

This formulation is a blend of an upwind and a central difference approximation. The parameter σ is defined in terms of the grid Peclet number (*Pe*):

$$\sigma = \coth(Pe) - (\frac{1}{Pe}) \qquad \textbf{Equation 5-54}$$

with the grid Peclet number (*Pe*) given by:

$$Pe = \frac{\omega \Delta x}{2D_b} \qquad \textbf{Equation 5-55}$$

Boudreau (1997) notes that Equation 5-54 has the following properties:

$$\sigma = 0 \quad \text{for } Pe \to 0$$

$$\sigma = 1 \quad \text{for } Pe \to \infty$$

The blended scheme therefore reduces to a central difference approximation at low grid Peclet numbers (diffusion dominated, $Pe \to 0$), but reverts to an upwind approximation when transport is advection dominated (high grid Peclet number, $Pe \to \infty$). The advantage of this scheme is that it ensures that an appropriate finite difference approximation is automatically used at all points in the solution domain. In addition, Boudreau (1997) notes that the scheme remains second order accurate even when it switches to the upwind approximation, which is nominally first order accurate.

5.12.1.2 Solution Algorithm

Discretising the model equations using the finite difference approximations discussed above reduces each diagenetic equation to a set of algebraic equations of the form:

$$\alpha C_{i+1}^{n+1} + \beta C_i^{n+1} + \gamma C_{i-1}^{n+1} = \delta_i$$

The variables ($\alpha, \beta, \gamma, \delta$) thus form a tridiagonal matrix that can be readily solved (inverted) species by species using a double sweep (Thomas) algorithm. The Thomas algorithm is an efficient and robust method for solving tridiagonal systems of equations. Its implementation,

including the incorporation of the various boundary conditions, is detailed in many numerical references (e.g. Press *et al.* 1992) and is not described herein.

The extensive coupling of the equations and non-linearity of some reaction terms means that a solution to the overall model can only be obtained iteratively. Two levels of iteration are therefore incorporated into the steady state solution algorithm. The first is a local iteration loop that accounts for the non-linearity in the reaction terms of each equation. The convergence of this local loop is improved by a Newton-Raphson iteration, which gives quadratic convergence, and is based on the following formulation:

$$R_i^k = R_i^{k-1} + \left.\frac{\partial R}{\partial C}\right|_{i,k-1} \left\{C_i^k - C_i^{k-1}\right\} \qquad \textbf{Equation 5-56}$$

where R is the reaction term of the model equation being solved and k indicates the iteration number. The derivative with respect to the dependent variable in Equation 5-56 can be calculated analytically.

The second level of iteration is a global loop that accounts for the coupling between the model equations and uses functional iteration. In functional iteration the solution vector from the previous iteration is simply used as an input to the next iterative step. Iteration continues until a user defined convergence criterion is met. The criterion for both iteration loops is defined as:

$$\varepsilon \leq \frac{\left|C_{new} - C_{old}\right|}{C_{new}} \qquad \textbf{Equation 5-57}$$

where C_{new} is the concentration calculated in the current iteration, C_{old} is the concentration calculated during the previous iteration, and ε is a user defined tolerance typically of the order 10^{-6} to 10^{-8}. This version of the redox model is hereafter referred to as the 'steady state version'.

5.12.2 Transient Solution

As noted above, the full differencing method described in the previous section could be extended to model the transient behaviour of the sedimentary system. However, an alternative approach using the Numerical Method of Lines (NMOL) has been used, which has a number of significant advantages associated with it. This version of the redox model is hereafter referred to as the 'NMOL version'.

5.12.2.1 Discretisation Scheme

In the NMOL, the spatial derivatives on the RHS of the model equations (Equations 5-27, 5-29, and 5-30) are replaced with the finite difference approximations discussed above. This has the effect of reducing the RHS of the equation to an algebraic expression. However, the first derivative in time on the LHS is left in analytical form. Hence, the partial differential equations in two independent variables (t, x) are converted to a large system of autonomous ordinary differential equations in one independent variable (t). (NB: additional model details can be found in Appendix I.)

5.12.2.2 Boundary Conditions

Dirichlet boundary conditions can be easily incorporated into the NMOL without any additional discretisation. The known concentrations are simply substituted into the ordinary differential equation (ODE) written for the first internal node.

The known-flux boundary condition for organic carbon (Equation 5-47), however, involves a derivative that must be implemented numerically. The derivative is replaced with a central difference approximation and the flux condition is then given by:

$$J_{org} = -\xi_{swi} D_b(0)\left(\frac{G_1 - G_{-1}}{2\Delta x}\right) + \xi_{swi}\omega(0)G(0) \qquad \textbf{Equation 5-58}$$

G_{-1} indicates a concentration defined at a node outside the model domain, that is, at an imaginary point. This imaginary concentration represents an additional model indeterminacy. This is removed by solving Equation 5-58 for G_{-1} and substituting the result into an additional

ODE written at the boundary, as illustrated by Boudreau (1996, 1997). An analogous process is carried out when implementing the no-flux condition for the three authigenic species.

Concentrations at imaginary nodes can be avoided altogether if an alternative difference approximation is used:

$$\left.\frac{dC}{dx}\right|_{x=0} = \frac{-3G(0)+4G(1)-G(2)}{2\Delta x} \qquad \textbf{Equation 5-59}$$

This approximation is also second order but its error term has a higher coefficient than that associated with a central difference approximation (Schiesser, 1991). Hence, the more accurate central difference approximation has been used.

The zero gradient condition at the lower boundary (Equation 5-49) is also implemented using a central difference approximation. The boundary condition can then be written as:

$$\left.\frac{dC}{dx}\right|_{x=N\Delta x} = \frac{C(N+1)-C(N-1)}{2\Delta x} = 0 \qquad \textbf{Equation 5-60}$$

As Boudreau (1996, 1997) notes this relationship implies that:

$$C(N+1) = C(N-1)$$

where C(N+1) is a concentration at an imaginary point. Writing an additional ODE at the boundary again eliminates this indeterminacy.

5.12.2.3 Solution Method

Each dependent variable (that is, the concentrations at each node) in the system of ODEs ultimately depends upon all other dependent variables. Hence, the whole system of equations must be integrated simultaneously. Moreover, the equations involve reaction rates that vary over a number of orders of magnitude. Hence, the solution could contain transients that are fast when compared to the time span of integration; that is, the system of equations must be considered stiff. Following the example of Boudreau (1996, 1997), the system of ODEs is therefore solved using the stiff ODE integrator VODE (Brown *et al.*, 1989).

VODE is a public domain software package for solving systems of first-order initial-value ODEs. The package uses the variable-order, fixed-leading-coefficient Backward Differentiation Formula (BDF) method to solve stiff problems. The Jacobian matrix can be treated as full or banded -- in this study the form of the model equations allows the dependent variables to be indexed so as to take advantage of the banded form, which can be solved more efficiently. VODE incorporates many useful functions, such as automatic error estimation and adaptive step size control. The package also automatically deals with floating point exceptions. Finally, VODE allows the Jacobian matrix to be approximated numerically.

The ability to integrate the system of ODEs using a well-tested peer reviewed integrator is a significant advantage since it removes a large part of the coding effort. Code must be written to input and output data and to define the RHS of the ODEs. However, no explicit consideration of the solution algorithms is required. The NMOL therefore allows a modular approach to be taken in code development.

The NMOL version of the redox model can also be used to generate steady state profiles simply by specifying constant parameters and boundary conditions and then integrating the model equations over a sufficiently long period. However, such calculations take much longer to converge ($\approx$ order 10 times) than an equivalent run using the steady state code described above. This is especially true when the initial guesses of the concentration profiles are poor because the integrator (VODE) controls the step size (Δt) so as to maintain a user defined accuracy level. Hence, small time steps are still selected by the integrator at the beginning of the run, even though there is actually no interest in the profiles calculated at this time.

5.13 Model Implementation

The redox model is implemented as a number of FORTRAN 77 computer programs, which can compile under both Windows and UNIX operating systems. Some common non-standard FORTRAN extensions have been used, so the portability of the code is likely but not

guaranteed. Input to the programs is mainly via a simple template that is modified by the user. In addition, the programs also require some manual input at the beginning of each run. Various data are output, including:

1. The concentration profile of each component species.
2. Internal model checks (mass balances and residuals).
3. The percentage of organic carbon oxidised via each metabolic pathway.
4. The percentage of carbon buried.
5. The depth profile of the rates of organic carbon oxidation for each metabolic pathway.
6. The depth profile of redox intensity.

5.14 Model Summary

The redox model is based on a multi component early diagenetic model and can be summarised thus:

1. The model consists of fifteen coupled 1-D reaction-transport equations.
2. Local transport is both advective and diffusive.
3. Coupling is through the reaction terms.
4. The rate laws and stoichiometries of reactions are taken from the literature.
5. The model is discretised using a blended/centred finite difference scheme and solved numerically.
6. A redox profile is calculated from the vertical distribution of the component species.
7. Unsteady and steady state versions of the model have been written

The main modelling assumptions include:

1. The sediment can be represented as a continuum.
2. A 1-D approximation is adequate; horizontal heterogeneity can be 'averaged out'.
3. The physical structure of the sediment is adequately parameterised by porosity (sediment texture has more influence on the metazoa then the microbial assemblage, so this assumption is not too limiting in terms of the overall modelling approach).

4. Compaction is at steady state.
5. Molecular/ionic diffusion and bioturbation are adequately described using a simple Fickian analogue.
6. Tortuosity is related to the porosity of the sediment.
7. The effect of irrigation can be represented using a non-local exchange function.
8. The composition of the POM can be expressed as the average C:N:P ratio.
9. The boundary condition for organic carbon is assumed to be the net flux of carbon that is available for incorporation into the sediment; post-depositional redistribution of organic carbon is implicit in the specified carbon flux.
10. Inputs of dissolved organic matter (DOM) into the sediment are not significant.
11. POM degradation can be represented using simple bulk (G-type) reactions.
12. Metabolic succession is represented using an inhibition scheme.
13. pH is constant through the model domain.
14. Reactions between component species are adequately modelled using simple rate laws.
15. Heterogeneous reactions can be modelled as pseudo-homogenous.
16. Interfacial (adsorped) phases of Mn and Fe can be considered as part of the corresponding authigenic component species.
17. Adsorption of ammonia follows a simple linear isotherm.
18. Total activities can be estimated using a simplified treatment (e.g. the Davies formula).
19. The redox potential at any depth can be calculated from the total activities of the oxidant and associated reduced product of the dominant metabolic pathway.

Chapter 6

6. MODEL VERIFICATION AND ANALYSIS

6.1 Introduction

Chapter 5 described the mathematical formulation and computer implementation of a sedimentary redox model. Both these stages of model development are central to the overall modelling process. However, once coded the model must still be verified to ensure that the computer algorithms have been implemented correctly. When this has been accomplished, the model can be analysed.

This Chapter describes the verification and analysis of the redox model. A description of the internal checks that have been included in the model code is presented first. An account is then given of the methods used to verify the implementation of the model equations. A sensitivity analysis using a simple parameter perturbation technique is then outlined and results discussed. This is followed by a consideration of various empirical relationships given in the literature that allow various important parameter values to be estimated. These empirical relationships are then used to examine the response of the model for a range of idealised depositional environments.

The Chapter ends by considering the modelling of transient systems. The simple functions used to represent the seasonal variations in sedimentary processes are discussed. The influence of initial conditions on the model output is then demonstrated. Finally, it is shown that steady state solutions can be related to the yearly averaged solutions of an equivalent transient case.

6.2 Model Internal Checks

The computer programs that implement the redox model incorporate two internal checks -- the mass balance of each component species and the residuals of each diagenetic equation:

6.2.1 Mass Balances

At steady state the mass flux into and out of the model domain must, by definition, be balanced by the reactions occurring within. Hence, the steady state mass balance for each component can be expressed as:

$$\text{Mass balance} = \frac{\text{Flux in} - \text{Flux out}}{\int \text{Reaction rate } dx} \cdot 100\ \% \qquad \textbf{Equation 6-1}$$

The mass balance is therefore calculated as the percentage of mass accounted for. The flux at the upper boundary (Flux in) is calculated numerically using a four-point (third order) approximation of the concentration gradient (see Boudreau, 1997 p. 360). The integral of the reaction rate is calculated using Simpson's rule.

The mass balance for unsteady conditions must take into account any accumulation that is not balanced by fluxes out of the model domain. Hence, for the transient case the mass balance for each component can be expressed as:

$$\textit{Accumulation} = \textit{Flux in} - \textit{Flux out} \pm \int \textit{Reaction}\ dx \qquad \textbf{Equation 6-2}$$

evaluated over the interval Δt (that is, the time step), with accumulation calculated as:

$$\textit{Accumulation} = \int C dx\Big|_{t+\Delta t} - \int C dx\Big|_{t} \qquad \textbf{Equation 6-3}$$

with all terms having units of mass/area. The fluxes and integrals are again evaluated numerically using a four-point approximation of the concentration gradient and Simpson's rule.

The mass balances of all species improve if the step size (Δx) is reduced. However, the mass balances of a number of components (for example, NO_3^-, Fe^{2+}, Mn^{2+}, CH_4, and TS) do not give a consistent indication of the model performance. This can be illustrated by considering the steady state nitrate profiles shown in Figure 15. These profiles were calculated for the same input conditions but with different space steps. The space steps used and mass balances are

detailed in Table 19. It can be seen that whilst the mass balance changes considerably over the range of Δx specified, the concentration profiles do not.

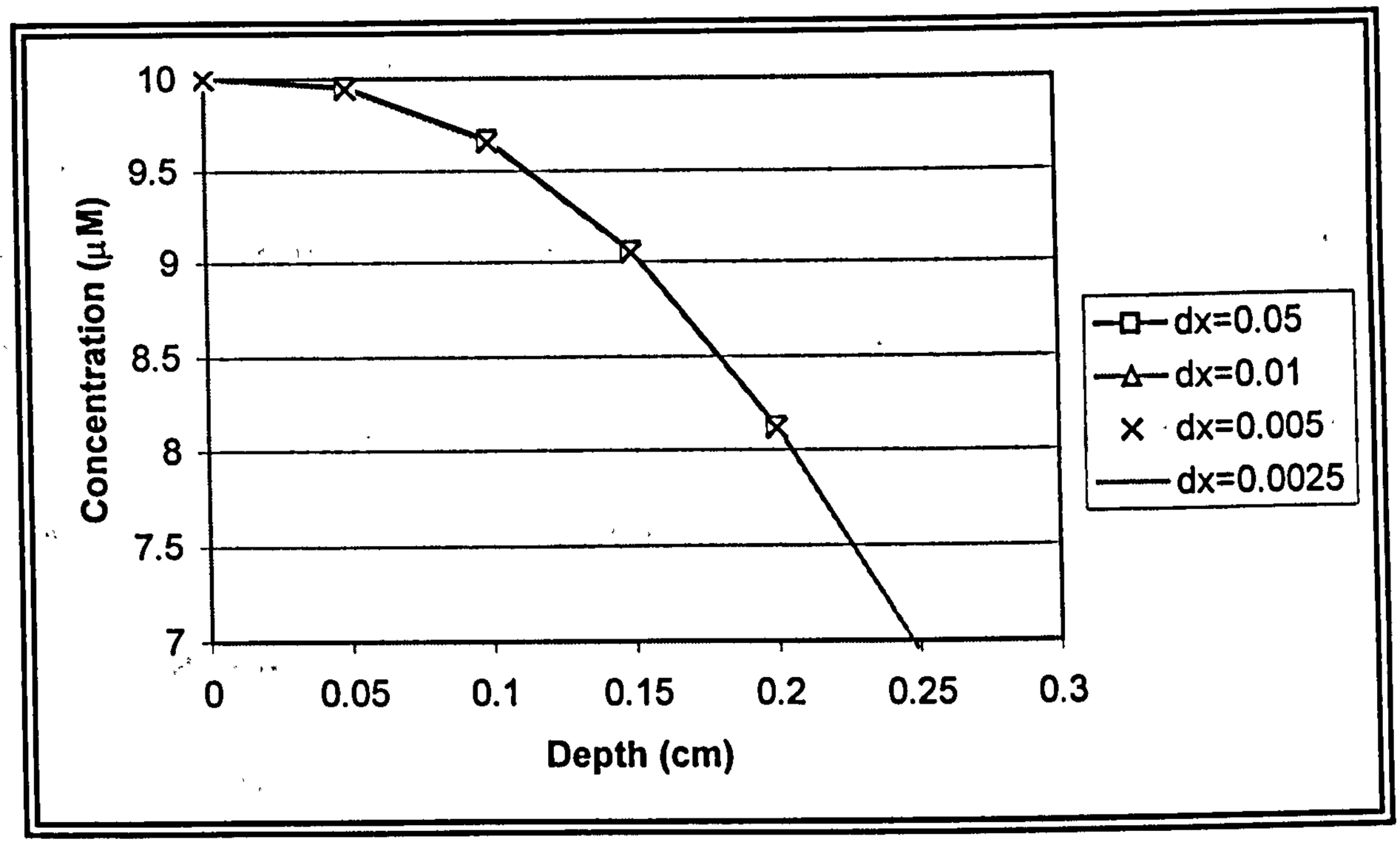

Figure 15 *Nitrate Profiles at Various Space Steps*

Space step Δx (cm)	Mass Balance (%)
0.05	429.3
0.01	106.8
0.005	101.5
0.0025	100.3

Table 19 *Mass Balances for the Nitrate Profiles*

The poor mass balance at coarser resolutions is related to the depth over which the flux at the upper boundary is estimated. As noted above, this flux is calculated using a four-point approximation of the concentration gradient. Hence, when a space step (Δx) of 0.05 cm is used the concentration gradient is approximated over a depth of 0.2 cm; that is, almost the whole depth illustrated in Figure 15. In contrast, when a space step of 0.0025 cm is specified this same gradient is estimated over a depth of just 0.01 cm. It is therefore not surprising that the

larger space step does not adequately resolve the gradient near the boundary and gives a poor estimate of the flux.

A poor mass balance can therefore be an artefact of a sharp gradient at the upper boundary. Consequently, the computational effort required to achieve a satisfactory mass balance for all species is not necessarily reflected in a significant change in the concentration profiles. The mass balance for organic carbon does, however, give a more consistent indication of the model performance. For this component species, a satisfactory mass balance (of the order 100 ±0.1 per cent) can usually be attained with a Δx of 0.025 cm.

6.2.2 Residuals

The residuals of each component are calculated by substituting the appropriate solution vector into a discrete analogue of the corresponding model equation, discretised using central differences. The residuals indicate if the solution vectors are satisfying the model equations under the prescribed conditions. As with mass balances, residuals improve (decrease) with decreasing space step (Δx).

6.3 Model Verification

A number of levels of testing were carried out to verify that the model equations had been implemented correctly. The model output was first compared with a simple analytical solution of the diagenetic equation. The output generated by the NMOL and the steady state versions of the model were then compared to ensure they were consistent under a range of input conditions. Finally, two peer-reviewed models were used as benchmarks. All three verification procedures examined the individual concentration profiles generated by the model, rather than the redox profile, and are described in more detail below.

6.3.1 A Simple Analytical Solution

As noted previously, the non-linearity and coupling of the model equations means that an analytical solution can not be obtained for the redox model as a whole, nor for most of the individual constituent equations. However, an analytical solution can be readily derived for the organic carbon species when degradation is specified as a 1-G formulation and the depth distribution of bioturbation is represented using a two-layer model, as shown in Appendix III.

Figure 16 compares this analytical solution with three equivalent profiles generated by the redox model, using space steps (Δx) of 0.1, 0.025 and 0.005 cm. The solutions have been plotted over a model depth of only 1 cm to allow the differences in the profiles to be seen more clearly. In addition, the plot focuses on the depth where the discontinuity in the bioturbation coefficient occurs, since this is where any numerical scheme is most susceptible to instabilities and inaccuracy.

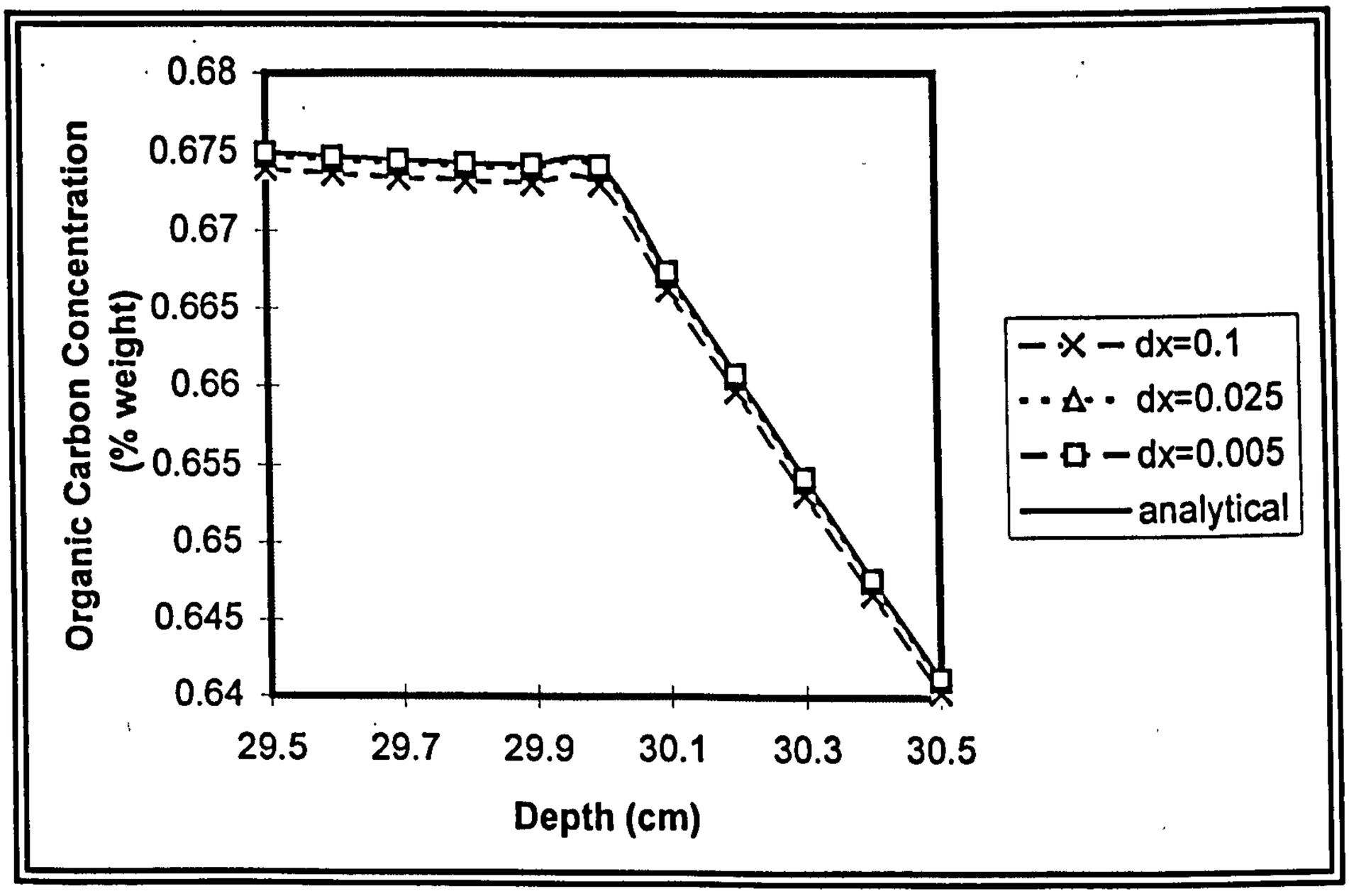

Parameter values: D_b; 10 cm^2/yr: ω; 1cm/yr: Jorg; 1050 $nm/cm^2/yr$: mixing depth X_L; 30cm: decay constant k_1=0.1/yr

Figure 16 *Comparison of the Model Output with a Simple Analytical Solution*

As the Figure indicates, the numerical model gives a reasonable approximation to the analytical solution for each of the space steps used. Furthermore, the numerical solution approaches the analytical solution as the space step is reduced. At a space step of 0.005 cm the numerical and analytical solutions are essentially indistinguishable (maximum error for all nodes: 0.006%).

6.3.2 Consistency of the Steady State and NMOL Versions

The two versions of the redox model use different solution techniques to solve what is essentially the same set of equations. Both versions of the model should therefore produce consistent outputs. To verify that this was the case, steady state outputs from both the NMOL and the steady state versions of the model were compared, using a range of input conditions. (As noted previously, the NMOL version of the model can be used to model steady state conditions simply by specifying constant boundary conditions and integrating over a sufficiently long period.)

It was found that the model outputs were consistent when a low flux of carbon was specified. However, the output from the two versions of the model started to diverge slightly as this flux was increased; that is, a difference in the concentration profiles of a number of component species was observed. It was subsequently determined that this divergence could be eliminated by running the steady state version of the model with a space step smaller than that used in the NMOL version.

The source of the divergence was identified as the numerical representation of the flux condition at the upper boundary. As discussed previously, this type of boundary condition is implemented in the NMOL version of the model using a second order accurate approximation of the spatial derivative (see Equation 5-58). Conversely, the tridiagonal scheme used to solve the steady state version employs a less accurate first order approximation for this boundary condition (e.g. Press *et al.*, 1992).

To confirm that this was the source of the divergence, Dirichlet boundary conditions were temporarily specified for all of the component species. (Since this type of boundary condition does not require a numerical approximation of a derivative, its representation is consistent in both versions of the model.) With the modification the two versions of the model gave the same output, at the same space step, for all input conditions tested. It was therefore concluded that whilst both versions of the model are consistent, the NMOL version is more accurate, at least for those components that have flux boundary conditions.

6.3.3 Comparisons with Benchmarks

Diagenetic models can be tested by fitting the model output to sedimentary data sets (e.g. Wang & Van Cappellen, 1996). However, given that the use of diagenetic equations is well established, this type of verification was considered unimportant. (Although, in Chapter 7 such an exercise is carried out to demonstrate various aspects of model calibration.) Nevertheless, it was still considered necessary to compare the model output to some independent benchmark. This was achieved by using two peer-reviewed diagenetic models to generate concentration profiles for a range of known conditions. The models used to generate these 'benchmarks' were: CANDI, a model written by Boudreau (1996) solved using the NMOL; and STEADYSED1 a model written by Van Cappellen & Wang (1995, 1996) solved using the Thomas algorithm.

The redox model and the two peer-reviewed models were compiled on a UNIX workstation using a SPARC compiler. Each model was then run for a variety of steady state scenarios, using the input conditions detailed in Appendix IV. The concentration profiles generated by each model were then plotted and compared. However, whilst the three models are similar, they are not exactly the same, and these differences had to be taken into account during the comparison. Simply setting appropriate rate constants in the peer-reviewed models to zero could accommodate some of the differences. In the case of CANDI, a zero rate constant was specified for a number of reactions involving solid sulphide phases (both AVSs and pyrite). In

the case of STEADYSED1, the rate constants of reactions involving interfacial Mn and Fe species were set to zero. Other differences required some modification of the model codes, as described below.

6.3.3.1 Comparison With CANDI

The profiles generated by the unmodified redox model followed the same general trends as those generated by CANDI. However, the fit of the individual concentration profiles was poor. For example, for test case 3 (see Appendix IV) the concentration of organic carbon at the SWI was nine per cent higher in the profile generated by CANDI. The difference between the model outputs were investigated and found to be due to the following factors:

1. CANDI uses a different tortuosity function.
2. The effect of bioturbation on the diffusion of solutes is ignored in CANDI; a reasonable assumption for most scenarios given the difference in the magnitude of the diffusion coefficients.
3. CANDI uses a modified inhibition scheme that does not require an inhibition constant for Mn and Fe oxides.
4. A different rate law for the oxidation of organic carbon via Mn and Fe oxide reduction is used in CANDI, which does not require a half saturation constant.
5. Different stoichiometries are used for the following reactions:
    - NO_3 reduction
    - NH_4 production
    - Oxidation of HS^- by $Fe(OH)_3$
    - Oxidation of CH_4 by O_2
6. The reaction rate for precipitation of FeS is specified with different units.

Appropriate modifications were made to the redox model code except for the tortuosity function, which was changed in the code for CANDI.

6.3.3.2 Comparison with STEADYSED1

The profiles generated by the unmodified redox model were again found to be different to those generated by STEADYSED1. These differences were investigated and found to be due to the following factors:

1. STEADYSED1 uses a modified monod scheme, the details of which can be found in Van Cappellen & Wang (1996).
2. Known flux boundary conditions are used for both the Mn and Fe oxides at the upper boundary.
3. STEADYSED1 calculates the pH of the sediment, which changes the values of various equilibrium constants used in the model.
4. A different function is used to calculate the temperature and salinity corrected diffusion coefficients; see Van Cappellen & Wang (1995) for details.

The code for the redox model was again modified in accordance with these factors except for the pH, which was made constant in the code of STEADYSED1.

The subsequent comparison between outputs of STEADYSED1 and the modified redox model highlighted one problem with this approach to verification; that it presupposes that the model being used as a benchmark is correct. However, two minor errors were identified in the STEADYSED1 code. The first error is associated with the precipitation reactions. Solute and particulate concentrations are calculated in different units in STEADYSED1 (mass/volume and mass/mass respectively) and porosity gradients are not considered. Hence, the authors apply a unit conversion factor to heterogeneous reaction terms. However, in the code for STEADYSED1 this conversion factor is applied incorrectly to the precipitation reactions, which results in terms with inconsistent units (see lines 1420, 1506, 1593 of STEADYSED1 code).

The second error is the omission of the hydrogen ion activity from the precipitation reaction in the sulphide species (see lines 2047, 2049, 2055 of STEADYSED1 code). In addition,

STEADYSED1 sets all O_2 concentration less than 10^{-8} M to zero. This had a noticeable effect on the hydrogen sulphide and sulphate profiles when input conditions produced a significant amount of sulphate reduction. These errors meant that the profiles output by the redox model could not be matched to those generated by STEADYSED1.

STEADYSED1 was modified to remove the second error and to allow oxygen concentrations to take non-zero values less than 10^{-8} M. Modification of STEADYSED1 to eliminate the first error was also attempted, but the resulting code did not converge. This problem was circumvented by rewriting the precipitation reactions in the redox model such that the rate constant was expressed in terms of mass/volume rather than in mass/mass as quoted in Van Cappellen & Wang (1995,1996).

6.3.3.3 Summary of Results

The concentration profiles generated by the models were compared visually to one another. In addition, the percentage difference between the concentrations at each node was calculated and then averaged over the whole domain to give a simple measure of the goodness of fit. As noted above, the unmodified model produced concentration profiles that only reflected the general trends of the peer-reviewed models. However, with appropriate modifications the output of the models matched to a high degree (percentage error at each node: order 0.1% or better). This confirmed that the diagenetic equations underlying the redox model had been implemented correctly. (Since the model outputs were effectively indistinguishable, comparative plots have not been included herein.)

At the end of the testing it had been established that the difference between the output of the unmodified redox model and the peer-reviewed models was due to a different formulation, rather than any errors. Furthermore, because of the verification procedure three versions of the redox model were available: the redox model as described in Chapter 5; a version consistent

with CANDI; and a version consistent with STEADYSED1. However, only the original version of the model is considered hereafter.

6.4 Sensitivity Analysis

The redox model contains a large number of parameters (listed in Appendix IV), each of which effects the model output to some degree. A sensitivity analysis was therefore carried out to examine the influence of each parameter on the model redox profile. Such an analysis serves two main functions. Firstly, it identifies parameters that must be accurately constrained if uncertainty in the model output is to be reduced. Secondly, it highlights the model processes that are of most significance to the redox state of the sediment. By inference, the analysis also identifies unimportant parameters and can thus guide any subsequent simplification of the model deemed appropriate. A sensitivity analysis can also be used to identify the range of parameter values to which the model output is most sensitive. However, as discussed below, this was not possible in this study.

6.4.1 Method

Various approaches to sensitivity analysis have been developed (e.g. Hamby, 1994; 1995). However, the complexity of the redox model, together with a lack of knowledge concerning the statistical distribution of parameter values, meant that the application of the more elegant techniques was problematic. A simple 'one at a time' parameter perturbation technique was therefore used, which involves the following steps:

1. A baseline condition is specified where all parameters are set to a 'typical' value for the scenario in question; in this case a coastal sediment.
2. The value of one parameter is changed from the baseline and the model output generated. All other parameters are held constant at their baseline values. This 'parameter perturbation' is then repeated until the parameter has been varied over a specified range.
3. The sensitivity of the model to the parameter in question is assessed by examining the range in model output associated with the range of parameter values.

4. The parameter perturbation (that is, step 2 & 3) is repeated for all model parameters.

6.4.1.1 The Baseline: a 'Typical' Coastal Sediment

Two baselines were used in the analysis, hereafter designated as base-case 1 (bc1) and base-case 2 (bc2). The typical parameter values used for both baselines are detailed in Appendix V, and are similar to those given in Van Cappellen & Wang (1995) for a 'typical' coastal sediment (see parameter listing 'coast 2' in Appendix IV). The main difference was that the Mn and Fe oxide concentrations were set at 0.25 per cent by weight, as in the test cases used by Boudreau (1996). For the main analysis, the transport coefficients and porosity were set constant throughout the model domain; that is the depth dependence was ignored. (However, the sensitivity of the model to these depth dependencies was subsequently examined, as described below.)

The two base-cases differ only in the way that the rate constants of the primary redox reactions were specified. This allowed the analysis to assess whether or not the model sensitivity depends upon the representation of degradation used. For base-case 1, all six rate constants were set to the same value; degradation was therefore modelled according to 1-G kinetics (referred to hereafter as the 1-G representation of degradation or 1-G case). In base-case 2, the rate constants were set at different values (referred to hereafter as the 6-D representation of degradation or 6-D case). The following arbitrarily selected relationships were used:

$$V_{o2}=V_{no3}$$

$$V_{mn4}=V_{fe3}=V_{o2}/2$$

$$V_{so4}=V_{ch4}=V_{o2}/10$$

As noted previously, this successive reduction in the value of the rate constants represents the decrease in the average lability of organic matter with depth. The relationships between the rate constants were maintained during the parameter perturbation; that is, all six rate constants were varied simultaneously, rather than one at a time.

6.4.1.2 Assessing Model Sensitivity

Model sensitivity could be assessed by visually comparing the full redox profiles generated by the model, as illustrated in Park & Jaffe (1996). However, this approach becomes cumbersome when a large number of model evaluations are considered. As an alternative, the analysis detailed herein examines just two points on the redox profile. The first point is the depth at which the dominant primary redox reaction switches from aerobic respiration to nitrate reduction (designated as characteristic depth d1). The second point is the depth where sulphate reduction becomes the predominant primary redox reaction (designated as characteristic depth d2).

As noted in Chapter 5, the transition from oxygen to nitrate reduction is assumed to occur when the inhibition factor for nitrate reduction exceeds 0.95. For the baselines used herein, this occurs when the oxygen concentration falls below 1 μM. The first characteristic depth (d1) can therefore be considered as a measure of the average depth of oxygen penetration. (Average because the 1-D approach taken herein assumes the horizontal heterogeneity is 'averaged out'.) The second point is the average depth at which the transition from a suboxic (that is, zones of Mn and Fe oxide reduction) to a sulphidic (anoxic) diagenetic regime occurs. Both points are therefore characteristic features of the redox profile in the top portion of the sediment. Furthermore, the depths both vary according to the prescribed sedimentary conditions. This variation can therefore be used to assess model sensitivity.

The sensitivity of the model to each parameter has been expressed in terms of a sensitivity index (e.g. Hamby, 1995). The sensitivity index (SI) was calculated as the ratio of the maximum characteristic depth to the minimum depth for each parameter analysed, that is:

$$SI = \frac{\text{max depth}}{\text{min depth}} \qquad \textbf{Equation 6-4}$$

Two index values were therefore calculated, one for each of the characteristic depths, which were then averaged to give a single sensitivity index for each parameter. This averaged value gives a better measure of model sensitivity since it reflects the effect of each parameter on the overall redox profile, rather than the individual characteristic depths.

6.4.1.3 Parameter Ranges

Wide ranges of parameter values have been determined in studies of the coastal environment. For example, bioturbation coefficients can vary over orders of magnitude, and the concentration of oxygen in the bottom water can vary from zero to supersaturating. This wide range of values was taken into account by perturbing each parameter over a two order of magnitude range.

Most of the parameters were varied over a range from one order of magnitude below the typical value (that is, the baseline parameter value) to one order of magnitude above. However, such a range would be meaningless for the bottom water concentrations of oxygen, sulphate, and total dissolved carbon (TC) because the typical values specified were approximately equal to the maximum observed in coastal waters. Hence, these parameters were perturbed over a range from a minimum value two orders of magnitude lower than the typical, to a maximum equal to the baseline parameter value. It should also be noted that the concentrations of reduced species at the SWI were zero for the baseline selected. These parameters were therefore not included in the analysis.

The parameter value range of two orders of magnitude was divided into thirty intervals using a logarithmic discretisation technique (e.g. Parker, 1997), which is based on a multiplier (b) calculated as:

$$b = \left(\frac{X_f}{X_o}\right)^{\frac{1}{m}} \qquad \textbf{Equation 6-5}$$

where X_f and X_o represent the maximum and minimum parameter values and m represents the number of intervals (30 in this case). The value of the parameter at each interval (X_i) is then calculated from:

$$X_i = b^i X_o \qquad \textbf{Equation 6-6}$$

where i represents the number of the interval ($i = 1..m$). This logarithmic approach ensures that each order of magnitude in the parameter range is adequately represented in the analysis.

The redox model involves three parameters that can not be meaningfully perturbed over a range of two orders of magnitude because the corresponding parameter value range is not observed in coastal sediments. These are the mole ratio of carbon (sx) to nitrogen (sy) in the organic matter (sx:sy is therefore the C:N ratio), the porosity (φ), and pH. The sensitivity of the model to these parameters was therefore tested over different ranges, as detailed in Table 20. These ranges encompass parameter values typically observed in coastal sediments. Since the ranges specified did not span an order of magnitude, a logarithmic discretisation was not required, and the ranges were therefore discretised using equal increments of the size indicated in the Table.

Parameter	*Range*	*Increment*
sx	50-210	10
φ (at SWI)	0.4-0.9	0.05
pH	7.1-8.1	0.1

NB: The value of sy was held constant at 11; the sx range specified corresponds to a C:N of 4.5 to 13.6.

Table 20 *Parameter Ranges used in Additional Analysis*

Finally, as discussed previously, the model involves a number of parameters that are depth dependent; namely the irrigation coefficient, bioturbation coefficient, and porosity. The sensitivity of the model to this depth dependence was examined using a range of both exponential and two-layer models. The form of the exponential profiles was varied by perturbing the decay constants (see Equations 5-31 to 5-33), again over a range of two orders of

magnitude. The 'typical' values of the decay constants were selected from the range of values given in Boudreau (1997). The form of the two-layer models was varied by changing the depth of the upper layer. (The details of the test cases used to examine this aspect of the model are summarised in Table 23 and Table 24.)

6.4.1.4 Model Version Analysed

The sensitivity analysis was carried out using the steady state version of the model. As noted previously, this model version is slightly less accurate than the NMOL version. However, the slight loss of accuracy incurred is far outweighed by the large saving in computational effort achieved. The model code was modified to automate the sensitivity analysis, and the output was changed to include only the following:

1. An integer code denoting the parameter being perturbed.
2. The value of the parameter.
3. The characteristic depths d1 and d2.
4. The mass balance of organic carbon (percentage of carbon accounted for).
5. Three integer flags:
    - Flag 1: Set to 1 if O_2 becomes the dominant oxidant below d1; 0 otherwise.
    - Flag 2: Set to 1 if SO_4 reduction is inhibited below d2; 0 otherwise.
    - Flag 3: Set to 1 if the model did not converge.

The mass balance and three integer flags were included to provide a means of monitoring the quality of the output. The modified code was compiled under a UNIX operating system and a space step (Δx) of 0.01 cm was used throughout.

6.4.1.5 Model Domain

As discussed in Chapter 5, Neumann boundary conditions are specified at the lower boundary of the redox model. The rates of reactions at the base of the model domain should therefore be sufficiently slow that concentration gradients approach zero. If this condition is not met then the Neumann boundary conditions can influence the form of the concentration profiles generated, which could influence the results of the sensitivity analysis. To assess this, the

sensitivity analysis was carried out using two different depths of model domain: 15 cm and 20 cm. The analysis showed that the two depths did result in slightly different characteristic depths (mean difference d1: 0.4%; d2: 0.79%). However, the overall sensitivity of the model was unaffected and the results presented herein refer solely to the model domain of 20 cm.

6.4.2 Results

The number of parameters considered in the main sensitivity analysis was forty-two, giving a total number of model evaluations of 1302 per base-case. The mass balances were better than 100 ±0.1 per cent carbon accounted for in all runs. All integer flags were zero indicating that the model converged and the diagenetic zonation was unidirectional; that is, oxidants became exhausted in sequential order, and significant concentrations below the depth of initial exhaustion did not occur.

The characteristic depths for each of the base-cases are shown in Table 21. The influence of the parameter perturbation on the model output was therefore exhibited in a change in these two depths.

Base-Case	d1 (cm)	d2 (cm)
bc1	0.72	3.46
bc2	1.27	6.37

NB: The characteristic depths for bc2 are deeper because of an implicit difference in the reactivity of the organic carbon.

Table 21 *Characteristic Depths for Base-case 1 & 2*

6.4.2.1 Main Parameter Group

The average sensitivity indices for the main parameter group are listed in Table 22 in descending order. It can be seen that the redox profile is most sensitive to the flux of organic carbon, the rate constants of degradation, and the oxygen concentration at the upper boundary. The model is also sensitive to the transport parameters; namely advection, irrigation, and

bioturbation. The redox profile exhibits only limited sensitivity to the rate constants of the secondary reactions. The model output is insensitive to the rate constants associated with reactions involving methane, and to the precipitation/dissolution reactions, as shown by the SI of 1.0.

The SI values detailed in Table 22 indicate that there is some difference in the model sensitivity for the two base-cases considered. This difference is illustrated in Figure 17, which shows the percentage difference between the average SIs, plotted as:

$$\% \; change = \frac{SI_{bc2} - SI_{bc1}}{SI_{bc1}} .100 \; \% \qquad \textbf{Equation 6-7}$$

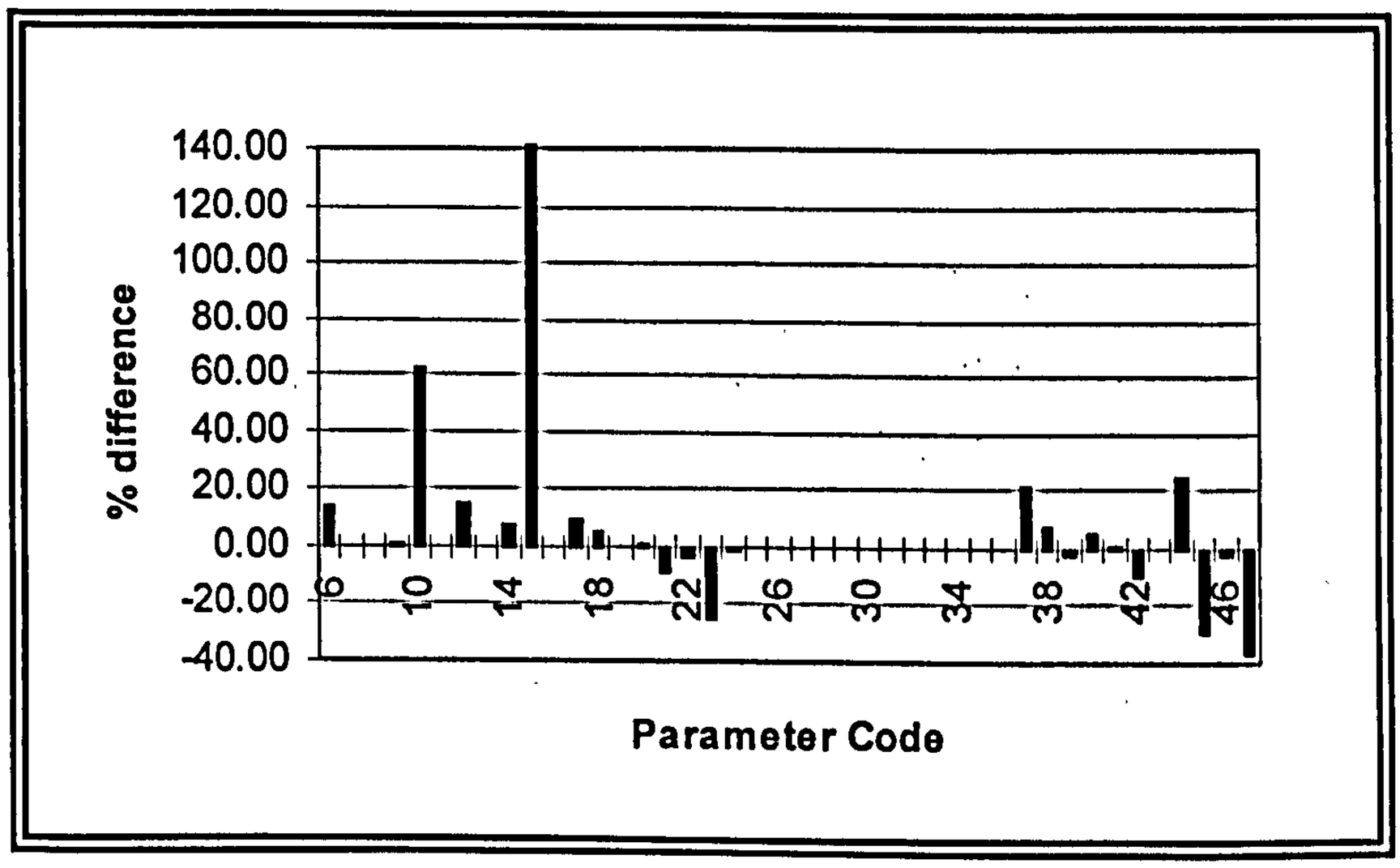

NB: A parameter key is given in Appendix VI; however, the interpretation of the graph is discussed in the text.

Figure 17 *Comparison of Sensitivity of the Two Base Cases*

A positive difference in Figure 17 indicates a parameter to which the model is more sensitive when conditions are specified as in base-case 2; a negative difference indicates the opposite. The Figure shows that when the 6-D representation of degradation is used, as in base-case 2, the model is more sensitive to parameters that characterise the primary redox reactions. The sensitivity of the model to transport processes is also affected. Overall, however, the most

striking difference is the increased sensitivity to parameters that characterise the metabolic reduction of Fe-oxide (that is, parameter 10 & 15; the inhibition constant and the half saturation constant for Fe-oxide reduction). This is hardly surprising given that the sensitivity analysis is based on the depth where this reaction becomes displaced by sulphate reduction.

The correlation between each parameter and the model response was examined by plotting the characteristic depths against the corresponding parameter values. Figure 18 shows examples of these plots for the ten most 'sensitive' parameters for base-case 1, ranked in terms of the SI associated with characteristic depth d2. The plots indicate that the response of the model to several of the parameters is non-linear. The correlations for all the parameter are summarised qualitatively in Appendix VII.

6.4.2.2 Other Parameters

The sensitivity index of the model to the C:N ratio was 1.02. The SI for the range of porosity values tested was 2.9. In terms of the SI of other parameters porosity therefore ranked seventh (bc1) and ninth (bc2). Whilst this comparison is not precise, since a different parameter range was used, it does suggest that the model is relatively sensitive to the value of porosity specified at the SWI. The model output was not sensitive to the value of pH (SI of 1.01).

Rank	Parameter	SI, bc1		Parameter	SI, bc2
1	Jorg	32.36		Jorg	39.35
2	k1	9.06		Vo2	10.29
3	O2BW	9.05		O2BW	9.72
4	Wf	6.88		Wf	8.55
5	irrigswi	5.88		Kfe3	3.71
6	Dbswi	4.89		irrigswi	3.71
7	InFE3	2.10		Dbswi	3.45
8	MN4BW	1.97		InFE3	3.42
9	FE3BW	1.65		MN4BW	2.08
10	k13	1.55		FE3BW	1.66
11	Kfe3	1.54		InO2	1.24
12	k11	1.32		Kmn4	1.24
13	InO2	1.24		k7	1.22
14	NO3BW	1.20		k11	1.20
15	Kmn4	1.15		Ko2	1.19
16	Kno3	1.13		k13	1.17
17	InNO3	1.12		NO3BW	1.17
18	k7	1.12		Kno3	1.12
19	Diswi	1.12		InNO3	1.11
20	SO4BW	1.11		Diswi	1.10
21	InMN4	1.07		InMN4	1.08
22	Kso4	1.07		k8	1.08
23	k12	1.06		Kso4	1.07
24	InSO4	1.05		InSO4	1.05
25	Ko2	1.04		k10	1.04
26	k8	1.03		k22	1.03
27	k10	1.03		kspfes	1.03
28	k22	1.03		k12	1.02
29	kspfes	1.03		k14	1.01
30	k14	1.02		k9	1.00
31	k9	1.00		k15	1.00
32	k15	1.00		k16	1.00
33	k16	1.00		k18	1.00
34	k18	1.00		k19	1.00
35	k19	1.00		k20	1.00
36	k20	1.00		k21	1.00
37	k21	1.00		k23	1.00
38	k23	1.00		kspfe	1.00
39	kspfe	1.00		kspmn	1.00
40	kspmn	1.00		NH4ads	1.00
41	NH4ads	1.00		SO4BW	1.00
42	TCBW	1.00		TCBW	1.00

See Appendix VI for a parameter key

Table 22 *Average SI values for Parameters; Base-Case 1 and 2*

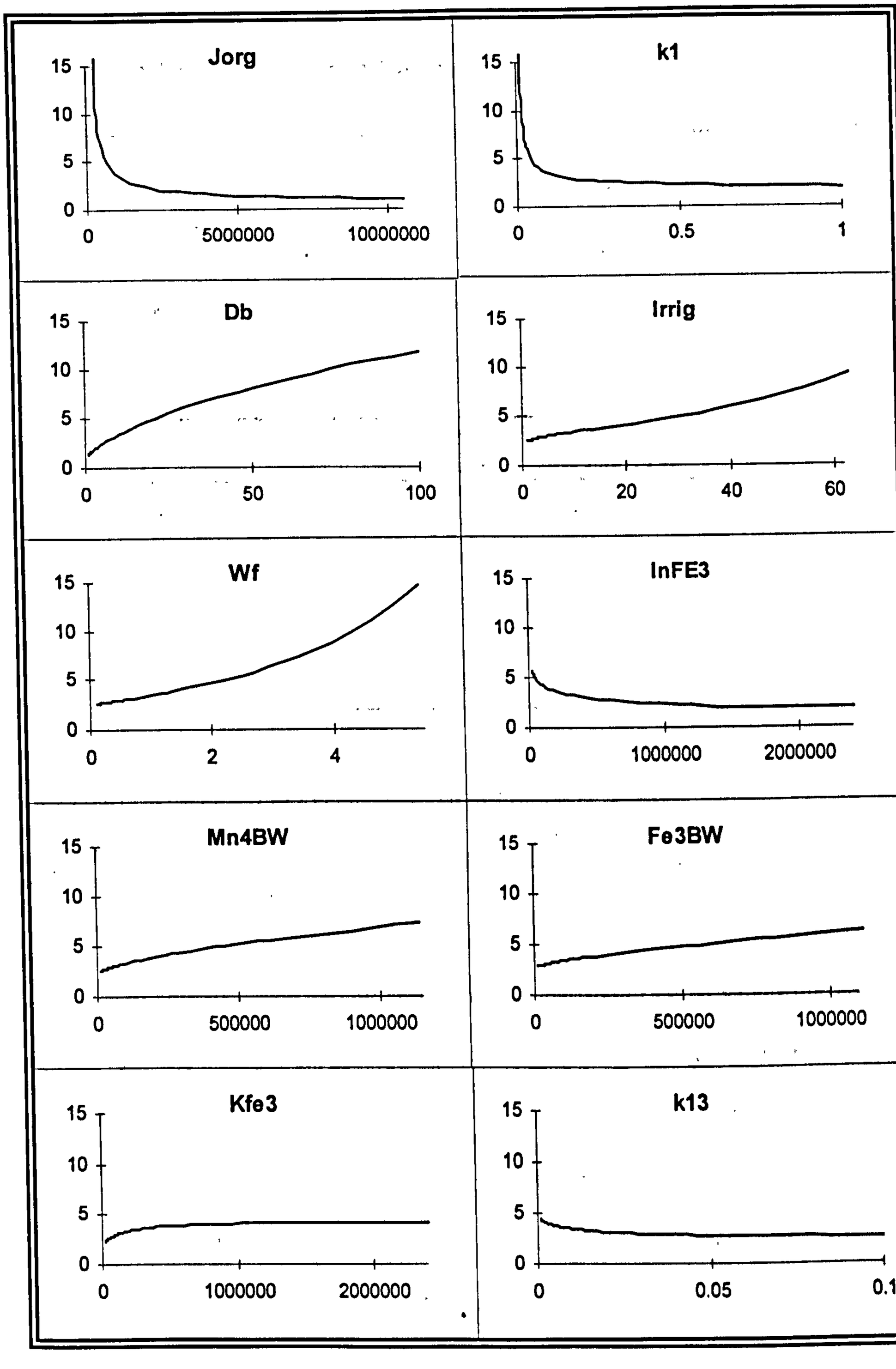

NB: all x axis parameter value (appropriate units); all y axis characteristic depth d2 (cm)

Figure 18 *Model Response (depth d2, base case 1) to Parameter Perturbation*

6.4.2.3 Depth Profiles of Bioturbation, Irrigation, and Porosity

The details of the test cases used to examine the effects of different depth profiles are summarised in Table 23 and Table 24. The SI values for the depth dependencies are also detailed in the Tables. (It should be noted that the results presented refer only to base-case 1, since the results from base-case 2 were qualitatively similar.)

Test Case	Profile	Porosity range	Decay constant	SI
P1	$D_b(x)$	0.9-0.9	0.1-10	2.60
P2	$D_b(x)$	0.8-0.8	0.1-10	3.03
P3	$\alpha(x)$	0.9-0.9	0.2-2	1.60
P4	$\alpha(x)$	0.8-0.8	0.2-2	1.62
P5	$\varphi(x)$	0.9-0.8	0.2-2	1.21
P6	$\varphi(x)$	0.9-0.7	0.2-2	1.51
P7	$\varphi(x)$	0.8-0.7	0.2-2	1.16

Table 23 *Test Cases and SI of Exponential Depth Profiles*

The SI values given in Table 23 indicate that the redox model exhibits some sensitivity to the depth profile of both irrigation and bioturbation. Comparison of the SI values for test cases P1 (profile of D_b with porosity of 0.9) and P2 (profile of D_b with porosity of 0.8) indicates that the sensitivity of the model to bioturbation is also influenced by the porosity (φ) specified at the SWI. If this were not the case then the SI values would be the same. Similarly, the SI values associated with P5, P6, and P7 (that is various porosity gradients) show that the form of the porosity gradient modifies the model sensitivity.

The SI values determined using the two-layer representation of irrigation and bioturbation are shown in Table 24. The SI values indicate that the model is less sensitive to variations in the two-layer model than to the range of exponential profiles tested.

Test Case	Profile	Depth 1st layer (cm)	SI
L1	Db(x)	1-15	1.03
L2	α(x)	1-15	1.07

Table 24 *Sensitivity of Two-Layer model*

6.4.3 Discussion

The redox profile exhibited some sensitivity (SI>1) to thirty of the forty-two parameters considered in the analysis. Furthermore, if a significant SI is arbitrarily defined as 1.2, which is equivalent to an average change in the characteristic depths of twenty per cent, the model is sensitive to fourteen parameters. In addition, seven (base-case 1) and nine (base-case 2) parameters have a SI of greater than two, which is equivalent to an average change in the characteristic depths of 100 per cent or more.

Whilst it is informative to consider the SI values in terms of the change in characteristic depths, the actual value of the SI determined for each parameter could be influenced by the base-case used (see Section 6.7). Consequently, the SIs can only be interpreted quantitatively for the specific base-cases analysed. However, given that the parameter values used are 'typical' of a coastal sedimentary system, the SI values should give an indication of relative sensitivity for most other coastal scenarios. Hence, the qualitative ranking of the parameters (as shown in Table 22) is more important than the actual value of the SIs.

The implication of this ranking is that the parameters with higher SI values must be constrained more accurately if the level of uncertainty in the model output is to be minimised. However, it should be remembered that the sensitivity was determined for a parameter value range spanning two orders of magnitude. Hence, order of magnitude estimates should suffice for those parameters exhibiting only a limited influence over the model output (that is, parameters that have a SI approaching one).

The insensitivity of the model to a parameter does not imply that the corresponding process is not significant in terms of overall diagenesis. It simply indicates that the process does not influence the redox profile when characterised by the two depths used in the analysis. Hence, in diagenetic studies with a different focus of attention an 'insensitive' parameter could be much more important. Consequently, the results from this analysis should not be interpreted in the wider context of early diagenetic modelling.

Insensitivity does, however, imply that a number of parameters and associated process could be excluded from a benthic impact model, at least when the redox state of the upper portion of the sediment column is the focus of the work. In particular, the model response indicates that the reactions detailed in Table 25 have little effect and could therefore be omitted from the governing equations without affecting the predicted redox state. However, it is noteworthy that these simplifications can be implemented in the redox model as written simply by setting the appropriate rate constants to zero.

Parameter	Reaction
k8	Fe^{2+} with O_2
k9	Fe^{2+} with MnO_2
k10	NH_4 with O_2
k12	MnO_2 with H_2S
k14	FeS with O_2
k15	CH_4 with O_2
k16	CH_4 with SO_4
k18	$MnCO_3$ precipitation
k19	$MnCO_3$ dissolution
k20	$FeCO_3$ precipitation
k21	$FeCO_3$ dissolution
k22	FeS precipitation
k23	FeS dissolution

Table 25 *'Insensitive' Reactions*

The results from the analysis indicate that the model output is insensitive to the hydrogen ion activity (pH). However, it should be noted that the hydrogen ion activity appears in the Nernst equation (Equation 4-1), which is used to calculate the model Eh. Hence, whilst the value of

pH specified does not modify the diagenetic zonation, as characterised by depths d1 and d2, it does modify the Eh calculated in each zone. Therefore, the same pH value should be used to ensure that a change in Eh indicates a shift in sediment conditions.

The response of the model to several of the parameters was found to be non-linear. For example, the flux of carbon and the rate constants of the primary redox reactions both exhibited a far greater sensitivity at the lower end of the parameter range (see Figure 18). In many mathematical models, such a response could be taken to indicate ranges of parameter values to which the model is most sensitive. However, the asymptotic response of the model implies that some other parameter value is controlling the minimum characteristic depth that can be generated for the base-line analysed; for example, the oxidant concentrations at the upper boundary. Furthermore, several of the processes included in the redox model correlate with one another (see Section 6.5 & 6.6), and the perturbation of these parameters in isolation is physically unrealistic. Using the results from this analysis to assess the parameter range to which the model is most sensitive would therefore be inappropriate.

The model output was sensitive to the depth profiles of bioturbation, irrigation, and porosity. For example, in the case of the bioturbation coefficient modelled as an exponential function (test case P1), an SI of 2.6 was determined, which is equivalent to an average change in the characteristic depths of 260 per cent. However, it should be noted that the range of decay constants used (see Table 23) characterise profiles that range from very sharp to very shallow gradients, and the sensitivity was associated more with the sharp gradients. Nevertheless, the results indicate that the selection of appropriate depth profiles could be an important modelling consideration.

The model exhibited less sensitivity when two-layer models were used to specify the depth dependencies. Moreover, it was found that when the mixed/irrigated layer extended below the suboxic zone (that is characteristic depth d2) the actual depth of the layer had a minimal

influence on the characteristic depths. In addition, the model was shown to be insensitive to other parameters that occur primarily below the suboxic zone, such as the rate constants of some secondary redox reactions. Both these findings indicate that the model is insensitive to processes associated with the deeper parts of the model domain, at least when the emphasis is placed on the upper part of the redox profile.

As discussed in Chapters 3 and 4, it is the upper part of the sedimentary redox profile that is used to characterise the redox state of the sediment and, by inference, the level of enrichment. The results of the analysis therefore indicate that the parameterisation of the upper sediment layer is more important than the parameterisation of processes occurring in the deeper layers. However, this is problematic because the upper sediment layer is also the most variable, both in time and space, and thus the most difficult to accurately parameterise.

The analysis was also intended to highlight the model processes that have the most effect on the redox state of the sediment. This can be illustrated more clearly if the model parameters are grouped together according to the following classification:

1. Environmental parameters:
    - The flux of carbon
    - The transport processes within the sediment
    - The composition at the SWI
    - The primary redox reactions
2. Reaction-specific parameters:
    - The secondary redox reactions
    - The precipitation/dissolution reactions

The environmental parameters are all related to the characteristics of the depositional environment and are thus inherently site-specific. The reaction-specific parameters are dependent upon the reaction pathways involved. The analysis demonstrated that the redox profile is insensitive to the reaction-specific parameters but is sensitive to the environmental

parameters. This can be clearly seen if the average SIs for the various groups of parameters are considered, as shown in Table 26.

Parameter Group	*SI (bc1)*	*SI (bc2)*
Carbon flux	32.36	39.35
Transport processes	4.69	4.20
Composition at the SWI	2.66	2.77
Primary redox reaction	1.96	2.41
Secondary redox reactions	1.11	1.07
Precipitation/dissolution reactions	1.01	1.01

Table 26 *Average SI of Parameter Groups*

The average SI values detailed in Table 26 show that each group of environmental parameters influence the redox profile (as defined by the model assumptions) to some degree. Consequently, the model response indicates that the redox state of the upper sediment layers depends upon both the abiotic characteristics (for example, the availability of reduced organic substrates and oxidants) and the biotic characteristics (for example, the macrofaunal assemblage present and the corresponding transport regime) of the depositional regime.

Table 26 also confirms that the representation of degradation influences the sensitivity of the model somewhat. In particular, the output for base-case 2 is more sensitive to those parameters that characterise the primary redox reactions. However, it should be noted that the qualitative ranking of the parameter groups is the same in both cases. As noted above, this ranking is more important than the numerical values of the SIs.

6.5 Parameterising the Model

The equations of the redox model describe an abstract 'model space' in which complex processes and interactions of the real world are represented in a simplified manner. Hence, the parameterisation of the model maps the processes of a sedimentary system into this idealised space. The correspondence between the model redox profile and the redox state of a

sedimentary system therefore depends upon the degree to which 'sensitive' parameters can be constrained.

Unfortunately, since the benthic environment is complex, and characteristics of the sediment depend upon a range of ecological interactions, there are no principles upon which to base a theoretical assessment of key parameter values. Extensive fieldwork could be carried out to parameterise sedimentary systems (e.g. Aller 1980a; 1980b; Canfield *et al.* 1993a; 1993b). However, for economic reasons it is desirable that the amount of fieldwork should be minimised. The only alternative is to use standard parameter values in conjunction with empirical regression models taken from the literature.

Standard parameter values were used in the sensitivity analysis to specify the 'typical' coastal sediment. However, this approach is really only justified for those parameters that are to some extent independent of the specific characteristics of a depositional regime; for example, the reaction-specific parameters. For site-specific parameters any correspondence between a 'typical' value selected and the actual value of a parameter at the site in question would be purely incidental.

Empirical regression models relate parameter values to other geochemical properties that can be determined independently. A number of such empirical relationships have been presented in the literature that use the burial rate, or rate of deposition, as a master variable, as discussed below. (Master variable in this context is a variable that characterises the overall nature of the depositional environment.) These models therefore provide a means of specifying site-specific parameter values that are more representative of a specific depositional regime, assuming that depositional regimes can be characterised by the burial velocity.

6.5.1 Empirical Models

Boudreau (1994) determined an empirical relationship that relates the magnitude of the bioturbation coefficient (D_b) to the burial velocity (ω), which can be written as:

$$D_b \approx 15.7\omega^{0.69} \qquad \textbf{Equation 6-8}$$

where D_b is in cm^2/yr and ω is in cm/yr. Boudreau noted that the correlation is statistically significant at the one per cent level, but explained only a relatively small percentage of the variance (thirty per cent) in the data set used. The physical significance of the regression model is therefore limited.

The correlation between the bioturbation coefficient and the burial velocity is explained by the positive correlation between the rate of deposition and the flux of carbon -- a high depositional rate therefore usually corresponds to a high flux of organic matter. This flux supports an elevated macrofaunal abundance and activity, which results in a more vigorous mixing of the sediment. The correlation between burial velocity and the flux of carbon (J_{org}) was examined explicitly by Henrichs & Reeburgh (1987), who determined the following relationship:

$$\log(J_{org}) \approx 0.69\log(\omega_\infty) + 2.27 \qquad \textbf{Equation 6-9}$$

where J_{org} is in $gC/m^2/yr$ and ω_∞ is the burial velocity after initial compaction near the SWI, with units of cm/yr.

Empirical models have also been derived that relate burial velocity to the rates of primary redox reactions. These correlations exist because reactive particulate organic matter (POM) is buried in rapidly accumulating sediments, whereas in slowly depositing sediments the organic matter is mineralised before it can be incorporated into the sediment (Boudreau, 1994). Boudreau (1997) examined the relationship between burial rate and the first order (G-type) rate constant for the k_1 fraction of organic matter (the k_1 fraction of the sedimentary POM decays within the top 10-20 cm of the sediment), and derived the following power law relationship:

$$k_1 \approx 0.4\omega^{0.6} \qquad \textbf{Equation 6-10}$$

where k_1 is in /yr and ω is in cm/yr.

It should be noted that the flux of carbon would actually consist of a number of fractions of organic matter, each having a different reactivity. Hence, the rate constant k_1 applies only to a portion of the organic matter delivered to the SWI. However, the redox model presented herein only conforms to the G-type modelling approach when the rate constants of the six primary redox reactions are set to the same value. Hence, only one fraction of organic matter can be specified. Some means of estimating the proportion of the organic matter belonging to this k_1 fraction would therefore be required if Equation 6-10 were to be used. Moreover, using Equation 6-10 to estimate the 1-G rate constant involves the implicit assumption that the other fractions do not have a significant effect on the concentration profiles of the component species.

For instance, it must be assumed that the highly reactive fraction that decomposes on a seasonal time scale (that is the k_0 fraction) can be ignored. This approach could only be justified if it was assumed that the degradation of the k_0 fraction occurs at the SWI. The oxygen used to mineralise the substrates would then be supplied from the water column. Similarly, any products of degradation would diffuse into the overlying water. Consequently, the mineralisation of the k_0 fraction would not produce a signal into the sediment column and, therefore, would not significantly influence the porewater chemistry. However, this approach is still conceptually limiting because it is likely to be the highly reactive k_0 fraction that drives much of the benthic metabolism.

Tromp *et al.* (1995) have published the following correlations between burial velocity and the rate constants for oxic respiration (V_{o2}), sulphate reduction (V_{so4}), and methanogenesis (k_{ch4}):

$$V_{o2} \approx 2.97\omega^{0.62} \qquad \textbf{Equation 6-11}$$

$$V_{so4} \approx 0.057\omega^{1.94}$$

$$k_{ch4} \approx 0.0072\omega^{2} \qquad \textbf{Equations 6-12 and 6-13}$$

again the rate constants are in /yr and ω is in cm/yr. Since these rate constants are associated with a specific diagenetic zone, their numerical value must reflect the average reactivity of the organic matter within that zone. Hence, these rate constants are not associated with a particular fraction of the sedimentary POM in the same way that the k_1 rate constant is, but are a function of the overall diagenetic regime.

To the author's knowledge, there are no equivalent empirical relationships for the rates of nitrate or metal-oxide reduction. However, the magnitude of the rate constants can be estimated from the relationships given in Equations 6-11 to 6-13. For instance, it is reasonable to assume that the rate constant for nitrate reduction is similar to that of oxic respiration, since both processes decompose organic matter of a similar reactivity. In contrast, Mn-oxide and Fe-oxide reduction decompose POM that has escaped oxic degradation and is therefore less reactive. Hence, the rate constants associated with these sub-oxic processes should be, on average, less than that of oxic processes, but higher than that of sulphate reduction. The applicability of this approach is discussed in the next section.

There are also no empirical relationships detailed in the literature for estimating the magnitude of the irrigation coefficient. However, under normal conditions the intensity of irrigation is determined by the type of animals present and their level of activity, as discussed in Chapter 5. Furthermore, all other things being equal, the magnitude of the irrigation coefficient should increase as the density of individuals increases (see Section 5.6.2.1). Similar factors produce an increase in bioturbation (e.g. Matisoff, 1982; Smith, 1992). It is therefore reasonable to assume that there is some correlation between the coefficient of irrigation and the bioturbation coefficient.

Bioturbation and irrigation are, however, distinct processes that are affected by a number of separate factors. For example, the rate of irrigation must be correlated with the oxygen concentration in the overlying water (e.g. Archer & Devol, 1992; Forster *et al.*, 1995). A depression in oxygen levels and corresponding rise in products of anaerobic degradation would therefore trigger an increase in irrigational activity, but not bioturbation. The strength of any correlation between the coefficients of bioturbation and irrigation would therefore depend upon a range of biotic factors, such as the species present and their behavioural responses, and the abiotic characteristics of the habitat.

There are also no empirical relationships for the depth dependency of the bioturbation and irrigation parameters. However, Boudreau (1994) considered the relationship between burial velocity and the depth of the bioturbated zone. The data used in the Boudreau's analysis suggested little correlation between the two variables ($r=0.032$). Nevertheless, the depth of the mixed layer was similar in environments with markedly different rates of deposition. Boudreau (1994) found a mean depth of 9.8 cm (standard deviation 4.5 cm) and suggested that the depth of mixing is limited by the physical difficulty and increasing energy costs of reworking and excavating deeper than 10-15 cm. This range can therefore be used as a guide value for the depth distribution of the macrofauna, and thus the depth of the mixed/irrigated layer in the two-layer representation of depth dependency.

The regression models given above only explain a limited percentage of the variance in the data sets from which they were derived. This means that factors other than the burial velocity must influence the numerical value of the parameters. For example, Boudreau (1994) noted that the unexplained variance in the regression of bioturbation coefficient on burial velocity could be attributed to:

1. The approximate nature of the diffusion model of bioturbation.
2. The temporal and spatial variability of the environment.
3. Differential mixing of different particle sizes.

4. Sampling and analytical artefacts.

5. The long chain of processes through which the two parameters are linked.

Hence, conceptual, analytical, and ecological factors can influence the physical significance of the regression models. Empirical relationships, therefore, can only constrain parameter values to a limited degree. However, the relationships do provide a means of assessing parameter values in the absence of any better information. Of course, the issue of uncertainty in the predicted values can not be ignored, and this matter is investigated in Section 6.7 and 6.8.

6.6 The Model Response for a Range of Idealised Depositional Regimes

The empirical models detailed in the previous section are all dependent on the burial rate. Hence, there is an implicit relationship between all the regression models, which indicates that the corresponding sedimentary processes correlate with one another. Perturbing the associated parameters in isolation is therefore physically unrealistic. Hence, the response of the model determined during the main sensitivity analysis was somewhat artificial and only a limited interpretation can be placed on the results obtained.

The empirical models detailed above, however, provide a means of simultaneously varying parameter values in a way that reflects the correlations between various processes. These empirical models can therefore be used to examine the model response for a range of idealised coastal scenarios, as described below. (In this context, an idealised scenario is a model depositional regime where parameter values are given by the empirical models and estimates taken from the literature.)

6.6.1 Method

Various idealised coastal scenarios were specified by assuming burial rate characterises the overall nature of the depositional regime. Burial velocities in the range of 0.1-10 cm/yr were considered, giving a two order of magnitude span about the 'typical' coastal value of 1 cm/yr

used in the main sensitivity analysis. This range was again divided into thirty increments using a logarithmic approach (see Section 6.4.1.3).

The empirical relationships discussed in Section 6.5.1 were used to estimate the values of the relevant parameters at each burial velocity. (Seventy percent of the flux of carbon calculated via Equation 6-9 was assumed labile.) All other parameter values were set according to the baseline condition used in the main sensitivity analysis; that is, were specified as the 'typical' values for a coastal sediment (see Appendix V). The influence of the overlying water composition was also examined by generating additional redox profiles at each burial velocity with reduced oxidant concentrations specified at the upper boundary.

Degradation was modelled with primary redox reactions specified according to both the 1-G and 6-D cases. In the 1-G case the labile POM was assumed to be degraded according to the rate constant k_1, estimated from Equation 6-10. In the 6-D case, the rate constants for nitrate and metal-oxide reduction were assumed to be related to the three empirical models given by Equations 6-11 to 6-13. A number of relationships were tested but for illustrative purposes only results using the following dependencies are presented herein:

$$V_{no3} = 0.75\, V_{o2}$$

$$V_{mn4} = 1.5\, V_{So4}$$

$$V_{fe3} = 1.25\, V_{So4}$$

The rate constants used in the 6-D case are shown in Figure 19. It can be seen that at low burial velocities the rate constants for suboxic (mn and fe) and anoxic processes (SO4 and CH4) are small compared to those of the oxic processes. This implies that oxic degradation predominates when the flux of carbon is low. The effect of assuming other relationships between the primary redox reactions is discussed below.

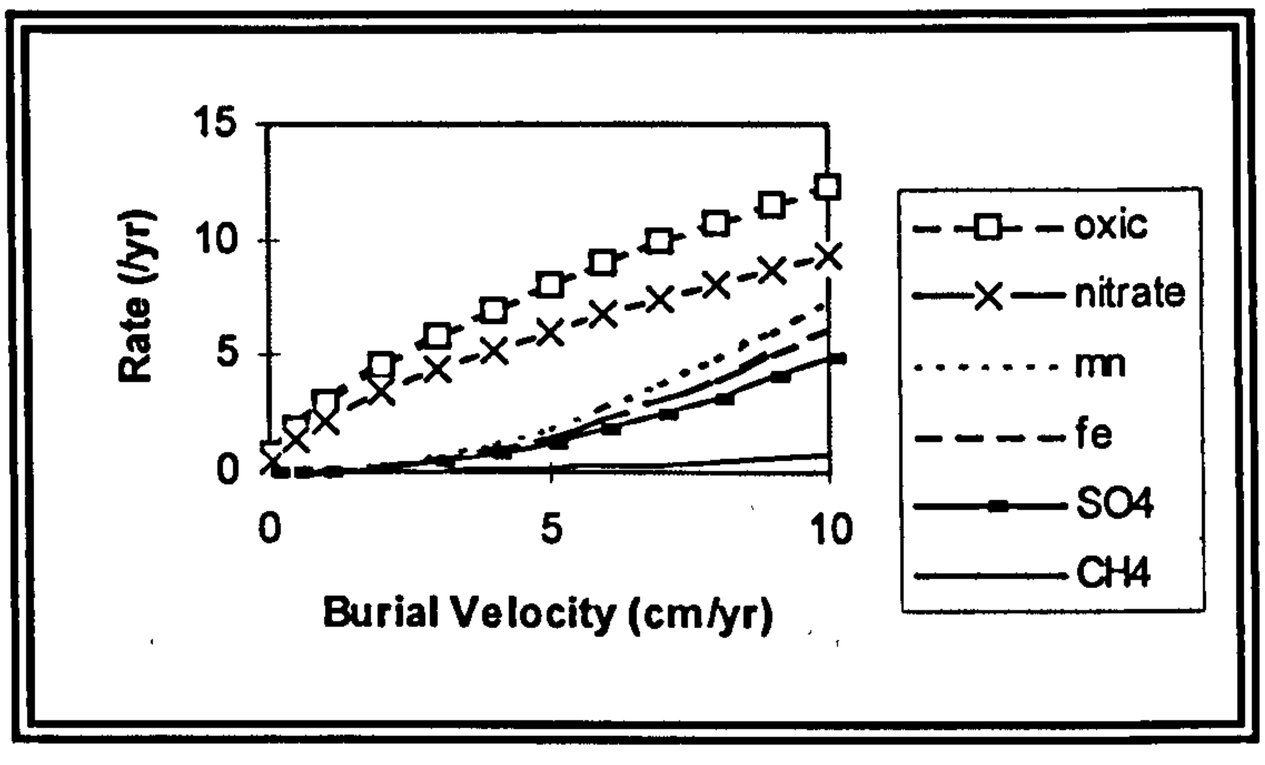

Figure 19 *Values of Rate Constants for the Six Primary Redox Reactions*

In the absence of any better guiding principle the change in irrigation over the range of depositional regimes was estimated from the same power law used to estimate D_b; that is:

$$\alpha \approx 15.7\omega^{0.69} \qquad \textbf{Equation 6-14}$$

This is equivalent to assuming that the level of irrigation and bioturbation are perfectly correlated. This must be considered a poorly constrained assumption because, as discussed previously, the two processes are in reality quite distinct. However, values of irrigation coefficient estimated in this way are sensible in that they fall within the range of values given in the literature (e.g. Boudreau, 1997). Additional runs were carried out with no irrigation and with irrigation specified as a diffusive flux.

The depth profile of the irrigation, and bioturbation coefficients were both assumed to follow a pseudo two-layer model; that is, Equation 5-34. The linear decrease in the parameter value was specified over the interval $9 < x < 11$ cm. This interval therefore brackets the average mixing depth of 9.8 cm determined by Boudreau (1994). For simplicity, porosity was assumed constant throughout the model domain. The steady state version of the model was used, with a model domain of 20 cm, and a space step (Δx) of 0.01 cm. The redox profiles were again summarised using the two characteristic depths d1 and d2.

6.6.2 Results

Figure 20 (legend label; 275) shows the plot of the characteristic depths against burial velocity for the 6-D case. As the Figure indicates, the characteristic depths exhibit an asymptotic response, with the sediment becoming more reducing as the burial velocity increases. The oxygen penetration depth (d1) ranges from 1.64 to 0.21 cm and the depth of the suboxic layer (d2) ranges between >20 cm to 2.07 cm. At low burial rates the rate constants for Mn and Fe-oxide reduction are small (see Figure 19). Consequently, the rate of metal oxide reduction is low and the depth of the suboxic layer (that is d2) exceeds the depth of the model domain (20 cm).

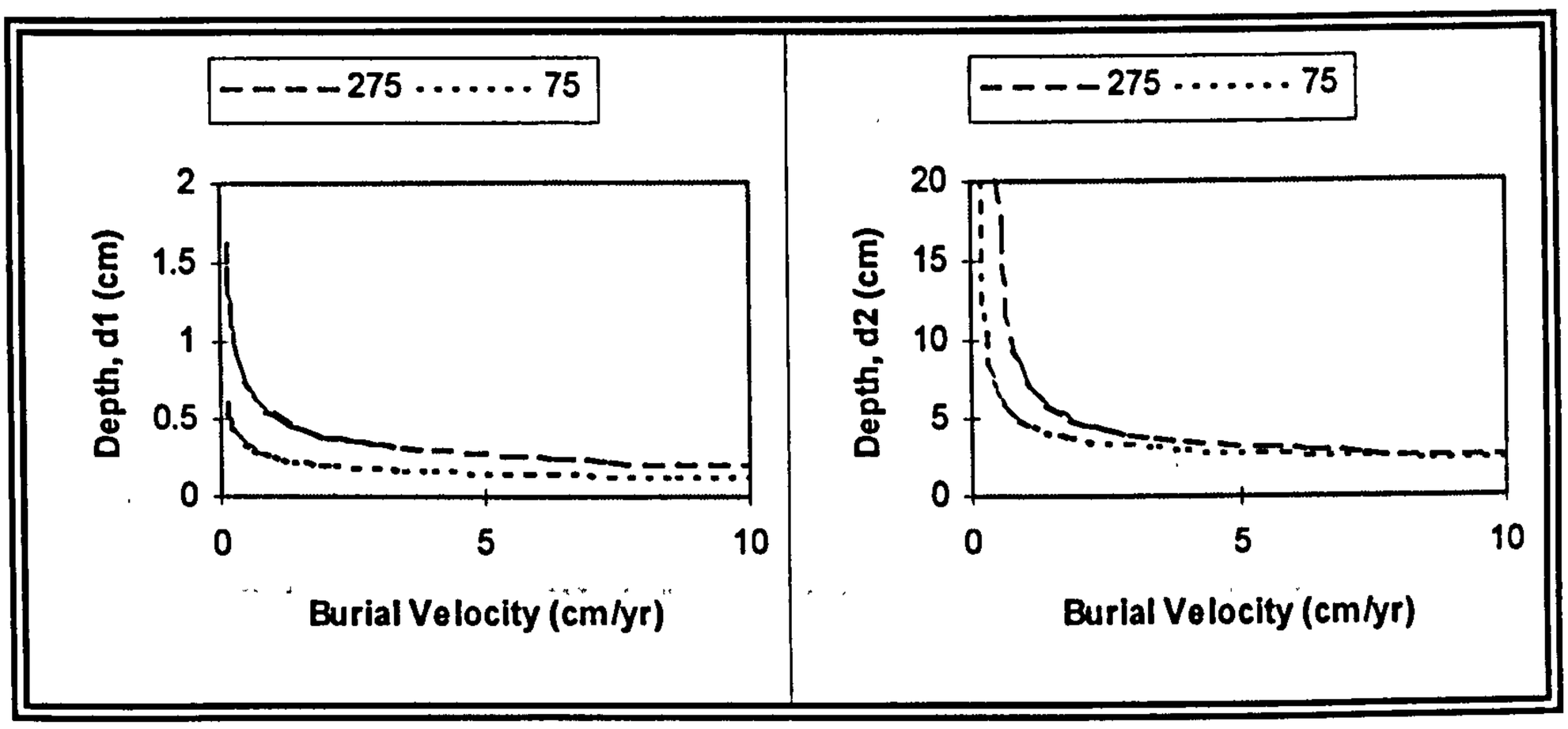

NB: The legends indicate oxygen concentrations at the SWI of 275 μM and 75 μM

Figure 20 *Characteristic Depths for a Range of Depositional Environments (6-D)*

As noted above, the influence of the overlying water composition was examined by generating redox profiles with reduced oxidant concentrations specified at the upper boundary. By way of illustration, Figure 20 (legend label; 75) shows the characteristic depths obtained when the oxygen concentration was specified as 75 μM (compared with the baseline concentration of 275 μM). It can be seen that the response remains asymptotic in form but the characteristic depths at each burial velocity are lower; which implies that reducing conditions are closer to the SWI.

The equivalent plots of characteristic depths for the 1-G case are shown in Figure 21. It can be seen that the oxygen penetration depth (that is d1) exhibits a similar asymptotic response to that observed in the 6-D case, with d1 ranging from 1.49 to 0.15 cm. However, the depth of the suboxic layer actually increases as burial rate increases, with depths ranging between 3.17 cm to 4.12 cm. The redox profiles characterised by the depth of the suboxic zone (d2) are, therefore, relatively constant across the whole range of depositional regimes. Figure 21 also shows that specifying lower oxidant concentrations at the upper boundary again had the effect of lowering the characteristic depths at each burial velocity.

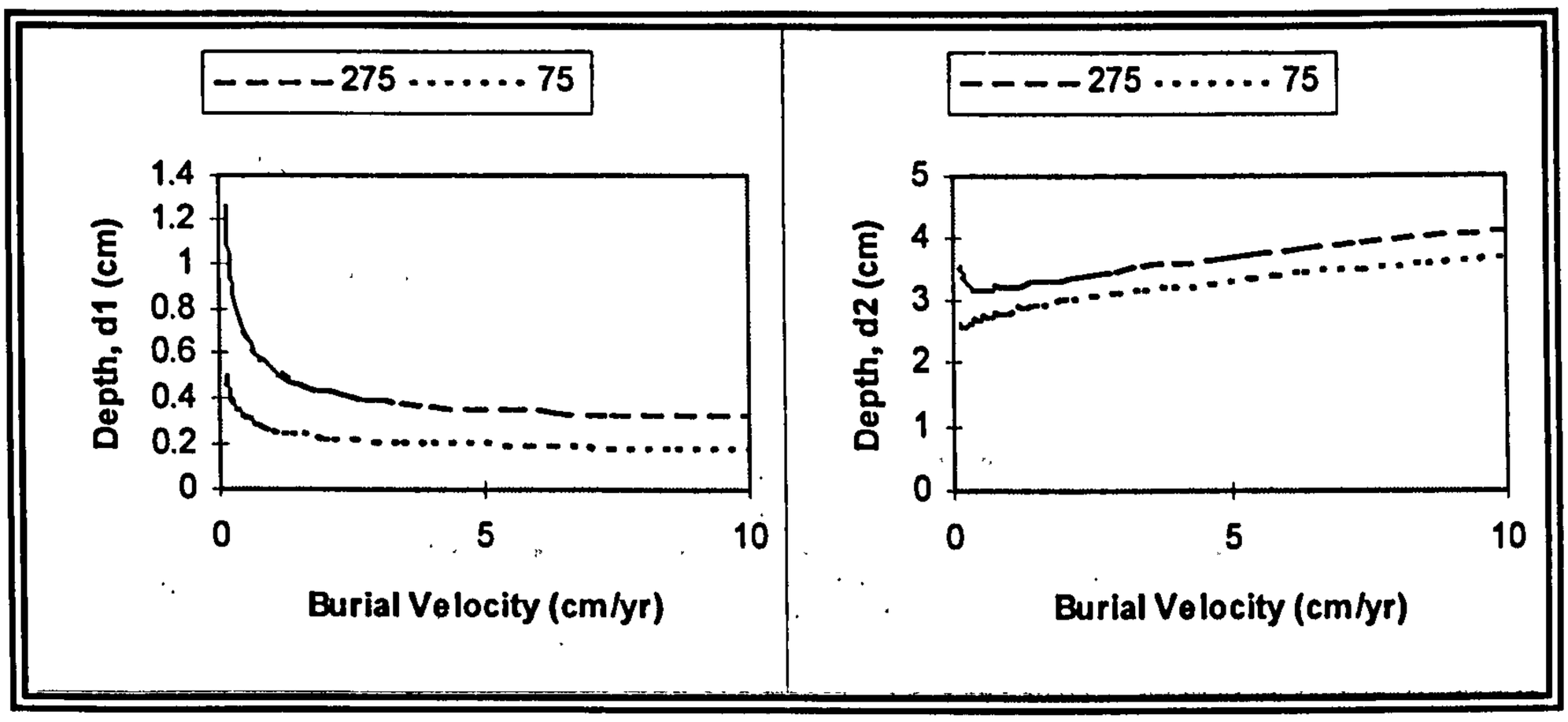

NB: The legends indicate oxygen concentrations at the SWI of 275 μM and 75 μM

Figure 21 *Characteristic Depths for a Range of Depositional Environments (1-G)*

As noted above, the redox profiles were also calculated for equivalent scenarios with both no irrigation and irrigation defined as a diffusive flux. However, the results were qualitatively the same as those obtained using the non-local exchange function and are thus not presented herein.

6.6.3 Discussion

The results of the 6-D case conform to the intuitive expectation that as the flux of carbon increases, oxidants are consumed more rapidly, and the sediment becomes reducing at a shallower depth. Similarly, in the 1-G case the oxygen penetration depth (that is depth d1) fell with increasing carbon flux, again implying an increasing rate of oxidant consumption in the

oxic zone. However, as shown in Figure 21, the depth of the suboxic layer remained approximately constant. Hence, the two representations of degradation produced quite different characteristic responses across the range of idealised depositional regimes considered.

These conflicting responses were investigated by assuming different relationships between the rate constants of the six primary redox reactions. It was found that when the rate constants of metal oxide reduction were estimated from the rate of oxic respiration, rather than sulphate reduction, the qualitative response for the 6-D case was the same as that observed in the 1-G case (that is, the response shown in Figure 21). However, the overall characteristics of the modelled system were still markedly different. This is illustrated in Table 27, which details the percentage of carbon oxidised via oxygen and sulphate reduction at burial velocities of 0.1 and 10 cm/yr for the two cases.

Case	*ω (cm/yr)*	*O_2 (%C)*	*SO_4 (%C)*
1-G	0.1	11.7	70
6-D	0.1	58.9	1.1
1-G	10	1.8	74.7
6-D	10	6.3	77.5

NB: Assumed relationships for the 6-D case were $V_{no3} = 0.75\ V_{ox}$; $V_{mn4} = 0.5\ V_{ox}$; *and* $V_{fe3} = 0.4\ V_{ox}$

Table 27 *The Percentage of Carbon Oxidised via Sulphate and Oxygen Reduction*

As indicated in the Table, when the burial velocity is low (0.1 cm/yr) oxygen reduction is much more important and sulphate reduction much less significant in the 6-D case. At the high burial velocity (10 cm/yr), the difference between the two cases is less marked. The two representations of degradation therefore produce markedly different diagenetic regimes at low burial velocities. Similar discrepancies were observed for a range of assumed dependencies between the various primary redox reactions. Consequently, the 1-G and 6-D cases appear to be inconsistent, at least when parameterised via the empirical relationships detailed above.

As discussed previously, the 6-D representation of degradation provides a means of modelling the change in the lability of the organic substrates with depth. However, both the qualitative and quantitative responses of the model are influenced by the assumed dependencies between the rates of nitrate and metal-oxide reduction and the other empirical relationships. Since these dependencies are not known, it would be inappropriate to use the empirical models to parameterise the 6-D representation of degradation in a practical modelling study.

In the 1-G case (and 6-D case with modified dependencies) the characteristic depth d2 increased with increasing burial rate. This is contrary to the expectation that the sediment should become more reducing as the flux of organic carbon increases. However, it should be remembered that there is a correlation between various processes, which is implicit in the empirical models. Hence, whilst the flux of carbon increases with increasing burial rate, there is a corresponding increase in the levels of bioturbation, irrigation, and the rates of the primary redox reaction. In the 1-G case, these changes in parameter values must therefore have acted together to redistribute oxidants and reductants, so as to maintain the upper sediment in a relatively constant redox state.

One possible interpretation of this is that the test cases used, and by inference the empirical models, represent scenarios in which an increasing flux of carbon would only have a 'beneficial' ecological effect. The carrying capacity of the habitat would then be increased without incurring any deleterious effects such as physical smothering or depression of oxygen concentrations at the SWI. The resulting elevated macrofauna abundance and activity would therefore induce a proportional increase in various reaction-transport processes, which would maintain the upper sediment in a relatively benign redox state. Making such inferences from the limited analysis detailed herein is, however, only speculative. Nevertheless, some conclusion can be drawn from the response of the model.

It was demonstrated in the main sensitivity analysis that a range of both biotic and abiotic factors influences the model redox profile. The relatively constant redox conditions across the whole range of parameter values used in the 1-G case indicate that the balance between these factors, rather than a single factor in isolation, determines the redox state of the upper sediment. This would in turn suggest that the increase in reducing conditions associated with organic enrichment is driven by a change in this balance and, consequently, a change in the relationship between the model parameters. Furthermore, the model response supports the interpretation of sediment redox intensity as an integrative measure of a number of benthic processes (see Davis *et al.*, 1998).

Although a similar characteristic depth d2 was obtained in the 1-G case using different combinations of parameter values, the concentration profiles of all the component species were not the same. For example, the profiles of organic carbon, ammonia, and authigenic mineral phases all varied considerably across the range of burial velocities considered. This observation has two main implications. Firstly, the model redox profile only characterises the distribution of some species and does not reflect, for instance, the distribution of highly reduced organic substrates. Hence, the redox profiles generated by the model are somewhat analogous to those produced by the models of Billen (1982) and Billen & Verbeustel (1979). Secondly, when the redox profile is considered in isolation the model has many degrees of freedom; that is, many combinations of parameter values can produce similar redox profiles in the upper portion of the model domain. This suggests that, even leaving aside the difficulty in interpreting electrode measurements, calibrating the model using measured redox profiles would be meaningless. Parameterisation and/or calibration would therefore have to be based on the overall chemistry of the sediment.

The influence of boundary conditions on the model response was examined by specifying reduced oxidant concentrations at the upper boundary. The resulting characteristic depths at each burial velocity were shallower, indicating that reducing conditions moved closer to the

SWI. As noted previously, redox intensity characterises oxidant concentrations. Hence, the reduction in oxidant concentration at the upper boundary simulates a transition to more reducing conditions in the overlying water. The shallower characteristic depths obtained in the analysis indicate that a similar transition would be generated within the sediment column; that is, the sediment would become more reducing.

The model response therefore illustrates that the redox state of the upper sediment layer is coupled to the redox state of the overlying water. It should also be noted that when sediment oxygen demand is high, flushing rates are low, and/or where stratification of the water column occurs, sedimentary processes can impose a control over the composition of the water at the SWI (e.g. Pearson & Rosenberg, 1978). Hence, in such situations the direction of this coupling is reversed; that is, the redox state of the upper sediment layer dictates the redox state of the overlying water. However, this effect cannot be predicted using the redox model alone, since the boundary conditions at the SWI are imposed and can not evolve out of the modelled conditions.

6.7 Model Sensitivity: Alternative Baselines

In the sensitivity analysis discussed in Section 6.4, the baseline parameter values were assumed to be representative of a 'typical' coastal scenario. However, the coastal environment is inherently heterogeneous. Hence, a range of such representative baselines could be specified. The question therefore arises as to whether or not the sensitivity of the model varies according to the baseline condition selected. Since empirical models can be used to estimate parameter values over a range of depositional regimes, these models provide a way of defining different baselines. The analysis of the redox model was therefore extended to assess if the sensitivity depends upon the baseline specified.

6.7.1 Method

Model sensitivity was again assessed using the parameter perturbation technique described previously. However, only those parameters that can be estimated via the empirical regression

models given in Section 6.5.1 were considered in this extended analysis. Irrigation was again assumed to be correlated with the bioturbation coefficient, and model sensitivity was assessed for both the 1-G and 6-D cases. The baseline parameter values at each burial velocity were calculated from the appropriate empirical models. All other parameter values were again specified as the 'typical values' for a coastal sediment. Burial velocities in the range of 0.1-10 cm/yr were again used, and the model domain was set at 20 cm with a space step of 0.01 cm.

The parameter values were varied over two orders of magnitude range, again divided into thirty increments using a logarithmic approach. In the case of k_1, V_{o2}, D_b, α, and J_{org} the range was taken about the baseline parameter value at each burial velocity. For primary redox reactions other than oxygen reduction (V_{o2}), the range was taken two orders of magnitude below the rate constant of the preceding reaction. For example, rate constant for nitrate reduction (V_{no3}) was varied over the range of V_{o2} to $V_{o2}/100$. This ensured that there was always a decrease in the rate constants with depth. The sensitivity of the model to each parameter was again expressed using the sensitivity index discussed previously.

6.7.2 Results

The results of the analysis are summarised in Table 28, which shows the maximum, minimum and mean sensitivity index for each parameter. The results confirm that the model is most sensitive to the flux of carbon across the whole range of burial velocities considered. The model redox profile is also influenced by the other parameters specified via the empirical relationships. The exception is that the model does not exhibit any sensitivity to the rate constant for methanogenesis, as shown by the SI of 1.0. This insensitivity is again probably due to the fact that this process is only associated with the anoxic zone and does not influence the depths of the oxic or suboxic zones, at least for the scenarios considered.

Parameter	*Min SI*	*Max SI*	*mean SI*
Jorg	22.26	90.85	52.58
Db	1.09	9.28	4.19
Wf	1.97	4.88	3.67
Irrig	1.72	5.12	2.75
Vo2	1.40	2.54	1.96
Vno3	1.03	2.56	1.34
Vmn4	1.20	1.32	1.26
Vfe3	1.03	1.60	1.23
Vso4	1.05	1.56	1.22
Kch4	1.00	1.01	1.00

Parameter	*Min SI*	*Max SI*	*mean SI*
Jorg	20.34	62.05	31.58
K1	3.02	18.64	8.45
Db	4.20	6.30	5.61
Wf	1.55	6.30	3.57
Irrig	2.95	3.81	3.46

NB: Upper table 6-D case; Lower table 1-G case

Table 28 *Sensitivity Index for a Range of Baselines*

Figure 22 and 23 shows the sensitivity index of each parameter plotted against the logarithm (base ten) of the burial velocity. The SI values were normalised by dividing by the mean SI of each parameter; a normalised SI of one therefore indicates that the sensitivity is equal to the mean SI.

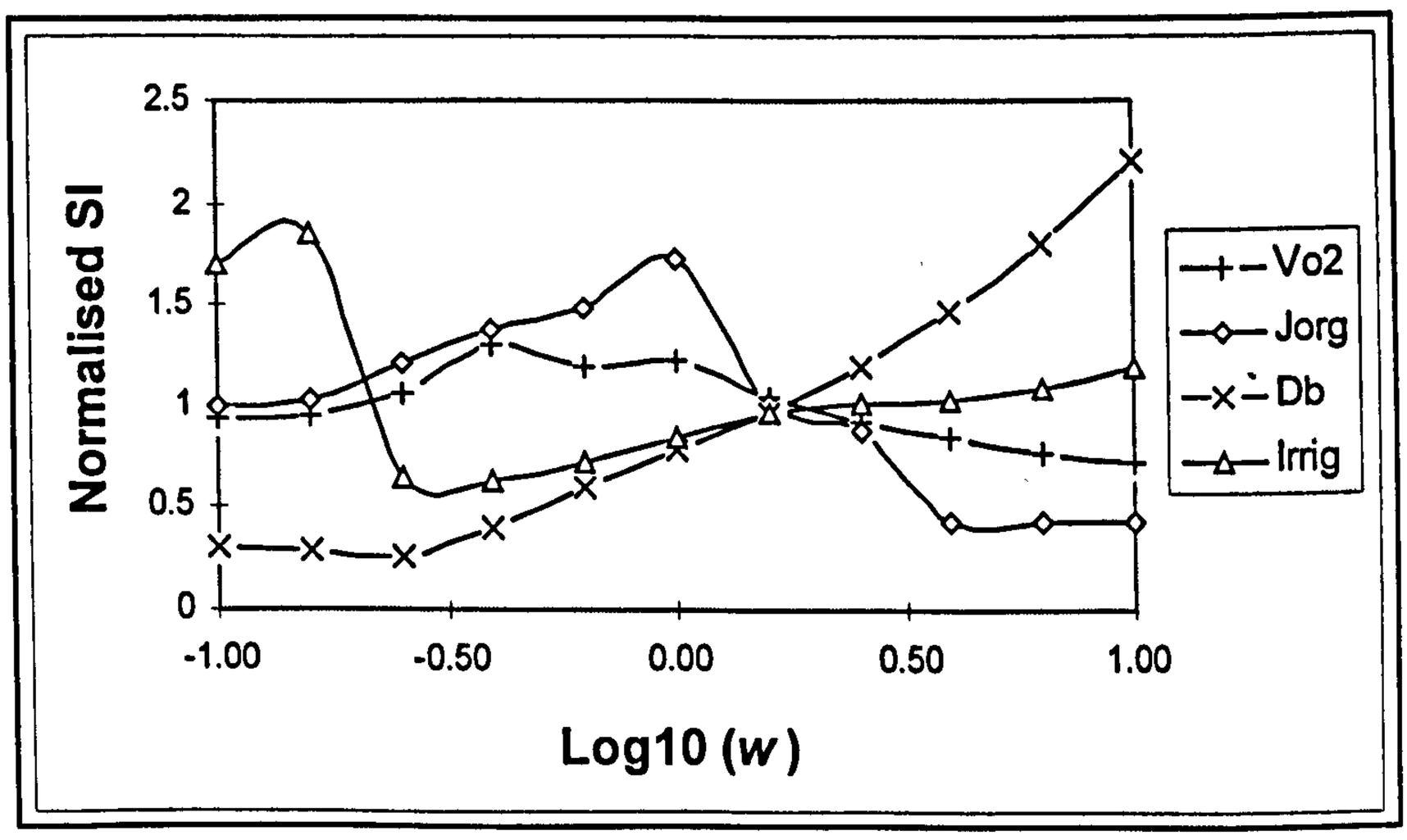

Figure 22 *Sensitivity to Alternative Base-lines (6-D case)*

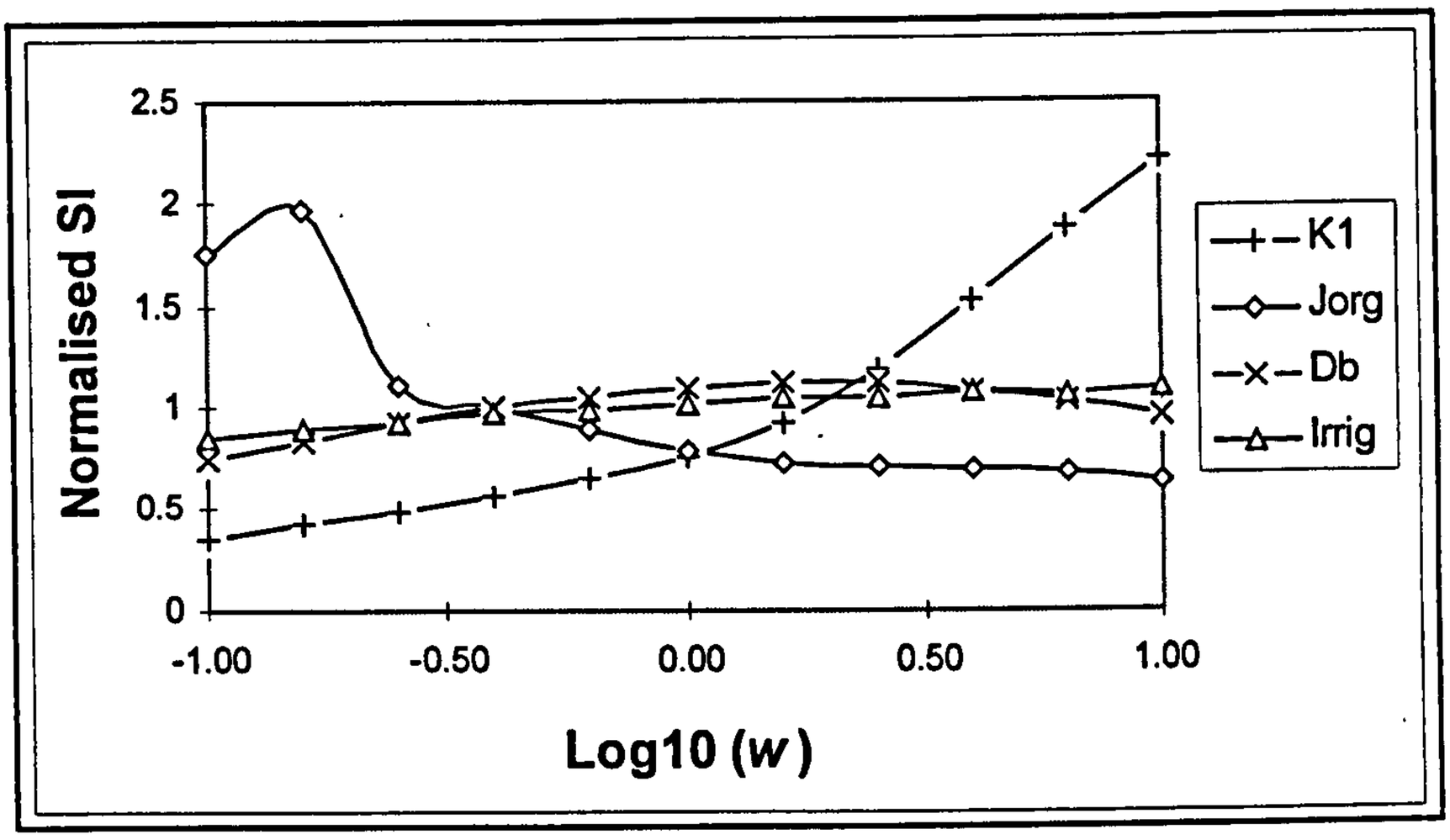

Figure 23 *Sensitivity to Alternative Base-lines (1-G case)*

6.7.3 Discussion

Figures 22 & 23 demonstrate that the sensitivity of the model does vary according to the baseline specified. This confirms that the results from the main sensitivity analysis, described in Section 6.4, can only be interpreted qualitatively. The Figures also indicate that the response of the model varies according to the representation of degradation used. For example, the SI values of the coefficients of irrigation and bioturbation remain reasonably constant when degradation is specified according to 1-G kinetics (see Figure 23). This is in contrast with the 6-D case where the SI values of these same parameters vary considerably (see Figure 22).

This different response reflects the implicit relationship between the rate constants of degradation and the transport regime in the two representations of degradation. For instance, when the 6-D representation of degradation is used any change in the transport parameters redistributes various reactants into diagenetic zones that have different rate constants associated with them. In contrast, redistribution of reactants in the 1-G case is less significant because the same rate constant is associated with each diagenetic zone.

The results of this analysis indicate that the model is more sensitive to the 1-G rate constant than to the individual rate constants of the 6-D case. This would seem to contradict the results of the main sensitivity analysis, which showed that the model was equally sensitive to these rate constants (see Table 22). However, in the main analysis, described in Section 6.4, the rate constants of the six primary redox reactions were varied simultaneously. Hence, the perturbation of the parameter values had a simultaneous effect on the rate of degradation in all the diagenetic zones. Likewise, perturbation of the 1-G rate constant influence degradation throughout the whole model domain. In contrast, in this analysis the rate constants of each primary redox reaction were varied separately. The parameter perturbation therefore only affected reactions occurring in one diagenetic zone. The overall effect on the model output was therefore less marked, as reflected by the lower sensitivity index values.

The results of this analysis, therefore, suggest that the model would be less sensitive to parameterisation errors if the 6-D formulation were used. However, if the rate constants of the separate reactions were poorly constrained, then the reduction in sensitivity would only be realisable by the introduction of additional model uncertainty.

6.8 A Simple Analysis of Uncertainty

Empirical regression models could be used to estimate the parameter values of a specific site. However, it has already been noted that these regression models only constrain parameter values to a certain degree. Hence, the actual value of a parameter could differ considerably from that given by the empirical model. Unfortunately, since it has been shown that the redox model is sensitive to all the parameters that can be estimated via regression models, any difference between the actual and estimated parameter value would have an influence on the model output. Using empirical models to parameterise a sedimentary environment could therefore introduce a significant amount of uncertainty into the redox profiles generated by the model. A simple assessment of this uncertainty was made using the results from the extended sensitivity analysis described in the previous Section.

6.8.1 Method

The effect of uncertainties in the empirical relationships was evaluated by plotting the changes in characteristic depths against the changes in parameter value for each of the baselines used in the analysis described in Section 6.7.

6.8.2 Results

For illustrative purposes, the responses of the model for the 1-G case at burial rates of 0.1, 1 and 10 cm/yr are shown in Figure 24. Before plotting, the parameter values at each burial velocity were normalised by dividing by the baseline value. Similarly, the characteristic depths were normalised by dividing by the depth calculated for this baseline condition. This allowed the model responses across a range of burial velocities to be plotted together. The results have been plotted as $\log_{10}$ (normalised value); the normalised base-line parameter value and characteristic depths are therefore positioned at the origin of each plot (since $\log_{10}(1) = 0$).

The curves illustrate how the characteristic depths would be affected by an under or over estimate of the parameter value. For example, a change in parameter value resulting in a ±0.3 on the y-axis would indicate that the characteristic depth had changed from the base-line value by a factor of two. As expected, the plots demonstrate uncertainties in J_{org} would have the greatest effect on the characteristic depth. The model shows less sensitivity to uncertainties in the other parameters. The plots also confirm that the sensitivity of the model varies according to the burial rate specified. (If this were not the case then the curves for each parameter would be the same at each of the burial velocities plotted.)

Visual inspection of the plots indicates that uncertainties in the parameters would influence both characteristic depths d1 and d2 to approximately the same degree. The exception to this is the bioturbation coefficient, which has a more pronounced influence over the characteristic depth d2. The plots also indicate that the model output would be influenced equally by both

under and over estimates. The most notable exception to this is the plot of k_1 at $\omega = 0.1$ cm/yr where the model exhibits less sensitivity to over-estimations of the parameter value.

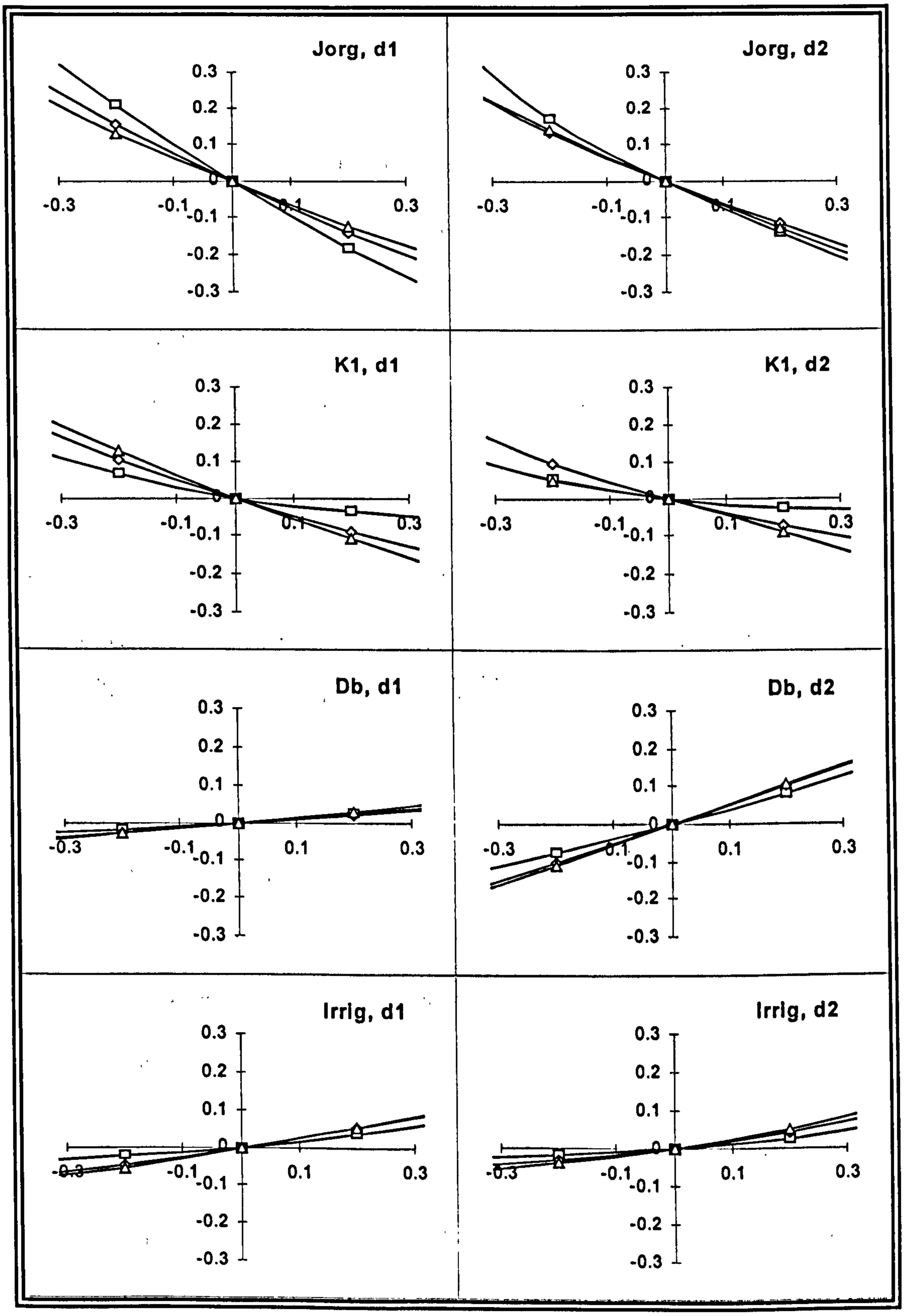

NB: all x axis; log10 (normalised parameter value); all y axis log10 (normalised depth)
Legend: square; ω =0.1 cm/yr: diamond; ω =1.0 cm/yr: triangle; ω =10.0 cm/yr

Figure 24 *Sensitivity of the Model to Variations in Parameter Value (1-G case)*

6.8.3 Discussion

The plots shown in Figure 24 can be used to give a quantitative assessment of uncertainty introduced by estimates of parameter values. For example, if the irrigation is estimated to within a factor of two (that is ± 0.3 on the x-axis), then the Figure indicates that both characteristic depths would be in error by approximately ±20% across the whole range of depositional regimes considered. Of course, the plots do not take into account the compound effect of errors in a number of parameter values. Nevertheless, even with this simplified treatment it is clear that even relatively small levels of uncertainty in some parameter values, especially J_{org}, would lead to significant changes in the redox profile generated by the model – parameter value uncertainty can lead to equivalent levels of uncertainty in the model output.

As noted in Section 6.5.1, the empirical models only explain a part of the variance observed in diagenetic data sets. For example, Boudreau (1994) notes that the regression model for bioturbation only constrains the coefficients associated with coastal sediments to within a factor of ten. The plots shown in Figure 24 indicate there is an almost one to one correspondence between the change in D_b and the change in characteristic depth d2. Hence, only constraining D_b to within an order of magnitude would introduce a high level of uncertainty in the model output. When the combined effect of uncertainties in all the parameter values are considered, any capacity to predict benthic impact is likely to be minimal. Hence, empirical regression models do not provide a practical means of parameterising the redox model, at least in the context of supporting management decisions (discussed further in Chapter 8).

The plots shown in Figure 24 illustrate the effect of any source of parameter uncertainty, not just that resulting from empirical models. Hence, other sources of errors, such as those introduced either through uncertainty in field measurements or the adoption of standard values taken from the literature, introduce uncertainty into the model output. These uncertainties also

influence the predictive capacity of the model. This matter is considered further in Chapter 7 and the implications to the modelling of benthic impact are discussed in Chapter 8.

6.9 Transient Response

The analysis of the redox model to this point has focused solely on steady state conditions. However, the sediments of temperate coastal waters are inherently variable, not only in space but also in time. For example, the rates of many important sedimentary processes are affected by temperature and therefore vary throughout the year. Similarly, seasonal fluctuations in the level of primary production within the water column result in a corresponding variation in the flux of carbon to the SWI. An overall stationary state would therefore not be expected in the redox chemistry of coastal sediments. The response of the redox model under idealised transient conditions has therefore been investigated.

6.9.1 Forcing Functions in Time

The seasonal variations of temperature and carbon flux have been modelled by assuming an idealised sinusoidal distribution in time with a period of one year. With this assumption, the temporal variation of the carbon flux (J_{org}) is given by:

$$J_{org} = F_o + F_a \sin(2\pi t) \qquad \textbf{Equation 6-15}$$

where F_o is the mean flux for the year, F_a is the amplitude and t is time in years. Assuming temperature gradients within the sediment column can be ignored, the seasonal variation in temperature in the model domain can be described by an analogous function. However, a lag/lead constant has also been included to allow the temperature and carbon flux to be specified either in phase or out of phase with one another. Hence, the forcing function for temperature is given by:

$$T = T_o + T_a \sin(2\pi(t+\tau)) \qquad \textbf{Equation 6-16}$$

where T_o is the mean temperature for the year, T_a is the amplitude and τ defines the lead time (or lag if negative) between the two functions, again in years.

The temperature dependence of other processes could be modelled using the Arrhenius equation (e.g. Aller, 1980a; Westrich & Berner, 1988; DiPasquale & Capone, 1998). For example, Aller (1980a) used this formulation to model the seasonal response of sulphate reduction, ammonium production, and bioturbation. However, this approach was considered overly complex for the purpose of this investigation. In any case, data was not available to allow the Arrhenius equation to be applied to all the temperature dependent reactions and processes included in the redox model.

Fortunately, a simplified model can be used for environments where only a narrow temperature range is observed (Chapra, 1997), as is the case for coastal waters. In this approach the temperature dependence of biologically mediated processes is approximated by:

$$k_{T2} = k_{T1} Q_{10}^{(T2-T1)/10} \qquad \textbf{Equation 6-17}$$

where k_{T1} is the rate constant/parameter value at temperature T_1 and k_{T2} is the rate constant or parameter value (as appropriate) at temperature T_2; Q_{10} is defined below. If both k_{T1} at a specific temperature (that is T_1) and the Q_{10} of the process are known, or can be estimated, Equation 6-17 allows the parameter value at any other temperature to be calculated. Given that the temperature variation over the year (that is the variation in T_2) is modelled as a sinusoidal function, the temperature response of parameter values calculated using this idealised approach would also be sinusoidal. The Q_{10} of a process is defined as:

$$Q_{10} = \frac{k_{T2}}{k_{T1}} \qquad \textbf{Equation 6-18}$$

Strictly speaking the Q_{10} is defined only for a given temperature range of 10°C (for example, 10°C to 20°C). However, for simplicity it has been assumed that the same Q_{10} is applicable to all temperatures considered.

It has also been assumed that the empirical relationships detailed in Section 6.5.1 give the parameter value (k_{T1}) at the yearly mean temperature (T_1) of the study area. The value of k_{T2} is then the parameter values at any other temperature (T_2). This assumption therefore allows the empirical equations to be used in the parameterisation of a transient case. It should be noted, however, that this assumption is not particularly significant because the empirical relationships are only used to illustrate the model response for idealised scenarios.

Most biological processes have a Q_{10} ranging between two and three (Valiela, 1995); that is, the rate of the processes increase by two to three times for every 10°C increase in temperature. Aller (1980a) found that macrofaunal activity exhibits a Q_{10} of approximately two. This value was therefore adopted for parameters that characterise macrofaunal activity; namely the bioturbation and irrigation coefficients. As discussed in Chapter 4, the microfauna of the sediment are stimulated by both an increase in temperature and by the activities of the macrofauna (see Table 7). A Q_{10} of three was therefore assumed for processes mediated by the microfauna; namely the rate constants of the primary redox reactions. This value is comparable with estimates of the Q_{10} for microbial processes given in the literature (e.g. Aller, 1980a; Westrich & Berner, 1988).

The redox model has been shown to be relatively insensitive to the rate constants of both the precipitation-dissolution and secondary redox reactions. Furthermore, the values of the rate constants used herein are the 'typical' values given by Van Cappellen & Wang (1995; 1996), which are only order of magnitude estimates. If it is assumed that reaction rates approximately double for each 10°C increase in temperature (e.g. Chapra, 1997), then even with a maximum temperature difference of say 20°C the reaction rates would only increase by a factor of four. Since this change is less than the precision to which the rate constants are constrained, any attempt to consider this variation would be somewhat arbitrary. Consequently, the temperature dependence of these reactions has not been considered.

6.9.2 Initial Conditions

The temporal response of the model output depends, in part, upon the type of boundary conditions specified. As noted above, periodic boundary conditions have been used to model the temporal variability of the sedimentary system. Consequently, the output of the model should also be periodic. However, a periodic solution is only produced from the start of a model run when the initial concentration profiles correspond to the starting parameter values; that is, when the initial conditions are consistent. If this is not the case then the initial conditions introduce some additional transients into the model output. These transients are spurious since they do not form part of the periodic solution vector being sought.

These spurious transients, however, eventually die away leaving only the periodic solution required. Hence, initial conditions could be specified simply by making a guess at the initial concentration profiles and then integrating the model equations over a sufficiently long time span. However, if the initial guess is very poor then the solution vectors could take a long time to settle, which is computationally expensive. Furthermore, the integrator can sometimes fail to maintain the specified accuracy levels, which causes VODE to raise an appropriate error flag and stop the integration.

These problems can be avoided by using the solution of an equivalent steady state problem to specify the initial conditions of the transient case. (Where the parameters for the 'equivalent' steady state problem are specified as the yearly mean values.) These initial conditions still introduce spurious transients but they should die away relatively quickly. Nevertheless, some modelling strategy must be adopted to ensure that these transients are not modifying the solution vectors at the time of output. The strategy taken in this work has been to compare the model output for two consecutive years. The output being considered of acceptable quality if when plotted no significant difference between the two years was observed.

As a rule, the output from the transient model was sufficiently settled after seven model years for the results to be accepted. However, under some input conditions the model can take longer to settle. For example, Figure 25 shows a case where the model response, characterised by the depth of the RPDL, did not settle until approximately twenty-two years (264 months) have been modelled. (The RPDL was assumed to occur at the depth where the model redox potential fell below zero Volts.)

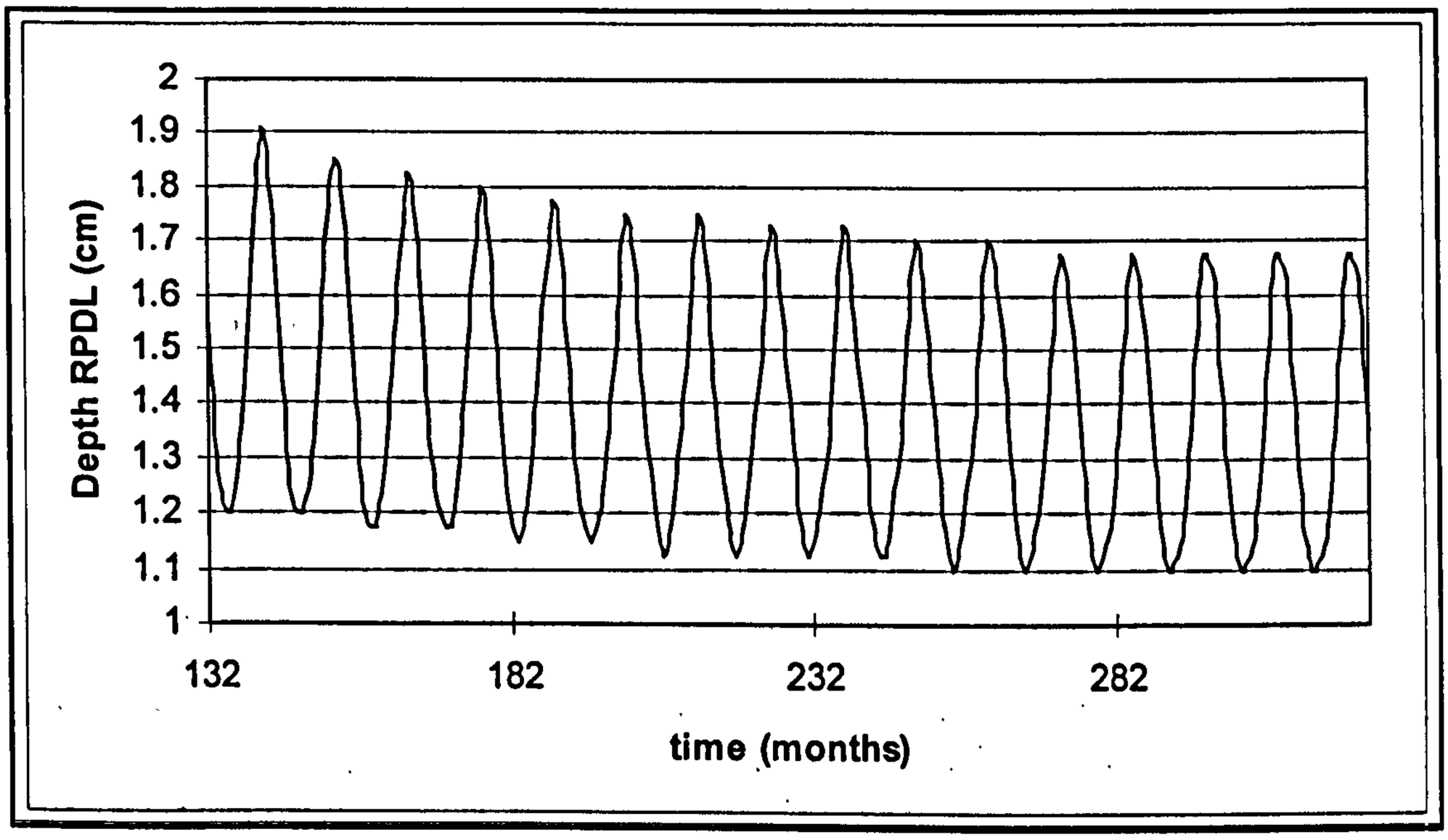

Figure 25 *The Transient Response of the RPDL*

6.9.3 Comparison of Steady State and Transient Outputs

In a simplified modelling study, Berner (1979) assumed that the yearly averaged response of an unsteady system could be modelled as an equivalent steady state problem. (The parameters in the steady state problem being specified as the mean annual values of the transient case.) This approach removes the need to consider the transient response explicitly, which simplifies the overall modelling problem. The validity of the assumption was therefore investigated by comparing the model output for equivalent steady and unsteady cases.

6.9.3.1 Method

The steady state solution for a range of cases was obtained using a space step of 0.025 cm and a model depth of 15 cm. The transient solution was then obtained for equivalent input conditions. The amplitude of the carbon flux (F_a in Equation 6-15) was specified as fifty per cent of the mean flux in all cases. The amplitude of the temperature (T_a in Equation 6-16) was varied over the range from zero to 100 per cent of the mean temperature. A Q_{10} of two was assumed for macrofaunal parameters, and a Q_{10} of three for microfaunal processes.

Output was taken after seven model years, which was sufficient to allow any initial transients to die away. The concentration profiles for each transient run were output at an interval of 1/12 a year. The average concentration at each node was then calculated to give the yearly mean concentration profile for each component. The averaged transient profiles were then compared to those generated by the steady state version of the redox model. (Concentration profiles were compared because the averaging of Eh values at each node gives essentially meaningless results.)

6.9.3.2 Results

Because they are representative of the overall model response, only the ammonia and the Mn^{2+} profiles are presented herein. Figure 26 and 27 show these profiles generated when parameters are specified according to the 'typical' values used previously.

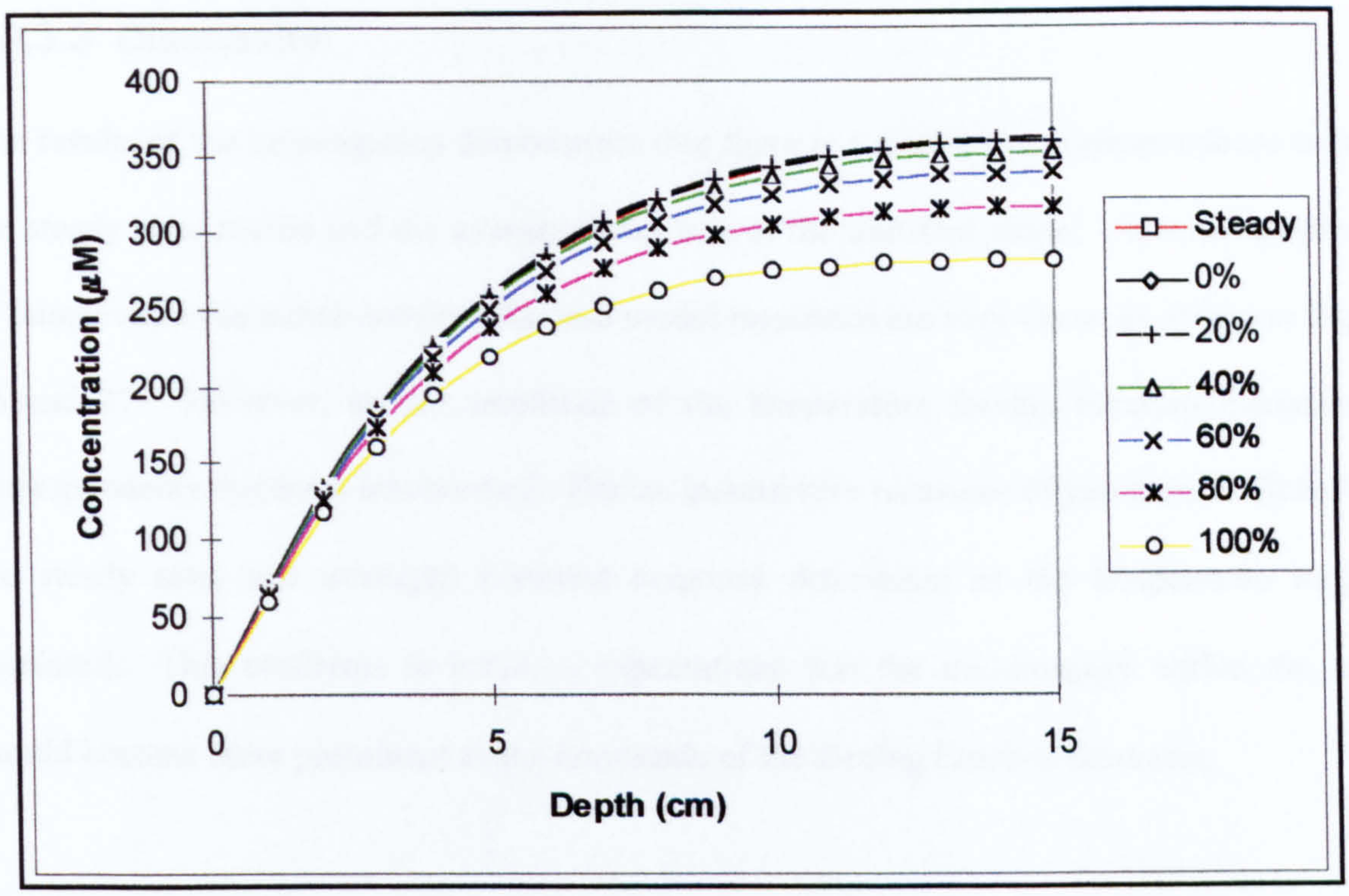

NB: The legend labels indicate the percentage of the mean used to specify the amplitude of the temperature forcing function; 'steady' indicates the steady state solution

Figure 26 *Comparison of Steady State and Averaged Transient Ammonia Profiles*

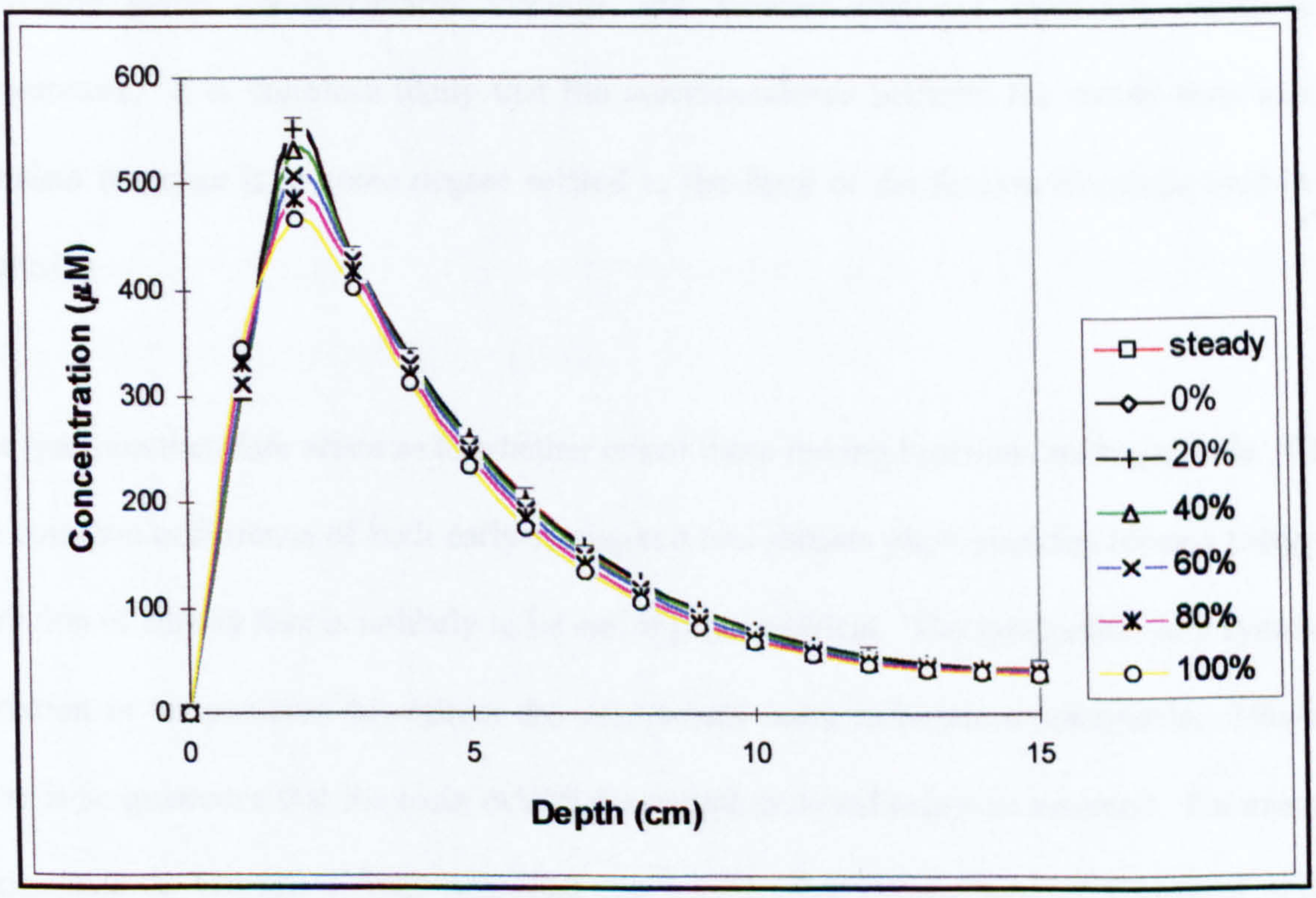

NB: The legend labels indicate the percentage of the mean used to specify the amplitude of the temperature forcing function; steady indicates the steady state solution

Figure 27 *Comparison of Steady State and Averaged Transient Mn^{2+} Profiles*

6.9.3.3 Discussion

The results of the investigation demonstrate that there is a qualitative correspondence between the steady state profile and the averaged response of the transient model. At small amplitudes of temperature the match between the two model responses are very close, as shown in Figures 26 and 27. However, as the amplitude of the temperature forcing function increases the correspondence becomes less marked. Hence, quantitative measures of goodness of fit between the steady state and averaged transient response deteriorate as the temperature range is increased. This conforms to intuitive expectations that the non-linearity within the model should become more prominent as the amplitude of the forcing function increases.

Some of these findings were corroborated by B.P. Boudreau (personal communication) who noted that if the forcing functions applied to the transient model are roughly symmetric in time, the yearly averaging should produce something 'like' the steady state response based on the yearly averaged parameters. However, Boudreau also indicated that this result was not inevitable given non-symmetric forcings and kinetics that are extremely sensitive to temperature. It is therefore likely that the correspondence between the steady state and the transient response is to some degree related to the form of the forcing functions used in the analysis.

The question therefore arises as to whether or not these forcing functions are reasonable. Given the common occurrence of both early-spring and late-autumn phytoplankton blooms the yearly variation of carbon flux is unlikely to be entirely symmetrical. The assumption of a symmetric variation in temperature throughout the year would seem to be more reasonable. However, there is no guarantee that the biota exhibit the simple seasonal response assumed. For example, Dipasquale & Capone (1998) note that the temperature dependence of microbial activity (specifically sulphate reduction) is mediated by an interaction of multiple factors including the quality and quantity of organic matter, redox conditions, and macrofaunal activity.

Consequently, the simple relationship between the rate of microbial activity and temperature is confounded by complex ecological interactions.

Similar complexities apply to the seasonal response of the macrofauna. For example, Boon & Duineveld (1998) found that seasonal variations in bioturbation can be positively correlated with the seasonal flux of POM (measured as Chlorophyll A in their study). It therefore seems likely that the response of the macrofauna to variations in the inputs of organic matter would be superimposed upon the temperature response, again confounding the simple temperature dependency.

Whilst accepting these conceptual limitations, it should be remembered that any model is a simplified representation of reality and must be considered in terms of its intended application. Therefore, if the purpose of the modelling study is to compare the response of a non stationary site under different conditions, then the steady state profiles should still give some indication of the system's response, yet allow a much simpler modelling approach to be taken. This observation is especially relevant to the current research since the assessment of benthic impact requires that the effects of various discharge options be either compared to some baseline condition or to each other. Hence, some assessment of benthic impact could be made without considering the transient response explicitly.

Finally, it should be noted that the correspondence between the transient and steady state response indicates that the sensitivity analysis detailed in this Chapter gives an indication of the sensitivity of the transient model, at least when simplified forcing functions in time are assumed

6.10 Summary

The model internal checks include the calculation of mass balances and the residuals of each component species. These calculations act as internal checks and allow the quality of each

model run to be assessed. Both mass balance and residuals improve if the space step is reduced. The redox model has been verified by comparing a steady state carbon profile to a simple analytical solution. Outputs from both the steady state and NMOL versions of the model have also been compared to ensure consistency. Finally, a benchmarking exercise was undertaken in which model outputs were compared to the output of two peer reviewed diagenetic models. The exercise demonstrated that the redox model equations have been implemented correctly.

A simple 'one at a time' parameter perturbation technique was used to examine model sensitivity. The analysis demonstrated that the model is most sensitive to site-specific factors, especially the flux of carbon, oxygen concentration at the SWI, transport processes, and primary redox reactions. The model is relatively insensitive to reaction-specific parameters such as the rate constants of secondary redox reactions, and is insensitive to precipitation and dissolution reactions. The sensitivity is influenced by the representation of degradation used, although the overall pattern of sensitivity is not altered. The analysis also indicated the selection of appropriate depth profiles of porosity, bioturbation, and irrigation could be an important modelling consideration.

The redox model can be parameterised through a combination of fieldwork, the adoption of 'typical' parameter values, and the use of empirical regression models. These regression models relate the value of a parameter to other geochemical properties. Empirical models taken from the literature have been used to examine the response of the redox model for a range of idealised depositional regimes. The results indicated that the model redox profile is dependent upon the balance between a number of interconnected processes. By inference, the change in sedimentary redox state associated with enrichment must be driven by a change in this balance.

The empirical regression models were also used to show that model sensitivity depends upon the baseline selected. Hence, the results from the main sensitivity analysis can only be

interpreted qualitatively. It was also demonstrated that any uncertainty in key parameter values can translate into equivalent levels of uncertainty in the model redox profiles. Furthermore, given the level of uncertainty inherent in any regression model, it is unlikely empirical models could be used to parameterise a specific site, at least when the aim of the study is to predict benthic impact.

Sediments of coastal waters are inherently variable in time and simplified sinusoidal functions have been used to represent the seasonal forcings. The initial concentration profiles for transient problems can be specified using the solutions from an equivalent steady state problem. However, the model user must still ensure that transients introduced by these initial conditions have died away before accepting any output. It has been demonstrated that there is a correspondence between the yearly averaged response and steady state response of the redox model. This suggests that the steady state version of the model could be used to compare the benthic impact of various disposal options. It also means that the sensitivity analysis of the steady state model gives an indication of the sensitivity of the transient model.

Chapter 7

7. MODEL APPLICATION

7.1 Introduction

In preceding Chapters, it has been shown that the redox state of sedimentary systems offers a potential focus for a benthic impact model. A description and analysis of a redox model developed to test this potential has also been given. It has been shown that the redox model, and by inference the redox state of the sediment, is sensitive to a relatively large number of parameters. Furthermore, when the redox profile is considered in isolation the model has many degrees of freedom. Hence, model calibration would have to be based on the overall chemistry of the sediment, not just redox measurements. Given the complexity of sedimentary systems and relative complexity of the redox model, it should therefore be anticipated that using the model in practice would require access to a large amount of data. This can be illustrated by applying the redox model to a data set taken from the literature.

The Chapter starts with the description of the data set used. Various parameter values and boundary conditions are then specified and a number of model parameters are calibrated using the steady state version of the model. The parameter values determined for the steady state case are then used to model transient conditions, with the output again being compared to the data. The empirical relationships described in the previous Chapter are also used to parameterise the model and to generate additional profiles for the site in question.

The Chapter closes by considering the practical application of the redox model to the assessment of benthic impact. The limitations of modelling the benthic impact directly are discussed first. A potential approach, which uses the redox model in a qualitative sense, is then investigated. Finally, the results of the investigation are considered and the potential for the modelling approach assessed.

7.2 Calibrating the Redox Model

In Chapter 6, the redox model was analysed using 'typical' values for the model parameters. The analysis provided a useful insight into the responses of both the model and sedimentary systems. However, the use of such idealised parameterisations fails to highlight the problems associated with the modelling of a real sedimentary system. A site-specific modelling exercise was therefore undertaken in which the redox model was calibrated using data published in the literature.

Model calibration is the process whereby key parameter values are adjusted until the output generated by the model matches (that is, fits) the data set in question (e.g. Chapra, 1997). In the context of this research, such an exercise provides a means of demonstrating the data requirements of a site-specific modelling study. The conclusions drawn from the study also help when assessing the potential for applying the redox model to the prediction of benthic impact, which is considered at the end of the Chapter.

7.2.1 Data Set Description

An exceptionally detailed data set would be required if all the processes included in the redox model were to be parameterised explicitly. However, it has already been demonstrated that the model redox profile is relatively insensitive to the parameters associated with both the precipitation-dissolution and secondary redox reactions. The approach taken herein has therefore been to assume that these reaction-specific parameters are sufficiently well constrained by estimates taken from the literature. Typical values have also been used for other parameters such as the half saturation constants. The effort required to parameterise the model is thereby much reduced. However, the data requirements are still relatively high because a range of site-specific parameters must be specified.

A complete data set giving values for each of these site-specific parameters has to the author's knowledge not been published in the literature. However, various data sets have been

published that include some parameter values and are comprehensive enough to allow most of the remaining parameters to be calibrated. Aller (1980a & 1980b) gives one such data set, which relates to a shallow station (15 m depth) in Long Island Sound and is designated as 'NWC'. This data set was selected for two main reasons. Firstly, the site is well studied and the data given by Aller (op. cit.) is supplemented by other published studies. Secondly, laterally averaged concentration profiles are available for a number of component species. The concentration profiles are therefore compatible with the 1-D approximation used in the redox model, which assumes that lateral heterogeneity is averaged in this way.

Rates of decomposition at the station have also been examined by Aller & Yingst (1980), who used anaerobic incubation techniques to determine the production of ammonia and the reduction of sulphate in the upper 10 cm of the sediment column. The authors determined that the rate of sulphate reduction and ammonia production decreased exponentially with depth. At 22°C, the distributions of these rates with depth were shown to be adequately described by the following functions:

$$R_{SO4} = 118\exp(-0.34x) + 5$$

$$\frac{R_{NH4}}{(1 + k_{NH4})} = 28.1\exp(-0.55x) + 0.57 \qquad \textbf{Equation 7-1 \& 7-2}$$

where R_{SO4} indicates the rate of sulphate reduction and $R_{NH4}/(1+k_{NH4})$ indicates the net rate of ammonia liberation, both rates in mM/yr. The gross rate of ammonia production can be estimated if the adsorption coefficient (k_{NH4}) is known. Aller & Yingst (1980) note that this coefficient is approximately one for sediments in Long Island Sound. Hence, the gross rate of ammonium production is given by:

$$R_{NH4} = 56.2\exp(-0.55x) + 1.14 \qquad \textbf{Equation 7-3}$$

As noted above, the empirical rate functions were generated using anaerobic incubation techniques. Obligate aerobes would therefore have died off in the initial part of the experiment, and the decomposition of the organic matter would have proceeded via anaerobic metabolic

pathways. As noted in Chapter 5, a significant difference in the rates of anaerobic and aerobic degradation is usually observed in marine sediments. However, this difference is created by the preferential use of labile substrates near the SWI; that is, the difference in rates is related to the quality of food that is normally available to different microbial assemblages.

The exclusion of obligate aerobes at the start of the experiments would have allowed anaerobic micro-organisms access to labile organic substrates normally associated with oxic degradation. The use of anaerobic incubation techniques should therefore have had little effect on the rate of degradation observed in each sediment interval (see also Canfield *et al.*, 1993b). Hence, it can be assumed that the empirically determined degradation rates are representative of the reactivity of the organic matter, not the metabolic pathway being used.

7.2.2 Calibrating the Carbon Flux and Rate Constant of Degradation

The empirical rate functions (Equation 7-1 and 7-3) could be directly incorporated into a diagenetic model, as demonstrated by Wang & Van Cappellen (1996) using the data given in Canfield *et al.* (1993b). However, the rate functions can also be used to calculate a first order rate constant of degradation (that is, a G-type rate constant) over the depth of interest (10 cm), as described below. This approach has been taken since it is more compatible with the data requirements of the redox model.

As noted previously, when the rate constants of the primary redox reactions are set to the same value the representation of degradation is equivalent to a 1-G model. The rate constant of degradation (k) was therefore estimated by fitting a 1-G model to the empirical rate function of sulphate reduction. The overall stoichiometry of sulphate reduction has a C:S ratio of 2:1; that is, two moles of carbon are oxidised for every one mole of sulphate reduced (see Chapter 5, Table 10). Hence, the relationship between the rate of carbon oxidation and rate of sulphate reduction can be written as:

$$R_{SO4}(x) = 0.5(\frac{1-\varphi}{\varphi})R_G(x) = 0.5(\frac{1-\varphi}{\varphi})kG(x) \qquad \textbf{Equation 7-4}$$

in units of mass/volume/year.

In Equation 7-4, sulphate reduction is represented as a first order rate law. In contrast, the redox model uses a monod type rate law for this reaction. However, the concentration of sulphate only affects the rate of sulphate reduction when concentrations have fallen below ten per cent of the sea water value (Boudreau & Westrich, 1984). In the incubation experiments, this concentration was only reached towards the end of the incubation period and only in the top 2 cm of the sediment (see Fig. 2 in Aller & Yingst, 1980). Hence, in this instance it is reasonable to assume that the overall rate of sulphate reduction is independent of sulphate concentration and can be represented as a simplified first order rate law (that is, Equation 7-4).

Aller (1980a) notes that the average porosity at NWC is 0.74. If this value is applied throughout the depth of interest (that is, porosity gradients are ignored) then $R_{SO4}(x)$ and the porosity in Equation 7-4 are both known. The term $kG(x)$ can be estimated by solving a 1-G model of the form:

$$\frac{\partial G}{\partial t} = D_b \frac{\partial^2 G}{\partial x^2} - \omega \frac{\partial G}{\partial x} - kG \qquad \textbf{Equation 7-5}$$

with $D_b(x) = D_b(0)$ for $0 < x < X_L$; 0 otherwise. Aller (1980a) notes that the apparent burial velocity (ω) at NWC is 0.5 cm/yr. The bioturbation coefficient (D_b) at the site is 13.6 cm^2/yr at 20°C (Aller *et al.*, 1980; see also Aller & Cochran, 1976).

The rate of sulphate reduction can only be used to determine the 1-G rate constant if it is assumed that the rates of degradation measured in the laboratory are a reasonable approximation of the rates occurring *in situ*. (Aller & Yingst (1980) give a number of arguments which indicate that this is the case.) Furthermore, it must also be assumed that

sulphate is the dominant oxidant being used during the period of incubation. It could therefore be argued that the rate of ammonia liberation is a better measure of degradation since it does not require this assumption to be made. The rate of ammonia production (R_{NH4}) is related to the rate of carbon degradation (R_G) via:

$$R_{NH4}(x) = \frac{1-\varphi}{\varphi}\frac{sy}{sx}R_G(x) = \frac{1-\varphi}{\varphi}\frac{sy}{sx}kG(x) \qquad \textbf{Equation 7-6}$$

where R_{NH4} is in units of mass/volume/year, *sx* represents the number of moles of carbon, and *sy* the number of moles of nitrogen in the organic substrates. (As noted previously, *sy:sx* represents the molar ratio of carbon to nitrogen (C:N) in the organic matter.) The term *kG(x)* could therefore be estimated from the depth profile of ammonia production. However, with the data available the C:N ratio of the organic matter could only be estimated by comparing the rate of sulphate reduction to ammonia production (discussed further below). Consequently, fitting the solution of the 1-G model to the rate of ammonia liberation was, in practice, no better than using the sulphate reduction data directly.

There was insufficient data to allow the unsteady formulation of the 1-G model (that is, Equation 7-5) to be calibrated. However, as shown in Chapter 6, if parameter values are specified as yearly means a steady state model can be used to represent a non-stationary system. The steady state version of Equation 7-5 can be written as:

$$0 = D_b \frac{\partial^2 G}{\partial x^2} - \omega \frac{\partial G}{\partial x} - kG \qquad \textbf{Equation 7-7}$$

again with $D_b(x) = D_b(0)$ for $0 < x < X_L$; 0 otherwise. If the upper boundary condition is expressed as J_{org}, then Equation 7-7 is the 1-G model used in the verification of the redox model, and its solution is detailed in Appendix III. As noted in the Appendix, the main modelling assumptions are that a steady state condition exists, bioturbation is represented as a two-layer model, and porosity is constant.

The bioturbation coefficient at the station is given for a temperature of 20°C and the rates of sulphate reduction were determined at 22°C. To allow the steady state model to be used, these parameters had to be normalised to the mean annual temperature of 12°C. This was accomplished by using the simplified treatment of temperature dependence described in Chapter 6. A Q_{10} of three was assumed for sulphate reduction (a microbial process) and a Q_{10} of two was assumed for the bioturbation coefficient (a macrofaunal process). From Equation 6-17, the bioturbation coefficient (D_b) at 12°C is then 7.8 cm^2/yr. Similarly, the depth distribution of the rate of sulphate reduction at this temperature is:

$$R_{SO4} = 39.3\exp(-0.34x) + 1.67 \qquad \text{Equation 7-8}$$

again in units of mM/yr.

The parameters in the 1-G model are all known except for the first order rate constant (k) and the flux of organic carbon (J_{org}). These parameters can, however, be constrained somewhat. For instance, it is known that the primary production in the water overlying the station is approximately 210 gC/m^2/yr of which around thirty per cent is ultimately delivered to the benthos (Aller & Yingst, 1980). Furthermore, the rate constant of degradation can be estimated from the empirical relationships discussed previously. For a burial velocity of 0.5 cm/yr the k_1 rate constant is 0.26 /yr. However, given the uncertainty inherent in such estimates the actual value of k (in Equation 7-7) is likely to be of the order 0.1 to 1 /yr. Improved estimates were obtained by fitting the solution of the 1-G model to the depth distribution of sulphate reduction (that is, Equation 7-8).

The fitting procedure was carried out by solving the 1-G model with various combinations of carbon flux and 1-G rate constants. Calculations were made with fluxes (J_{org}) in the range of 12 to 72 gC/m^2/yr, with the range divided into 500 equal increments. At each flux, the rate constant (k) was varied over a range from 0.01 to 3 /yr, with this range divided into 300 equal intervals. The 1-G model was solved for each combination of J_{org} and k to give the depth

distribution of G(x). This was then converted into a depth distribution of sulphate reduction rates (that is, R_{so4}) using Equation 7-4. The fit of the model-generated profile of sulphate reduction rates was then compared to the empirically determined profile using a chi squared goodness of fit; that is:

$$\chi^2 = \sum_{all\ x} \frac{(R_m - R_e)^2}{R_e} \qquad \textbf{Equation 7-9}$$

where R_m represents the model rate and R_e represents the empirically determined rate. Reasonable fits ($\chi^2 \leq 2$ mM/yr) were obtained for J_{org} in the range 22.45 to 23.9 gC/m^2/yr and k in the range 0.81 to 0.94 /yr. The overall best fit ($\chi^2 = 0.13$ mM/yr) was with k of 0.84 /yr and J_{org} of 23.4 gC/m^2/yr (195 μmole/cm^2/yr).

The rate constant (k) estimated in this way must reflect the average reactivity of the organic material in the top 10 cm of the sediment column. This rate constant is therefore somewhat analogous to that of the k_1 fraction, which decays on a time scale represented by a depth of 10 to 20 cm (see Chapter 6, Section 6.5.1). However, the k_1 rate constant is usually interpreted as being an intrinsic function of the organic compounds undergoing degradation (Aller & Aller, 1998). In contrast, the rate constant estimated from the incubation data reflects the *in situ* distribution of reactive sedimentary particulate organic matter (POM). This distribution depends upon the net result of a range of sedimentary processes, as well as the nature of the organic substrate delivered to the SWI.

The calculated flux of 23.4 gC/m^2/yr represents only thirty-seven per cent of the total organic carbon flux delivered to the SWI (that is, approximately 63 gC/m^2/yr). However, it should be remembered that the total flux would also include very reactive material that degrades at the SWI and would not be incorporated into the sediment column. Furthermore, some material would have been refractory on the time scale of the incubation experiments. The fitting

procedure used above can therefore only estimate part of the total flux; that is, the estimated flux must be less than the total available flux.

In the parameter calibration procedure described above, it was assumed that both the bioturbation coefficient (D_b) and burial velocity (ω) were well constrained. In reality, there is a great deal of uncertainty associated with the measurement of these parameters. A brief sensitivity analysis was therefore carried out to determine the level of uncertainty introduced by the parameter values used. The fitting procedure was repeated with D_b specified as twice and half the value given for NWC. Similarly, the value of burial velocity was specified as half the value quoted. (The burial velocity was not doubled since the apparent burial velocity of 0.5 cm/yr used is likely to be a high estimate.)

The results of the sensitivity analysis indicated that the flux and rate constants would fall in the range of 23.2 to 23.8 $gC/m^2/yr$ and 0.4 to 1.3 /yr respectively. These ranges can be used to give a simple assessment of the uncertainty introduced into the model output. For example, if the value of 0.84/yr is taken as the baseline rate constant, then the range of normalised k determined in the analysis was 0.5 to 1.5 (normalised to the baseline estimate). From Figure 24 (in Chapter 6), it can be estimated that the maximum range in characteristic depths d_1 and d_2 associated with this range of normalised k is approximately sixty per cent of the baseline depths. It is therefore quite possible that the values of D_b and ω used have already introduced a significant level of uncertainty into the model redox profile. This analysis would be more meaningful if the experimental error associated with the parameters (D_b and ω) was known. However, this information is not normally provided in the diagenetic literature, presumably because the parameters are themselves determined by fitting models to data, rather than being measured directly.

7.2.3 Dirichlet Boundary Conditions

Aller (1980a; 1980b) measured the nitrate, ammonia, and sulphate concentrations at the SWI but did not determine the concentrations of other solutes. However, from the site description it is reasonable to assume that the water was well saturated with oxygen. Given this assumption it is also reasonable to assume that the concentration of reduced solutes at the SWI approached zero. The boundary conditions of nitrate, ammonia, and sulphate, were therefore specified according to the data given in Aller (op. cit.). The boundary conditions for other solutes were specified as the typical value for a coastal scenario used previously.

Specifying the boundary condition for the Mn and Fe oxides was, however, problematic because Aller (1980b) used an aggressive extraction technique to determine the total concentration of Fe and Mn in the solid fraction. Therefore, the concentrations would have included:

1. A structurally stable lithogenic fraction extracted from the matrices of sediment particles.
2. A reactive fraction consisting of:
    - Reactive metal-oxides.
    - Adsorbed reduced phases (that is, Fe^{2+}, Mn^{2+}).
    - Solid reduced phases such as pyrite, AVS, and various carbonates.

The total reactive fraction can be estimated by subtracting the background concentration of total Fe or Mn measured at depth from the concentrations measured at the SWI (e.g. Aller, 1994). However, no estimate could be made of the proportions of the various species that make up this reactive phase. Hence, accurate estimates could not be made of the MnO_2 and $Fe(OH)_3$ boundary conditions. There is thus a great deal of uncertainty associated with the modelling of Mn and Fe phases at NWC. (Canfield *et al.* (1993b) describe analytical techniques that allow the concentrations of these components to be determined.)

7.2.4 Depth Profiles of AVS

All cores at NWC showed a subsurface peak in the concentration of AVS at a depth of approximately 4 cm. Below this depth the concentration fell, indicating that conversion to pyrite (FeS_2) was occurring. However, pyrite conversion is not included within the redox model. Consequently, the depth distribution of iron-sulphides at NWC can not be reproduced. The conversion of AVS to pyrite can be modelled as a first order reaction in AVS concentration (Boudreau, 1996) and the modification required to include this reaction is quite trivial. However, its inclusion would not add anything to the current exercise because the data available does not allow the accurate modelling of the authigenic metal species.

7.2.5 Calibrating the Irrigation Coefficient

The irrigation coefficient can be calibrated by fitting the model ammonia profile to measured ammonia profiles (e.g. Van Cappellen & Wang, 1996). However, before doing this it is desirable to constrain all other parameters (other than irrigation) that influence the distribution of ammonia. Ammonia distribution depends upon both transport processes and the rate of production. The rate of ammonia production at any depth depends upon the quantity and quality of the organic matter. In terms of model parameters these factors are represented by:

1. The concentration of organic matter.
2. The rate constant of degradation.
3. The C:N ratio of the organic matter being degraded.

The rate constant of degradation and concentration of organic matter have already been determined by fitting the solution of the 1-G model to the depth distribution of sulphate reduction. Hence, the only unknown is the C:N ratio of the organic matter.

Aller & Yingst (1980) estimated that the depth averaged C:N ratio at NWC was 6.5:1. However, a preferential degradation of nitrogenous compounds is normally observed in sediments (e.g. Kristensen & Blackburn, 1987). Consequently, the C:N ratio of sedimentary organic matter increases with depth. The use of an average C:N ratio would therefore distort

the rates of ammonia production, especially in the top portion of the sediment. Before calibrating the irrigation coefficient it is, therefore, desirable to constrain the depth distribution of C:N in some way.

If sulphate reduction is the dominant metabolic process used, and assuming k_{NH4} is one and the C:S of sulphate reduction is 2:1, there is a direct correspondence between the ratio R_{SO4}:$R_{NH4}/(1+k_{NH4})$ and the ratio of the rate of carbon mineralisation to gross ammonia production (that is, $R_{\Sigma CO2}$:R_{NH4}). Under these conditions the C:N ratio of the organic matter being mineralised can be estimated from the ratio R_{SO4}:R_{NH4} /$(1+k_{NH4})$. The ratios of these two rates were therefore calculated and polynomials of various orders fitted through the resulting depth distribution. A fifth order polynomial gave a good fit (assessed visually) to the depth profile; that is:

$$\frac{R_{SO4}}{R_{NH4}(1+k_{NH4})^{-1}}(x) = 0.0006x^5 - 0.014x^4 + 0.09x^3 - 0.013x^2 + 1.13x + 4.24 \qquad \textbf{Equation 7-10}$$

Equation 7-10 indicates that the ratio R_{SO4}:R_{NH4} /$(1+k_{NH4})$ in the upper portion of the sediment column was low (4.2:1 at x = 0) with respect to the Redfield ratio (C:N ratio of 106:16 or 6.6:1). This probably indicates a preferential oxidation of nitrogenous compounds was occurring. It could, however, indicate that oxidants other than sulphate were being used to oxidise the organic matter in the incubation experiments -- the rate of sulphate reduction (R_{SO4}) would then not correspond to the rate of carbon mineralisation ($R_{\Sigma CO2}$). However, the ratio R_{SO4}:$R_{NH4}/(1+k_{NH4})$ at the SWI (4.24:1) is within the range reported for the ratio $R_{\Sigma CO2}$:R_{NH4} determined for the decomposition of relatively fresh organic matter in marine sediments (see Canfield *et al.*, 1993b and references therein). This lends some support to the assumption that sulphate reduction was the dominant pathway of decomposition being used in the incubation experiments.

It therefore seems likely that the low R_{SO4}:$R_{NH4}/(1+k_{NH4})$ ratio at the SWI indicates a preferential degradation of nitrogenous compounds. Consequently, in the top portion of the sediment this ratio gave an 'apparent' C:N ratio rather than the true C:N ratio of the organic matter. This apparent C:N ratio reflects both the actual C:N ratio of the organic matter and the preferential degradation of nitrogenous material. Nevertheless, for the current purposes the apparent ratio is actually more useful since it forces the modelled rates of ammonia production at each depth to match those determined empirically. Hence, the apparent C:N ratio ensures there is a good correspondence between the depth distribution of rates in the model and those occurring within the sediment column. (Again assuming the rates determined in the laboratory are reasonable approximations of those occurring *in situ*.)

As noted above, the profile of ammonia also depends upon transport processes. Since the values of transport parameters other than the irrigation coefficient are known, the ammonia profiles measured at NWC can be used to calibrate the irrigation coefficient. This was achieved by running the redox model with different values of irrigation coefficient and comparing the resultant ammonia profiles to the profiles given in Aller (1980a, Appendix B).

Aller (1980a) measured six ammonia profiles at NWC over a period of two years. The ammonia concentrations were determined for depth intervals, rather than at specific points in the sediment column. The yearly mean ammonia profile at NWC was therefore calculated by taking the average concentration in each depth interval over the six profiles given. The concentrations were then assumed to occur in the centre of each interval. This yearly mean profile could then be compared to the profile generated by the steady state redox model.

Ammonia profiles were generated with the model parameterised according to the parameter values and boundary conditions discussed above (the parameter values are summarised in Appendix VIII, designated as NWC1). The model domain was specified as 20 cm with a space step of 0.025 cm. The additional 10 cm was modelled to ensure that the Neumann condition at

the lower boundary did not effect the concentration profiles in the interval of interest; that is, the top 10 cm. The profiles in the interval 10-20 cm were therefore not considered. The fifth order polynomial (Equation 7-10) was used to represent the apparent C:N ratio in the interval 0-10 cm; at a depth of 10 cm and below the C:N ratio was assumed constant.

As noted previously, the depth dependencies of various parameters could be an important modelling consideration. However, since there was no information concerning the depth profiles of parameters at NWC, the representation of depth dependency was somewhat arbitrary. In the face of this uncertainty the simplest model was selected, and the depth distribution of bioturbation and irrigation were represented as a two-layer model with 'mixing' depth of 10 cm. The values of other parameters were again assumed equal to the 'typical' values of a coastal sediment used previously. A range of irrigation coefficients was specified and the resulting ammonia profiles compared to the average of the measured concentration profiles, as shown in Figure 28. It can be seen that a non-local exchange coefficient of 3/yr gives a reasonable fit to the data.

Aller (1980a) also modelled the ammonia distribution at NWC using a 2-D radial diffusion model. It was noted earlier that there is an equivalence between this 2-D model and the non-local exchange model of irrigation. This equivalence involves $\bar{r}$ the radius where the concentration of the diffusing solute is equal to the laterally averaged concentration (see Section 5.6.2.1). The value of $\bar{r}$ is not known but must lie in the interval between the inner and outer radii of the micro-environment (that is, $r_1 < \bar{r} < r_2$). Aller (1980a, p.299) used an inner radius (r_1) of 0.14 cm, an outer radius (r_2) of 5.9 cm, and a diffusion coefficient for ammonia of 264 cm^2/yr. Substituting these values into Equation 5-20 gives a non-local irrigation coefficient ranging between 0.21 and 17.7 /yr. Hence, the value of irrigation coefficient determined in this study (3 /yr) is comparable with the estimate of irrigation parameters made by Aller.

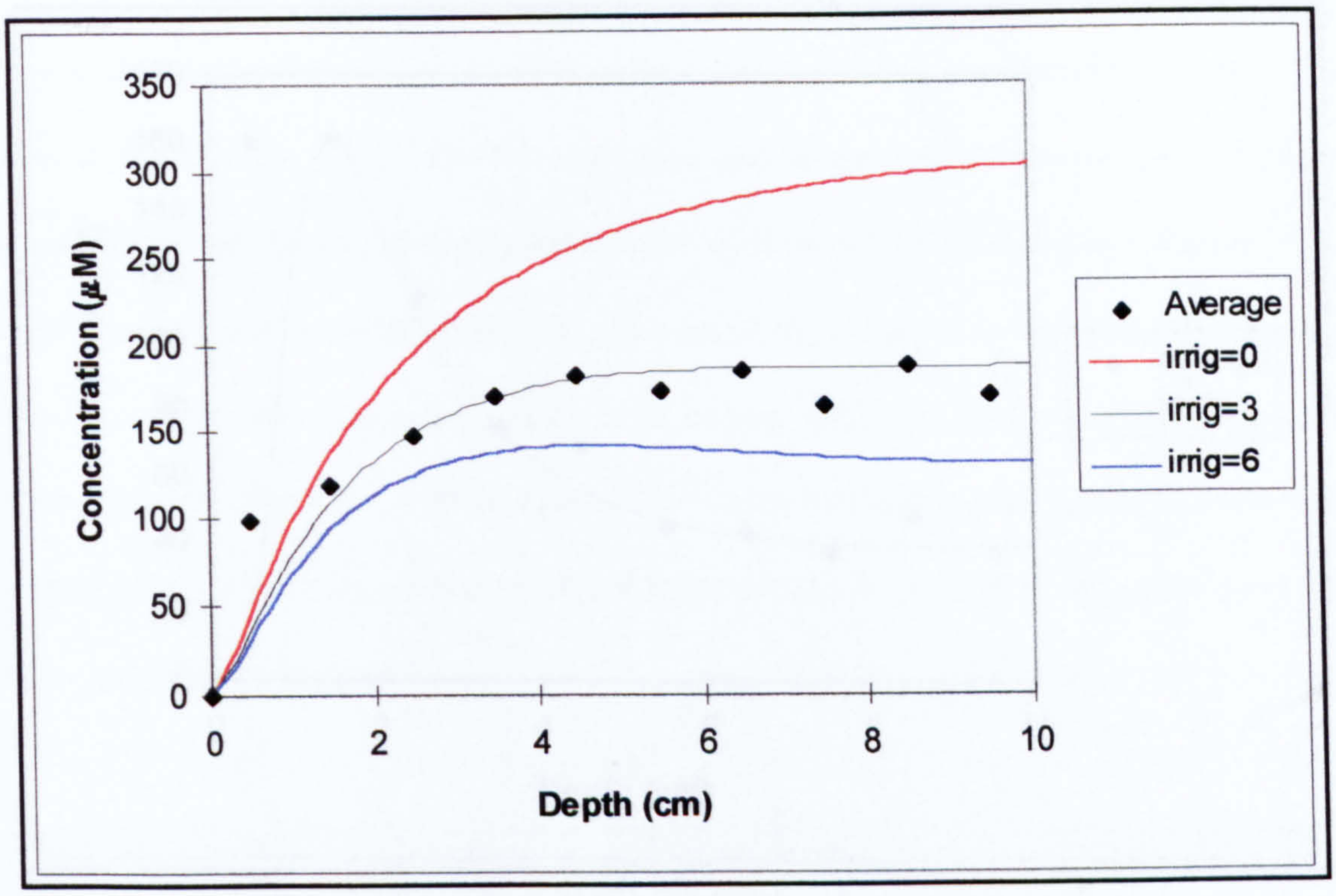

NB: 'Average' in the legend indicates the yearly averaged ammonia concentrations at NWC; 'irrig' indicate the value of the non local exchange coefficient used

Figure 28 *Model Ammonia Profile and Averaged Analytical Profiles*

7.2.6 Calibrating Parameters Associated with Metal Species

As noted above, the accurate modelling of Mn and Fe at NWC was not possible using the data presented by Aller (1980a; 1980b). However, the values of various parameters associated with these components could still be calibrated to some extent. This was achieved by adjusting the boundary conditions of the metal-oxides and the parameter values associated with the precipitation/dissolution of the authigenic phases until the model output matched the profiles measured at NWC. For example, Figure 29 compares the averaged Mn^{2+} depth profile at NWC with the model Mn^{2+} profile after parameter values have been calibrated in this way.

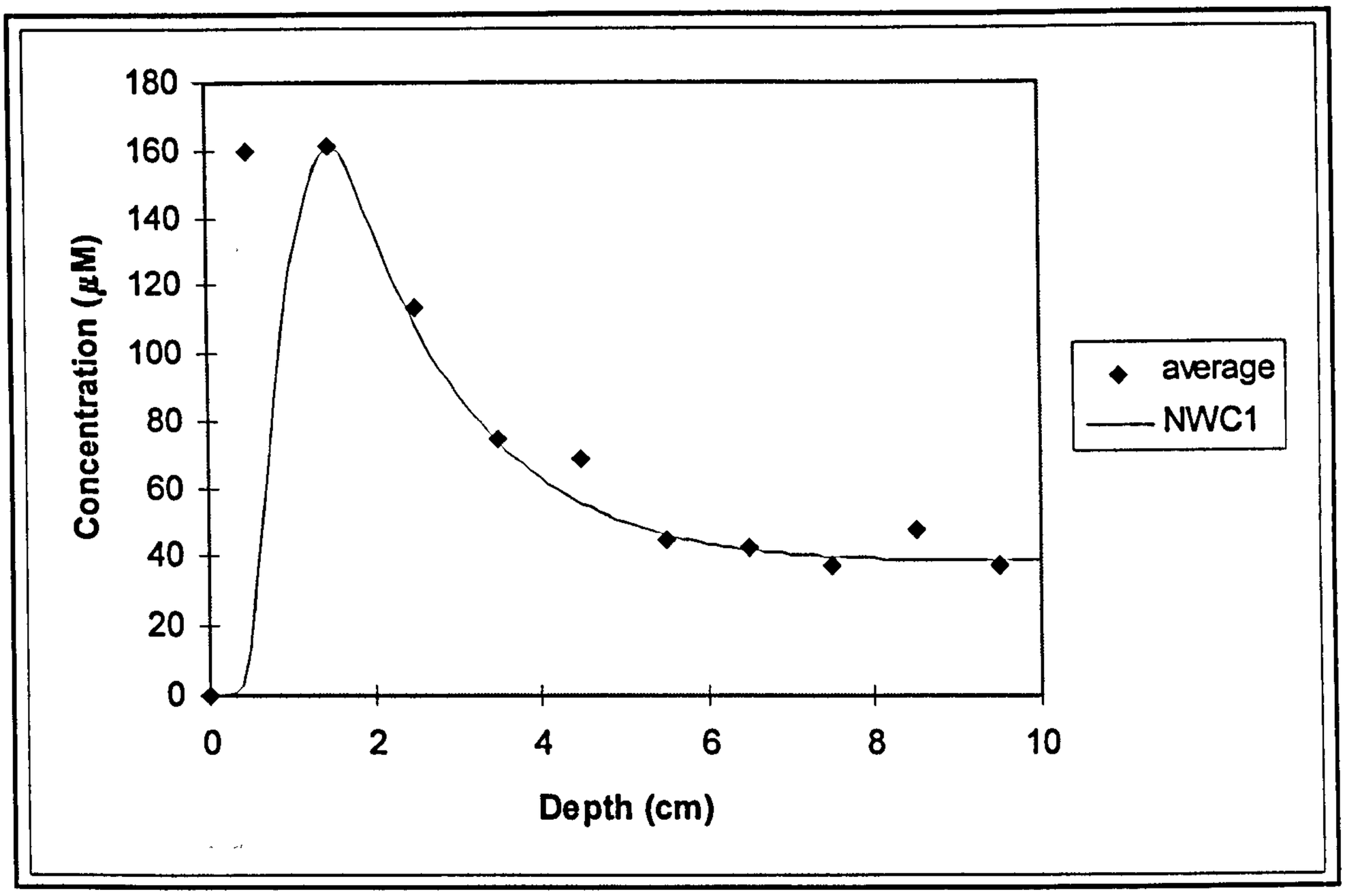

NB: Average in the legend indicates the yearly averaged Mn^{2+} concentrations at NWC; NWC1 indicates the profile generated by the model

Figure 29 *Model Mn^{2+} Profile and Averaged Analytical Profiles*

7.3 Transient Response

The parameter values determined above were used to examine the transient response of the model. (The parameter values used are summarised in Appendix VIII, designated as case NWC1.) Temperature and carbon flux were specified using the simple sinusoidal forcing functions given in Chapter 6. Microbial and macrofaunal activities were assumed to exhibit a temperature response that is adequately described using a simplified Q_{10} treatment, as discussed previously.

The temperature at NWC follows an approximately sinusoidal distribution in time (Aller, 1980a). Aller & Yingst (1980) state that the lowest temperatures (2°C) are found in February-March and the highest temperatures (22°C) in August-September. The amplitude of the temperature forcing function (Equation 6-16) was therefore specified as 10°C. The annual primary production in Long Island Sound is characterised by a major late winter-early spring

bloom and a lesser autumn bloom. The spring bloom results in a substantial export of organic matter to the benthos (Aller, 1994b). Because only a portion of the total flux of carbon is considered in the model, the amplitude of the carbon flux temperature forcing function (Equation 6-15) was assumed to be 100 per cent of the mean value determined during model calibration. The maximum carbon flux occurs in May when the spring temperature is equal to the yearly mean (see Aller, 1994b; Figure 4). The seasonal response of the carbon flux was therefore represented by specifying a lag of three months between the temperature and flux of carbon, as shown in Figure 30.

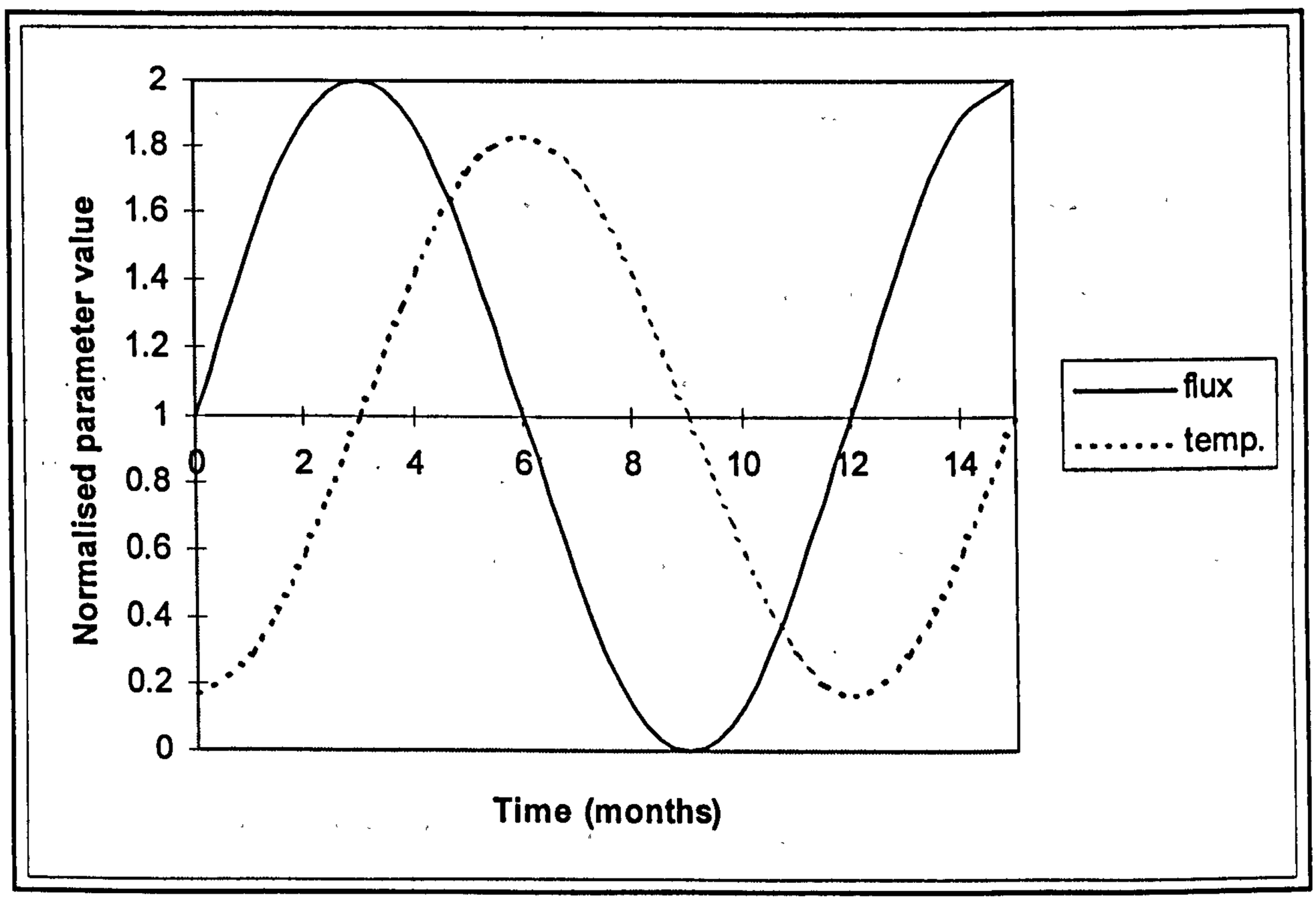

NB: The forcing functions were normalised before plotting by dividing by the mean.

Figure 30 *Relationship between the Carbon Flux and Temperature Forcing Functions*

The model domain was specified as 20 cm with a space step of 0.025 cm. The model was run for nine model years and the concentration profiles for years eight and nine saved. No significant difference between the output for these years was observed, indicating that all transients associated with the initial conditions had died away. The concentration profiles generated by the model were again compared with the profiles given in Aller (1980a). For

consistency with results presented so far, only the concentration profiles of ammonia and Mn^{2+} are included herein. (NB: In the context of this exercise, ammonia represents a component species for which the associated parameters are relatively well constrained; Mn^{2+} is a component for which parameter estimates are poor.)

Figures 31 to 36 compare measured and modelled profiles for spring (March), summer (July), and autumn (November). The interval 10 to 20 cm was again modelled to account for the Neumann condition at the lower boundary (see page 216). The concentration profiles plotted in each Figure, designated as Year 1 and Year 2, correspond to the data for the two sample years given in Aller (1980a; 1980b). It can be seen that the transient version of the model produces depth profiles that are qualitatively similar to the depth profiles at NWC. Furthermore, the quantitative agreement between the measured and model profiles are reasonable given the number of assumptions made during the calibration exercise and in the modelling of the transient case. It is also noteworthy that there is a considerable difference between the concentration profiles measured in each year. This is especially noticeable in the ammonia profiles of the summer sampling period shown in Figure 32. These differences further emphasise the heterogeneous nature of the coastal environment.

The correspondence between the model and measured transient response lends some support to the estimates of parameter values determined during the model calibration exercise. As noted above, however, there is considerable uncertainty associated with the metal-oxide components and associated phases. Nevertheless, for the purposes of the present discussion it can be assumed that the model does give a reasonable reproduction of the concentration profiles at NWC, at least within the constraints imposed by the modelling assumptions. The model redox profile can then be used to give a summary of the redox state of the system.

By way of illustration, the spring, summer, and autumn redox profiles calculated for NWC are shown in Figure 37. It can be seen that the redox state of the sediment is more reducing in

summer and more oxidised in spring, with autumn representing an intermediate case. It should be noted that in parts of each profile there is a slight increase in model redox potential with depth. This slight increase occurs in the zones of MnO_2 and $Fe(OH)_3$ reduction and is related to a fall in the concentration (activity) of the dissolved metal ions, which are used to calculate the Eh within these zones.

Figure 38 illustrates the seasonal response of redox state at NWC when characterised by the depth of the RPDL (again assumed to be the depth where Eh < 0). As expected, the depth of the RPDL is shallowest during the summer and deepest during the winter months. However, the seasonal response is not smooth, even though smooth forcing functions are specified for the temperature and carbon flux. This irregular response is related to the way in which the RPDL has been specified, coupled with the predicted distribution of metal-oxides and reduced metal ions throughout the year (discussed further below).

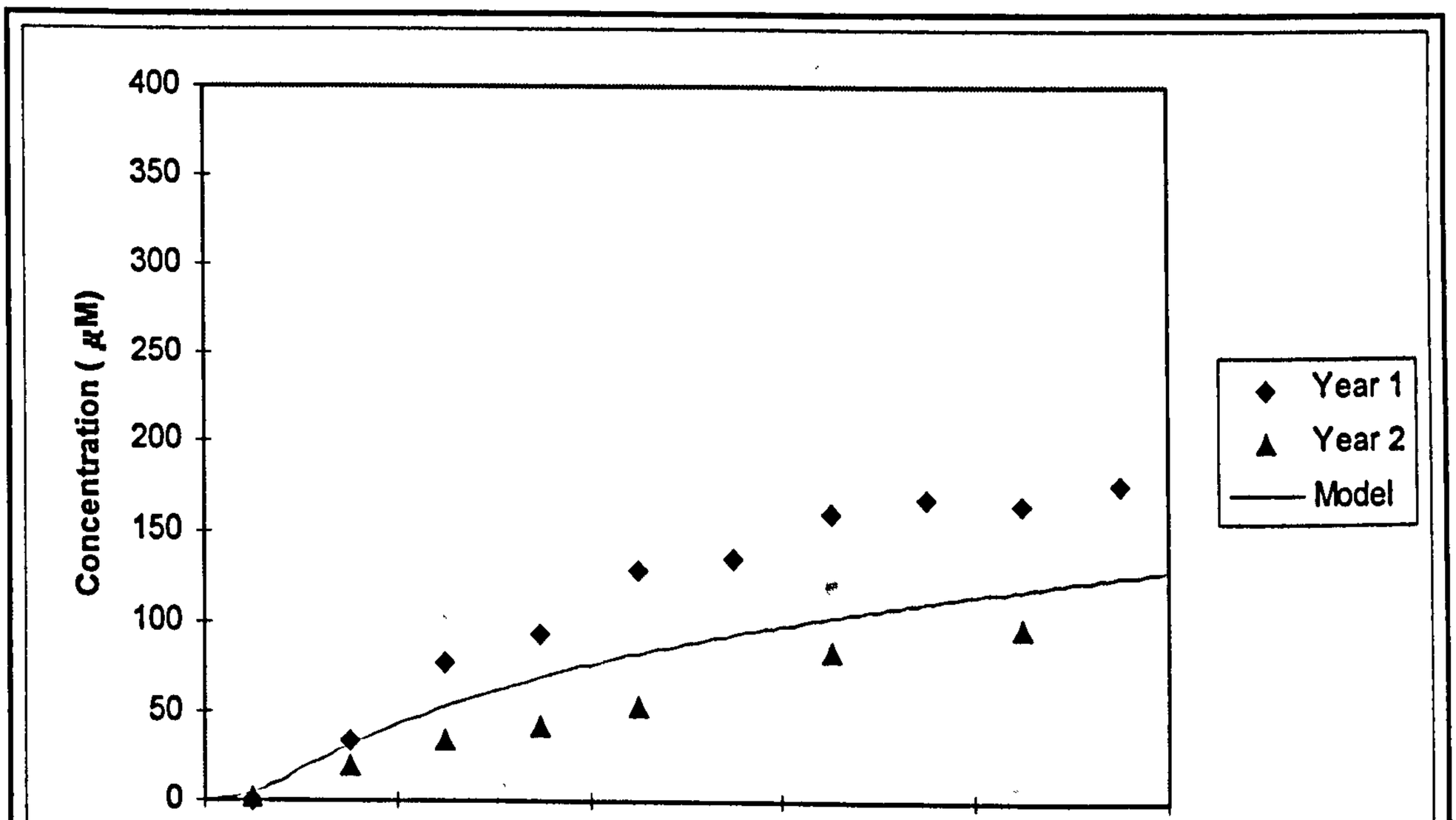

Figure 31 *Spring Ammonia Profiles*

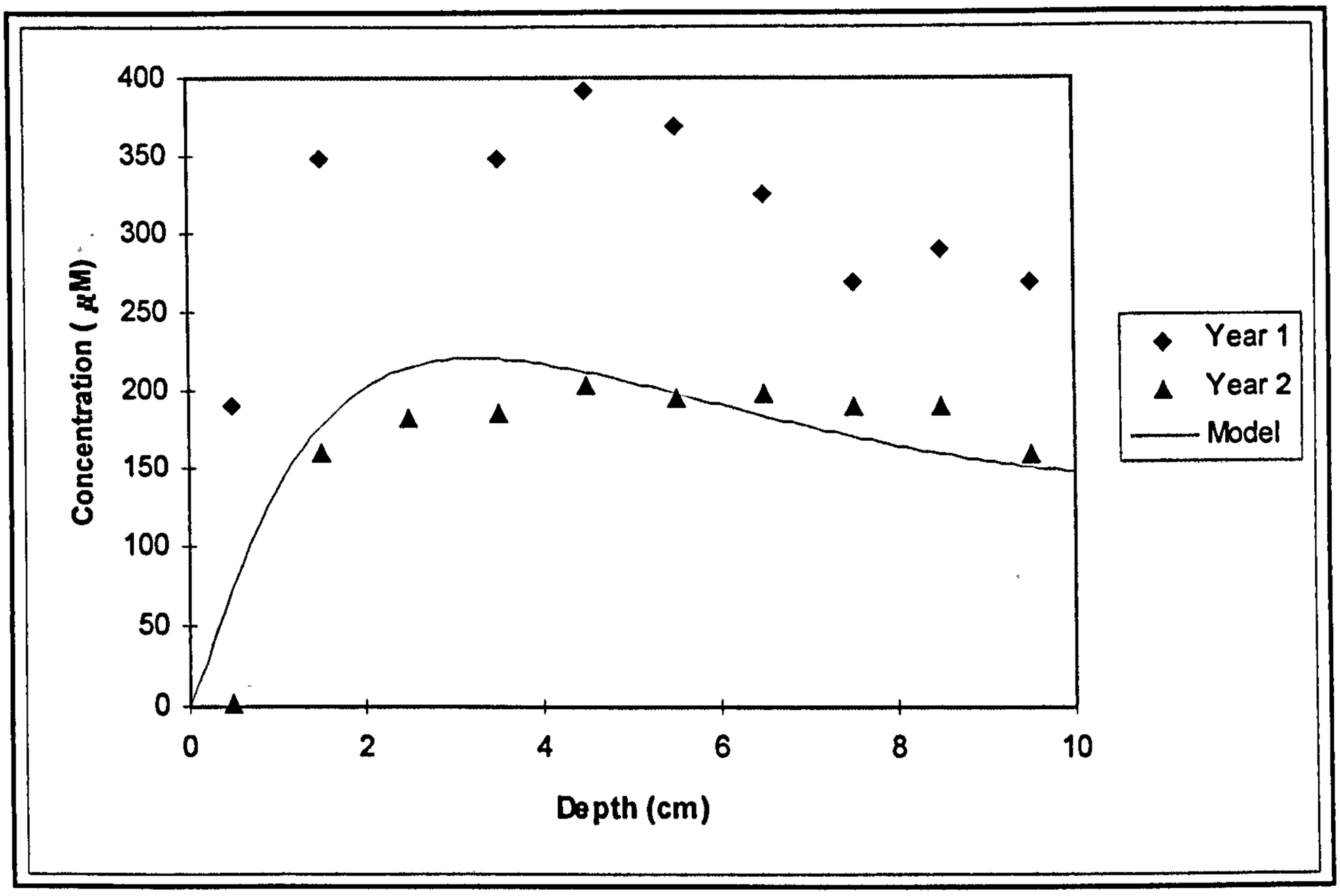

Figure 32 *Summer Ammonia Profiles*

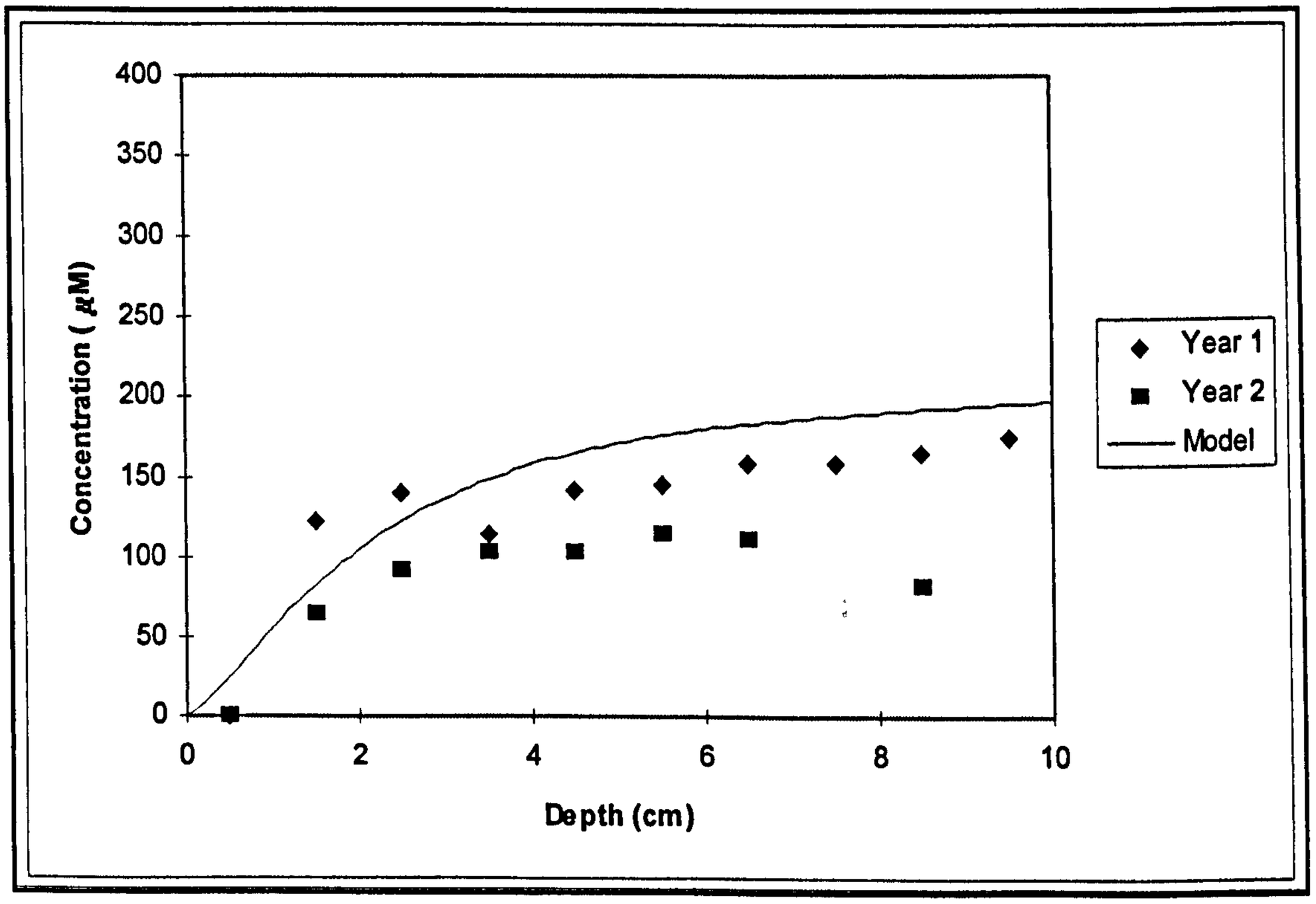

Figure 33 *Autumn Ammonia Profiles*

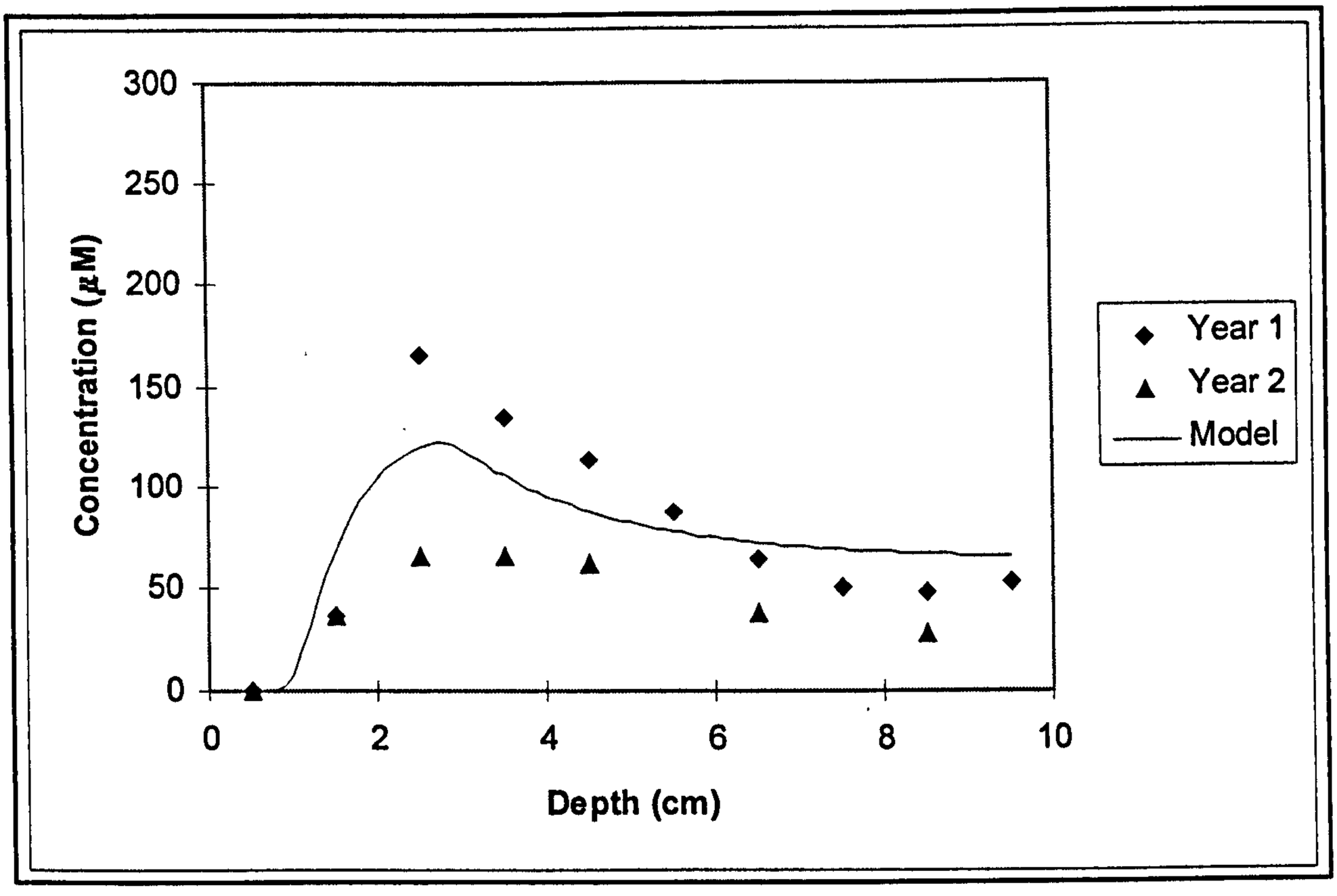

Figure 34 *Spring Mn^{2+} Profiles*

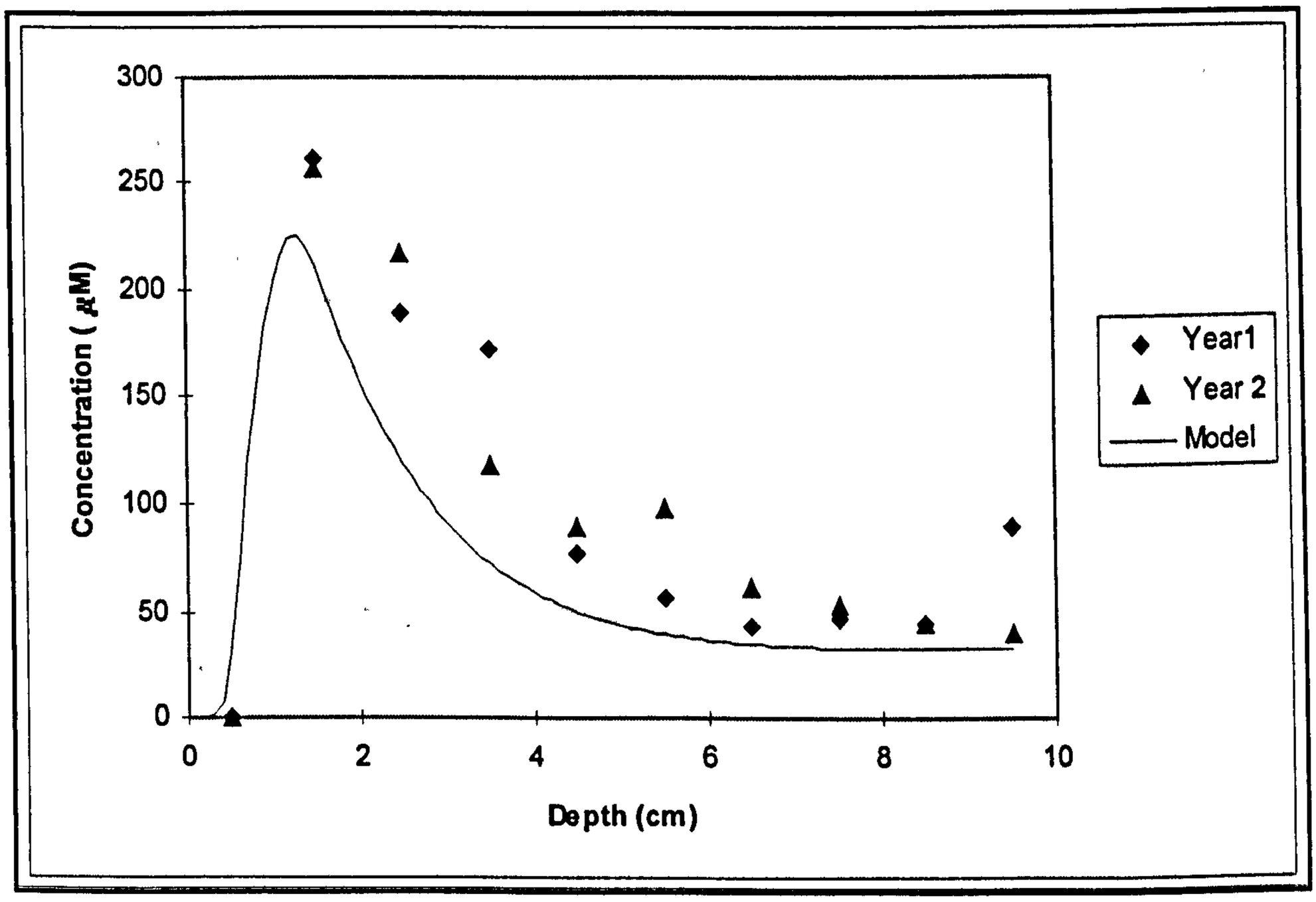

Figure 35 *Summer Mn^{2+} Profiles*

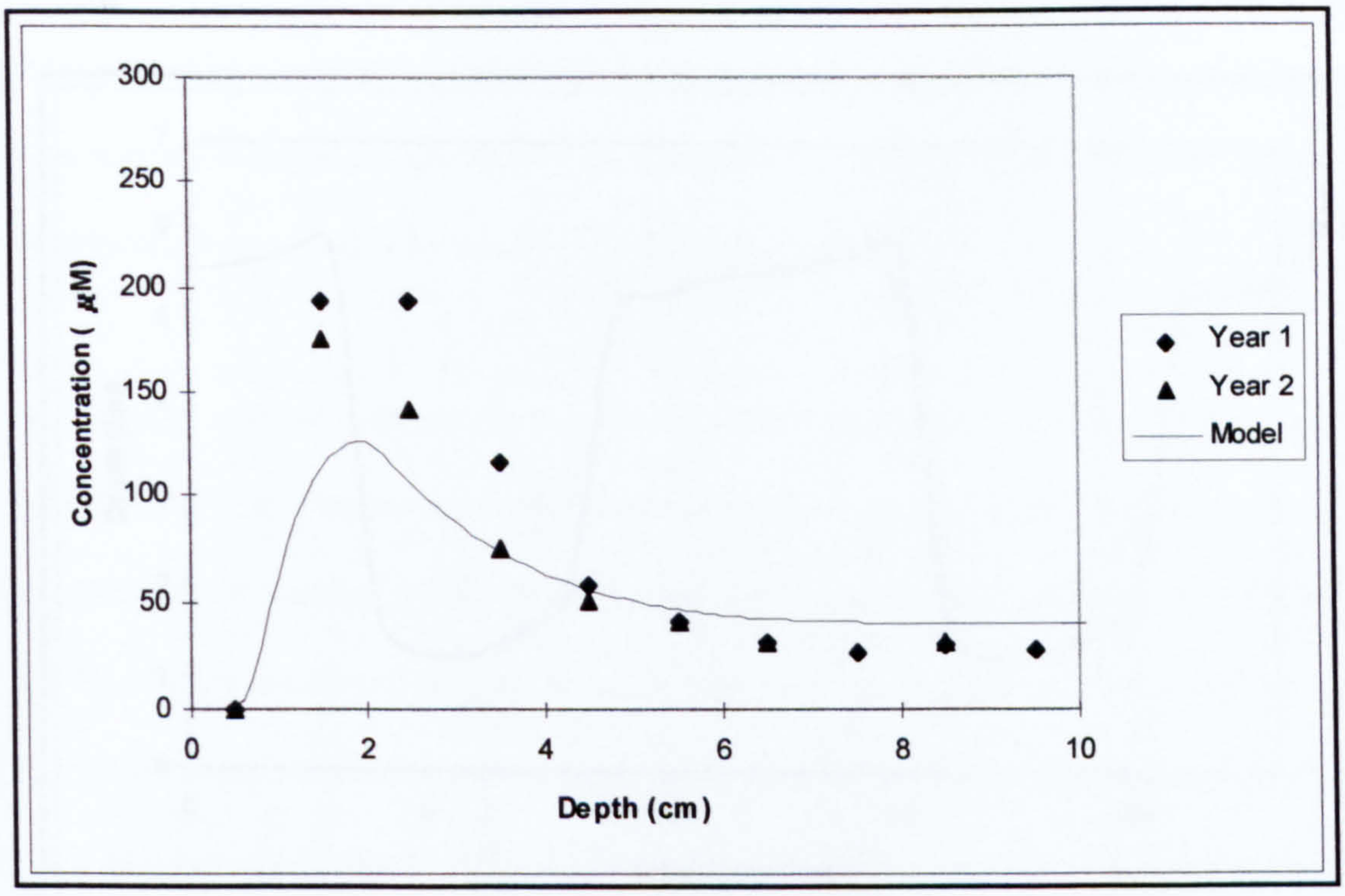

Figure 36 *Autumn Mn^{2+} Profiles*

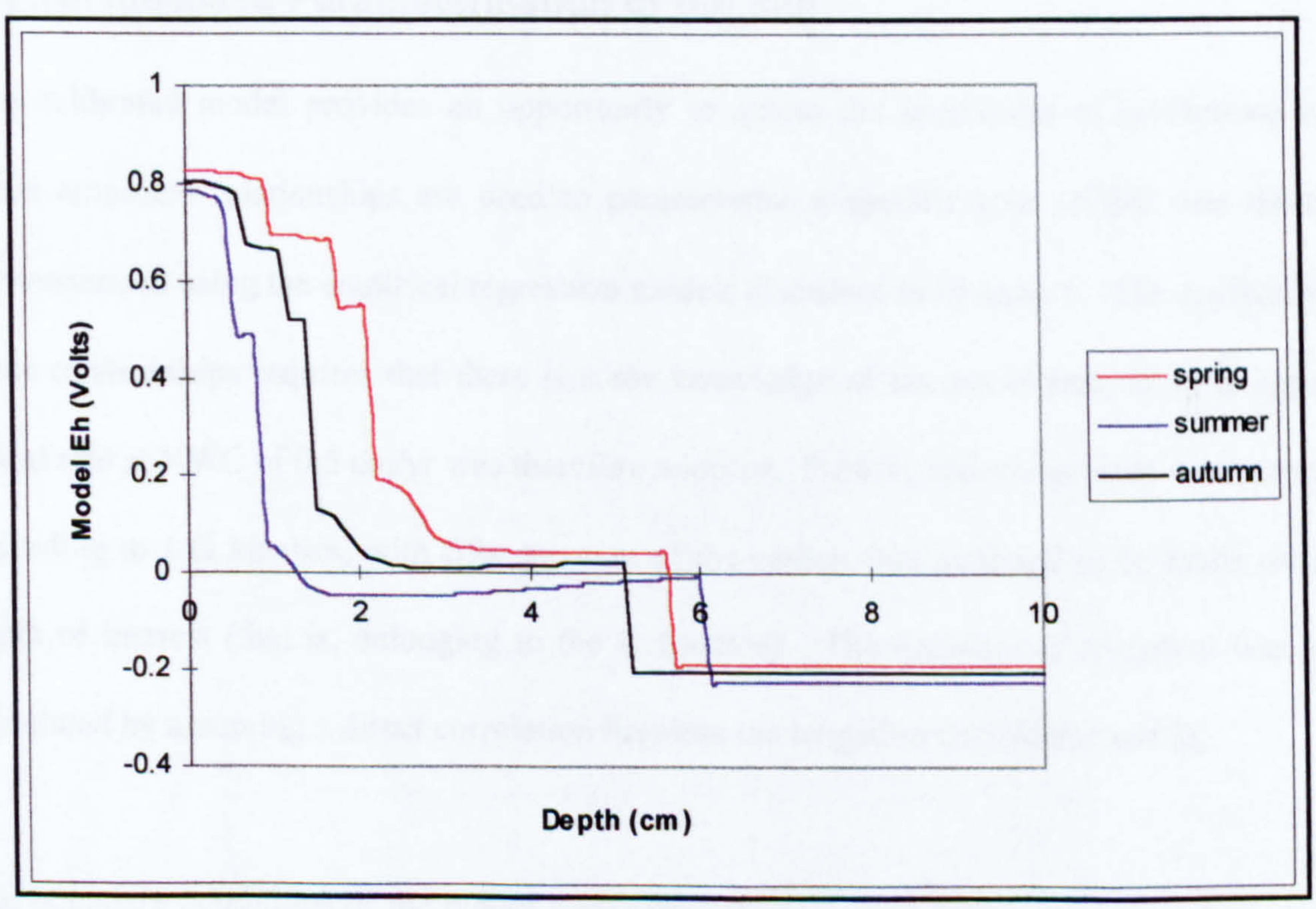

Figure 37 *Seasonal Change in Model Eh Profiles at NWC*

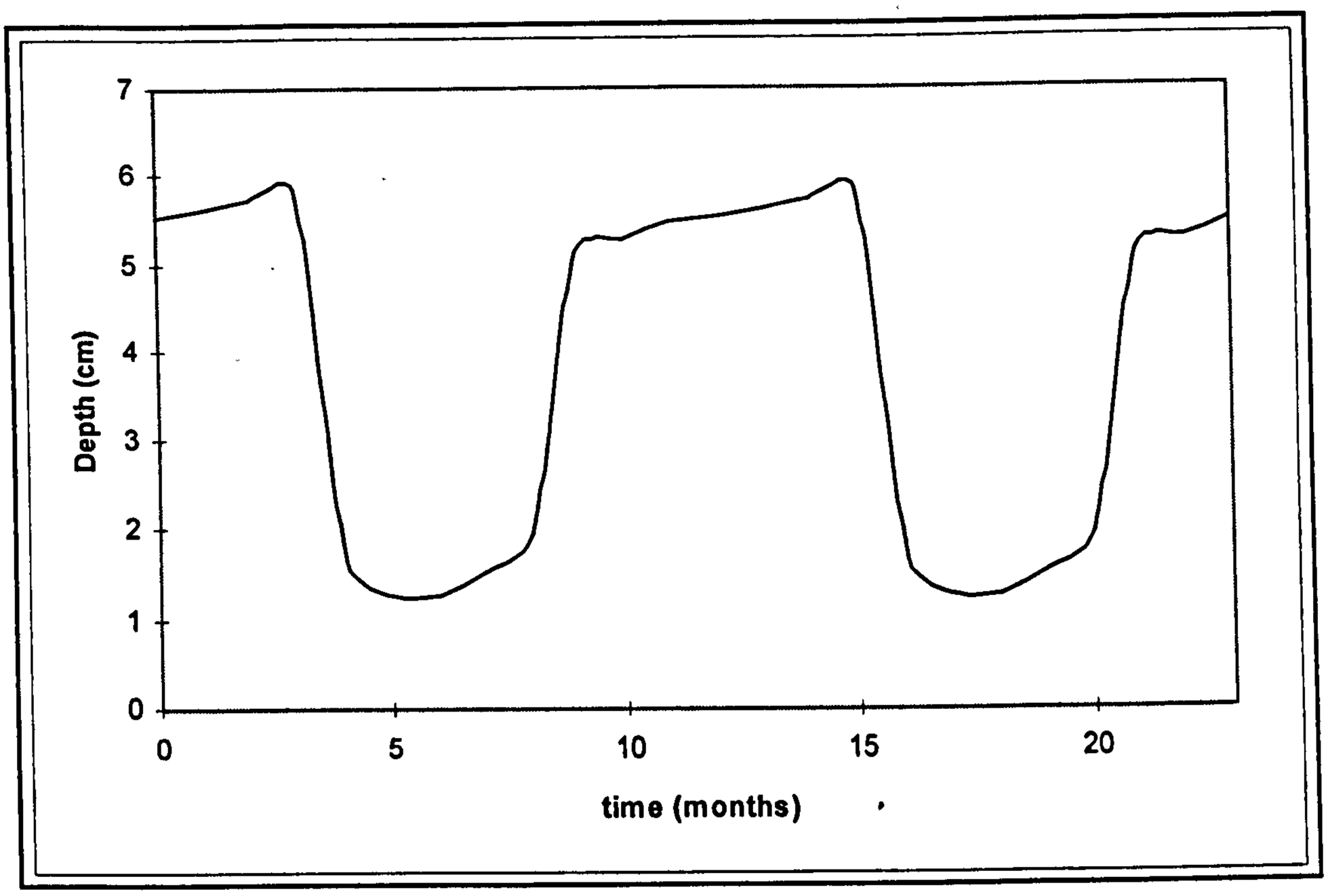

Figure 38 *Seasonal Change in Model RPDL at NWC*

7.4 An Idealised Parameterisation of the Site

The calibrated model provides an opportunity to assess the usefulness of predictions made when empirical relationships are used to parameterise a specific site. NWC was therefore parameterised using the empirical regression models discussed in Chapter 6. The application of these relationships requires that there is some knowledge of the burial rate, and the apparent burial rate at NWC of 0.5 cm/yr was therefore adopted. Primary redox reactions were specified according to 1-G kinetics, with fifty per cent of the carbon flux assumed to be labile over the depth of interest (that is, belonging to the k_1 fraction). The intensity of irrigation was again calculated by assuming a direct correlation between the irrigation coefficient and D_b.

The boundary conditions of the model were specified according to the 'typical' values used in the sensitivity analysis. Similarly, 'typical' values were used for the rate constants of the secondary redox reactions, the precipitation/dissolution reactions, and the C:N ratio. A constant porosity of 0.74 was again used. The depth dependence of bioturbation and irrigation

were specified as a two-layer model with a 'mixing depth' of 10 cm. The full input conditions for the runs are detailed in Appendix VIII, designated as NWC2. The model domain and space step were again specified as 20 cm and 0.025 cm respectively.

The ammonia, reduced manganese, and redox profiles generated by the steady state version of the model have again been used to illustrate the model output. Figure 39 and Figure 40 show the concentration profiles for the NWC2 case. For comparative purposes, the Figures also show the average concentration profiles calculated from the data given in Aller (1980a) and the steady state model outputs for the calibrated case (that is, NWC1). Figure 39 shows the depth profiles of ammonia concentration. It can be seen that when parameterised using the empirical equations the model does not produce a good fit to the data. In contrast, the equivalent plot of the Mn^{2+} profiles, given in Figure 40, indicates that the model profile still exhibits a reasonable fit to the data. This is somewhat surprising since different boundary conditions, reaction rates, irrigation, and solubility product were specified for the NWC2 case. This again illustrates the number of degrees of freedom available in the model.

Figure 41 compares the Eh profile generated by the model for both the NWC1 and NWC2 input conditions. To aid the interpretation of the redox profiles Table 29 details the relationship between the model redox potentials and the diagenetic zonation for both cases.

Model Eh (Volts)	***Diagenetic Zone***
Eh>0.7	Oxygen reduction (oxic)
0.7>Eh>0.6	Nitrate reduction (oxic)
0.6>Eh>0.5	MnO_2 reduction (suboxic)
0.5>Eh>0	$Fe(OH)_3$ reduction (suboxic)
Eh < 0	Sulphate reduction (anoxic)

Table 29 *Model Redox Potentials and Diagenetic Zonation*

The redox profiles shown in Figure 41 indicate that there is a significant difference in the diagenetic zonation of the sediment. In particular, the zone of MnO_2 reduction is much more extensive in the case of NWC2, and the zone of $Fe(OH)_3$ reduction is more extensive in NWC1.

There are also slight differences in the oxygen penetration depths, as indicated by the longer initial plateau in the profile of NWC1.

It is noteworthy that there was a reasonable correspondence between the depth of the model RPDL predicted for the NWC1 and NWC2 cases (NWC1: 4.3 cm; NWC2: 4.9 cm). As discussed previously, the depth of the RPDL determined from electrode measurements gives a qualitative assessment of the sedimentary redox conditions. However, in the redox model the depth of the RPDL is sensitive to the extent of the metal-oxide reduction zones and to the concentration of associated metal ions within the zones. For example, the redox profile for case NWC1, shown in Figure 41, exhibits a model Eh that is only slightly above zero from a depth of 2 to 4.3 cm. The depth of the model RPDL is therefore 4.3 cm but a slight change in model parameters could result in a RPDL of 2 cm. Therefore, the depth of the model RPDL does not provide a consistent summary of the predicted sedimentary redox state.

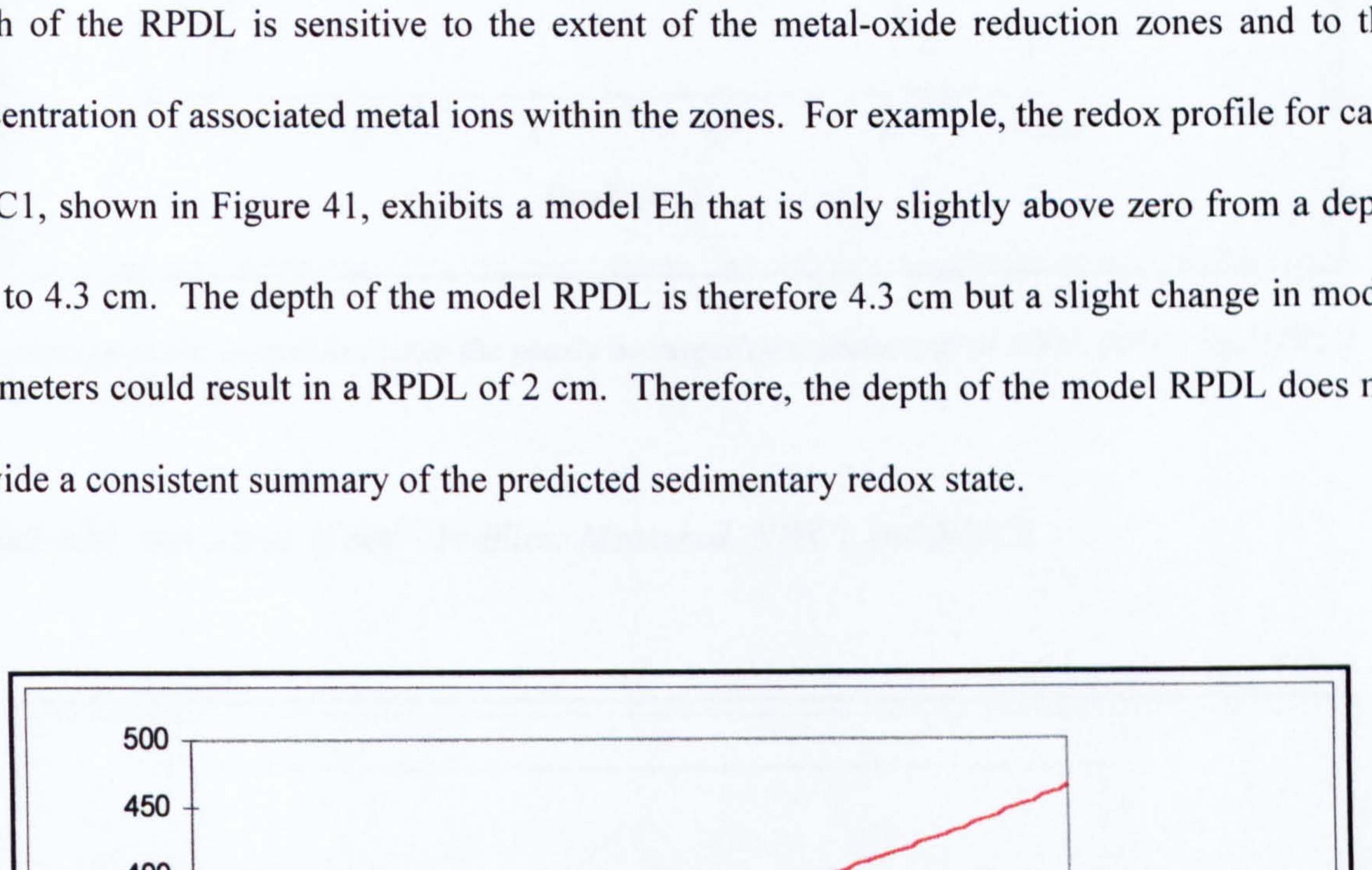

NB: Average in the legend indicates the yearly averaged concentrations at NWC; NWC1 and NWC2 denote the model output

Figure 39 *Comparison of Ammonia Profiles; Measured, NWC1 and NWC2*

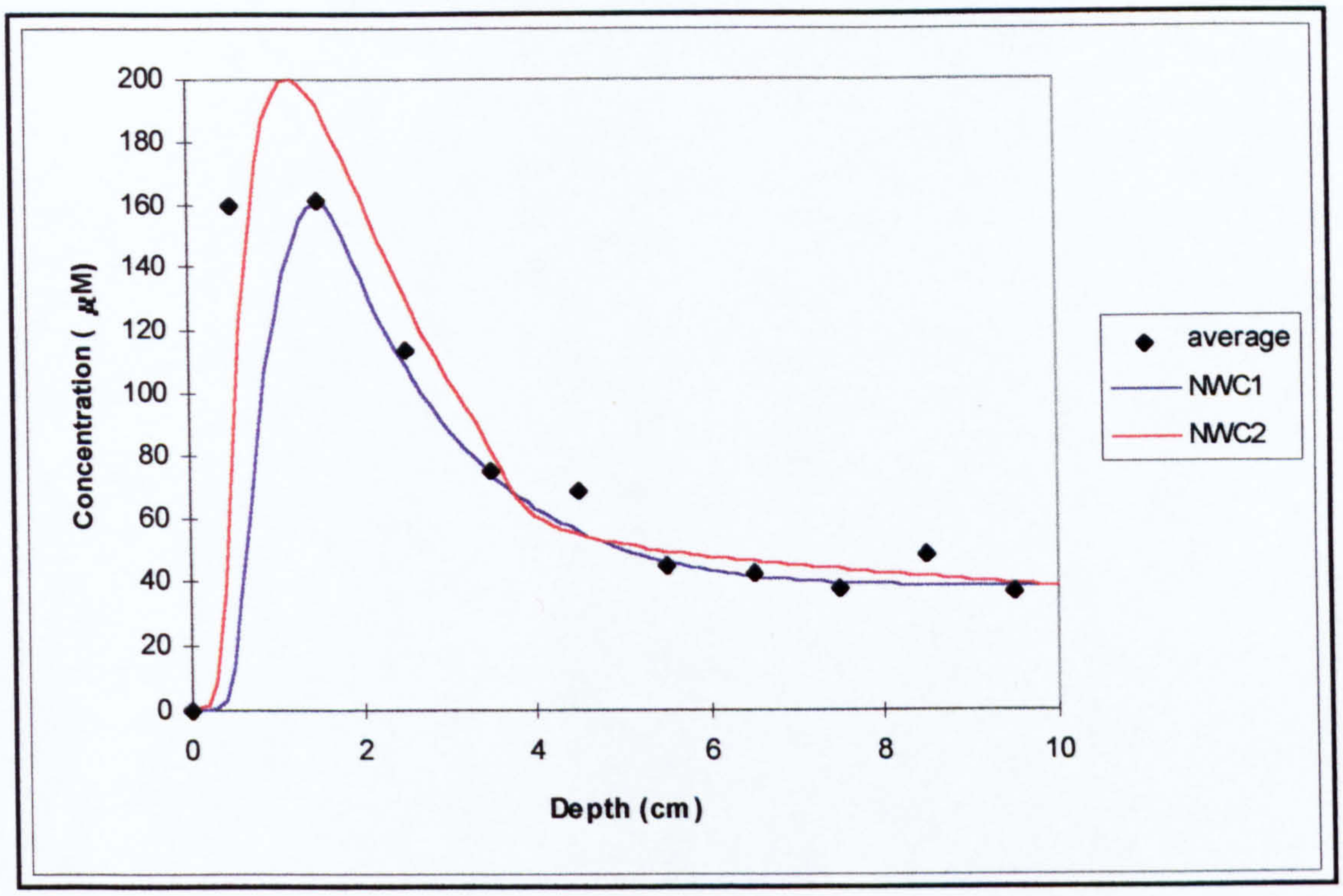

NB: Average in the legend indicates the yearly averaged concentrations at NWC; NWC1 and NWC2 denote the model output

Figure 40 *Comparison of Mn^{2+} Profiles; Measured, NWC1 and NWC2*

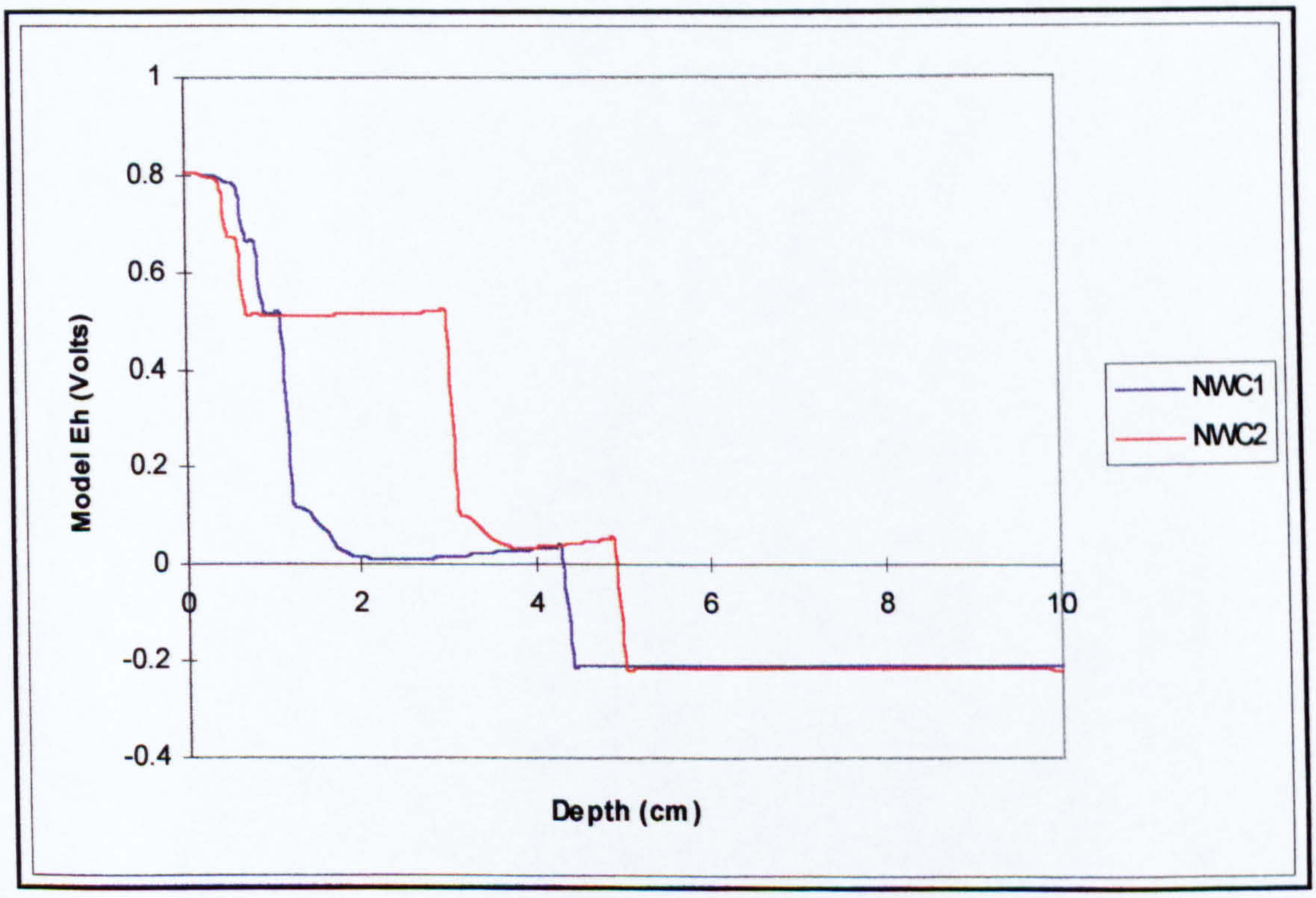

Figure 41 *Comparison of Eh Profiles; NWC1 and NWC2 Cases*

7.5 Implications of the Site-Specific Modelling Exercise

The data given by Aller (1980a; 1980b) relates to a number of years of field studies and the data set is therefore quite comprehensive. However, it has been demonstrated that the data set is still incomplete with regard to the requirements of the redox model. Furthermore, it is possible that there is a relatively large amount of uncertainty in the model parameters given. Consequently, the correspondence between model and measured profiles does not give any absolute assurances with respect to the accuracy of the model calibration. This is certainly the case when the parameters associated with the Mn and Fe component species are considered because the available data did not allow the boundary conditions of the solid-oxide phases to be specified with any certainty. This indeterminacy introduces an additional degree of freedom into the calibration process that increases the uncertainty in the resulting parameter values.

It is therefore desirable to constrain independently as many parameters as possible before attempting to calibrate the model. However, the number of parameters in the redox model means that this would involve a substantial effort. Furthermore, the parameterisation and measurement of many benthic processes is inherently difficult for a number of reasons (Blackford, 1997), including:

1. The relative inaccessibility of the environment.
2. The difficulty in establishing benthic communities in mesocosms.
3. High degrees of heterogeneity even at small scales, which makes blind sampling prone to high variability.

In addition to these difficulties, many critical parameters are only poorly constrained by analytical work and subsequent model calibration.

For instance, even when accurate estimates of mineralisation rates are available, acceptable fits to the data can be achieved through numerous combinations of bioturbation and degradation rates (Soetaert *et al.*, 1998). Some knowledge of the bioturbation coefficient is therefore desirable. However, standard approaches for estimating the intensity of bioturbation (that is,

D_b) usually involve the calibration of a diagenetic equation against the depth profile of some tracer. The mixing coefficient obtained in this way is influenced by the tracer used (e.g. Smith, 1992 and references therein) and artefacts associated with the model fitting procedure. There is thus a considerable amount of uncertainty associated with the estimate of D_b. Consequently, any calibration of parameter values using this value of D_b would also be uncertain, even when a considerable amount of field data is available. The model output must therefore be interpreted with care, and appropriate considerations given to uncertainty in the parameter values.

One further problem associated with the application of the redox model to a particular site is that the technical difficulty and expense of fieldwork means that the coverage of data in time and space will always be relatively sparse. In fact, it is perhaps for this reason that diagenetic models are usually applied -- to fill in gaps and elicit the maximum amount of information from the data collected. The scarcity of data is therefore not as restrictive in many diagenetic modelling studies because predictions are used to generate and support hypothesis, which can always be tested with additional experimental, modelling, or field work, as appropriate. It is only when the model is intended for use as a management tool that sparse data, and the concomitant parameter value uncertainty, becomes an intractable problem

Given the effort required to calibrate the redox model it is desirable that the empirical regression models should provide an adequate assessment of critical parameter values. However, as noted previously, the heterogeneous nature of coastal sediments means that any quantitative correspondence between measured and modelled diagenetic characteristics would be purely incidental. Consequently, empirical regression models do not provide a viable alternative to the calibration of the model using data gathered at the site in question. Two important conclusions can be therefore be drawn from the modelling exercise presented in this Chapter:

1. Site specific modelling studies must be supported by fieldwork. Any study not supported by fieldwork can only provide a qualitative description of the generic

characteristics of a depositional regime; any attempt to interpret the model output quantitatively would be inappropriate.

2. The data requirements of model calibration are high, and are likely to be excessive with regard to both the resources generally available for fieldwork and the quality of the results that can be realised; especially given the uncertainty inherent in the estimates of critical parameter values.

This second point implies that the scope for applying the redox model to the prediction of benthic impact is limited; a supposition that is considered explicitly in the next section.

7.6 Predicting Benthic Impact

The analysis given in Chapter 6 demonstrated that the redox model is sensitive to a relatively large number of parameters, some of which are only poorly constrained by analytical work, empirical relationships, or estimates taken from the literature. Furthermore, it has been shown above that calibration of the model requires access to a considerable amount of data. It must therefore be anticipated that use of the model in a predictive sense would be problematic. This is especially true if the direct modelling of benthic impact was attempted, as discussed below.

7.6.1 Limitations of a Direct Modelling Approach

Direct modelling of the benthic impact implies that that the redox model could be used to make a quantitative assessment of the change in sedimentary redox conditions associated with a discharge. This would require estimates of parameter values along a predicted gradient of J_{org}. If such estimates were available, the redox conditions at discrete points along this gradient could be modelled and the results assessed. However, it has already been shown that parameterisation of the model equations is difficult even for a non-impacted sediment for which measured concentration profiles are available. Any attempt to predict the change in parameter values associated with the enrichment would be even more problematic.

This can be illustrated by considering the intensity of bioturbation along a gradient of enrichment. The level of bioturbation is in part related to the macrofaunal abundance and both

the size and feeding rates of individual animals (Smith, 1992). All these factors change along a gradient of enrichment (see Chapter 3; Section 3.4.3). Consequently, there must also be a spatial gradient in the level of bioturbation. However, it is not known how the various structural and functional changes in the macrofauna community effect the intensity of bioturbation (Wheatcroft & Martin, 1996).

Under normal conditions there is a positive correlation between the bioturbation coefficient and the flux of organic matter. In fact, it is noteworthy that the empirical relationship linking burial rate to carbon flux (Equation 6-9) can be rewritten as:

$$\log(J_{org}) = \log(\omega^{0.69}) + 2.27 \qquad \textbf{Equation 7-11}$$

Compare this to Equation 6-8, repeated here for completeness:

$$D_b \approx 15.7\omega^{0.69} \qquad \textbf{Equation 6-8}$$

Clearly, the two equations can be combined to give an explicit relationship between the flux of carbon and the bioturbation coefficient. This provides a way of roughly calculating the change in bioturbation intensity induced by an elevated flux of carbon. However, as noted previously, such empirical models only explain a limited amount of the variance observed in data sets. Hence, this approach could not possibly give precise estimates of the bioturbation coefficient.

In any case, the relationship would only apply to situations where the flux of carbon and bioturbation are positively correlated. However, foraging models for individual deposit feeders suggest that the rate of feeding can reach a maximum at intermediate food concentrations (Smith, 1992 and references therein). Since deposit feeding has a strong influence on the intensity of bioturbation, it is therefore conceivable that an enhanced carbon flux would result in a lower value of D_b.

Furthermore, at extreme levels of enrichment, where the flux of carbon generates anoxic conditions at the SWI, the macrofauna are excluded from the sediment. The level of bioturbation must therefore fall to zero. This response indicates that the flux of carbon has a subsidy-stress effect on bioturbation (see Odum *et al.*, 1979 for a general discussion of subsidy-stress effects). Hence, at some level of enrichment a switch must occur where the subsidy effect of extra food is displaced by stress effects related to changes in the physical and chemical characteristics of the depositional regime. At this level and beyond the flux of carbon can not be positively correlated with bioturbation. The level of enrichment at which this switch occurs is not known, but is likely to depend upon a combination of factors and therefore be site specific.

The intensity of irrigation must also vary along a gradient of enrichment in response to changes in the sediment redox conditions and the succession in the benthic community structure. Furthermore, any shift in the transport regime within the sediment could also modify the rate constants of the primary redox reactions. These rates would be modified further by changes in the amount and nature of the organic matter deposited at the SWI.

The processes that drive all these changes depend upon many ecological interactions, which are likely to vary both in time and space. Hence, whilst one can make qualitative statements regarding the likelihood of change, estimating the magnitude of change in parameter values would be extremely difficult. Any attempt to parameterise the model along a predicted gradient of enrichment would therefore be problematic and almost certainly entirely arbitrary.

Finally, if the benthic impact was modelled directly the question could arise as to what oxygen concentration to specify at the SWI. Specifying the same boundary condition along the predicted gradient of carbon flux would be equivalent to assuming that the composition of the overlying water was unaffected by the benthic metabolism, irrespective of the sediment oxygen demand (SOD). For well-mixed dynamic receiving waters, this assumption is perhaps

reasonable because the flux of oxygen into the sediment would be balanced by transport mechanisms in the water column. However, for areas with poor flushing characteristics and/or a stratified water column, a high SOD could depress oxygen concentrations in the water overlying the sediment (e.g. Pearson & Rosenberg, 1978; Jørgensen, 1980; Findlay & Watling, 1997a). Furthermore, at times of low flow a viscous sub-layer can develop which limits the rate of transport of oxygen to the SWI (e.g. Jørgensen & Revsbech, 1985), which could, in conjunction with a high SOD, depress oxygen concentrations at the SWI.

Additional modelling work would be required to take these factors into account. For example, the boundary condition for solutes could be modified to include the effect of the diffusive sub-layer (see Boudreau, 1997) and the redox model could be coupled to a water quality model. However, this would require a significant amount of effort to implement. Given the uncertainty in parameterising the model along a gradient of enrichment this work could not be justified

7.6.2 An Alternative Approach

Various parameter value uncertainties therefore preclude the adoption of a direct modelling approach. However, it should be remembered that the aim of a benthic impact model is to compare various disposal options and to predict if a significant impact is likely to occur. To achieve these aims it is not actually necessary to model the level of impact explicitly. It is sufficient to use the model in a qualitative sense; to estimate and compare trends, rather than to quantify bio-chemical and physical gradients. A qualitative modelling approach was therefore investigated that focused on determining the sensitivity of the sedimentary redox state to increases in carbon flux. The redox model would therefore be used to assess the assimilative capacity of the sedimentary environment with respect to the carbon load imposed by a discharge.

Any attempt to determine the sensitivity of a sedimentary system to an increased flux of carbon must still take into account changes in biogenic parameters induced by the increased food

supply. However, it has already been shown that correlations between various model parameters mean that similar redox states can be predicted for a wide range of scenarios (see Section 6.6). As a consequence, if biogenic transport parameters were increased in line with the flux of carbon, the model could predict a relatively unchanged redox profile over a wide range of fluxes. However, this would not indicate the absence of impact, since the parameters would have been shifted considerably from their baseline values. Some means of placing a threshold upon the acceptable change in biogenic parameters is therefore required.

It has been noted previously that wide ranges of bioturbation coefficients have been reported in the literature. This variability was considered by Matisoff (1982) who suggested that reported values of D_b should be considered as net coefficients that are the product of the biomass density diffusivity of a particular macrofaunal species (D_b*, cm^4/g per yr) and the biomass (b, in g dry weight organism/cm^2). The bioturbation coefficient defined in this way can be written as:

$$D_b = bD_b^* \qquad \textbf{Equation 7-12}$$

D_b* is therefore effectively D_b normalised to the biomass of the macrofauna. By taking this approach, Matisoff (op. cit.) was able to account for much of the variation in published values of D_b; variations between studies were improved by a factor of eight. The author noted that other factors such as temperature differences, effects of other organisms, sampling error, and physical mixing could account for the remaining variation. Matisoff also asserted that coefficients for irrigation should also be normalised to the biomass densities.

The purpose of Matisoff's analysis was to try to explain the variance in the reported values of D_b. However, for the purposes of the current discussion it is informative to consider Equation 7-12 in reverse. The relationship implies that if the biomass density diffusivity remains reasonably constant, then an increase in macrofaunal biomass would produce a proportional increase in the bioturbation coefficient. It can also be assumed that a similar increase in the

irrigation coefficient would also occur (see the discussion of Aller's radial diffusion model in Section 5.6.2).

If it is assumed that biogenic transport parameters are related to biomass in this way, the upper threshold of the transport coefficients can be specified if an acceptable increase in biomass can be defined. The MPMMG (1994) state that a fifty per cent increase in biomass over non-impacted levels is considered acceptable. By inference, therefore, a corresponding increase (fifty per cent) in the level of bioturbation and irrigation would also be deemed acceptable; assuming that the relationship implicit in Equation 7-12 holds for both processes.

The link between the standing crop biomass and bioturbation is, however, complex and would depend upon many site-specific factors. For example, Boon & Duineveld (1998) studied the relationship between bioturbation and macrofaunal abundance at two stations in the North Sea (one at a depth of 39m and one at 28m). Although the deeper site had a biomass and abundance twice that of the shallower station, the calculated bioturbation rates were only higher for two months of the year.

Even at a given site, the standing crop biomass depends upon temporal factors such as recruitment success. In fact, Matisoff (op. cit.) includes the caveat that the community at the time of sampling could be significantly different to that which produced the mixing. In other words, it might actually be quite difficult to define the biomass (b) from which the value of D_b is calculated. In addition, the change in food input is likely to induce some shift in community structure, which could alter the biomass density diffusivity (D_b*). However, because only the initial stages of enrichment are considered here this complication can be ignored, at least for the purposes of the present discussion.

For the sake of the current investigation, it has therefore been assumed that bioturbation and irrigation at a given site are proportional to the biomass of the macrofauna. A fifty per cent

increase in the bioturbation and irrigation coefficients would therefore be considered acceptable. This then constrains the level to which the biogenic transport parameters can be increased over and above the baseline values. This meets one criterion for applying the redox model. However, the modelling approach also requires some definition of an acceptable change in model redox conditions. The most obvious constraint is that redox state of the sediment should not change from the baseline and this condition is therefore adopted.

With these constraints, the model can be used to determine the maximum carbon flux that can be assimilated by the benthos without inducing a change in the modelled redox conditions and, by inference, an unacceptable change in the benthic community. This flux is hereafter designated as the acceptable effect flux (AEF). The approach still requires that the fluxes of carbon be predicted via the modelling of physical processes. However, the level of impact throughout the discharge area would then be expressed simply as the ratio of the predicted flux to the AEF. Hence, any areas of sediment where this ratio is greater than one would indicate a risk of unacceptable enrichment. Larger values would indicate higher levels of risk.

The modelling approach outlined above would therefore involve the following steps:

1. The parameterisation of the depositional environment according to baseline (pre-implementation) conditions.
2. The use of the redox model to determine the baseline redox conditions in the model space.
3. The use of the redox model to determine the maximum flux that can be assimilated without inducing a change in redox conditions, assuming biogenic transport parameters are limited to an increase of fifty per cent.
4. The modelling of physical processes to estimate the net carbon flux associated with the discharge (NB: as noted previously, post-depositional redistribution of organic carbon via processes such as resuspension and lateral advection must be accounted for in this physical process modelling).

The main advantage of such a modelling approach is that because low levels of enrichment are considered, the assumption of normal correlations between the carbon flux and biogenic transport parameters is reasonable. In addition, the sediment could be parameterised according to baseline conditions rather than degraded ones; that is, the model could be calibrated using concentration profiles measured at the site prior to the implementation of the discharge. Finally, since there would be no need to explicitly model impact at different points along a gradient of enrichment, the modelling effort would be much reduced -- the approach only requires one characteristic AEF to be determined for the discharge site.

7.6.3 Assessment of Approach

The validity of this modelling approach can not be confirmed without supporting experimental work. However, numerical experiments were carried out to ascertain if the approach is worth investigating further, as described below.

7.6.3.1 Method

The modelling approach was tested for a range of idealised scenarios in which empirical regression models were used to specify key parameter values. Burial rates in the range 0.1-10 cm/yr were again used. Primary redox reactions were specified according to the 1-G and 6-D cases used previously. Other parameters were specified according to the 'typical' values for a coastal sediment. A range of porosities and different depth profiles of bioturbation and irrigation were applied. The details of the parameter values used in the analysis are given in Appendix IX.

The redox model was used to determine the baseline redox profile for each scenario considered. The irrigation and bioturbation parameters were then increased by fifty per cent in accordance with the acceptable increase in biomass. For simplicity, the rate constants of the primary redox reactions were assumed to be unchanged by the additional organic matter. This is equivalent to assuming that the average reactivity of the organic matter within the sediment is unaffected by the discharge. The flux of carbon was then increased incrementally until the redox state

deteriorated. This was assessed by comparing three points on the redox profile; the two points used previously (the oxygen penetration depth, d1 and the depth of the sub-oxic zone, d2) and the depth of the RPDL. The depth of the RPDL was again taken to be the depth where the model redox potential fell below zero. It was assumed that deterioration in redox state was indicated when all these depths were either equal to or shallower than the depths calculated for the baseline condition.

The numerical experiments were carried out using the steady state code, which was modified to automate the analysis. The flux of carbon was increased in increments of one per cent of the baseline flux. Output was generated at each incremental value of carbon flux. The output from the model was modified to include the following:

1. The burial rate.
2. The flux of carbon.
3. The mass balance.
4. The three characteristic depths.
5. Four integer flags.

The four integer flags were again used to indicate the quality of the runs, as discussed in Chapter 6. A model domain of 20 cm and space step of 0.01 cm was used throughout.

7.6.3.2 Results

The mass balances for all runs were better than order of 0.01%. All integer flags were zero indicating that the model converged and the diagenetic zonation was unidirectional; that is, oxidants became exhausted in sequential order, and increased concentrations below the depth of initial exhaustion did not occur. The results of the analysis are shown in Table 30, which shows the initial flux of carbon (J_i) and the AEF for a range of cases (case 1 to 10), expressed in $gC/m^2/yr$. Table 31 details the ratio of the baseline flux to the final flux (AEF). No result is given for case 2 (burial velocity of 0.1) since the characteristic depth d2 and the RPDL exceeded the depth of the model domain (20 cm).

ω	J_i	*case 1*	*case 2*	*case 3*	*case 4*	*case 5*	*case 6*	*case 7*	*case 8*	*case 9*	*case 10*
0.10	27	38	-	32	39	40	37	37	38	36	36
0.16	37	53	43	45	55	57	53	53	54	51	52
0.25	50	76	62	63	78	81	76	76	76	73	73
0.40	69	108	92	89	110	113	108	107	108	104	104
0.63	95	151	133	127	155	157	151	151	153	148	147
1.00	130	210	188	180	215	219	211	210	214	207	207
1.58	179	294	270	260	301	301	292	294	299	288	290
2.51	246	409	386	369	416	413	406	409	413	401	401
3.98	338	568	548	531	571	565	565	568	571	555	555
6.31	465	776	767	762	781	771	781	781	785	767	771
10.00	638	1066	1066	1073	1066	1047	1066	1073	1066	1047	1047

NB: Fluxes expressed in $gC/m^2/yr$, J_i denotes baseline flux

Table 30 *Baseline and AEF for a variety of depositional regimes*

ω	*case 1*	*case 2*	*case 3*	*case 4*	*case 5*	*case 6*	*case 7*	*case 8*	*case 9*	*case 10*
0.10	1.41	-	1.19	1.45	1.51	1.40	1.4	1.41	1.35	1.35
0.16	1.46	1.17	1.22	1.50	1.57	1.46	1.46	1.47	1.4	1.41
0.25	1.51	1.24	1.25	1.55	1.61	1.51	1.51	1.52	1.46	1.46
0.40	1.56	1.33	1.29	1.59	1.64	1.56	1.55	1.57	1.51	1.51
0.63	1.59	1.40	1.34	1.63	1.66	1.59	1.59	1.61	1.56	1.55
1.00	1.61	1.44	1.38	1.65	1.68	1.62	1.61	1.64	1.59	1.59
1.58	1.64	1.51	1.45	1.68	1.68	1.63	1.64	1.67	1.61	1.62
2.51	1.66	1.57	1.50	1.69	1.68	1.65	1.66	1.68	1.63	1.63
3.98	1.68	1.62	1.57	1.69	1.67	1.67	1.68	1.69	1.64	1.64
6.31	1.67	1.65	1.64	1.68	1.66	1.68	1.68	1.69	1.65	1.66
10.00	1.67	1.67	1.68	1.67	1.64	1.67	1.68	1.67	1.64	1.64

Table 31 *Ratios of AEF to Baseline Flux*

7.6.3.3 Discussion

It can be deduced from the ratios shown in Table 31 that for all cases the AEF lies in the range seventeen to sixty-eight per cent of the base-line flux. For the modelling approach to have any validity, it would therefore have to be possible for an increase in flux of seventeen to sixty-eight per cent to support an increase in macrofaunal biomass of fifty per cent. The complexities of ecological interactions involved make it very difficult to make any categorical statement about this. However, it is informative to consider an idealised situation where ecological interactions are much simplified.

Therefore, consider a benthic community with a simple food chain consisting of one bacterial, one meiofaunal, and one macrofaunal species. It is assumed that the micro-organisms consume all the detrital material entering the system. Hence, the meiofauna obtain food by grazing the bacteria, and the macrofauna obtain food through consumption of micro-organisms and/or meiofauna. It is further assumed that these ecological interactions remain the same under the enriched conditions; that is, the trophic relationships are unaffected by the increased food supply.

If an increase in the flux of labile carbon of fifty per cent above the baseline condition is considered (equivalent to 1.5 in Table 31 above), there is a corresponding increase in food supply to the bacteria of fifty per cent. The efficiency with which bacteria transform carbon in substrates to cells is in the range ten to fifty per cent (Valiela, 1995). Assuming a thirty per cent efficiency, the increase in food supply to the meiofauna is therefore only fifteen per cent of the total input. However, this still represents a fifty per cent increase in the food available to the meiofauna since they previously had access to only thirty per cent of the original food supply. Similar arguments can be made for the increase in food supply to the macrofaunal assemblage. Hence, under these idealised conditions each trophic group 'sees' an increase in food supply of fifty per cent, compared to the baseline condition. The percentage increase in flux of carbon therefore represents the increase in food supply at each trophic level.

Table 31 indicates that an increase in flux of seventeen to sixty-eight per cent was calculated for the scenarios considered. This therefore represents a seventeen to sixty-eight per cent increase in food supply to the macrofauna. Hence, for the model assumptions to hold for even this simple scenario, this increase in food supply must be sufficient to support a fifty per cent increase in macrofaunal biomass. It is conceivable that this could be the case. However, it is noteworthy that in one case detailed in the literature a fifty per cent increase in macrofaunal biomass was attributed to a ten-fold (that is, 1000%) increase in carbon input (Pearson, 1982). Furthermore, production/biomass ratios of the macrofauna are commonly greater than one (Valiela, 1995). Hence, even if it is assumed that a fifty per cent increase in food supply would correspond to a fifty per cent increase in production, this would not normally correspond to a fifty per cent increase in biomass.

Of course, the situation is more complex in real sediments since benthic food webs are highly complex. Furthermore, in ecological terms it is not just the carbon input that is important, since the food value of the organic matter is dependent upon the C:N:P ratio. Nevertheless, it can be surmised that the AEF fluxes predicted by the model are ecologically unrealistic. This could be due to a number of factors. For example, the maintenance of sedimentary redox conditions (as defined above) is not necessarily implicit in the environmental quality standard defining the acceptable change in biomass. Furthermore, the ecological interactions implicit in the diagenetic equations are by necessity simplistic and the assumed relationship between biomass, irrigation, and bioturbation might be unjustified in terms of this approach. In any case, it can be concluded that the redox model does not allow a qualitative prediction of benthic impact to be made with any certainty. This matter is considered further in Chapter 8.

7.7 Summary

A modelling study has been carried out using data taken from the literature. The data set includes concentration profiles of various components, estimates of the bioturbation coefficient and burial rate, and results from incubation experiments. The 1-G rate constant, carbon flux,

and irrigation coefficient were calibrated using the data provided. It was assumed that various other parameter values were sufficiently well constrained by estimates taken from the literature.

Boundary conditions for the Mn and Fe oxides were, however, not known with any certainty. A higher level of uncertainty was therefore implicit in parameter values calibrated using the depth profiles of the Mn and Fe phases. It is therefore desirable to determine independently as many parameters as possible before carrying out any model calibration. Unfortunately, empirical models do not constrain parameter values sufficiently to allow meaningful application to a site-specific study. The amount of data required to parameterise the model is therefore high and excessive in terms of the quality of the predictions that could be made.

Application of the model to a site-specific study is therefore problematic. Such problems would be even more apparent if the model were used predictively -- any attempt to predict changes in parameter values along a gradient of enrichment would almost certainly be entirely arbitrary. However, given that the aim of the modelling study is to compare the effect of various disposal options and to predict if a significant impact is likely to occur, a qualitative modelling approach could be adopted. An approach has been investigated in which the model was used to assess the sensitivity of idealised sedimentary systems to increases in carbon load. However, results from numerical experiments demonstrate that using the model in this way is still problematic.

Chapter 8

8. CRITIQUE OF THE MODELLING APPROACH

8.1 Introduction

The aim of this research was to consider the application of mechanistic models to the prediction of environmental impacts associated with coastal discharges. The modelling of benthic impacts was subsequently identified as an area for which a limited amount of research had previously been undertaken. The redox state of the sediment was then selected as a specific focus of the modelling effort. All these aspects of the research are considered in this Chapter by giving a critique of the modelling approach taken.

The Chapter starts by considering the model redox profile and the limited interpretation that can be placed on the calculated Eh values. The deterministic nature of the model is then briefly discussed and it is indicated that a stochastic model would be more appropriate. A general consideration of benthic impact modelling is then given. It is noted that uncertainties arising from various sources mean that explicit benthic impact models are unlikely to provide any real capacity for recommending action. The overall model development cycle is then considered in an attempt to explain why, in the face of these uncertainties, any attempt has been made to model benthic impacts generically. Specific reference is made to factors that appear to have influenced the development of Benoss. Finally, an approach to benthic impact modelling is suggested that is based solely on the output of physical process models, rather than on an explicit model of benthic processes.

8.2 Interpretation of the Model Redox Profile

As noted in Chapter 4, the redox potential of sediments is often measured with electrodes and expressed as Eh. For consistency with this practice, it is desirable that a sedimentary redox model should also express redox state in terms of Eh. However, the chemistry of marine

sediments is highly complex. Much of this complexity is ignored in the model to allow the Eh to be calculated. Interpretation of the model output should therefore be made with appropriate consideration given to the assumptions and simplifications made.

One of the principal assumptions made is that the redox potential within each diagenetic zone can be calculated from the activities of the dominant oxidant and corresponding reduced species (see Section 5.9). However, if this assumption is invalid then the redox potential at any given depth only characterises the distribution of one oxidant and/or reduced species. Even if the assumption is satisfactory, the model response indicates that the redox profile only reflects certain aspects of the overall sediment chemistry. For example, the model Eh does not characterise the distribution of highly reduced organic substrates. Furthermore, pH is assumed constant throughout the model domain. Consequently, the calculated value of Eh can only provide a semi-quantitative indication of the overall redox state of the system.

The model redox profiles are therefore most suitable for comparative purposes; that is, for comparing gross features of redox chemistry. Hence, the model output suffers from the same limitations as those associated with Eh measurements made with electrodes. Whilst acknowledging these limitations, however, expressing the sediment chemistry in terms of Eh still facilitates comparison of different early diagenetic regimes because only one profile need be considered. This statement applies equally to the model Eh and measurements made with an electrode.

The calculated value of Eh is quite insensitive to the activities of the oxidised/reduced species within each diagenetic zone. This can be illustrated by considering the O_2/H_2O couple, which can be represented by the half reaction (see Table 17):

$$O_2(g) + 4H^+ + 4e^- \rightarrow 2H_2O$$

Assuming the activity of water is one, the temperature is 25°C, and the pH is 7.5 the Nernst equation for this couple can be written as:

$$Eh = 0.78 + 0.0148 \log_{10}(P_{O_2}) \qquad \textbf{Equation 8-1}$$

where P_{O2} is the partial pressure of oxygen. A plot of Equation 8-1 is given in Figure 42 below. It can be seen that even when the oxygen partial pressure falls to less than 0.5% saturation (less than 0.001 atmospheres) the Eh has only fallen by 0.034 volts; a less than five per cent decrease. Similar conclusions can be drawn for the other redox couples of interest. Hence, the model Eh profile is influenced more by the metabolic succession than the activities of the component species. The fact that this succession is highly idealised further emphasises the need to interpret the Eh profile with care.

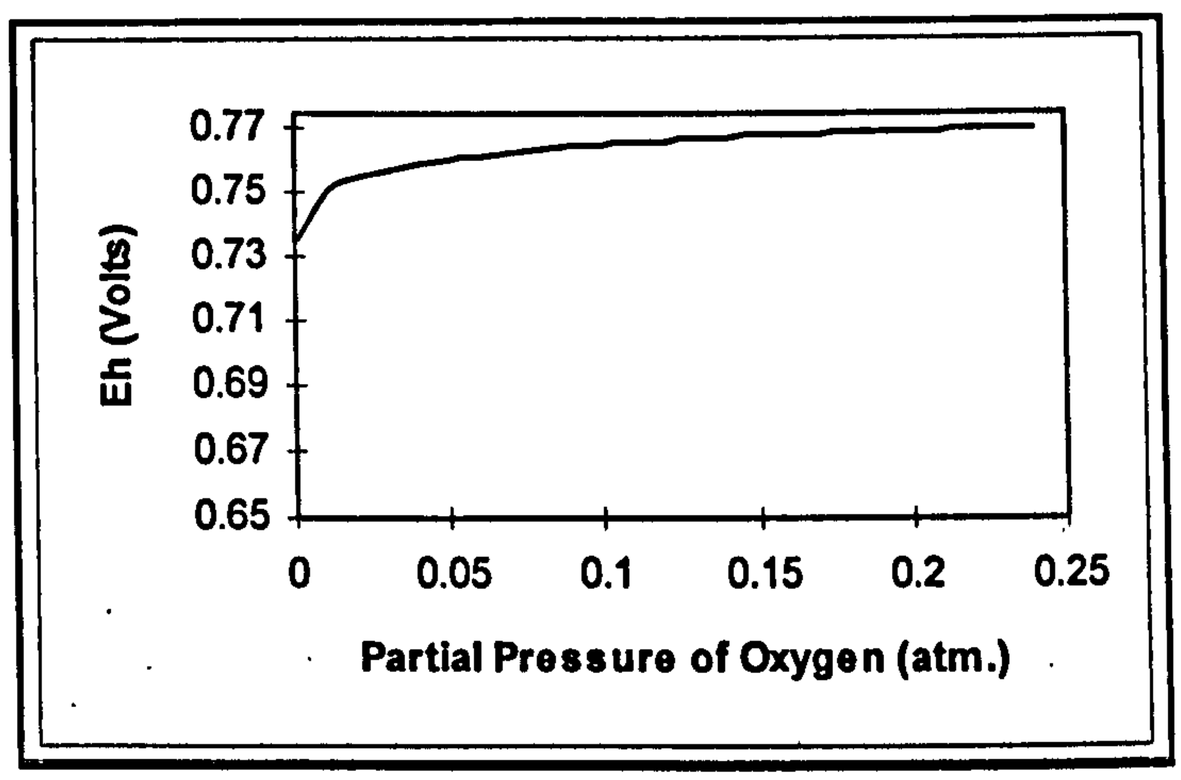

Figure 42 *The Eh of O_2/H_2O Couple at Various Partial Pressures of O_2*

Since the calculated value of Eh is insensitive to the activities of the component species, the redox profile is also insensitive to any inaccuracies introduced by the use of the Davies formula (see Section 5.9.1). A more exact treatment of ionic interactions is therefore not required. In fact, it could be argued that any consideration of activities is superfluous, especially given the qualitative nature of the model redox profile.

As discussed in Chapter 6, the model Eh is calculated using an approach similar to that taken by Park & Jaffe (1996). These authors state that their redox model could be coupled to a chemical equilibrium model to allow post-depositional metal mobility to be assessed. This implies that

the model redox potential gives a thermodynamically valid measure of the redox state of the system. As noted above, the model Eh only gives a semi-quantitative indication of the redox conditions. It therefore seems questionable that a sedimentary redox model based on diagenetic equations could be used in the application proposed by Park & Jaffe.

As noted earlier, many redox couples in natural systems are not electro-active (that is, they are irreversible in a thermodynamic sense). In addition, platinum electrodes usually measure mixed potentials that are not amenable to thermodynamic interpretation. Consequently, redox potentials calculated from the theoretical half reactions used in the model will not correspond to potentials measured with an electrode. As a result, there is no way of directly comparing the model output to electrode measurements.

The H_2O_2-O_2 half-cell can be used to estimate the electrode potential of aerobic seawater (e.g. Berner, 1971). Furthermore, Berner (1963) found that the potential adopted by a platinum electrode in sulphide rich sediment was controlled by the HS^--S^0 half cell. Hence, the H_2O_2-O_2 and HS^--S^0 half-cells could provide a means of calculating Eh values that correspond more closely to potentials measured with an electrode. However, given the assumptions underlying the model it is still unlikely that Eh values calculated in this way could be meaningfully compared to electrode measurements. This is especially true for measurements made in coastal sediments because micro-environments create a 3-D mosaic rather than the simple 1-D diagenetic zonation assumed.

8.3 Deterministic Models of Stochastic Systems

The diagenetic equations used in this work are deterministic; that is, there is a fixed relationship between the model input and output. However, factors such as recruitment success, storm events, and fine scale heterogeneity impose a stochastic (that is, random) component on the redox chemistry of coastal sediments. A purely deterministic modelling approach is therefore inappropriate. Stochasticity can be readily incorporated into a

mechanistic model by expressing the parameters as random variables. This allows parameter values for a particular model run to be randomly generated. The analysis of the input-output relationships for a large number of model runs can then be used to determine the statistical properties of the system. This technique is termed Monte Carlo simulation (e.g. Haefner, 1996).

With the redox model in its current form, the application of Monte Carlo techniques would be problematic because of the number of parameters involved and the computational effort required to solve the equations. As discussed previously, the sensitivity analysis indicated that some model simplification was justified. However, the analysis also showed the most critical parameters are those that characterise transport processes and degradation. Therefore, these processes can not be eliminated from the model.

Unfortunately, the parameters associated with these processes can not be directly measured. For example, the value of the bioturbation coefficient, irrigation coefficient, and rate constants of primary redox reactions must all be inferred from other characteristics of the sediment. It has already been shown that empirical models do not allow these parameters to be estimated with any certainty. Furthermore, the heterogeneity of the coastal environment means that a wide range of depositional regimes can be encountered. It is therefore not possible to make an *a priori* estimate of likely ranges or statistical distributions of these critical parameter values. Since these estimates are required in Monte Carlo simulation, the application of this technique would be problematic. It would perhaps be possible to apply these techniques on a site by site basis, given sufficient fieldwork. However, various uncertainties mean that the application of benthic impact models in a management context is considered inappropriate, as discussed in the next Section. Monte Carlo techniques have therefore not been applied to the redox model.

8.4 Benthic Impact Models

It was shown in previous Chapters that horizontal gradients in sedimentary redox conditions can reflect the impact and, by inference, the performance of an effluent disposal scheme. However, whilst it has proved possible to develop a model that gives a mechanistic description of vertical gradients in redox intensity, the application of the model in a predictive sense has proved problematic. One of the main sources of difficulty has been the level of uncertainty associated with the modelling of benthic processes. Since these processes are obviously central to the mechanistic modelling of benthic impact, it can be inferred that any explicit benthic impact model would be similarly affected by these uncertainties.

In any mathematical model there are two types of uncertainty:

1. Type I or model uncertainty
2. Type II or parameter value uncertainty

Type I uncertainty stems from the simplifications necessary to form a mathematical model of a complex physical system. These simplifications mean that the output from a particular model represents just one estimate of the true behaviour of the modelled system. The influence of this type of uncertainty can therefore be minimised by aggregating the results from multiple model methodologies (e.g. Cardwell & Ellis, 1996). However, the lack of other mechanistic models for predicting benthic impact means that such an approach is not possible at present.

Type I uncertainty would be particularly important if the model was used to give a quantitative prediction of impact. However, if the model was used to compare the effect of different management or engineering options, this type of uncertainty would be less critical. Such comparisons only require that the model gives an indication of the relative impact of each option. From this perspective, it does not matter if the measure of impact in the model space is not entirely consistent with that observed in real space, as long as the mapping into the model space is representative and meaningful. Unfortunately, this is not the case in the present study because of type II uncertainties.

Type II uncertainties arise in the redox model for three interconnected reasons. Firstly, critical parameters such as the bioturbation coefficient, irrigation coefficient, and G-type rate constants can not be measured directly. In effect, these parameters are simplified models of complex processes themselves and therefore have type I uncertainty associated with them. Type I uncertainty in these subsidiary models leads to parameter value uncertainty in the redox model. Secondly, there are analytical uncertainties associated with any parameters that are measured (e.g. background carbon flux and other boundary conditions, etc.), especially when limited data sets are extrapolated to a wider domain in either space or time. Finally, significant uncertainty is introduced because the mechanisms that drive ecological changes associated with enrichment are poorly understood. As discussed previously, there is also a high level of uncertainty in parameter values taken from the literature or estimated from empirical relationships.

As noted in Chapter 7, this parameter value uncertainty prevents the quantitative modelling of benthic impact. It has also been shown that applying the redox model in a qualitative sense is problematic. It was suggested that one possible reason for this was that diagenetic equations only give a very simplistic mathematical treatment of the overall ecology of the benthos. For example, in diagenetic models organisms are treated essentially as 'black boxes' that mineralise organic matter and induce transport of particulates and solutes. However, in using the model to assess benthic impact it becomes necessary to try to incorporate the ecological effect of the increased carbon flux in some way. In the qualitative approach described in Chapter 7, this was achieved by assuming that the flux would induce an increase in the biomass. However, even this simple approach violates the assumption that the biota can be treated as 'black boxes'. The implication of this is that a meaningful mechanistic benthic impact model would require ecological interactions to be modelled in more detail.

Smith *et al.* (1992) suggest a way of recasting the G-type representation of degradation so as to include ecological characteristics of the biota. In addition, explicit ecosystem models have been developed that represent benthic processes on a coarse scale (e.g. Beretta *et al.*, 1995;

Blackford, 1997). However, the use of these models as quantitative management tools would still be problematic, again because of uncertainty associated with limited mechanistic understanding, estimates of key parameter values, and fine-scale heterogeneity. Furthermore, benthic production can be disseminated through the overall ecosystem of the receiving waters by mechanisms such as predation of infauna by demersal fish (Pearson, 1987). Any model of benthic ecology should therefore also consider benthic-pelagic coupling. Clearly, any attempt to model ecological interactions explicitly would be a highly complex undertaking.

Of course, this complexity does not mean that a quantitative model could not be produced. In fact, with the advent of cheap, readily available computing power there is an increasing capacity to develop complex models that are convincing in both their construction and output. However, the model output can not be meaningfully applied to a management problem if there is significant uncertainty in the underlying processes and parameter values.

The type of problem to which any model can be applied is therefore constrained by the quality of the available data and the level of understanding of important processes. This is clearly illustrated in Figure 43 (after Haefner, 1996) which shows graphically the appropriate use of models according to the degree of understanding and data quality and, by inference, the degree of uncertainty in the model.

As the Figure indicates, models should only be used to recommend action (that is, used as the basis for a management decision) when the degree of understanding and the quality of data are both relatively high. It has been shown throughout this work that this is clearly not the case for a model of benthic impact. Current understanding of important ecological interactions and the quality of available data are not sufficient to allow meaningful predictions to be made. Consequently, whilst any model of benthic processes, including diagenetic equations, can be used for testing theory or gaining insight, recommending action on the basis of the model output would be inappropriate

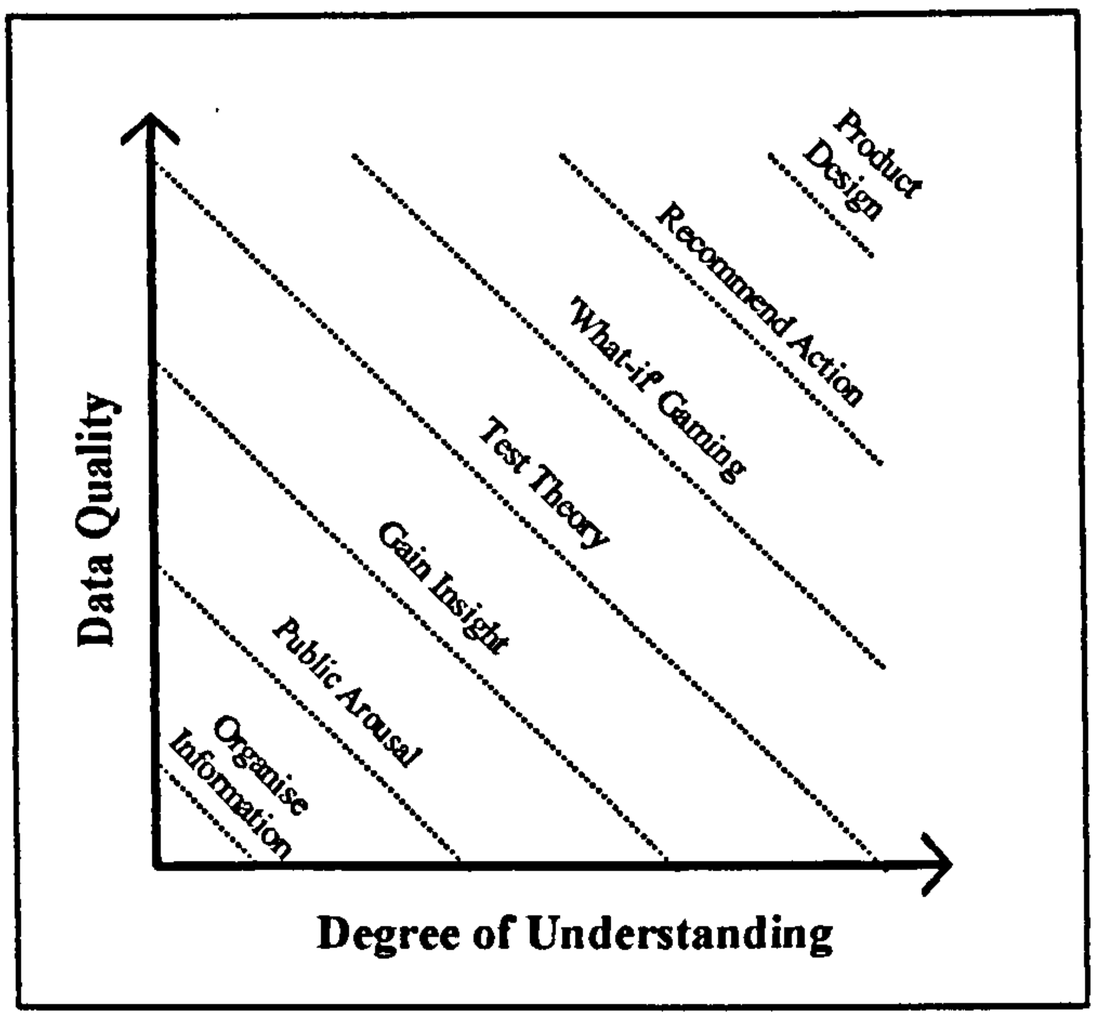

Figure 43 Appropriate Use of Models According to the Level of Uncertainty

Such arguments apply if the model is used as a quantitative management tool. However, it could be argued that complex mechanistic models can serve a number of other purposes; for example:

1. The ability to use complex models demonstrates a certain level of competence within an institution or company.
2. The modelling work acts as a focus for the overall study.
3. The model output can be used to give tangible results that demonstrate the impact of various options to non-experts.

Consequently, the modelling of benthic impact could perhaps be justified in some studies. However, a quantitative interpretation of the model output would be inappropriate.

Sources of uncertainty are particularly noticeable when mechanistic models are used since processes must be parameterised explicitly. As noted previously, one alternative to a mechanistic modelling approach is the use of empirical models. However, this type of model can only circumvent the limitations of mechanistic models if either the processes being modelled are sufficiently similar at different sites or site specific data is available to modify the empirical equations.

As discussed earlier, inter-site similarities are not the norm for effluent disposal schemes. In addition, empirical models are essentially a black box approach; that is, the relationship between input and output is defined statistically, and no consideration is given to the processes or mechanisms linking them. Sources of uncertainty are therefore not explicitly highlighted during model application. For example, consider the models of Mearns & Word (1982) described in Section 3.5.1. These models require only that the mass emission rate is specified. Hence, with a minimum of effort a seemingly convincing evaluation of potential impact can be made. However, as discussed previously, quantitative interpretation of the model output is really only justified for the sites studied by Mearns & Word (op. cit.). Empirical models are therefore more susceptible to misapplication than mechanistic models.

It has been noted a number of times throughout this work that the mechanisms that drive the ecological changes associated with enrichment are not well understood. Furthermore, the ability of a sedimentary system to assimilate a carbon load is dependent upon a number of interconnected site specific factors. Given the complexity of the problem and the lack of mechanistic understanding it is interesting to consider why any attempt has been made to develop a generic management tool for predicting benthic impact.

As noted previously, this research was partly conceived as an extension to the work carried out by the developers of Benoss. The main impetus for developing Benoss was the need to predict benthic impact associated with discharges of primary treated sewage. This need arose from the requirements of the Urban Waste Water Treatment Directive (UWWTD -- DIR 91/271 EEC) and the desire in the UK to implement only primary treatment where appropriate. Under the terms of the Directive, predictive assessments were required to show that the implementation of primary treatment was satisfactory and that secondary treatment would not accrue any additional environmental benefits. All impacts associated with the primary treated effluent had to be examined, including the impact of the suspended solid load. However, the task team that considered the implications of the UWWTD to UK disposal practices identified that there were

no predictive tools available for assessing the impact of suspended solids deposition (MPMMG, 1994). Funding was subsequently made available to develop Benoss. Benoss was therefore shaped by a range of institutional pressures associated with the new legislative framework, the perceived need for a predictive tool, and the availability of funding.

The factors influencing the development of a model such as Benoss are illustrated schematically in Figure 44. The two opposing arrows on the Figure can be considered as 'forces' that influence the level of predictive capacity the model developers aim to achieve. Various institutional pressures force the model towards a higher level of predictive capacity. However, model uncertainties and insufficient understanding of key mechanisms limit the predictive capacity that is actually achievable. The ultimate claim of predictive capacity depends upon the balance between these 'forces'.

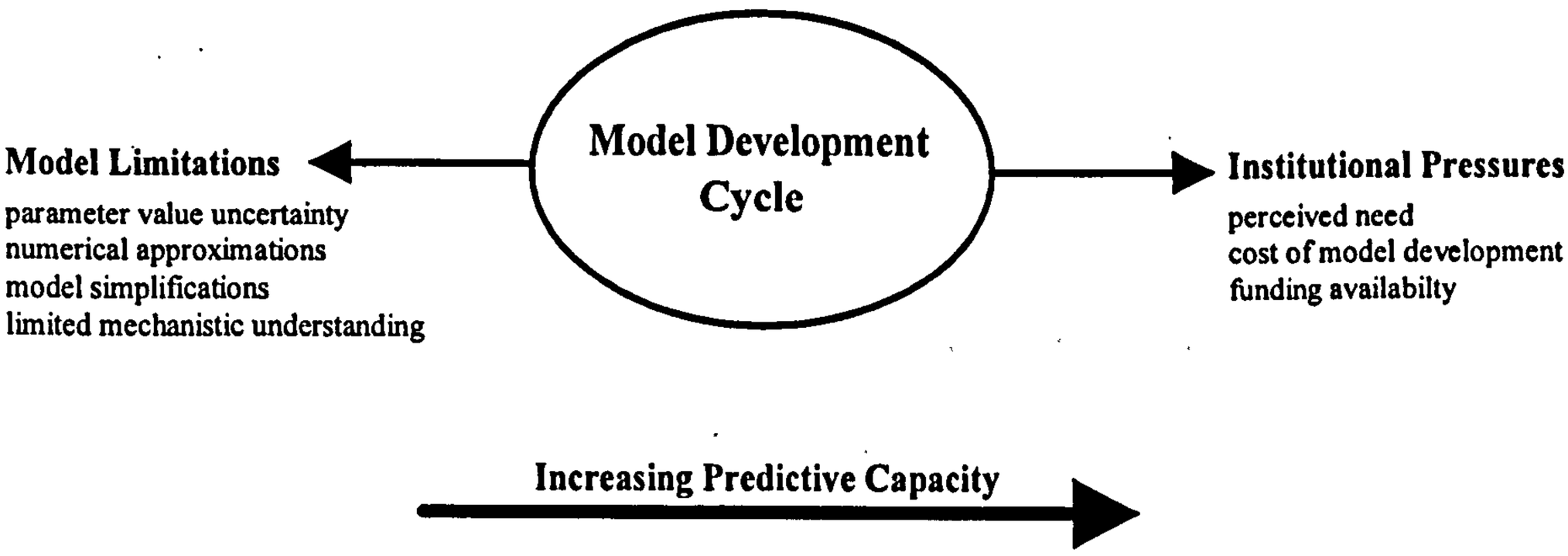

Figure 44 *Factors Influencing the Model Development Cycle*

It is conceivable that institutional pressures could over-ride explicit consideration of model uncertainties, so as to allow a greater predictive capacity to be claimed. This appears to have been the case in the development of Benoss. Institutional pressures required a model with a convincing predictive capacity. As a result, the issue of model uncertainty has not been addressed explicitly in Benoss. (However, a caveat is given to the effect that the model is not intended to replace other methodologies such as monitoring -- see UKWIR, 1996.)

It is noteworthy that much of the type II uncertainty in the redox model is associated with parameters that describe the influence of the macrofauna on early diagenetic processes. Hence, representing the influence of the macrofauna in the relatively simple way used in diagenetic equations does not circumvent the problems associated with modelling this assemblage explicitly, as was originally intended. Furthermore, the problems encountered when applying the redox model in a predictive sense are no less prevalent in Benoss because the macrofauna are considered explicitly. The spatial and temporal heterogeneity and uncertainty in the ecological succession still make this assemblage intractable to any predictive modelling effort, at least in the context of recommending action. The semi-empirical modelling approach used in Benoss avoids some of the problems associated with the parameterisation of various critical processes. However, as noted above, empirical approaches applied generically are unlikely to allow any meaningful quantitative prediction of benthic impact to be made.

The application of a generic model to a site specific study is also influenced by factors similar to those shown in Figure 44. For example, it could be argued that Benoss gives an adequate description of physical processes as long as sufficient work is carried out to parameterise the models. However, the fieldwork required is expensive since it is off-shore. It would therefore be tempting to limit the amount of fieldwork undertaken and use default values for key parameters. In other words, institutional pressures would tend to force the model to be used at a predictive level that would not be justified by the quality of the input data.

Whilst this discussion has focused on the development and application of benthic impact models, it seems reasonable to assume that similar considerations apply to all mathematical models. For example, consider the application of computation fluid dynamic (CFD) models. For a well defined (that is, artificial) system a CFD model can give a representation of fluid flow that is accurate enough to facilitate product development. The expenditure of resources can also be justified since the cost of the modelling work can be recovered through product sales. However, if CFD models are used to assess tidal flows and/or effluent dispersion then

the problem is poorly defined. Sources of uncertainties include the parameterisation of turbulence and boundary conditions, model resolution, and the representation of complex geometries. Furthermore, the cost of the modelling study can not be recovered since a marketable product is not produced. Consequently, there must be institutional pressures to limit the amount of work carried out to parameterise and verify the model. Again the danger is that seemingly convincing quantitative output can be obtained and used in a predictive sense that is not justified by the quality of the modelling study.

8.5 A Possible Alternative to Explicit Modelling of Benthic Impact

From a purely academic point of view, an attempt to explicitly model benthic impact is an interesting problem in itself. Furthermore, had this research shown that impact could be easily and meaningfully modelled this approach could be incorporated into the practical assessment of an effluent disposal scheme. However, it has been shown that the modelling of benthic impact is difficult and, by inference, would require significant effort to implement. For this effort to be justified the interest in protecting the benthic component of the receiving waters would have to be high.

In many coastal areas public health concerns mean that the most critical impact associated with the discharge of effluents is the contamination of water and shellfish fisheries by sewage derived pathogens. Consequently, for such discharges only limited resources would be made available to consider the impact on the benthos. Furthermore, an effective way of controlling pathogenic contamination is the implementation of secondary/tertiary treatment with some form of disinfection (e.g. UV disinfection). Secondary treatment involves a considerable reduction in both BOD and SS load. Hence, except for the most sensitive of areas, this level of treatment would also ensure that significant benthic impacts were not produced. Similarly, the legal requirements associated with the implementation of the UWWTD only require predictive studies to be undertaken when a discharge of primary treated effluent is proposed (see

MPMMG, 1994). Hence, the implementation of secondary treatment would effectively remove any obligation to predict benthic impact.

For other sources of organically rich effluents, such as industrial wastewater, microbial contamination is not necessarily a major concern. Furthermore, the use of primary treatment plus a long sea outfall can still be used to protect near-shore water quality. In both cases, the focus of any predictive assessment could then shift towards ensuring benthic impacts were not excessive. However, economic considerations would still restrict the amount of modelling work justified. In any case, any explicit benthic impact model must rely on physical process models to predict the flux of carbon to the sediment. However, there is a great deal of uncertainty inherent in the use of these models.

We therefore return to the issue of uncertainty in model predictions. The complexities of the coastal environment mean these uncertainties can not be removed, although the application of methodologies such as Monte Carlo simulation and model aggregation allow the implications of such uncertainties to be minimised. It is, however, clear that using the output of physical process models as an input to an explicit benthic impact model can only compound the level of uncertainty. Nevertheless, there is still a desire to predict the level of benthic impact in some way. The results of the model analysis indicated that the flux of carbon is the main factor influencing the redox state of the sediment. Furthermore, there is a culture of applying models of physical processes to environmental problems. It would therefore seem sensible to concentrate on this modelling approach. The question is, can the output of these models be expressed in a way that reflects benthic impact.

The simplest approach would be to express the benthic impact directly in terms of the predicted carbon fluxes. This would then allow the differential effect of various disposal options to be compared. However, the flux of carbon in itself does not necessarily provide an indication of ecological impact. A conceptually more satisfying approach would therefore be to define an

acceptable effect flux (AEF) through experimental work. The output of the physical models could then be expressed using the same qualitative measure of predicted impact suggested at the end of Chapter 7; that is, the ratio of the predicted flux to an AEF. However, in this case the AEF would be determined empirically.

An empirically determined AEF is at least compatible with the common use of empirical data to summarise complex physical and/or ecological interactions. Furthermore, the ratio of fluxes would give some indication of the possible ecological consequences of the discharge. Again, the results of the modelling study would only give a qualitative indication of risk, but this would at least allow some comparison of the benthic impact of different options. Furthermore, the ratios could be combined with results from other predictive tools to give an aggregate assessment of the overall impact and performance of the disposal scheme. In addition, if physical process modelling was required for assessment of other impacts, such as those associated with water quality, the cost of carrying out the benthic impact modelling would be minimised.

Some work has already been published in the literature that can be used to constrain the AEF. For example the Marine Ecosystem Research Laboratory has used mesocosm experiments to determine the effect of organic enrichment (e.g. Kelly & Nixon, 1984; Oviat *et al.*, 1987; Maughan & Oviatt, 1993). Results indicated that organic loadings of less than 36 $gC/m^2/yr$ had little effect. Enriched conditions were produced for loadings in the range 36-365 $gC/m^2/yr$. Degraded conditions were produced when loadings exceeded 548 $gC/m^2/yr$. It is noteworthy that the AEF fluxes calculated in Chapter 7 compare reasonably well with these estimates.

The AEF flux would of course depend upon the level of impact deemed acceptable. For example, Findlay & Wattling (1997a) note that the State of Maine (USA) has specified that an unacceptable impact from maricultural activities is indicated by the development of azoic conditions or *Beggiatoa* spp. mats. As noted previously, this impact represents a very high

level of enrichment. Consequently, a very high AEF would be implied by the adoption of this environmental quality standard. A much lower level of impact is implicit in standards applied to other point sources; for example, the fifty per cent increase in macrofaunal biomass referred to earlier. The experimental results referred to above suggest that a conservative (that is, low risk) AEF would fall in the range 10 to 100 $gC/m^2/yr$.

The problem of heterogeneity in benthic response would, however, still have to be considered. For example, Schratzberger & Warwick (1998) determined that nematode communities from organic-rich muddy sediments were more resistant to enrichment than those from organic-poor sandy sediments. The authors found that an input equivalent to 100 $gC/m^2/yr$ did not affect the mud community but did effect the sand community. This suggests that the AEF would depend upon the characteristics of the non-impacted habitat and the adaptations of associated fauna. The impact of enrichment is also affected by processes in the water column that influence the supply of oxygen to the SWI (e.g. Findlay & Watling, 1994; 1997a). Much experimental work would therefore be needed to determine if meaningful AEFs could be specified for different depositional regimes. Consequently, this issue is not considered further herein.

8.6 Summary

The model redox profiles give limited quantitative information concerning the redox state of the overall system. The redox profile should therefore only be considered as a semi-quantitative summary of the oxidant distribution within the sediment.

Although deterministic diagenetic equations have been implemented in the redox model, a stochastic formulation would be more appropriate. However, limitations in the overall modelling approach mean that the incorporation of stochasticity into the redox model is not warranted. These limitations are related to the degree of uncertainty inherent in the model. The uncertainties are associated with both model simplifications and parameter values.

Much of the uncertainty originates from the limited mechanistic understanding of key processes. The question therefore arises as to why any attempt has been made to model benthic impact generically. Specific reference is made to the development of Benoss, and it is noted that a range of factors can influence the model development cycle. In particular, institutional pressures mean that there is a tendency to interpret model output more rigorously than is justified by the degree of mechanistic understanding or the quality of input data.

Finally, any explicit model of benthic impact must rely on other physical process models to supply an estimate of carbon flux. Consequently, any uncertainty in the physical process modelling would be compounded by the subsequent modelling of benthic impact. A modelling approach is therefore suggested that expresses the output of physical process models in such a way as to give a qualitative assessment of benthic impact.

Chapter 9

9. Conclusions and Recommendations

9.1 Introduction

The three initial aims of this research were to:

1. investigate the environmental impact of organically rich effluents discharged to the marine environment.
2. examine the modelling tools available for predicting these impacts.
3. develop and test additional modelling tools.

These aims were subsequently refined such that only the benthic impacts of organic enrichment were examined. Conclusions and recommendations are therefore considered with respect to this focus. Furthermore, since summaries of each Chapter have already been given, the conclusions refer only to these three main research aims.

9.2 Conclusions

The first research aim was met by considering the nature of the coastal resource and environmental impacts. The characteristics of effluents, effluent disposal practices, and various forms of benthic impacts were also investigated. The unifying conclusion drawn from these considerations was that high levels of treatment are not necessarily synonymous with good environmental practice.

A balance should therefore be struck between alleviating the immediate environmental impacts associated with a discharge and those associated with treatment. Hence, from a scientific viewpoint the assimilative capacity of the receiving waters should be utilised. However, public opinion, to a degree, determines what is considered an acceptable disposal practice. Nevertheless, implementation of 'excessive' levels of treatment is undesirable because it diverts funds away from other projects that could realise a greater level of environmental improvement.

Therefore, discharges should be considered on a case by case basis, rather than dictating that a uniformly high level of treatment should be implemented.

The second aim of the research was met by examining published benthic impact models. Only two explicit benthic impact models were identified, both of which use empirical relationships to quantify the impact. Given that a single 'efficient' effluent disposal strategy can not be specified due to the heterogeneity of the coastal environment, it is highly unlikely that a universally applied empirical model could give a meaningful quantitative prediction of benthic impact. Therefore, it must be concluded that the models do not provide realistic predictions, at least when applied generically.

The third research aim was met by developing and analysing a mechanistic model that describes the vertical gradient in sedimentary redox potential. By definition, a mechanistic model gives an explicit mathematical description of processes occurring in the system of interest. Therefore, the redox model allows the heterogeneity of the environment to be taken into account, and can thus provide useful insights with respect to the development of vertical redox gradients in sediment systems. In addition, comparison of the calibrated model output with measured concentration profiles taken from the literature indicated that the model could give a reasonable reproduction of data.

The redox model therefore provides a diagnostic capacity with respect to the redox state of sedimentary systems. However, the idealised nature of the calculated Eh values means that the model Eh profiles should be considered only as an integrative summary of the diagenetic characteristics of the modelled system. Consequently, the redox model is not suitable for applications that require a definite thermodynamic interpretation of Eh. It is therefore unlikely that the model could be coupled to an equilibrium model to give a meaningful assessment of metal mobility, as suggested by Park & Jaffe (1996).

A sensitivity analysis indicated that a simplified model could be used to model the redox state of the upper portion of the sediment. However, the analysis also showed that the redox state is sensitive to various reaction-transport parameters that introduce considerable uncertainty into the model output. Since these processes can not be ignored, any model simplification would reduce the data requirements somewhat, but would not facilitate the application of the model in a management context.

The ability of the model to give convincing fits to measured concentration profiles does not give any absolute assurances with respect to the quality of subsequent model predictions. Furthermore, application of the redox model in a predictive sense is impeded by uncertainty in parameter values, especially when a data set is extrapolated to a wider domain, either in time or space. Finally, it is difficult to estimate even qualitatively how organic enrichment would effect various parameter values; especially those associated with the macrofaunal assemblage. Since uncertainty in critical parameter values translates into equivalent levels of uncertainty in the model redox profiles, it can be concluded that the redox model does not offer a viable management tool, at least in a quantitative sense.

Some of the model uncertainties are associated with the mathematical representations of sedimentary processes. However, in the context of predicting benthic impact, a more important source of uncertainty is the lack of mechanistic understanding and the stochastic nature of key ecological interactions that drive the macrofaunal succession, as well as the effect that this succession has on the parameter values. The introduction of additional model complexity could improve the mathematical representation of benthic processes. However, this would not improve the predictive capacity of the modelling approach because the parameter value uncertainty would remain. These same uncertainties would be encountered in the predictive application of any model of benthic processes; that is, any quantitative predictions would have a high level of uncertainty associated with them. It can be concluded, therefore, that explicit benthic impact models do not provide a solid basis for decision support and, in this respect,

would not facilitate the proactive management of coastal resources. The outcome of the modelling work in terms of the third research aim was therefore negative; that is, a viable modelling tool was not developed.

9.3 Suggestions for Further Work

The computational effort required to solve the transient case rapidly increases as the space step is reduced. It is therefore not desirable to have to reduce the space step in order to improve the mass balance. This can be avoided if the diagenetic equations are discretised using a formulation that is inherently mass conserving, such as the numerical scheme used by Soetaert *et al.* (1996a). Any development of the redox model should incorporate this improvement.

The redox model is a versatile diagnostic tool that could provide useful information with respect to the interactions of a complex system, which would be difficult or impossible to gather in other ways. For example, coupling the redox model to a water quality model could provide useful insights into the dynamic interaction between the water column and organically enriched sediments.

Additional research into the development of an explicit benthic impact model is not recommended. Nevertheless, some ability to predict benthic impact is desirable. Therefore, it is recommended that a qualitative modelling approach using an empirically determined Acceptable Effect Flux should be investigated. Much experimental work could be carried out to determine if a meaningful AEF could be defined for a range of depositional regimes. The development of a modelling approach based on this qualitative measure of impact should pay due attention to stochasticity and uncertainties. Furthermore, the modelling approach should be incorporated into an overall risk assessment methodology, and not be considered in isolation.

APPENDICES

Appendix I: Additional Model Details

Governing Equations

Organic Carbon (G)

$$(1-\varphi)\frac{\partial G}{\partial t} = (1-\varphi)D_b\frac{\partial^2 G}{\partial x^2} + \frac{\partial G}{\partial x}\left[(1-\varphi)\frac{dD_b}{dx} - D_b\frac{d\varphi}{dx} - \xi_f\omega_f\right]$$

$$-(1-\varphi)G\left\{\frac{V_{O_2}C_{O_2}}{(K_{O_2}+C_{O_2})} + \frac{V_{NO_3}C_{NO_3}}{(K_{NO_3}+C_{NO_3})}\cdot\frac{K_{in}^{O_2}}{C_{O_2}+K_{in}^{O_2}}\right\}$$

$$-(1-\varphi)G\left\{\frac{V_{Mn}C_{Mn}}{(K_{Mn}+C_{Mn})}\cdot\frac{K_{in}^{O_2}}{C_{O_2}+K_{in}^{O_2}}\cdot\frac{K_{in}^{NO_3}}{C_{NO_3}+K_{in}^{NO_3}}\right\}$$

$$-(1-\varphi)G\left\{\frac{V_{Fe}C_{Fe}}{(K_{Fe}+C_{Fe})}\cdot\frac{K_{in}^{O_2}}{C_{O_2}+K_{in}^{O_2}}\cdot\frac{K_{in}^{NO_3}}{C_{NO_3}+K_{in}^{NO_3}}\cdot\frac{K_{in}^{Mn}}{C_{Mn}+K_{in}^{Mn}}\right\}$$

$$-(1-\varphi)G\left\{\frac{V_{SO_4}C_{SO_4}}{(K_{SO_4}+C_{SO_4})}\cdot\frac{K_{in}^{O_2}}{C_{O_2}+K_{in}^{O_2}}\cdot\frac{K_{in}^{NO_3}}{C_{NO_3}+K_{in}^{NO_3}}\cdot\frac{K_{in}^{Mn}}{C_{Mn}+K_{in}^{Mn}}\cdot\frac{K_{in}^{Fe}}{C_{Fe}+K_{in}^{Fe}}\right\}$$

$$-(1-\varphi)G\left\{k_{CH_4}\cdot\frac{K_{in}^{O_2}}{C_{O_2}+K_{in}^{O_2}}\cdot\frac{K_{in}^{NO_3}}{C_{NO_3}+K_{in}^{NO_3}}\cdot\frac{K_{in}^{Mn}}{C_{Mn}+K_{in}^{Mn}}\cdot\frac{K_{in}^{Fe}}{C_{Fe}+K_{in}^{Fe}}\cdot\frac{K_{in}^{SO_4}}{C_{SO_4}+K_{in}^{SO_4}}\right\}$$

Mn-Oxide (C_{Mn})

$$(1-\varphi)\frac{\partial C_{Mn}}{\partial t} = (1-\varphi)D_b\frac{\partial^2 C_{Mn}}{\partial x^2} + \frac{\partial C_{Mn}}{\partial x}\left[(1-\varphi)\frac{dD_b}{dx} - D_b\frac{d\varphi}{dx} - \xi_f\omega_f\right]$$

$$-2(1-\varphi)G\left\{\frac{V_{Mn}C_{Mn}}{(K_{Mn}+C_{Mn})}\cdot\frac{K_{in}^{O_2}}{C_{O_2}+K_{in}^{O_2}}\cdot\frac{K_{in}^{NO_3}}{C_{NO_3}+K_{in}^{NO_3}}\right\}$$

$$+\varphi k_7\left(C_{mnii}C_{O_2}\right) - (1-\varphi)k_9\left(C_{Feii}C_{Mn}\right) - (1-\varphi)k_{12}\left(C_{Mn}C_{TS}\right)$$

Fe-Oxide (C_{Fe})

$$(1-\varphi)\frac{\partial C_{Fe}}{\partial t} = (1-\varphi)D_b\frac{\partial^2 C_{Fe}}{\partial x^2} + \frac{\partial C_{Fe}}{\partial x}\left[(1-\varphi)\frac{dD_b}{dx} - D_b\frac{d\varphi}{dx} - \xi_f\omega_f\right]$$

$$-4(1-\varphi)G\left\{\frac{V_{Fe}C_{Fe}}{(K_{Fe}+C_{Fe})}\cdot\frac{K_{in}^{O_2}}{C_{O_2}+K_{in}^{O_2}}\cdot\frac{K_{in}^{NO_3}}{C_{NO_3}+K_{in}^{NO_3}}\cdot\frac{K_{in}^{Mn}}{C_{Mn}+K_{in}^{Mn}}\right\}$$

$$+k_8\varphi(C_{O_2}C_{feii}) + 2k_9(1-\varphi)(C_{Mn}C_{feii}) - 2k_{13}(1-\varphi)(C_{Fe}C_{TS})$$

$MnCO_3$ (C_R: subscript 'R' denotes Rhodochrosite)

$$(1-\varphi)\frac{\partial C_R}{\partial t} = (1-\varphi)D_b\frac{\partial^2 C_R}{\partial x^2} + \frac{\partial C_R}{\partial x}\left[(1-\varphi)\frac{dD_b}{dx} - D_b\frac{d\varphi}{dx} - \xi_f\omega_f\right]$$

$$+k_{18}(1-\varphi)\delta_{18}\left\{\frac{C_{mnii}C_{CO_3^{2-}}}{K'_{spMnCO_3}} - 1\right\} - k_{19}(1-\varphi)\delta_{19}C_R\left\{1 - \frac{C_{mnii}C_{CO_3^{2-}}}{K'_{spMnCO_3}}\right\}$$

$FeCO_3$ (C_S: where the subscript 'S' denotes Siderite)

$$(1-\varphi)\frac{\partial C_S}{\partial t} = (1-\varphi)D_b\frac{\partial^2 C_S}{\partial x^2} + \frac{\partial C_S}{\partial x}\left[(1-\varphi)\frac{dD_b}{dx} - D_b\frac{d\varphi}{dx} - \xi_f\omega_f\right]$$

$$+k_{20}(1-\varphi)\delta_{20}\left\{\frac{C_{feii}C_{CO_3^{2-}}}{K'_{spFeCO_3}} - 1\right\} - k_{21}(1-\varphi)\delta_{21}C_S\left\{1 - \frac{C_{feii}C_{CO_3^{2-}}}{K'_{spFeCO_3}}\right\}$$

FeS (C_A: where the subscript 'A' denotes AVS)

$$(1-\varphi)\frac{\partial C_A}{\partial t} = (1-\varphi)D_b\frac{\partial^2 C_A}{\partial x^2} + \frac{\partial C_A}{\partial x}\left[(1-\varphi)\frac{dD_b}{dx} - D_b\frac{d\varphi}{dx} - \xi_f\omega_f\right]$$

$$+k_{22}(1-\varphi)\delta_{22}\left\{\frac{C_{feii}C_{HS}}{a_{H^+}K'_{spFeS}} - 1\right\} - k_{14}(1-\varphi)(C_{O_2}C_A) - k_{23}\delta_{23}(1-\varphi)C_A\left\{1 - \frac{C_{feii}C_{HS}}{a_{H^+}K'_{spFeS}}\right\}$$

Oxygen (C_{0_2})

$$\varphi\frac{\partial C_{0_2}}{\partial t}=\varphi D_{tot}\frac{\partial^2 C_{0_2}}{\partial x^2}+\frac{\partial C_{0_2}}{\partial x}\left[\varphi\frac{dD_{tot}}{dx}+D_{tot}\frac{d\varphi}{dx}-\varphi_f\omega_f\right]+\alpha\varphi(C_{0_2}|_{x=0}-C_{0_2})$$

$$-\left(\frac{x+2y}{x}\right)(1-\varphi)G\frac{V_{0_2}C_{0_2}}{(K_{0_2}+C_{0_2})}-\frac{1}{2}k_7\varphi(C_{0_2}C_{mnii})-\frac{1}{4}k_8\varphi(C_{0_2}C_{feii})$$

$$-2\ \left\{k_{10}\varphi(C_{0_2}C_{NH4})+k_{11}\varphi(C_{0_2}C_{TS})+k_{14}(1-\varphi)(C_{0_2}C_A)+k_{15}\varphi(C_{0_2}C_{CH_4})\right\}$$

Nitrate(C_{N0_3})

$$\varphi\frac{\partial C_{N0_3}}{\partial t}=\varphi D_{tot}\frac{\partial^2 C_{N0_3}}{\partial x^2}+\frac{\partial C_{N0_3}}{\partial x}\left[\varphi\frac{dD_{tot}}{dx}+D_{tot}\frac{d\varphi}{dx}-\varphi_f\omega_f\right]+\alpha\varphi(C_{N0_3}|_{x=0}-C_{N0_3})$$

$$+\left(\frac{y}{x}\right)(1-\varphi)G\frac{V_{0_2}C_{0_2}}{(K_{0_2}+C_{0_2})}-\left(\frac{4x+3y}{5x}\right)(1-\varphi)G\left\{\frac{V_{N0_3}C_{N0_3}}{(K_{N0_3}+C_{N0_3})}\cdot\frac{K_{in}^{0_2}}{C_{0_2}+K_{in}^{0_2}}\right\}$$

$$+k_{10}\varphi(C_{0_2}C_{NH4})$$

Sulphate(C_{SO_4})

$$\varphi\frac{\partial C_{SO_4}}{\partial t}=\varphi D_{tot}\frac{\partial^2 C_{SO_4}}{\partial x^2}+\frac{\partial C_{SO_4}}{\partial x}\left[\varphi\frac{dD_{tot}}{dx}+D_{tot}\frac{d\varphi}{dx}-\varphi_f\omega_f\right]+\alpha\varphi(C_{SO_4}|_{x=0}-C_{SO_4})$$

$$-\frac{1}{2}(1-\varphi)G\left\{\frac{V_{SO_4}C_{SO_4}}{(K_{SO_4}+C_{SO_4})}\cdot\frac{K_{in}^{0_2}}{C_{0_2}+K_{in}^{0_2}}\cdot\frac{K_{in}^{N0_3}}{C_{N0_3}+K_{in}^{N0_3}}\cdot\frac{K_{in}^{Mn}}{C_{Mn}+K_{in}^{Mn}}\cdot\frac{K_{in}^{Fe}}{C_{Fe}+K_{in}^{Fe}}\right\}$$

$$+k_{11}\varphi(C_{0_2}C_{TS})+k_{14}(1-\varphi)(C_{0_2}C_A)-k_{16}\varphi(C_{SO_4}C_{CH_4})$$

Ammonia (C_{NH4})

$$[\varphi+(1-\varphi)k_{NH4}]\frac{\partial C_{NH4}}{\partial t}=(\varphi D_{tot}+(1-\varphi)k_{NH4}D_b)\frac{\partial^2 C_{NH4}}{\partial x^2}$$

$$+\frac{\partial C_{NH4}}{\partial x}\left[\varphi\frac{dD_{tot}}{dx}+(1-\varphi)k_{NH4}\frac{dD_b}{dx}+D_{tot}\frac{d\varphi}{dx}-k_{NH4}D_b\frac{d\varphi}{dx}-\varphi_f\omega_f-k_{NH4}\xi_f\omega_f\right]$$

$$+\alpha\varphi(C_{NH4}|_{x=0}-C_{NH4})+\frac{y}{x}(1-\varphi)G\left\{\frac{V_{Mn}C_{Mn}}{(K_{Mn}+C_{Mn})}\cdot\frac{K_{in}^{O_2}}{C_{O_2}+K_{in}^{O_2}}\cdot\frac{K_{in}^{NO_3}}{C_{NO_3}+K_{in}^{NO_3}}\right\}$$

$$+\frac{y}{x}(1-\varphi)G\left\{\frac{V_{Fe}C_{Fe}}{(K_{Fe}+C_{Fe})}\cdot\frac{K_{in}^{O_2}}{C_{O_2}+K_{in}^{O_2}}\cdot\frac{K_{in}^{NO_3}}{C_{NO_3}+K_{in}^{NO_3}}\cdot\frac{K_{in}^{Mn}}{C_{Mn}+K_{in}^{Mn}}\right\}$$

$$+\frac{y}{x}(1-\varphi)G\left\{\frac{V_{SO_4}C_{SO_4}}{(K_{SO_4}+C_{SO_4})}\cdot\frac{K_{in}^{O_2}}{C_{O_2}+K_{in}^{O_2}}\cdot\frac{K_{in}^{NO_3}}{C_{NO_3}+K_{in}^{NO_3}}\cdot\frac{K_{in}^{Mn}}{C_{Mn}+K_{in}^{Mn}}\cdot\frac{K_{in}^{Fe}}{C_{Fe}+K_{in}^{Fe}}\right\}$$

$$+\frac{y}{x}(1-\varphi)G\left\{k_{CH_4}\cdot\frac{K_{in}^{O_2}}{C_{O_2}+K_{in}^{O_2}}\cdot\frac{K_{in}^{NO_3}}{C_{NO_3}+K_{in}^{NO_3}}\cdot\frac{K_{in}^{Mn}}{C_{Mn}+K_{in}^{Mn}}\cdot\frac{K_{in}^{Fe}}{C_{Fe}+K_{in}^{Fe}}\cdot\frac{K_{in}^{SO_4}}{C_{SO_4}+K_{in}^{SO_4}}\right\}$$

$$-k_{10}\varphi(C_{O_2}C_{NH4})$$

Mn^{2+}(C_{mnii})

$$\varphi\frac{\partial C_{mnii}}{\partial t}=\varphi D_{tot}\frac{\partial^2 C_{mnii}}{\partial x^2}+\frac{\partial C_{mnii}}{\partial x}\left[\varphi\frac{dD_{tot}}{dx}+D_{tot}\frac{d\varphi}{dx}-\varphi_f\omega_f\right]+\alpha\varphi(C_{mnii}|_{x=0}-C_{mnii})$$

$$+2(1-\varphi)G\left\{\frac{V_{Mn}C_{Mn}}{(K_{Mn}+C_{Mn})}\cdot\frac{K_{in}^{O_2}}{C_{O_2}+K_{in}^{O_2}}\cdot\frac{K_{in}^{NO_3}}{C_{NO_3}+K_{in}^{NO_3}}\right\}$$

$$-k_7\varphi(C_{O_2}C_{mnii})+k_9(1-\varphi)(C_{feii}C_{Mn})+k_{12}(1-\varphi)(C_{Mn}C_{TS})$$

$$-k_{18}(1-\varphi)\delta_{18}\left\{\frac{C_{mnii}C_{CO_3^{2-}}}{K'_{spMnCO_3}}-1\right\}+k_{19}(1-\varphi)\delta_{19}C_R\left\{1-\frac{C_{mnii}C_{CO_3^{2-}}}{K'_{spMnCO_3}}\right\}$$

Fe^{2+} (C_{feii})

$$\varphi\frac{\partial C_{feii}}{\partial t}=\varphi D_{tot}\frac{\partial^2 C_{feii}}{\partial x^2}+\frac{\partial C_{feii}}{\partial x}\left[\varphi\frac{dD_{tot}}{dx}+D_{tot}\frac{d\varphi}{dx}-\varphi_f\omega_f\right]+\alpha\varphi(C_{feii}\big|_{x=0}-C_{feii})$$

$$+4(1-\varphi)G\left\{\frac{V_{Fe}C_{Fe}}{(K_{Fe}+C_{Fe})}\cdot\frac{K_{in}^{O_2}}{C_{O_2}+K_{in}^{O_2}}\cdot\frac{K_{in}^{NO_3}}{C_{NO_3}+K_{in}^{NO_3}}\cdot\frac{K_{in}^{Mn}}{C_{Mn}+K_{in}^{Mn}}\right\}$$

$$-k_8\varphi(C_{O_2}C_{feii})-2k_9(1-\varphi)(C_{feii}C_{Mn})+2k_{13}(1-\varphi)(C_{Fe}C_{TS})$$

$$+k_{14}(1-\varphi)(C_{O_2}C_A)-k_{20}(1-\varphi)\delta_{20}\left\{\frac{C_{feii}C_{CO_3^{2-}}}{K'_{spFeCO_3}}-1\right\}+k_{21}(1-\varphi)\delta_{21}C_S\left\{1-\frac{C_{feii}C_{CO_3^{2-}}}{K'_{spFeCO_3}}\right\}$$

$$-k_{22}(1-\varphi)\delta_{22}\left\{\frac{C_{feii}C_{HS}}{a_{H^+}K'_{spFeS}}-1\right\}+k_{23}\delta_{23}(1-\varphi)C_A\left\{1-\frac{C_{feii}C_{HS}}{a_{H^+}K'_{spFeS}}\right\}$$

Total Sulphides -- TS (C_{TS})

$$\varphi\frac{\partial C_{TS}}{\partial t}=\varphi D_{tot}\frac{\partial^2 C_{TS}}{\partial x^2}+\frac{\partial C_{TS}}{\partial x}\left[\varphi\frac{dD_{tot}}{dx}+D_{tot}\frac{d\varphi}{dx}-\varphi_f\omega_f\right]+\alpha\varphi(C_{TS}\big|_{x=0}-C_{TS})$$

$$+\frac{1}{2}(1-\varphi)G\left\{\frac{V_{SO_4}C_{SO_4}}{(K_{SO_4}+C_{SO_4})}\cdot\frac{K_{in}^{O_2}}{C_{O_2}+K_{in}^{O_2}}\cdot\frac{K_{in}^{NO_3}}{C_{NO_3}+K_{in}^{NO_3}}\cdot\frac{K_{in}^{Mn}}{C_{Mn}+K_{in}^{Mn}}\cdot\frac{K_{in}^{Fe}}{C_{Fe}+K_{in}^{Fe}}\right\}$$

$$-k_{11}\varphi(C_{O_2}C_{TS})-k_{12}(1-\varphi)(C_{Mn}C_{TS})-k_{13}(1-\varphi)(C_{Fe}C_{TS})+k_{16}\varphi(C_{SO_4}C_{CH_4})$$

$$-k_{22}(1-\varphi)\delta_{22}\left\{\frac{C_{feii}C_{HS}}{a_{H^+}K'_{spFeS}}-1\right\}+k_{23}\delta_{23}(1-\varphi)C_A\left\{1-\frac{C_{feii}C_{HS}}{a_{H^+}K'_{spFeS}}\right\}$$

Methane (C_{CH_4})

$$\varphi\frac{\partial C_{CH_4}}{\partial t}=\varphi D_{tot}\frac{\partial^2 C_{CH_4}}{\partial x^2}+\frac{\partial C_{CH_4}}{\partial x}\left[\varphi\frac{dD_{tot}}{dx}+D_{tot}\frac{d\varphi}{dx}-\varphi_f\omega_f\right]+\alpha\varphi(C_{CH_4}\big|_{x=0}-C_{CH_4})$$

$$+\frac{1}{2}(1-\varphi)G\left\{k_{CH_4}\cdot\frac{K_{in}^{O_2}}{C_{O_2}+K_{in}^{O_2}}\cdot\frac{K_{in}^{NO_3}}{C_{NO_3}+K_{in}^{NO_3}}\cdot\frac{K_{in}^{Mn}}{C_{Mn}+K_{in}^{Mn}}\cdot\frac{K_{in}^{Fe}}{C_{Fe}+K_{in}^{Fe}}\cdot\frac{K_{in}^{SO_4}}{C_{SO_4}+K_{in}^{SO_4}}\right\}$$

$$-k_{15}\varphi(C_{O_2}C_{CH_4})-k_{16}\varphi(C_{SO_4}C_{CH_4})$$

Total Carbonate -- TC (C_{TC})

$$\varphi\frac{\partial C_{TC}}{\partial t}=\varphi D_{tot}\frac{\partial^2 C_{TC}}{\partial x^2}+\frac{\partial C_{TC}}{\partial x}\left[\varphi\frac{dD_{tot}}{dx}+D_{tot}\frac{d\varphi}{dx}-\varphi_f\omega_f\right]+\alpha\varphi(C_{TC}|_{x=0}-C_{TC})$$

$$+(1-\varphi)G\left\{\frac{V_{O_2}C_{O_2}}{(K_{O_2}+C_{O_2})}+\frac{V_{NO_3}C_{NO_3}}{(K_{NO_3}+C_{NO_3})}\cdot\frac{K_{in}^{O_2}}{C_{O_2}+K_{in}^{O_2}}\right\}$$

$$+(1-\varphi)G\left\{\frac{V_{Mn}C_{Mn}}{(K_{Mn}+C_{Mn})}\cdot\frac{K_{in}^{O_2}}{C_{O_2}+K_{in}^{O_2}}\cdot\frac{K_{in}^{NO_3}}{C_{NO_3}+K_{in}^{NO_3}}\right\}$$

$$+(1-\varphi)G\left\{\frac{V_{Fe}C_{Fe}}{(K_{Fe}+C_{Fe})}\cdot\frac{K_{in}^{O_2}}{C_{O_2}+K_{in}^{O_2}}\cdot\frac{K_{in}^{NO_3}}{C_{NO_3}+K_{in}^{NO_3}}\cdot\frac{K_{in}^{Mn}}{C_{Mn}+K_{in}^{Mn}}\right\}$$

$$+(1-\varphi)G\left\{\frac{V_{SO_4}C_{SO_4}}{(K_{SO_4}+C_{SO_4})}\cdot\frac{K_{in}^{O_2}}{C_{O_2}+K_{in}^{O_2}}\cdot\frac{K_{in}^{NO_3}}{C_{NO_3}+K_{in}^{NO_3}}\cdot\frac{K_{in}^{Mn}}{C_{Mn}+K_{in}^{Mn}}\cdot\frac{K_{in}^{Fe}}{C_{Fe}+K_{in}^{Fe}}\right\}$$

$$+\frac{1}{2}(1-\varphi)G\left\{k_{CH_4}\cdot\frac{K_{in}^{O_2}}{C_{O_2}+K_{in}^{O_2}}\cdot\frac{K_{in}^{NO_3}}{C_{NO_3}+K_{in}^{NO_3}}\cdot\frac{K_{in}^{Mn}}{C_{Mn}+K_{in}^{Mn}}\cdot\frac{K_{in}^{Fe}}{C_{Fe}+K_{in}^{Fe}}\cdot\frac{K_{in}^{SO_4}}{C_{SO_4}+K_{in}^{SO_4}}\right\}$$

$$+k_{15}\varphi(C_{O_2}C_{CH_4})+k_{16}\varphi(C_{SO_4}C_{CH_4})$$

$$-k_{18}(1-\varphi)\delta_{18}\left\{\frac{C_{mnii}C_{CO_3^{2-}}}{K'_{spMnCO_3}}-1\right\}+k_{19}(1-\varphi)\delta_{19}C_R\left\{1-\frac{C_{mnii}C_{CO_3^{2-}}}{K'_{spMnCO_3}}\right\}$$

$$-k_{20}(1-\varphi)\delta_{20}\left\{\frac{C_{feii}C_{CO_3^{2-}}}{K'_{spFeCO_3}}-1\right\}+k_{21}(1-\varphi)\delta_{21}C_S\left\{1-\frac{C_{feii}C_{CO_3^{2-}}}{K'_{spFeCO_3}}\right\}$$

Notes

x:y in the equations is equal to the assumed C:N ratio of the POM. D_{tot} is equal to $D_b+D_i+D_{sed}$; with D_{sed} being given by Boudreau's subroutine, adjusted for tortuosity. When irrigation is represented using the non-local exchange function, and in the absence of other additional diffusional fluxes of interest, D_i can be set to zero. Other parameters are as defined within the text (see Chapter 5).

The non-component concentrations involved in the precipitation and dissolution reactions (that is, CO_3^{2-}+ HS^-) are calculated thus:

$$C_{CO_3^{2-}}=c_1C_{TC}$$

$$C_{HS}=h_1C_{TS}$$

where c_1 and h_1 are constants that can be calculated from equilibrium relationships such as those detailed in Van Cappellen & Wang (1995, Table 8).

The values of delta in the precipitation/dissolution reactions are set to one or zero according to the Ion Activity Product (IAP) of the solutes involved in the reaction. Hence:

$\delta_{18}; \delta_{20}; \delta_{22} = 0$ for IAP $\leq K'_{sp}$ $\quad$ $\delta_{19}; \delta_{21}; \delta_{23} = 1$ for IAP $\leq K'_{sp}$

$\delta_{18}; \delta_{20}; \delta_{22} = 1$ for IAP $\geq K'_{sp}$ $\quad$ $\delta_{19}; \delta_{21}; \delta_{23} = 0$ for IAP $\geq K'_{sp}$

Additional Notes on Model Implementation

The value of the depth dependent parameters (α, φ, D_b, D_i) were calculated at each depth ($x=i.\Delta x$) from the appropriate analytical functions. Likewise, the derivatives of the parameters were calculated analytically (see Section 5.8). In the specific implementation of the redox model used in this research, all of the functions (and corresponding derivatives) discussed in the text were incorporated into the same code. The selection of the depth dependency for any particular run was made by specifying integer switches (set to one or zero). Hence, the function to be used was specified at the start of each run by setting integer switches in the input template to one or zero accordingly -- the integer switch being used in the code to automatically select the appropriate functional form of the depth dependencies and associated derivatives. However, as noted in "Suggestions for Further Work" (Chapter 9), a flux based discretisation is recommended, which would require the derivatives of these parameters to be treated numerically.

Finally, in the transient version of the model, various parameter values (at the SWI) at time t were calculated according to the assumed temperature forcing function, in conjunction with the simple Q_{10} treatment of temperature dependency discussed in the text.

Additional Notes on Discretisation

As discussed in the main text, the governing equations given above must be solved numerically. Hence, the derivatives at each node were approximated using finite difference formulations. The concentrations in the reaction terms were taken at the node in question.

For the NMOL solution, only the terms on the RHS were discretised, as discussed in the text. For solutes, the first and second derivatives in space were replaced by central difference approximations. For solids, the second derivative was replaced by central difference approximation, but a blended scheme was used to represent the first derivative in space. Both sides of the resulting ODEs were then divided by $(1-\varphi)$, φ, or $(\varphi + k_{NH4}(1-\varphi))$ as appropriate (see the governing Equations given above) to leave just the derivative in time on the LHS. This then formed the system of ODEs that could be solved using VODE.

For the steady state solution, both the derivatives in time and space were replaced by the difference scheme discussed in the text (and above). The resulting set of algebraic equations could then be rearranged into a tridiagonal matrix of the form:

$$\alpha C_{i+1}^{n+1} + \beta C_i^{n+1} + \gamma C_{i-1}^{n+1} = \delta_i$$

where δ_i is a function of the concentrations calculated at the previous time step (or iteration). This set of equations was solved using the Thomas algorithm. With constant boundary conditions, integrating the governing equations over a sufficiently long time span gives the steady state solution. In the main text, this process is termed 'Global iteration' in an attempt to emphasise the steady state nature of the solution algorithm.

Additional Notes on Redox Calculation

As noted in the main text, the model redox potential at any depth was calculated from the concentration of the component species using the Nernst Equation. The subroutine written to calculate Eh values included an algorithm to determine the dominant metabolic pathway being used at each node (see main text, Section 5.9 for details on the selection criteria used in this study). Once the dominant metabolic pathway had been determined, the activities of the oxidant and corresponding reduced species associated with the respiratory metabolism could be used to calculate the redox potential.

By way of illustration, consider the calculation of Eh at depths where Mn-oxide is the main oxidant being used; that is, at depths where Mn-oxide reduction is not inhibited but is inhibiting the reduction of Fe-oxide, sulphate, and methanogenesis (see Section 5.9). The Nernst Equation (Equation 4-1) has the form:

$$Eh = E^o + \frac{RT}{nF} \ln \frac{\{a_{ox}\}^c}{\{a_{red}\}^d}$$

From Table 17, the degradation of POM via Mn-oxide reduction is assumed to involve the following half reaction:

$$MnO_2 + 4H^+ + 2e^- \rightarrow Mn^{2+} + 2H_2O$$

Hence, two electrons are transferred between the oxidant and reductant; that is, '*n*' in the Nernst Equation is two. At 25°C, E° for this half reaction is 1.23V (which can be calculated from the thermodynamic data given in Appendix II or obtained from many physical chemistry texts). Noting that $\ln(x)=2.3\log_{10}(x)$, the Nernst Equation for this half reaction is:

$$Eh = 1.23 + 0.0295 \log_{10}\left(\frac{\{a_{MnO_2}\}\{a_{H^+}\}^4}{\{a_{Mn^{2+}}\}\{a_{H_2O}\}^2}\right)$$

which can be rewritten as:

$$Eh = 1.23 + 0.0295\left(\log_{10}\{a_{MnO_2}\} + 4\log_{10}\{a_{H^+}\} - \log_{10}\{a_{Mn^{2+}}\} - 2\log_{10}\{a_{H_2O}\}\right)$$

The activity of solids and water can be assumed to be one, and the hydrogen ion activity throughout the model domain is given by the assumed pH. Hence, the Equation can be simplified to:

$$Eh = 1.23 - 0.0295\left(\log_{10}\{a_{Mn^{2+}}\} + 4\text{pH}\right)$$

Finally, for a pH of 7.5 this equation reduces to:

$$Eh = 0.345 - 0.0295\log_{10}\{a_{Mn^{2+}}\}$$

The activity of the Mn^{2+} ion can then be calculated from the concentration of Mn^{2+} (output by the diagenetic part of the model) at each depth where Mn-oxide reduction predominates, as:

$$a_{Mn^{2+}} = \gamma C_{mnii}$$

with the activity coefficient calculated using the Davies formula (with an ionic charge of 2; see Equation 5-41). The ionic strength I used in the Davies formula can be calculated from the specified salinity/chlorinity (see Van Cappellen & Wang, 1995, Table 8 for the appropriate formula).

The calculation of Eh for metabolic pathways involving neutral species is carried out in the same way, except that the concentration of the solute must be converted to a partial pressure using Henry's Law. An activity coefficient is then applied to account for the decrease in solubility with increasing ionic strength (that is, to account for 'salting out'), as discussed in the text.

Finally, as mentioned in Chapter 8, the insensitivity of the redox potential to the activities of the component species means that any consideration of activities could be superfluous. In that case, a redox potential could be calculated simply by substituting the concentrations output by the model into the Nernst equation; that is, without applying any activity coefficients.

APPENDIX II: Thermodynamic Data

Species	ΔG_f^o *(kj/mol)*	ΔH_f^o *(kj/mol)*
$O_2(g)$	0	0
$O_2(aq)$	16.32	-11.71
$H_2O_2(aq)$	-134.1	-191.17
$H_2O(l)$	-237.18	-285.83
$NO_3^-(aq)$	-111.3	-207.3
$NH_4^+(aq)$	-79.37	-132.5
$N_2(g)$	0	0
$MnO_2(s)$	-465.1	-520.0
$Mn^{2+}(aq)$	-228.0	-220.7
$Fe(OH)_3(s)$	-696.5	-823.0
$Fe^{2+}(aq)$	-78.87	-89.10
$SO_4^{2-}(aq)$	-744.6	-909.2
$HS^-(aq)$	12.05	-17.6
$HCO_3^-(aq)$	-586.8	-692.0
$CH_4(g)$	-50.79	-74.80
$CH_4(aq)$	-34.39	-89.04
$H^+(aq)$	0	0
$H_2(g)$	0	0
e^-	0	See Notes

Data from Stumm & Morgan (1996)

The free energies are used to calculate the equilibrium constant at 25°C. The standard enthalpies are used to calculate the equilibrium constants at other temperatures.

For any given reaction the standard free energy change (ΔG°) and standard enthalpy change (ΔH°) is calculated as:

$$\Delta G^o = \sum \Delta G_f^o(\text{products}) - \sum \Delta G_f^o(\text{reactants})$$

$$\Delta H^o = \sum \Delta H_f^o(\text{products}) - \sum \Delta H_f^o(\text{reactants})$$

When calculating the standard enthalpy change of a half reaction the electron can be ignored because redox potentials are referred to the hydrogen scale. Hence, the standard hydrogen electrode is implied in each of the half reactions considered. When the H_2/H^+ couple is included explicitly the electron e^- in the half reaction cancels. Furthermore, since the Standard Enthalpy of Formation for the H_2/H^+ couple is zero by convention, it does not influence the calculation.

APPENDIX III: Analytical Solution for Organic Carbon

Assumptions:

1. Steady State
2. 1-G formulation
3. Two layer model of bioturbation
4. Known flux boundary condition
5. Constant porosity

Model Definition

$$0 = D_b \frac{\partial^2 G}{\partial x^2} - \omega \frac{\partial G}{\partial x} - kG \qquad \textbf{Equation A-1}$$

with $D_b(x) = D_b(x)$; $0 < x < X_L$; 0 otherwise. Hence, X_L is the depth at which bioturbation falls to zero.

Boundary Conditions

$$J_{org} = -D_b \frac{\partial G}{\partial x} + \omega G\Big|_{x=0} = known\ value \qquad \textbf{Equation A-2}$$

$$\frac{\partial G}{\partial x}\Big|_{x \to \infty} = 0 \qquad \textbf{Equation A-3}$$

In addition flux continuity is required at the interface $x = X_L$ which implies that:

$$-D_b \frac{\partial G}{\partial x} + \omega G\Big|_{x=X_L} = \omega G\Big|_{x=X_L} \qquad \textbf{Equation A-4}$$

Solution

For the top layer: $0 < x < X_L$:

$$G(x) = \frac{a}{k} J_{org} \exp(aX_L + bx) - \frac{b}{k} J_{org} \exp(bX_L + ax)$$

where

$$a = \frac{\omega + \sqrt{\omega^2 + 4D_b k}}{2D_b} \qquad \text{and} \qquad b = \frac{\omega - \sqrt{\omega^2 + 4D_b k}}{2D_b}$$

Equation A-5

For the bottom layer: $X_L < x < \infty$

$$G(x) = \frac{J_{org}}{k} \exp((a+b)X_L).(a-b)\exp(-\frac{k}{\omega}(x - X_L)) \qquad \textbf{Equation A-6}$$

with a and b as defined in Equation A-5 above

APPENDIX IV: Model Input Conditions (Verification)

Parameter Definitions (Input Template)

```
'Temperature ----', in °C
'Salinity -------', in ppt
'Pressure--------', in atm
'pH -------------', usually set to 7.5
'Xbphi ----------', decay constant for porosity
'initial phi ----', initial porosity (unitless)
'final phi ------', final porosity (unitless)

'W @ infinity ---', sedimentation rate (cm/yr)

'Option Db-------', integer flag for choice of bioturbation function
'Option Di-------', integer flag for choice of diffusion function
'Option Irrig----', integer flag for choice of irrigation function

'Db SWI ---------', Bioturbation at SWI(cm^2/yr)
'Di SWI ---------', Enhanced Diffusion Coefficient at SWI
'irrig SWI ------', Irrigation at SWI (/yr)

'DBzb -----------', depth of mixed layer/decay constant for bioturbation (cm)
'DBz0 -----------', depth of zero bioturbation (cm)

'Dizb -----------', as Dbzb but for enhanced diffusion
'Diz0 -----------', as Dbzb but for enhanced diffusion

'Dirrigzb -------', as Dbzb but for irrigation
'Dirrigz0 -------', as Dbzb but for enhanced diffusion

'density solid --', in g/cm^3
'adsorb NH4 -----', constant for linear adsorption isotherm (unitless)

'kspfe ----------', Ksp feco3 ((nm/cm^3)^2)
'kspfes ---------', Ksp fes ((nm/cm^3)^2)
'kspmn ----------', Ksp mnco3 ((nm/cm^3)^2)

'Vo2 ------------', rate constant for oxygen reduction (/yr)
'Vno3 -----------', rate constant for nitrate reduction (/yr)
'Vmn4 -----------', rate constant for mn oxide reduction (/yr)
'Vfe3 -----------', rate constant for fe oxide reduction (/yr)
'Vso4 -----------', rate constant for sulfate reduction (/yr)
'Kch4 -----------', rate constant for methane production (/yr)

'k7: mnii.o2 ----', rate constant (1/nm/cm^3/yr)
'k8: feii.o2 ----', rate constant (1/nm/cm^3/yr)
'k9: feii.mno2 --', rate constant (1/nm/cm^3/yr)
'k10: nh4.o2 ----', rate constant (1/nm/cm^3/yr)
'k11: o2.h2s ----', rate constant (1/nm/cm^3/yr)
'k12: mno2:h2s --', rate constant (1/nm/cm^3/yr)
'k13: fe3:h2s ---', rate constant (1/nm/cm^3/yr)
'k14: fes.o2 ----', rate constant (1/nm/cm^3/yr)
'k15: ch4.o2 ----', rate constant (1/nm/cm^3/yr)
'k16: ch4.so4 ---', rate constant (1/nm/cm^3/yr)
'k18: mnco3P ----', rate constant (nm/cm^3/yr)
'k19: mnco3D ----', rate constant (/yr)
'k20: feco3P ----', rate constant (nm/cm^3/yr)
'k21: feco3D ----', rate constant (/yr)
'k22: fesP ------', rate constant (nm/cm^3/yr)
'k23: fesD ------', rate constant (/yr)

'inhibit o2 -----', inhibition constant: by oxygen (nm/cm^3)
'inhibit no3 ----', inhibition constant: by nitrate (nm/cm^3)
'inhibit mn4 ----', inhibition constant: by mn oxide (nm/cm^3)
'inhibit fe3 ----', inhibition constant: by fe oxide (nm/cm^3)
'inhibit so4 ----', inhibition constant: by sulphate (nm/cm^3)

'1/2 sat o2 -----', half saturation constant of oxygen (nm/cm^3)
'1/2 sat no3 ----', half saturation constant of nitrate (nm/cm^3)
'1/2 sat mn4 ----', half saturation constant of mn oxide (nm/cm^3)
'1/2 sat fe3 ----', half saturation constant of fe oxide (nm/cm^3)
'1/2 sat so4 ----', half saturation constant of sulphate (nm/cm^3)
```

```
'stoich sx ------', number atoms of carbon in organic matter
'stoich sy ------', number atoms of nitrogen in organic matter
'stoich sz ------', number atoms of phosphorous in organic matter

'Boundary G -----', boundary condition (nm/cm^2/yr)
'Boundary O2 ----', boundary condition (nm/cm^3)
'Boundary NO3 ---', boundary condition (nm/cm^3)
'Boundary MN4 ---', boundary condition (nm/cm^3)
'Boundary FE3 ---', boundary condition (nm/cm^3)
'Boundary SO4 ---', boundary condition (nm/cm^3)
'Boundary H2S ---', boundary condition (nm/cm^3)
'Boundary CH4 ---', boundary condition (nm/cm^3)
'Boundary NH4 ---', boundary condition (nm/cm^3)
'Boundary MN2 ---', boundary condition (nm/cm^3)
'Boundary FE2 ---', boundary condition (nm/cm^3)
'Boundary TC ----', boundary condition (nm/cm^3)
'Boundary MNCO3 -', boundary condition (nm/cm^2/yr)
'Boundary FECO3 -', boundary condition (nm/cm^2/yr)
'Boundary FES ---', boundary condition (nm/cm^2/yr)
```

Test Cases – CANDI

Parameter	case 1	case 2	case 3	case 4	case 5	case 6	case 7	case 8	case 10
'Temperature ----'	5	2	5	5	5	5	5	10	5
'Salinity -------'	35	35	35	35	35	35	35	35	35
'Pressure--------'	100	200	100	100	100	100	100	1	100
'pH ------------'	7.5	7.5	7.5	7.5	7.5	7.5	7.5	7.5	7.5
'Xbphi ----------'	4	4.0	4.0	4.0	8.0	2.0	1.0	4.0	8.0
'initial phi ----'	0.8	0.8	0.8	0.8	0.8	0.8	0.8	0.8	0.8
'final phi ------'	0.8	0.8	0.8	0.8	0.7	0.7	0.7	0.8	0.7
'W @ infinity ---'	3.0E-02	3.0E-03	3.0E-02	3.0E-02	3.0E-02	3.0E-02	3.0E-02	3.0E-01	3.0E-02
'Option Db--------'	2	2	2	1	1	1	1	2	1
'Option Di--------'	2	2	2	2	2	2	2	2	2
'Option Irrig----'	2	2	2	2	2	2	2	2	2
'Db SWI ---------'	1.350	0.269	1.350	1.350	1.350	1.350	1.350	6.760	1.350
'Di SWI ---------'	0	0	0	0	0	0	0	0	0
'irrig SWI ------'	0	0	0	5	5	5	5	0	5
'DBzb -----------'	8	8	8	8	8	8	8	8	8
'DBz0 -----------'	10	10	10	10	10	10	10	10	10
'Dizb -----------'	10	10	10	10	10	10	10	10	10
'Diz0 -----------'	12	12	12	12	12	12	12	12	12
'Dirrigzb -----------'	10	10	10	8	8	8	8	10	8
'Dirrigz0 -----------'	12	12	12	8	8	8	8	12	8
'density solid --'	2.5	2.5	2.5	2.5	2.5	2.5	2.5	2.5	2.5
'adsorb NH4 -----'	0	0	0	2	10	10	10	0	10
'kspfe ----------'	1	na	na	na	na	na	na	na	na
'kspfes ---------'	1	na	na	na	na	na	na	na	1.0
'kspmn ----------'	1	na	na	na	na	na	na	na	na
'Vo2 ------------'	1	0.05	0.6	0.6	0.6	0.6	0.6	1.0	0.6
'Vno3 -----------'	1	0.05	0.6	0.6	0.6	0.6	0.6	1.0	0.6
'Vmn4 -----------'	1	0.05	0.6	0.6	0.6	0.6	0.6	1.0	0.6
'Vfe3 -----------'	1	0.05	0.6	0.6	0.6	0.6	0.6	1.0	0.6
'Vso4 -----------'	1	0.05	0.6	0.6	0.6	0.6	0.6	1.0	0.6
'Kch4 -----------'	1	0.05	0.6	0.6	0.6	0.6	0.6	1.0	0.6
'k7: mnii.o2 ----'	2000	1000	2000	2000	2000	2000	2000	2000	2000
'k8: feii.o2 ----'	2000	1000	2000	2000	2000	2000	2000	2000	2000
'k9: feii.mno2 --'	0	0	0	0	0	0	0	0	0
'k10: nh4.o2 ----'	10	10	10	10	10	10	10	10	10
'k11: o2.h2s ----'	600	300	600	600	600	600	600	600	600
'k12: mno2:h2s --'	0	0	0	0	0	0	0	0	0
'k13: fe3:h2s ---'	0	0	0	0	0	0	0	0	0
'k14: fes.o2 ----'	220	200	220	220	220	220	220	220	220
'k15: ch4.o2 ----'	10000	10000	10000	10000	10000	10000	10000	10000	10000
'k16: ch4.so4 ---'	10000	10000	10000	10000	10000	10000	10000	10000	10000
'k18: mnco3P ----'	0	0	0	0	0	0	0	0	0
'k19: mnco3D ----'	0	0	0	0	0	0	0	0	0

'k20: feco3P ----'	0	0	0	0	0	0	0	0	0
'k21: feco3D ----'	0	0	0	0	0	0	0	0	0
'k22: fesP ------'	0	0	0	0	0	0	0	0	0
'k23: fesD ------'	0	0	0	0	0	0	0	0	0
'inhibit o2 -----'	4	4	4	4	4	4	4	4	4
'inhibit no3 ----'	5	5	5	5	5	5	5	5	5
'inhibit mn4 ----'	10	10	10	10	10	10	10	10	10
'inhibit fe3 ----'	10	10	10	10	10	10	10	10	10
'inhibit so4 ----'	500	500	500	500	500	500	500	500	500
'1/2 sat o2 -----'	8	8	8	8	8	8	8	8	8
'1/2 sat no3 ----'	10	10	10	10	10	10	10	10	10
'1/2 sat mn4 ----'	1	1	1	1	1	1	1	1	1
'1/2 sat fe3 ----'	1	1	1	1	1	1	1	1	1
'1/2 sat so4 ----'	1000	1000	1000	1000	1000	1000	1000	1000	1000
'stoich sx ------'	200	200	200	200	200	200	200	106	200
'stoich sy ------'	21	21	21	21	21	21	21	16	21
'stoich sz ------'	1	1	1	1	1	1	1	1	1
'Boundary G -----'	130000	18500	130000	130000	130000	130000	130000	985000	130000
'Boundary O2 ----'	250	180	250	250	250	250	250	275	250
'Boundary NO3 ---'	15	30	15	15	15	15	15	10	15
'Boundary MN4 ---'	113761	113761	113761	113761	113761	113761	113761	113761	113761
'Boundary FE3 ---'	111907	111907	111907	111907	111907	111907	111907	111907	111907
'Boundary SO4 ---'	29149	29290	29149	29149	29149	29149	29149	28999	29149
'Boundary H2S ---'	0	0	0	0	0	0	0	0	0
'Boundary CH4 ---'	0	0	0	0	0	0	0	0	0
'Boundary NH4 ---'	0	0	0	0	0	0	0	0	0
'Boundary MN2 ---'	0	0	0	0	0	0	0	0	0
'Boundary FE2 ---'	0	0	0	0	0	0	0	0	0
'Boundary TC ----'	2200	2200	2200	2200	2200	2200	2200	2200	2200
'Boundary MNCO3 -'	0	0	0	0	0	0	0	0	0
'Boundary FECO3 -'	0	0	0	0	0	0	0	0	0
'Boundary FES ---'	0	0	0	0	0	0	0	0	0

Test Cases -- STEADYSED1

Parameter	coast 1	coast 2	coast 3	shelf	deep
'Temperature ----'	18	18	18	10	2
'Salinity -------'	20	20	20	35	35
'Pressure--------'	1	1	1	1	1
'pH -------------'	7.5	7.5	7.5	7.5	7.5
'Xbphi ----------'	4	4	4	4	4
'initial phi ----'	0.9	0.9	0.9	0.85	0.8
'final phi ------'	0.9	0.9	0.9	0.85	0.8
'W @ infinity ---'	1	1	1	0.04	0.001
'Option Db-------'	2	2	2	2	2
'Option Di-------'	2	2	2	2	2
'Option Irrig----'	2	2	2	2	2
'Db SWI ---------'	10	10	10	3	0.1
'Di SWI ---------'	0	0	0	0	0
'irrig SWI ------'	10	10	10	5	0
'DBzb -----------'	30	30	30	30	20
'DBz0 -----------'	30	30	30	30	20
'Dizb -----------'	10	10	10	10	10
'Diz0 -----------'	12	12	12	12	12
'Dirrigzb -------'	30	30	30	30	10
'Dirrigz0 -------'	30	30	30	30	12
'density solid --'	2.4	2.4	2.4	2.5	2.5
'adsorb NH4 -----'	1.4	1.4	1.4	1.4	1.4
'kspfe ----------'	4.0E+03	4.0E+03	4.0E+03	4.0E+03	4.0E+03
'kspfes ---------'	6.3E+09	6.3E+09	6.3E+09	6.3E+09	6.3E+09
'kspmn ----------'	3.2E+03	3.2E+03	3.2E+03	3.2E+03	3.2E+03
'Vo2 ------------'	0.1	0.1	0.1	0.01	0.003
'Vno3 -----------'	0.1	0.1	0.1	0.01	0.003
'Vmn4 -----------'	0.1	0.1	0.1	0.01	0.003
'Vfe3 -----------'	0.1	0.1	0.1	0.01	0.003
'Vso4 -----------'	0.1	0.1	0.1	0.01	0.003
'Kch4 -----------'	0.1	0.1	0.1	0.01	0.003
'k7: mnii.o2 ----'	2000	2000	2000	2000	1000
'k8: feii.o2 ----'	2000	2000	2000	2000	1000
'k9: feii.mno2 --'	200	200	200	200	0.01
'k10: nh4.o2 ----'	15	15	15	15	10
'k11: o2.h2s ----'	600	600	600	600	300
'k12: mno2:h2s --'	0.01	0.01	0.01	0.01	0.01
'k13: fe3:h2s ---'	0.01	0.01	0.01	0.01	0.01
'k14: fes.o2 ----'	22	22	22	22	20
'k15: ch4.o2 ----'	10000	10000	10000	10000	10000
'k16: ch4.so4 ---'	10000	10000	10000	10000	10000
'k18: mnco3P ----'	0	100	100	100	100
'k19: mnco3D ----'	0	0.80	0.80	0.80	0.80
'k20: feco3P ----'	0	450	450	450	450
'k21: feco3D ----'	0	0.25	0.25	0.25	0.25
'k22: fesP ------'	0	15	15	15	15
'k23: fesD ------'	0	0.1E-2	0.1E-2	0.1E-2	0.1E-2
'inhibit o2 -----'	20	20	20	20	20
'inhibit no3 ----'	2	2	2	2	2
'inhibit mn4 ----'	3.84E+04	3.84E+04	3.84E+04	4.00E+04	4.00E+04

'inhibit fe3 ----'	2.40E+05	2.40E+05	2.40E+05	2.50E+05	2.50E+05
'inhibit so4 ----'	1.6E+03	1.6E+03	1.6E+03	1.6E+03	1.6E+03
'1/2 sat o2 -----'	20	20	20	20	20
'1/2 sat no3 ----'	2	2	2	2	2
'1/2 sat mn4 ----'	3.84E+04	3.84E+04	3.84E+04	4.00E+04	4.00E+04
'1/2 sat fe3 ----'	2.40E+05	2.40E+05	2.40E+05	2.50E+05	2.50E+05
'1/2 sat so4 ----'	1.6E+03	1.6E+03	1.6E+03	1.6E+03	1.6E+03
'stoich sx ------'	106	106	106	200	200
'stoich sy ------'	11	11	11	21	21
'stoich sz ------'	1	1	1	1	1
'Boundary G -----'	1050000	1050000	1050000	80000	7000
'Boundary O2 ----'	275	275	275	250	180
'Boundary NO3 ---'	10	10	10	15	30
'Boundary MN4 ---'	4000	4000	4000	12	0.04
'Boundary FE3 ---'	10000	10000	10000	100	0.01
'Boundary SO4 ---'	16000	16000	1600	28000	28000
'Boundary H2S ---'	0	0	0	0	0
'Boundary CH4 ---'	0	0	0	0	0
'Boundary NH4 ---'	0	0	0	0	0
'Boundary MN2 ---'	0	0	0	0	0
'Boundary FE2 ---'	0	0	0	0	0
'Boundary TC ----'	2200	2200	2200	2200	2200
'Boundary MNCO3 -'	0	0	0	0	0
'Boundary FECO3 -'	0	0	0	0	0
'Boundary FES ---'	0	0	0	0	0

NB: Boundary Conditions for the Mn and Fe oxide components were specified as known fluxes. Coast 2 parameter values are the typical values used in the analysis of the model, except for the Mn and Fe oxide boundary conditions, which were specified as Dirichlet boundary conditions; equivalent to a concentration of 0.25% by weight (assuming a constant sediment solids density).

APPENDIX V: Model Input Conditions (Sensitivity Analysis)

Parameter	bc1	bc2
'Temperature ----'	18	18
'Salinity -------'	20	20
'Pressure--------'	1	1
'pH ------------'	7.5	7.5
'Xbphi ----------'	4	4
'initial phi ----'	0.9	0.9
'final phi ------'	0.9	0.9
'W @ infinity ---'	1	1
'Option Db-------'	2	2
'Option Di-------'	2	2
'Option Irrig----'	2	2
'Db SWI ---------'	10	10
'Di SWI ---------'	0	0
'irrig SWI ------'	10	10
'DBzb -----------'	30	30
'DBz0 -----------'	30	30
'Dizb -----------'	10	10
'Diz0 -----------'	12	12
'Dirrigzb -------'	30	30
'Dirrigz0 -------'	30	30
'density solid --'	2.4	2.4
'adsorb NH4 -----'	1.4	1.4
'kspfe ----------'	4.0E+03	4.0E+03
'kspfes ---------'	6.3E+09	6.3E+09
'kspmn ----------'	3.2E+03	3.2E+03
'Vo2 ------------'	0.1	0.1
'Vno3 -----------'	0.1	0.1
'Vmn4 -----------'	0.1	0.05
'Vfe3 -----------'	0.1	0.05
'Vso4 -----------'	0.1	0.01
'Kch4 -----------'	0.1	0.01
'k7: mnii.o2 ----'	2000	2000
'k8: feii.o2 ----'	2000	2000
'k9: feii.mno2 --'	200	200
'k10: nh4.o2 ----'	15	15
'k11: o2.h2s ----'	600	600
'k12: mno2:h2s --'	0.01	0.01
'k13: fe3:h2s ---'	0.01	0.01
'k14: fes.o2 ----'	22	22
'k15: ch4.o2 ----'	10000	10000
'k16: ch4.so4 ---'	10000	10000
'k18: mnco3P ----'	100	100
'k19: mnco3D ----'	0.80	0.80
'k20: feco3P ----'	450	450
'k21: feco3D ----'	0.25	0.25
'k22: fesP ------'	15	15
'k23: fesD ------'	0.1E-2	0.1E-2
'inhibit o2 -----'	20	20
'inhibit no3 ----'	2	2
'inhibit mn4 ----'	3.84E+04	3.84E+04

'inhibit fe3 ----'	2.40E+05	2.40E+05
'inhibit so4 ----'	1.6E+03	1.6E+03
'1/2 sat o2 -----'	20	20
'1/2 sat no3 ----'	2	2
'1/2 sat mn4 ----'	3.84E+04	3.84E+04
'1/2 sat fe3 ----'	2.40E+05	2.40E+05
'1/2 sat so4 ----'	1.6E+03	1.6E+03
'stoich sx ------'	106	106
'stoich sy ------'	11	11
'stoich sz ------'	1	1
'Boundary G -----'	1050000	1050000
'Boundary O2 ----'	275	275
'Boundary NO3 ---'	10	10
'Boundary MN4 ---'	113761	113761
'Boundary FE3 ---'	111907	111907
'Boundary SO4 ---'	29290	29149
'Boundary H2S ---'	0	0
'Boundary CH4 ---'	0	0
'Boundary NH4 ---'	0	0
'Boundary MN2 ---'	0	0
'Boundary FE2 ---'	0	0
'Boundary TC ----'	2200	2200
'Boundary MNCO3 -'	0	0
'Boundary FECO3 -'	0	0
'Boundary FES ---'	0	0

APPENDIX VI: Parameter Key (Sensitivity Analysis)

Code	Parameter	Description
6	K1/Vo2	Rate constants for primary redox reactions
7	InO2	Inhibition constant for oxygen reduction
8	InNO3	Inhibition constant for nitrate reduction
9	InMN4	Inhibition constant for Mn-oxide reduction
10	InFE3	Inhibition constant for Fe-oxide reduction
11	InSO4	Inhibition constant for sulphate reduction
12	Ko2	Half saturation for oxygen reduction
13	Kno3	Half saturation for nitrate reduction
14	Kmn4	Half saturation for Mn-oxide reduction
15	Kfe3	Half saturation for Fe-oxide reduction
16	Kso4	Half saturation for sulphate reduction
17	k7	Rate constant -- Mnii.O2
18	k8	Rate constant -- Feii.O2
19	k9	Rate constant – Feii.MnO2
20	k10	Rate constant – NH4.O2
21	k11	Rate constant – O2.H2S
22	k12	Rate constant – MnO2:H2S
23	k13	Rate constant -- Fe3:H2S
24	k14	Rate constant – FeS.O2
25	k15	Rate constant -- CH4.O2
26	k16	Rate constant – CH4.SO4
27	k18	Rate constant -- MnCO3 precipitation
28	k19	Rate constant -- MnCO3 dissolution
29	k20	Rate constant -- FeCO3 precipitation
30	k21	Rate constant – FeCO3 dissolution
31	k22	Rate constant -- FeS precipitation
32	k23	Rate constant -- FeS dissolution
33	kspfe	Apparent solubility Constant FeCO3
34	kspfes	Apparent solubility Constant FeS
35	kspmn	Apparent solubility Constant MnCO3
36	NH4ads	Adsorption Coefficient (NH4)
37	Jorg	Boundary Condition G
38	O2BW	Boundary Condition oxygen
39	NO3BW	Boundary Condition nitrate
40	MN4BW	Boundary Condition Mn-oxide
41	FE3BW	Boundary Condition Fe-oxide
42	SO4BW	Boundary Condition Sulphate
43	TCBW	Boundary Condition Total Carbonate
44	Wf	Burial rate (asymptotic)
45	Dbswi	Bioturbation coefficient at the SWI
46	Diswi	Diffusion coefficient at the SWI
47	irrigswi	Irrigation coefficient at the SWI

APPENDIX VII: Qualitative Correlations (Sensitivity Analysis)

Code	Parameter	d1, bc1	d2, bc1	d1, bc2	d2, bc2
6	K1/Vo2	I	I	I	I
7	InO2	I	I	I	IP
8	InNO3	I	I	I	I
9	InMN4	I	I	I	I
10	InFE3	I	I	I	I
11	InSO4	I	I	I	I
12	Ko2	P	I	P	P
13	Kno3	P	P	P	P
14	Kmn4	P	P	P	P
15	Kfe3	P	P	P	P
16	Kso4	P	P	P	P
17	k7	I	P	I	P
18	k8	NS	P	NS	P
19	k9	NS	NS	NS	NS
20	k10	I	NS	I	I
21	k11	I	I	I	I
22	k12	P	P	P	P
23	k13	P	I	P	I
24	k14	I	I	NS	I
25	k15	NS	NS	NS	NS
26	k16	NS	NS	NS	NS
27	k18	NS	NS	NS	NS
28	k19	NS	NS	NS	NS
29	k20	NS	NS	NS	NS
30	k21	NS	NS	NS	NS
31	k22	I	P	I	I
32	k23	NS	NS	NS	NS
33	kspfe	NS	NS	NS	NS
34	kspfes	P	I	P	P
35	kspmn	NS	NS	NS	NS
36	NH4ads	NS	NS	NS	NS
37	Jorg	I	I	I	I
38	O2BW	P	P	P	P
39	NO3BW	P	P	P	P
40	MN4BW	PI	P	I	P
41	FE3BW	PI	P	I	P
42	SO4BW	NS	NS	NS	NS
43	TCBW	NS	NS	NS	NS
44	Wf	P	P	P	P
45	Dbswi	P	P	IP	P
46	Diswi	P	P	P	P
47	irrigswi	P	P	P	P

I; INVERSLY CORRELATED: **P**; POSITIVLY CORRELATED: **NS**; NO SLOPE; **PI/IP**: MIXED CORRELATION (order of letters indicates shape of response curve)

APPENDIX VIII: Model Input Conditions (NWC)

Parameter	NWC1	NWC2
'Temperature ----'	12	12
'Salinity -------'	26	26
'Pressure--------'	1.5	1.5
'pH ------------'	7.5	7.5
'Xbphi ----------'	0.4	0.4
'initial phi ----'	0.74	0.74
'final phi ------'	0.74	0.74
'W @ infinity ---'	0.5	0.5
'Option Db-------'	2	2
'Option Di-------'	2	2
'Option Irrig----'	2	2
'Db SWI ---------'	7.8	9.73
'Di SWI ---------'	0	0
'irrig SWI ------'	3	9.73
'DBzb -----------'	10	10
'DBz0 -----------'	11	11
'Dizb -----------'	9	9
'Diz0 -----------'	11	11
'Dirrigzb -------'	10d0	10d0
'Dirrigz0 -------'	11d0	11d0
'density solid --'	2.4	2.4
'adsorb NH4 -----'	1	1.4
'kspfe ----------'	3200	4000
'kspfes ---------'	6.3d9	6.3d9
'kspmn ----------'	2200	3200
'Vo2 ------------'	0.84	0.26
'Vno3 -----------'	0.84	0.26
'Vmn4 -----------'	0.84	0.26
'Vfe3 -----------'	0.84	0.26
'Vso4 -----------'	0.84	0.26
'Kch4 -----------'	0.84	0.26
'k7: mnii.o2 ----'	2d3	2d3
'k8: feii.o2 ----'	2d3	2d3
'k9: feii.mno2 --'	2d2	2d2
'k10: nh4.o2 ----'	1.5d1	1.5d1
'k11: o2.h2s ----'	6d2	6d2
'k12: mno2:h2s --'	1d-2	1d-2
'k13: fe3:h2s ---'	1d-2	1d-2
'k14: fes.o2 ----'	2.2d1	2.2d1
'k15: ch4.o2 ----'	1d4	1d4
'k16: ch4.so4 ---'	1d4	1d4
'k18: mnco3P ----'	0.5d4	0.24d6
'k19: mnco3D ----'	0.8d0	0.8d0
'k20: feco3P ----'	1.08d6	1.08d6
'k21: feco3D ----'	0.25d0	0.25d0
'k22: fesP ------'	0.36d5	0.36d5
'k23: fesD ------'	0.1d-2	0.1d-2
'inhibit o2 -----'	20d0	20d0
'inhibit no3 ----'	2d0	2d0
'inhibit mn4 ----'	38.4d3	38.4d3

'inhibit fe3 ----'	240d3	240d3
'inhibit so4 ----'	1.6d3	1.6d3
'1/2 sat o2 -----'	20d0	20d0
'1/2 sat no3 ----'	2d0	2d0
'1/2 sat mn4 ----'	38.4d3	38.4d3
'1/2 sat fe3 ----'	240d3	240d3
'1/2 sat so4 ----'	1600d0	1600d0
'stoich sx ------'	n.a	106
'stoich sy ------'	n.a	16
'stoich sz ------'	n.a	1
'Boundary G -----'	195d3	480d3
'Boundary O2 ----'	275	275
'Boundary NO3 ---'	10	10
'Boundary MN4 ---'	10d3	113.76d3
'Boundary FE3 ---'	66d3	111.9d3
'Boundary SO4 ---'	23.1d3	28d3
'Boundary H2S ---'	0	0
'Boundary CH4 ---'	0	0
'Boundary NH4 ---'	0	0
'Boundary MN2 ---'	0	0
'Boundary FE2 ---'	0	0
'Boundary TC ----'	2200	2200
'Boundary MNCO3 -'	0	0
'Boundary FECO3 -'	0	0
'Boundary FES ---'	0	0

APPENDIX IX: Model Input Conditions (AEF analysis)

Parameter	case 1	case 2	case 3	case 4	case 5	case 6	case 7	case 8	case 9	case 10
'Temperature ----'	18	18	18	18	18	18	18	18	18	18
'Salinity -------'	20	20	20	20	20	20	20	20	20	20
'Pressure--------'	1	1	1	1	1	1	1	1	1	1
'pH ----------'	7.5	7.5	7.5	7.5	7.5	7.5	7.5	7.5	7.5	7.5
'Xbphi ----------'	30	30	30	30	30	30	30	30	30	30
'initial phi ----'	0.9	0.9	0.9	0.8	0.7	0.9	0.9	0.9	0.9	0.9
'final phi ------'	0.9	0.9	0.9	0.8	0.7	0.9	0.9	0.9	0.9	0.9
'W @ infinity ---'	n.a	n.a	n.a	n.a	n.a	n.a	n.a	n.a	n.a	n.a
'Option Db-------'	2	2	2	2	2	2	2	2	2	2
'Option Di-------'	2	2	2	2	2	2	2	2	2	2
'Option Irrig----'	2	2	2	2	2	2	2	2	2	2
'Db SWI ---------'	n.a	n.a	n.a	n.a	n.a	n.a	n.a	n.a	n.a	n.a
'Di SWI ---------'	n.a	n.a	n.a	n.a	n.a	n.a	n.a	n.a	n.a	n.a
'irrig SWI ------'	n.a	n.a	n.a	n.a	n.a	n.a	n.a	n.a	n.a	n.a
'DBzb ----------'	30	30	30	30	30	30	30	9	9	9
'DBz0 ----------'	30	30	30	30	30	30	30	11	11	11
'Dizb ----------'	30	30	30	30	30	30	30	9	9	9
'Diz0 ----------'	30	30	30	30	30	30	30	11	11	11
'Dirrigzb ----------'	30	30	30	30	30	30	30	9	9	9
'Dirrigz0 ----------'	30	30	30	30	30	30	30	11	11	11
'density solid --'	2.4	2.4	2.4	2.4	2.4	2.4	2.4	2.4	2.4	2.4
'adsorb NH4 -----'	1.4	1.4	1.4	1.4	1.4	1.4	1.4	1.4	1.4	1.4
'kspfe ----------'	4000	4000	4000	4000	4000	4000	4000	4000	4000	4000
'kspfes ---------'	6.3E+09	6.3E+09	6.3E+09	6.3E+09	6.3E+09	6.3E+09	6.3E+09	6.3E+09	6.3E+09	6.3E+09
'kspmn ----------'	3200	3200	3200	3200	3200	3200	3200	3200	3200	3200
'Vo2 ------------'	n.a	n.a	n.a	n.a	n.a	n.a	n.a	n.a	n.a	n.a
'Vno3 -----------'	n.a	n.a	n.a	n.a	n.a	n.a	n.a	n.a	n.a	n.a
'Vmn4 -----------'	n.a	n.a	n.a	n.a	n.a	n.a	n.a	n.a	n.a	n.a
'Vfe3 -----------'	n.a	n.a	n.a	n.a	n.a	n.a	n.a	n.a	n.a	n.a
'Vso4 -----------'	n.a	n.a	n.a	n.a	n.a	n.a	n.a	n.a	n.a	n.a
'Kch4 -----------'	n.a	n.a	n.a	n.a	n.a	n.a	n.a	n.a	n.a	n.a
'k7: mnii.o2 ----'	2.0E+03	2.0E+03	2.0E+03	2.0E+03	2.0E+03	2.0E+03	2.0E+03	2.0E+03	2.0E+03	2.0E+03
'k8: feii.o2 ----'	2.0E+03	2.0E+03	2.0E+03	2.0E+03	2.0E+03	2.0E+03	2.0E+03	2.0E+03	2.0E+03	2.0E+03
'k9: feii.mno2 --'	2.0E+02	2.0E+02	2.0E+02	2.0E+02	2.0E+02	2.0E+02	2.0E+02	2.0E+02	2.0E+02	2.0E+02
'k10: nh4.o2 ----'	1.5E+01	1.5E+01	1.5E+01	1.5E+01	1.5E+01	1.5E+01	1.5E+01	1.5E+01	1.5E+01	1.5E+01
'k11: o2.h2s ----'	6.0E+02	6.0E+02	6.0E+02	6.0E+02	6.0E+02	6.0E+02	6.0E+02	6.0E+02	6.0E+02	6.0E+02
'k12: mno2:h2s --'	1.00E-02	1.00E-02	1.00E-02	1.00E-02	1.00E-02	1.00E-02	1.00E-02	1.00E-02	1.00E-02	1.00E-02
'k13: fe3:h2s ---'	1.00E-02	1.00E-02	1.00E-02	1.00E-02	1.00E-02	1.00E-02	1.00E-02	1.00E-02	1.00E-02	1.00E-02
'k14: fes.o2 ----'	2.2E+01	2.2E+01	2.2E+01	2.2E+01	2.2E+01	2.2E+01	2.2E+01	2.2E+01	2.2E+01	2.2E+01
'k15: ch4.o2 ----'	1.0E+04	1.0E+04	1.0E+04	1.0E+04	1.0E+04	1.0E+04	1.0E+04	1.0E+04	1.0E+04	1.0E+04
'k16: ch4.so4 ---'	1.0E+04	1.0E+04	1.0E+04	1.0E+04	1.0E+04	1.0E+04	1.0E+04	1.0E+04	1.0E+04	1.0E+04
'k18: mnco3P ----'	1.0E+02	1.0E+02	1.0E+02	1.0E+02	1.0E+02	0	1.0E+02	1.0E+02	1.0E+02	0
'k19: mnco3D ----'	8.00E-01	8.00E-01	8.00E-01	8.00E-01	8.00E-01	0	8.00E-01	8.00E-01	8.00E-01	0
'k20: feco3P ----'	4.5E+02	4.5E+02	4.5E+02	4.5E+02	4.5E+02	0	4.5E+02	4.5E+02	4.5E+02	0
'k21: feco3D ----'	2.50E-01	2.50E-01	2.50E-01	2.50E-01	2.50E-01	0	2.50E-01	2.50E-01	2.50E-01	0
'k22: fesP ------'	1.5E+01	1.5E+01	1.5E+01	1.5E+01	1.5E+01	0	1.5E+01	1.5E+01	1.5E+01	0
'k23: fesD ------'	1.00E-03	1.00E-03	1.00E-03	1.00E-03	1.00E-03	0	1.00E-03	1.00E-03	1.00E-03	0
'inhibit o2 -----'	2.0E+01	2.0E+01	2.0E+01	2.0E+01	2.0E+01	2.0E+01	2.0E+01	2.0E+01	2.0E+01	2.0E+01
'inhibit no3 ----'	2.0E+00	2.0E+00	2.0E+00	2.0E+00	2.0E+00	2.0E+00	2.0E+00	2.0E+00	2.0E+00	2.0E+00
'inhibit mn4 ----'	3.84E+4	3.84E+4	3.84E+4	3.84E+4	3.84E+4	3.84E+4	3.84E+4	3.84E+4	3.84E+4	3.84E+4

'inhibit fe3 ----'	2.4E+05	2.4E+05	2.4E+05	2.4E+05	2.4E+05	2.4E+05	2.4E+05	2.4E+05	2.4E+05	2.4E+05
'inhibit so4 ----'	1.6E+03	1.6E+03	1.6E+03	1.6E+03	1.6E+03	1.6E+03	1.6E+03	1.6E+03	1.6E+03	1.6E+03
'1/2 sat o2 -----'	2.0E+01	2.0E+01	2.0E+01	2.0E+01	2.0E+01	2.0E+01	2.0E+01	1.0E+01	2.0E+01	2.0E+01
'1/2 sat no3 ----'	2.0E+00	2.0E+00	2.0E+00	2.0E+00	2.0E+00	2.0E+00	2.0E+00	1.0E+00	2.0E+00	2.0E+00
'1/2 sat mn4 ----'	3.84E+4	3.84E+4	3.84E+4	3.84E+4	3.84E+4	3.84E+4	3.84E+4	1.94E+4	3.84E+4	3.84E+4
'1/2 sat fe3 ----'	2.40E+5	2.40E+5	2.40E+5	2.40E+5	2.40E+5	2.40E+5	2.40E+5	1.20E+6	2.40E+5	2.40E+5
'1/2 sat so4 ----'	1.6E+03	1.6E+03	1.6E+03	1.6E+03	1.6E+03	1.6E+03	1.6E+03	1.0E+03	1.6E+03	1.6E+03
'stoich sx ------'	106	106	106	106	106	106	106	106	106	106
'stoich sy ------'	11	11	11	11	11	11	11	11	11	11
'stoich sz ------'	1	1	1	1	1	1	1	1	1	1
'Boundary G -----'	n.a	n.a	n.a	n.a	n.a	n.a	n.a	n.a	n.a	n.a
'Boundary O2 ----'	275	275	275	275	275	275	275	275	275	275
'Boundary NO3 --'	10	10	10	10	10	10	10	10	10	10
'Boundary MN4 --'	1.14E+5	1.14E+5	1.14E+5	1.14E+5	1.14E+5	1.14E+5	1.14E+5	1.14E+5	1.14E+5	1.14E+5
'Boundary FE3 ---'	1.12E+5	1.12E+5	1.12E+5	1.12E+5	1.12E+5	1.12E+5	1.12E+5	1.12E+5	1.12E+5	1.12E+5
'Boundary SO4 ---'	2.80E+4	2.80E+4	2.80E+4	2.80E+4	2.80E+4	2.80E+4	2.80E+4	2.80E+4	2.80E+4	2.80E+4
'Boundary H2S ---'	0	0	0	0	0	0	0	0	0	0
'Boundary CH4 --'	0	0	0	0	0	0	0	0	0	0
'Boundary NH4 --'	0	0	0	0	0	0	0	0	0	0
'Boundary MN2 --'	0	0	0	0	0	0	0	0	0	0
'Boundary FE2 ---'	0	0	0	0	0	0	0	0	0	0
'Boundary TC ----'	2200	2200	2200	2200	2200	2200	2200	2200	2200	2200
'Bndry MNCO3 -'	0	0	0	0	0	0	0	0	0	0
'Bndry FECO3 -'	0	0	0	0	0	0	0	0	0	0
'Bndry FES ---'	0	0	0	0	0	0	0	0	0	0

Case 2 used a 6-D representation of degradation with Vmn4, Vfe3 calculated from Vso4

Case 3 used a 6-D representation of degradation with Vmn4, Vfe3 calculated from Vo2

Case 7 used a modified function to describe Db

REFERENCES

Abbott, M.B., & Basco, D.R., (1989) "Computational Fluid Dynamics: An Introduction For Engineers", Longman

Aller, R., (1980a) "Diagenetic Processes Near the Sediment Water Interface of Long Island Sound I. Decomposition and Nutrient Element Geochemistry (S.N.P)", in *Estuarine Physics and Chemistry: Studies in Long Island Sound*, B. Saltzman (Ed.), Academic Press, New York, pp 238-350

Aller, R.C., (1980b) "Diagenetic Processes Near the Sediment Water Interface of Long Island Sound II: Fe & Mn", in *Estuarine Physics and Chemistry: Studies in Long Island Sound*, B. Saltzman (Ed.), Academic Press, New York, pp 351-416

Aller, R.C., (1980c) "Quantifying Solute Distributions in the Bioturbated Zones of Marine Sediments by Defining an Average Microenvironment", Geochimica et Cosmochimica Acta, 44, 1955-1966

Aller, R.C., (1982) "The Effects of Macrobenthos on Chemical Properties of Marine Sediments and Overlying Water", In *Animal-Sediment Relationships*, P.L.McCall & M.J.S.Tevesz (Eds.), New York, Plenum, 53-102

Aller, R.C., (1994a) "Bioturbation and Mineralisation of Sedimentary Organic Matter: Effects of Redox Oscillations", Chemical Geology, 114, 331-345

Aller, R.C., (1994b) "The Sedimentary Mn Cycle in Long Island Sound: Its Role an Intermediate Oxidant and the Influence of Bioturbation, $O_2$and C_{org} Flux on Diagenetic Reaction Balances", Journal of Marine Research, 52, 2, 259-295

Aller, R.C., & Cochran, J.K., (1976) "$^{234}Th/^{238}U$ Disequilibrium in Near-Shore Sediment: Particle Reworking and Diagenetic Time Scales", Earth Planetary Science Letters, 29, 37-50

Aller, R.C., & Yingst, J.Y., (1980) "Relationships Between Microbial Distributions and Anaerobic Decomposition of Organic Matter in Surface Sediments of Long Island Sound, USA", Marine Biology, 56, 29-42

Aller, R.C., Benninger, L.K., & Cochran, J.K., (1980) "Tracking Particle Associated Processes in Nearshore Sediment by use of the $^{234}Th/^{238}U$ Disequilibrium", Earth Planetary Science Letters, 47, 161-175

Aller, R.C., & Yingst, J.Y., (1985) "Effects of the Marine Deposit *Feeders Heteromastus filiformis* (Polychaeta), *Macoma balthica* (Bivalvia), and *Tellina texana* (Bivalvia) on Averaged Sedimentary Solute Transport, Reaction Rates, and Microbial Distributions", Journal of Marine Research, 43, 615-645

Aller, R.C., & Aller, J.Y., (1998) "The Effect of Biogenic Irrigation Intensity and Solute Exchange on Diagenetic reaction Rates in Marine Sediments", Journal of Marine research, 56, 905-936

Archer, D., & Devol, A., (1992) "Benthic Oxygen Fluxes On The Washington Shelf And Slope – A Comparison Of In situ Microelectrode And Chamber Flux Measurements", Limnology and Oceanography, 37(3), 614-629

Balzer, W., (1982) "On the Distribution of Iron and Manganese at The Sediment Water Interface - Thermodynamic Versus Kinetic Control", Geochimica et Cosmochimica Acta, 46 (7), 1153-1161

Baretta, J.W., Ebenhoh, W., & Ruardij, P., (1995) "The European Regional Seas Ecosystem Model, A Complex Marine Ecosystem Model", Netherlands Journal of Sea Research, 33(3/4), 233-246

Bascom, W., (1982) "The Effects of Waste Disposal on the Coastal Waters of Southern California", Environmental Science and Technology, 16(4), 227A-236A

Ben-Yaakov, S., (1973) "pH Buffering of Pore Water of Recent Anoxic Sediments", Limnology & Oceanography, 18 (1), 86-94

Berner, R.A., (1963) "Electrode Studies of Hydrogen Sulfide in Marine Sediments", Geochimica et Cosmochimica Acta, 27, 563-575

Berner, R.A., (1964) "An Idealised Model of Sulfate Distribution in Recent Sediments", Geochimica et Cosmochimica Acta, 28, 1497-1503

Berner, R.A., (1971) "Principles of Chemical Sedimentology", McGraw-Hill, New York

Berner (1979) "A Rate Model For Organic Matter Decomposition During Bacterial Sulfate Reduction in Marine Sediments", BioGeochimie de la Matiere Organique A L'Interface Eau Sediment Marin, 293, 35-44

Berner, R.A., (1980) "Early Diagenesis: A Theoretical Approach", Princeton University Press, Princeton

Berner, R.A., (1981) "A New Geochemical Classification of Sedimentary Environments", Journal of Sedimentary Petrology, 51 (2), 359-365

Berner, R.A., (1984) "Sedimentary Pyrite Formation - An Update", Geochimica et Cosmochimica Acta, 48(4), 605-615

Billen G., (1978) "The Dependence of the Various Kinds of Microbial Metabolisms on the Redox State of the Medium", in Biogeochemistry of Estuarine Sediments, Proceedings of the UNESCO/SCOR workshop, Melreux (Belgium) 1976, 254-261

Billen, G., (1982) "An Idealised Model of Nitrogen Recycling in Marine Sediments", American Journal of Science, 282, 512-541

Billen, G., & Verbeustel, S., (1979) "Distribution of Microbial Metabolisms in Natural Environments Displaying Gradients of Oxidation-Reduction Conditions", BioGeochimie de la Matiere Organique A L'Interface Eau Sediment Marin, 293, 291-300

Blackford, J. C., (1997) "An Analysis of Benthic Biological Dynamics in a North Sea Ecosystem Model", Journal of Sea Research, 38, 213-230

Boon, A.R., & Duineveld, G.C.A., (1998) "Chlorophyll A as a Marker for Bioturbation and Carbon Flux in Southern and Central North Sea Sediments", Marine Ecology-Progress Series, 162, 33-43

Boudreau, B.P., (1984) "On the Equivalence of Non-local and Radial Diffusion Models for Porewater Irrigation", Journal of Marine Research, 42, 731-735

Boudreau, B.P., (1986) "Mathematics of Tracer Mixing in Sediments I: Spatially-Dependent, Diffusive Mixing", American Journal of Science, 286, 161-198

Boudreau, B.P., (1992) " A Kinetic Model for Microbic Organic Matter Decomposition in Marine Sediments", FEMS Microbiology Ecology, 102, 1-14

Boudreau, B.P., (1994) "Is Burial Velocity a Master Parameter for Bioturbation", Geochimica et Cosmochimica Acta, 58(4), 1243-1249

Boudreau, B.P., (1996) "A Method of Lines Code for Carbon and Nutrient Diagenesis in Aquatic Sediments", Computers and Geosciences, 22(5), 479-496

Boudreau, B.P., (1997) "Diagenetic Models and Their Implementation: Modelling Transport and Reactions in Aquatic Sediments", Springer-Verlag, New York

Boudreau, B.P., & Westrich, J.T., (1984) "The Dependence of Bacterial Sulphate Reduction on Sulphate Concentrations in Marine Sediments", Geochimica et Cosmochimica Acta, 48, 2503-2516

Boudreau, B.P., & Canfield, D.E., (1988) "A Provisional Diagenetic Model for Ph in Anoxic Porewaters -Application to the Foam Site", Journal Of Marine Research, 46(2), 429-455

Boudreau, B.P., & Ruddick, B.R., (1991) "On a Reactive Continuum Representation of Organic Matter Diagenesis", American Journal of Science, 291, 507-538

Boudreau, B.P., & Marinelli, R.L., (1994) "A Modelling Study of Discontinuous Biological Irrigation", Journal of Marine Research, 52, 947-968

Brown, J.R., Gowen, R.J., & McLusky, D.S., (1987) "The Effect of Salmon Farming on the Benthos of a Scottish Sea Loch", Journal of Experimental Marine Biology and Ecology, 109, 39-51

Brown, P. N., Byrne, G. D., & Hindmarsh, A. C., (1989) "VODE: A Variable Coefficient ODE Solver," Siam Journal On Scientific and Statistical Computing, 10, 1038-1051

Bruntland Commission (1987) "Our Common Future", World Commission on Environment & Development, OUP

Burdige, D.J., (1993)" The Biogeochemistry of Manganese and Iron Reduction in Marine-Sediments", Earth-Science Reviews, 35 (3), 249-284

Canfield, D.E., (1993) "Organic Matter Oxidation in Marine Sediments", in *Interactions of C.N.P and S Biogeochemical Cycles and Global Change*, Wollast, R., Mackenzie, F.T., & Chou, L., (Eds.), NATO ASI Series, V.14, 333-363

Canfield, D.E., Jørgensen, B.B., Fossing, H., Glud, R., Gundersen, J.M., Ramsing, N.B., Thamdrup, B., Hansen, J.W., Nielson, L.P., & Hall, P.O., (1993a) "Pathways of Organic Carbon Oxidation in three Continental Marine Sediments", Marine Geology, 113, 27-40

Canfield, D.E., Thamdrup, B., & Hansen, J.W., (1993b) "The Anaerobic Degradation of Organic Matter in Danish Coastal Sediments: Iron Reduction, Manganese Reduction and Sulfate Reduction", Geochimica et Cosmochimica Acta, 54, 1247-1254

Cardwell, H., & Ellis, H, (1996) "Model uncertainty and model aggregation in environmental management", Applied Mathematical Modelling, 20 (2), 121-134

CASSS, (1997) http://freespace.virgin.net/malcolm.hooper/index.html

Chapra, S.C., (1997) "Surface Water Quality Modelling", McGraw-Hill, Singapore

Christensen, E.R., (1982) "A Model for Radionuclides in Sediments Influenced by Mixing and Compaction", Journal of Geophysical Research-Oceans and Atmospheres, 87, No.NC1, 566-572

Clark, R.B., (1992) "Marine Pollution", OUP, New York

Cooper, V.A., & Lack, T.J., (1987) "Environmental Effects of Discharges", The Public Health Engineer, 14 (5), 22-25

Coull, B.C., & Chandler, G.T., (1992) "Pollution and Meiofauna - Field, Laboratory, and Mesocosm Studies", Oceanography and Marine Biology, 30, 191-271

Crank, J., (1975) "Mathematics of diffusion", 2nd Ed., Clarendon, Oxford

Cromey, C.J., Black, K.D., Edwards, A., & Jack, I.A., (1998) "Modelling the Deposition and Biological Effects of Organic Carbon from Marine Sewage Discharges", Estuarine, Coastal and Shelf Sciences, 47, 295-308

CRPB, (1990) "An Assessment of the Impact of Fish Farming Activities to the Waters and Sediments of Fishnish Bay, Sound of Mull", Clyde River Purification Board Report, 22-06-90, unpublished report

CRPB, (1991a) "An Assessment of the Impact of Fish Farming Activities to the Waters and Sediments of Port Lunna, Loch Sween", Clyde River Purification Board Report, 15/16-10-91, unpublished report

CRPB, (1991b) "An Assessment of the Impact of Fish Farming Activities to the Waters and Sediments of Cairndow, Loch Fyne", Clyde River Purification Board Report, 30/31-10-91, unpublished report

Dauwe, B., Herman, P.M.J., & Heip, C.H.R. (1998) "Community Structure and Bioturbation Potential of Macrofauna at Four North Sea Stations With Contrasting Food Supply", Marine Ecology-Progress Series, 173, 67-83

Davies, G.L., & Wade, K.R., (1985) "Studies of the Intertidal Benthic Fauna in the Usk Estuary in Relation to BSC ORB Works No. 1 Outfall", Welsh Water, SE/14/85, unpublished report

Davis, W.R., Draxler, A.F.J., Paul, J.F., & Vitaliano, J.J., (1998) "Benthic Biological Processes and Eh as a Basis for a Benthic Index", Environmental Monitoring and Assessment, 51, 1-2, 259-268

Dempsey, P., & Lack, T.J., (1989) "Environmental Impact Assessment of Coastal Schemes", in *Long Sea Outfalls*, Institution of Civil Engineers, Thomas Telford, London, 41-50

Dhaker, S.P., & Burdige, D.J., (1996) "A Coupled, Non-Linear, Steady State Model for Early Diagenetic Processes in Pelagic Sediments", American Journal of Science, 296 (3), 296-330

Diaz, R.J., & Rosenberg, R., (1995) "Marine Benthic Hypoxia: a Review of its Ecological Effects and the Behavioural Responses of the Benthic Macrofauna", Oceanography & Marine Biology: An Annual Review, 33, 245-303

DiPasquale, M.C., & Capone, D.G., (1998), "Benthic Sulfate Reduction along the Chesapeake Bay Central Channel. I. Spatial Trends and Controls", Marine Ecology-Progress Series, 168, 213-228

Di Toro, D.T., Paquin, P.R., Subburamu, K., Gruber, D.A. (1990) "Sediment Oxygen Demand Model: Methane and Ammonia Oxidation", Journal of Environmental engineering, 116(5), 945-986

Duplissa, D.E., & Hargrave, B.T., (1996) "Response of Meiobenthic Size-Structure, Biomass and Respiration to Sediment Organic Enrichment", Hydrobiologia, 339, 161-170

Emerson, S., Jahnke, R., & Heggie, D., (1984) "Sediment-Water Exchange In Shallow-Water Estuarine Sediments", Journal Of Marine Research, 42 (3), 709-730

Ernest, A.N., Bonner, J.S., & Autenreith, R.L., (1995) "Determination of Particle Collision Efficiencies for Flocculent Transport Models", Journal of Environmental Engineering, 121(4), 320-329

Fairweather, P.G., (1993) "Links Between Ecology and Ecophilosophy, Ethics and the Requirements of Environmental Management", Australian Journal of Ecology, 18, 3-19

Farley, K.J., (1990) "Predicting Organic Accumulation in Sediments Near Marine Outfalls", Journal of Environmental Engineering, 116 (1), 144-165

Fenchel, T.M., & Riedl, R.J. (1970) "The Sulfide System: a New Biotic Community Underneath the Oxidised Layer of Marine Sand Bottoms", Marine Biology, 7, 255-268

Fenchel, T.M., & Finlay, B.L., (1995) "Ecology and Evolution in Anoxic Worlds", OUP, New York

Ferraro, S.P., Swartz, R.C., Cole, F.A.& Schults, D.W., (1991) "Temporal Changes in The Benthos Along a Pollution Gradient - Discriminating The Effects of Natural Phenomena From Sewage Industrial Waste-Water Effects", Estuarine Coastal and Shelf Science, 33 (4), 383-407

Fiadeiro, M.E., & Veronis, G., (1977) "On Weighted-mean Schemes for the Finite Difference Approximation to the Advection-Diffusion Equation", Tellus, 29, 512-522

Findlay, R.H., & Watling, L., (1994) "Toward a Process Level Model to Predict the Effects of Salmon Net-Pen Aquaculture on the Benthos", in *Modelling Benthic Impacts of Organic Enrichment from Marine Aquaculture*, B.T. Hargrave (Ed.), Canadian Technical Report of Fisheries and Aquatic Sciences, 1949

Findlay, R.H., & Watling, L., (1997a) "Prediction of Benthic Impact for Salmon Net-Pens Based on the Balance of Benthic Oxygen Supply and Demand", Marine Ecology-Progress Series, 155, 147-157

Findlay, R.H., & Watling, L., (1997b) "Seasonal Variation in a Sedimentary Microbial Community Structure as a Backdrop for the Detection of Anthropogenic Stress", in The Application of Molecular Markers in Environmental Geochemistry, ACS Symposium, 671, Orlanod Florida, August 1996, 49-64

Forster, S. (1996) "Spatial and Temporal Distribution of Oxidation Events Occurring Below the Sediment-Water Interface", Marine Ecology, 17(1-3), 309-319

Forster, S., & Graf, G., (1995) "Impact of Irrigation on Oxygen Flux Into The Sediment - Intermittent Pumping by *Callianassa-Subterranea* and Piston-Pumping by *Lanice-Conchilega*", Marine Biology, 123 (2), 335-346

Forster, S., Graf, G., Kitlar, J., & Powilleit, M., (1995) "Effects of Bioturbation in Oxic and Hypoxic Conditions - a Microcosm Experiment With a North-Sea Sediment Community", Marine Ecology-Progress Series, 116 (1-3), 153-161

FRPB, (1984) "Inverkeithing Bay A Paper-Mill Effluent Discharge: An Environmental Impact of its Effects", Forth River Purification Board, Report ES3/84

FRPB, (1987) "Largo Bay: An Assessment of the Benthic Sediments and Fauna, 1985", Forth River Purification Board, Report ES4/87, unpublished report

FRPB, (1994a) "Seafield Long Sea Outfall Survey of the Benthos and Sediments, 1993", Forth River Purification Board, Report TW 3/94, unpublished report

FRPB, (1994b) "A Comprehensive Study of the Sewage Outfall for the Purposes of Article 6 of DIR 91/271 EEC, The Urban Waste Water Treatment Directive", Forth River Purification Board, Report TW 16/94, unpublished report

Froelich, P.N., Klinkhammer, G.P., Bender, M.L., Luedtke, N.A., Heath, G.R., Cullen, D., Dauplin, P., Hammond, D., & Maynard, V., (1979) "Early Oxidation of Organic Matter in Pelagic Sediments of the Eastern Equatorial Atlantic: Suboxic Diagenesis", Geochimica et Cosmochimica Acta, 43, 1075-1090

Gee, J.M., Warwick R.M., Schaanning, M., Berge, J.A., & Ambrose, W.G., (1985) "The Effects of Organic Enrichment on Meiofaunal Abundance and Community Structure in Sublittoral Soft Sediments", Journal of Experimental Marine Biology and Ecology, 91(3), 247-262

Gerlach, S.A., (1981) "Marine Pollution, Diagnosis and Therapy", Springer-Verlag, Berlin

GESAMP (1990) "The State of the Marine Environment", UNEP Regional Seas Report & Studies, 115, UNEP

Gowen, R.J., & Bradbury, N.B., (1987) " The Ecological Impact of Salmonid Farming in Coastal Waters: A Review", Oceanography and Marine Biology Annual Review, 25, 563-575

Grace, R.A., (1978) "Marine Outfall Systems: Planning, Design and Construction", Prentice Hall Inc., Toronto, 54

Gray, J.S., (1979) "Pollution-induced Changes in Populations", Philosophical Transactions of the Royal Society of London B, 286, 545-561

Gray, J.S., (1981) "The Ecology of Marine Sediments", CUP, Cambridge, 152

Grizzle, R.E., & Penniman, C.A., (1991) "Effects of Organic Enrichment on Estuarine Macrofaunal Benthos: a Comparison of Sediment Profile Imaging and Traditional Methods", Marine Ecology Progress Series, 74, 249-262

Grundl, T., (1995) "Determination of Redox Status in Sediments", in *Metal Contaminated Aquatic Sediments* H.E. Allen (Ed.), Chap. 6, Ann Arbor Press, Michigan, 149-167

Haefner, J.W., (1996) "Modelling Biological Systems: Principles and Applications", Chapman & Hall, New York

Hamby, D.M., (1994) "A Review Of Techniques For Parameter Sensitivity Analysis of Environmental-Models", Environmental Monitoring and Assessment, 32 (2), 135-154

Hamby, D.M., (1995) "A Comparison of Sensitivity Analysis Techniques", Health Physics, 68 (2), 195-204

Hansen, S.R., & Blackburn, T.H., (1991) "Aerobic and Anaerobic Mineralization of Organic Material in Marine Sediment Microcosms", Marine Ecology Progress Series, 75, 283-291

Hargrave, B.T., Duplisea, D.E., Pfeiffer, E., & Wildish, D.J., (1993) "Seasonal-Changes in Benthic Fluxes of Dissolved-Oxygen and Ammonium Associated With Marine Cultured Atlantic Salmon", Marine Ecology-Progress Series, 96 (3), 249-257

Harvey, S.M., & Phillips, C.J., (1995) "Organic Waste Disposal in the Marine Environment", MAFF project AE 0511, Final Report, Dunstaffange Marine Laboratory

Heip, C. (1995) "Eutrophication and Zoobenthos Dynamics", Ophelia, 1995, 41, 113-136

Heip, C., Warwick, R.M., Carr, M.R., Herman, P.M.J., Hays, R., Smol, N., & Van Holsbeke, K., (1988) "Analysis of Community Attributes of the Benthic Meiofauna of Frierfjord/Langesundfjord", Marine Ecology Progress Series, 46, 171-180

Heip, C., & Craeymeersch, J.A., (1995) "Benthic Community Structures in the North-Sea", Helgolander Meeresuntersuchungen, 49 (1-4), 313-328

Hendricks, T.J., (1992) "Sediment Model Verification" in *Southern California Coastal Water Research Project, Annual Report 1990-1991 and 1991-1992*, J.N. Cross (Ed.), SCCWRP, California, USA, 61-69

Henrichs, S.M., (1992) "Early Diagenesis of Organic Matter in Marine Sediments: Progress and Perplexity", Marine Chemistry, 39, 119-149

Henrichs, S.M., & Reeburgh, W.S., (1987) "Anaerobic Mineralisation of Marine Sediment Organic Matter: Rates and the Role of Anaerobic Processes in the Oceanic Carbon Economy", Geomicrobiology Journal, 5(3/4) pp 191-237

Hevia, M., Rosenthal, H., & Gowen, R.J., (1996) "Modelling Benthic Deposition Under Fish Cages", Journal of Applied Ichthyology, 12, 71-74

Hostettler, J.D., (1984) "Electrode Electrons, Aqueous Electrons, and Redox Potentials in Natural Waters", American Journal of Science, 284, 734-759

Houston-Kempton, J., Lindburg, R.D., Runnels, D.D., (1990) "Numerical Modelling of Platinum Eh Measurements using Heterogeneous Electron Transfer Kinetics", In *Chemical Modelling of Aqueous Systems II*, D.C.Melchior, R.L.Bassett (Eds.), ACS Symposium Series 416, Chap. 29, American Chemical Society, Washington

Hughes, J.M.R., & Goodall, B., (1992) "Marine Pollution", in *Environmental Issues in the 1990's*, A.M. Mannion & S.R.Bowlby (Eds.), John Wiley & Sons, Chichester, 97-114

IUCN (1991) "Oceans", D.Alder (Ed.), Mitchel Beazley Publishers, London

Jørgensen, B.B., (1977a) "Bacterial Sulfate reduction Within Reduced Microniches of Oxidised Marine Sediments", Marine Biology, 41, 19-28

Jørgensen, B.B., (1977b) "The Sulfur Cycle of a Coastal Marine Sediment (Limfjorden, Denmark)", Limnology and Oceanography, 22(5), 814-832

Jørgensen, B.B., (1979) "A Comparison of Methods for the Quantification of Bacterial Sulfate Reduction in Coastal Marine Sediments. II. Calculation from Mathematical Models", Geomicrobiology Journal, 1, 29-47

Jørgensen, B.B., (1980) "Seasonal Oxygen Depletion in the Bottom Waters of a Danish Fjord and its Effects on the Benthic Community", OIKOS, 34, 68-76

Jørgensen, B.B., (1983) "Processes at the Sediment Water Interface", in *The Major Biogeochemical Cycles and Their Interactions*, Bolin, B., & Cook, R.B. (Eds.), SCOPE 21, John Wiley & Sons, New York, 477-515

Jørgensen, B.B., & Revsbech, N.P., (1985) "Diffusive Boundary Layers and the Oxygen Uptake of Sediments and Detritus", Limnology and Oceanography, 30(1), 111-122

Jumars, P.A., & Wheatcroft, R.A., (1989) "Responses of Benthos to Changing Food Quality and Quantity, With a Focus on Deposit Feeding and Bioturbation", in *Productivity of the Oceans Present and Past*, W.H.Berger *et al.* (Eds.), 235-253

Keller, M., (1985) " Quantitative Distribution of The Meiofauna in the Vicinity of Marseilles Sewage Outfall", Marine Biology, 89(3), 293-302

Kelly, J.R., & Nixon, S.W., (1984) "Experimental Studies of The Effect of Organic Deposition on the Metabolism of a Coastal Marine Bottom Community", Marine Ecology-Progress Series, 17(2), 157-169

Kerr, S., & Side, J., (1994) "An Assessment of the Applicability of Cost-Benefit Analysing in Determining BATNEEC", in *The Determination of BATNEEC*, IOE report 93/066, Volume 1

Kristensen, E., & Blackburn, T.H., (1987) "The Fate of Organic Carbon in Experimental Marine Sediment Systems: Influences of Bioturbation and Anoxia", Journal of Marine Research, 45, 231-257

Lindberg, R. D., & Runnels, D.D., (1984) "Ground Water Redox Reactions: An Analysis of Equilibrium State Applied to Eh Measurements and Geochemical Modelling", Science, 225, 925-927

Litchner, P.C., (1996) "Continuum Formulation of Multi-Component-Multiphase Reactive Transport", in *Reactive Transport in Porous Media*, P.C. Lichtner, C.I. Steefel & E.H. Oelkers (Eds.), Reviews in Minerology, 34, 1-81

Mackin, J.E., & Swider, K.T., (1989) "Organic Matter Decomposition Pathways and Oxygen Consumption in Coastal Marine Sediments", Journal of Marine Research, 47, 681-716

MAFF (1993) "Analysis and Interpretation of Benthic Community Data at Sewage-Sludge Disposal Sites", Aquatic Environment Monitoring report, No. 37, Directorate of Fisheries Research, Lowestoft

Makay, D.W., & Haig, A.J.N., (1989) "Long Sea Outfalls - Environmental Considerations", in *Long Sea Outfalls*, Institution of Civil Engineers, Thomas Telford, London, 17-26

Marinelli, R.L., & Boudreau, B.P., (1996) "An Experimental and Modelling Study of Ph And Related Solutes in an Irrigated Anoxic Coastal Sediment", Journal of Marine Research, 54 (5), 939-966

Martin, W.R., & Banta, G.T., (1992) "The Measurement of Sediment Irrigation Rate: a Comparison of the Br Tracer and 222 Rn/226 Ra Disequilibrium Technique", Journal of Marine Research, 50, 125-154

Matisoff, G., (1982) "Mathematical Models of Bioturbation", In *Animal-Sediment Relationships*, P.L.McCall & M.J.S.Tevesz (Eds.), New York, Plenum, 289-330

Matisoff, G., (1995) "Effects of Bioturbation on Solute and Particle Transport in Sediments", in *Metal Speciation and Contamination of Aquatic Sediments*, Allen, H.E. (Ed.), Ann Arbor Press, 201-272

Maughan, J.T., & Oviatt, C.A., (1993) "Sediment and Benthic Response to Waste-Water Solids in a Marine Mesocosm", Water Environment Research, 65(7), 879-889

Mayer, L.M., (1989) "The Nature and Determination of Non-Living Sedimentary Organic Matter as a Food Source for Deposit Feeders", in *Lecture Notes in Coastal and Estuarine Studies 31:Ecology of Marine Deposit Feeders*, G.Lopez, G.Taghon, J.Levington (Eds.), Springer Verlag, New York, 98-113

McEldowney, J.F., & McEldowney, S. (1996) "Environment & the Law: an Introduction for Environmental Scientists and Lawyers", Longman, Harlow, Essex

Meadows, P.S., & Campbell, J.I., (1993) "An Introduction to Marine Science", Second Edition, Balckie Academic & Professional, Glasgow

Mearns, A.J., & Word, J.Q., (1982) "Forecasting Effects of Sewage Solids on Marine Benthic Communities", in *Ecological Stress and the New York Bight*, G.F. Mayer (Ed.), Estuarine Research Foundation, Columbia, South Carolina, USA, 495-512

Metcalf & Eddy inc., (1991) "Wastewater Engineering: Treatment, Disposal, and Reuse", McGraw-HIll, Singapore

Middelburg, J.J., (1989) "A Simple Rate Model for Organic Matter Decomposition in Marine Sediments", Geochimica et Cosmochimica Acta, 53, 1577-1581

Miller, M.L., & Kirk, J., (1992) "Marine Environmental Ethics", Ocean and Coastal Management, 17 (3-4), 237-251

Morel, F.M.M., & Hering, J.G., (1993) "Principles and Applications of Aquatic Chemistry", John Wiley and Sons, New York, 421-508

Morris J.C., & Stumm, W., (1967) "Redox Equilibria and Measurements in the Aquatic Environment", Advances in Chemistry Series, 67, 270-285

MPMMG, (1994) "Comprehensive Studies for the Purposes of Article 6 of Dir 91/271 EEC, the Urban Waste Water Treatment Directive", Final Report, FRPB, Edinburgh

Mulsow, S., Boudreau, B.P., & Smith, J.N. (1998) "Bioturbation and Porosity Gradients", Limnology and Oceanography, 43(1), 1-9

Myers, C.R., & Nealson, K.H. (1988) "Microbial Reduction of Manganese Oxides: Interaction with Iron and Sulfur", Geochimica et Cosmochimica Acta, 52, 2727-2732

NRC (1993), "Managing Wastewater in Coastal Urban Areas", National Research Council, National Academy Press, Washington

O'Conner, B., Costelloe, J., & Rhoads, D., (1989) "Report on the Firth of Clyde Sewage Dumping Ground REMOTS® Survey, May 1989", unpublished report

Odum, E.P., Finn, J.T., & Franz, E.H., (1979) "Perturbation Theory and the Subsidy-Stress Gradient", Bioscience, 29, 349-352

Omori, K., Kirano, T., & Takeoka, H., (1994) "The Limitations to Organic Loading on a Bottom of a Coastal Ecosystem", Marine Pollution Bulletin, 28(2), 73-80

O'Sullivan, A.J., (1971) "Ecological Effects of Sewage Discharge in the Marine Environment", Proceedings of the Royal Society of London, B, 117, 331-351

Otway, N.M., Gray, C.A., Craig, J.R., McVea, T.A., & Ling, J.E., (1996) "Assessing the Impacts of Deep-Water Sewage Outfalls on Spatially-variable and Temporally-variable Marine Communities", Marine Environmental Research, 41(1), 45-71

Oviatt, C.A., Quinn, J.G., Maughan, J.T., Ellis, J.T., Sullivan, B.K., Gearing, J.N., Gearing, P.J., Hunt, C.D., Sampou, P.A., & Latimer, J.S., (1987) "Fate and Effects of Sewage-Sludge in the Coastal Marine-Environment - A Mesocosm Experiment", Marine Ecology-Progress Series, 41(2), 187-203

Park, S.S., & Jaffe, P.R., (1996) "Development of a Sediment Redox Potential Model for the Assessment of Postdepositional Metal Mobility", Ecological Modelling, 91, 169-181

Parker, W.J., (1997) "A Multi-Parameter Sensitivity Analysis of a Model Describing the Fate of Volatile Organic Compounds In Trickling Filters", Journal of The Air & Waste Management Association, 47(8), 871-880

Paul, P.N., & Midmer, F.N., (1989) "Marine Treatment", Water Science and Technology, 21, 1517-1526

Pearson, T.H., (1975) "The Benthic Ecology of Loch Linnhe and Loch Eil, A Sea-Loch System on The West Coast of Scotland. IV. Changes in the Benthic Fauna Attributable to Organic Enrichment", Journal of Experimental Marine Biology And Ecology, 20, 1-41

Pearson, T.H., (1982) " The Loch Eil Project - Assessment and Synthesis With a Discussion of Certain Biological Questions Arising From a Study Of The Organic Pollution Of Sediments", Journal of Experimental Marine Biology And Ecology, 57 (1), 93-124

Pearson, T.H., (1987) "Benthic Ecology in an Accumulating Sludge-Disposal Site", in *Oceanic Processes in Marine Pollution 1, Biological Processes and Wastes in the Ocean*, J.M. Capuzzo & D.R. Kester (Eds.), Robert E Kreiger Publishing Co., Malabar, Florida, 195-200

Pearson, T.H., & Rosenberg, R., (1978) "Macrobenthic Succession in Relation to Organic Enrichment and Pollution of the Marine Environment", Oceanography and Marine Biology Annual Review, 16, 229-311

Pearson, T.H., & Stanley, S.O., (1979) "Comparative Measurement of Redox Potential of Marine Sediments as a Rapid Means of Assessing the Effect of Organic Pollution", Marine biology, 53, 371-379

Peiffer, S., Klemm, O., Pecher, K., & Hollerung, R., (1992) "Redox Measurements in Aqueous Solutions - A Theoretical Approach to Data Interpretation Based on Electrode Kinetics", Journal of Contaminant Hydrology, 10, 1-18

Perkins, E.J., (1979) "The Effects of Marine Discharges on the Ecology of Coastal Waters", in *Biological Indicators of Water Quality*, A. James & L. Evison (Eds.), John Wiley & Sons, Chichester, Chapter 12

Picket, S.T.A., & White, P.S. (1985) "The Ecology of Natural Disturbance and Patch Dynamics", Academic Press, London

Press, W.H., Teukolsky, S.A., Vetterling, W.T., & Flannery, B.P., (1992) "Numerical Recipes in FORTRAN: The Art of Scientific Computing", Second Edition, CUP, Cambridge

Rabouille, C., & Gaillard, J.F., (1991a) "A Model Representing the Deep Sea Organic Carbon Mineralization and Oxygen Consumption in Surfacial Sediments", Journal of Geophysical Research, 96, 2761-2776

Rabouille, C., & Gaillard, J.F., (1991b) "Towards the EDGE: Early Diagenetic Global Explanation. A Model Depicting the Early Diagenesis of Organic Matter, O_2, NO_3, and PO_4", Geochimica et Cosmochimica Acta, 55, 2511-2525

Raffaelli, D., (1987) "The Behaviour of The Nematode Copepod Ratio in Organic Pollution Studies", Marine Environmental Research, 23 (2), 135-152

Raffaelli, D., & Mason, C.F., (1981) "Pollution Monitoring with Meiofauna Using the ratio of Nematodes to Copepods", Marine Pollution Bulletin, 12(5), 158-163

Ray, B.T., (1995) "Environmental Engineering", PWS Publishing Company, Boston

Rhoads, D.C., (1974) "Organism-Sediment Relations on the Muddy Sea Floor", Oceanography and Marine Biology: an Annual Review, 12, 263-300

Rhoads, D.C., & Boyer, L.F. (1982) "The Effects of Marine Benthos on Physical Properties of Sediments: a Successional Perspective", In *Animal-Sediment Relationships*, P.L.McCall & M.J.S.Tevesz (Eds.), New York, Plenum, 3-52

Rhoads, D.C., & Germano, J.D., (1982) "Characterisation of Organism-Sediment Relations Using Sediment Profile Imaging: An Efficient Method of Remote Ecological Monitoring of the Seafloor (REMOTS System)", Marine Ecology: Progress Series, 8, 115-128

Rhoads, D.C., & Germano, J.D., (1986) "Interpreting Long-term Changes in Benthic Community Structure: a New Protocol", Hydrobiologia, 142, 291-308

Rice, D.L., & Rhoads, D.C., (1989) "Early Diagenesis of Organic Matter and the Nutritional Value of Sediment", in *Lecture Notes in Coastal and Estuarine Studies 31: Ecology of Marine Deposit Feeders*, G.Lopez, G.Taghon, J.Levington (Eds.), Springer Verlag, New York, 59-97

Ruddy, G., (1997) "An Overview of Carbon and Sulphur Cycling in Marine Sediments", in *Biogeochemistry of Intertidal Sediments*, T.D. Jickells and J.E. Rae (Eds.), Cambridge Environmental Chemistry Series 9, Cambridge University Press, Cambridge, 99-118

Sandulli, R., & de Nicola, M., (1991) "Responses of Meiobenthic Communities Along a Gradient of Sewage Pollution", Marine Pollution Bulletin, 22(9), 463-467

Sawyer, C.N., McCarty, P.L., Parkin, G.F., (1994) "Chemistry for Environmental Engineers", McGraw-Hill, Singapore

Schratzberger, M., & Warwick, R.M., (1998) "Effects Of The Intensity and Frequency of Organic Enrichment on Two Estuarine Nematode Communities", Marine Ecology-Progress Series, 164, 83-94

Scheisser, W.E., (1991) "The Numerical Method of Lines: Integration of Partial Differential Equation", Academic Press

Scott, M.J., & Morgan, J.J., (1990) "Energetics and Conservative Properties of Redox Sytems", In *Chemical Modelling of Aqueous Systems II*, D.C.Melchior, R.L.Bassett (Eds.), ACS Symposium Series 416, Chap. 29, American Chemical Society, Washington

Seas Ltd, (1994) "Garroch Head Sludge Disposal Ground Survey - 1993", Final Report, Scottish Environmental Advisory Service Report, unpublished report

Seas Ltd, (1997) "Garroch Head Sludge Disposal Ground Survey - 1996", Final Report on the Monitoring Survey Carried out Between the 27th May and 6th June 1996, Scottish Environmental Advisory Service Report, No SR 128, unpublished report

Segar, D., (1985) "Beneficial Use of Municipal Sludge in the Ocean", Marine Pollution Bulletin, 16(5), 186-191

SEPA (1996) "untitled report", data from a study of Loch Spelve, Isle of Mull, 20th June 1996, unpublished report

Silvert, W., & Sowles, J.W., (1996) "Modelling Environmental Impacts of Marine Finfish Aquaculture", Journal of Applied Icthyology, 12, 75-81

Smith, C.R., (1992) "Factors Controlling Bioturbation in Deep-Sea Sediments and Their Relation to Models of Carbon Diagenesis", in *Deep Sea Food Chains and the Global Carbon Cycle*, G.T Rowe & V. Pariente (Eds.), Kluwer Academinc Publishers, Netherlands, 375 -393

Smith, C.R., Walsh, I.D., Jahnke, R.A., (1992) "Adding Biology to One-Dimensional Models of Seidment-Carbon Degradation: the Multi-B Approach", in *Deep Sea Food Chains and the Global Carbon Cycle*, G.T Rowe & V. Pariente (Eds.), Kluwer Academinc Publishers, Netherlands, 395-400

SNIFFER (1994) "Forecasting the Deposition and Biological Effects of Excess Organic Carbon from Sewage Discharges - a Review of the Literature", Final Report no. SR6002

Soetaert, K., Herman, P.M.J., & Middelburg, J.J, (1996a) "A model of early diagenetic processes from the shelf to abyssal depths", Geochimica et Cosmochimica Acta, 60 (6), 1019-1040

Soetaert, K., Herman, P.M.J., Middelburg, J.J., Heip, C., deStigter, H.S., van Weering, T.C.E., Epping, E., & Helder, W., (1996b) "Modelling Pb-210 Derived Mixing Activity in Ocean Margin Sediments: Diffusive Versus Non-local mixing", Journal of Marine Research, 54 (6), 1207-1227

Soetaert, K., Herman, P.M.J., & Middelburg, J.J & Heip, C., (1998) "Assessing Organic Matter Mineralization, Degradability and Mixing Rate in an Ocean Margin Sediment (Northeast Atlantic) by Diagenetic Modelling", Journal of Marine Research, 56, 519-534

Spies, R., (1984) "Benthic Pelagic Coupling in Sewage Affected Marine Ecosystems", Marine Environmental Research, 13, 195-230

Stumm, W., (1965) " Redox Potential as an Environmental Parameter: Conceptual Significance and Operational Limitation", In: *Advances in Water Pollution Research*, 1, O. Jaag (Ed.), Proc. Int. Water Polut. Res. Conf., 2nd, Tokyo, Pergamon Press, 283-308

Stumm, W., & Morgan, J., (1996) " Aquatic Chemistry: Chemical Equilibria and Rates in Natural Waters", John Wiley and Sons, New York

Tebo, B.M., Nealson, K.H., Emerson, S., Jacobs, L., (1984) "Microbial Mediation of Mn (II) and Co(II) Precipitation at the O_2/H_2S Interface in Two Anoxic Fjords", Limnology and Oceanography, 29(6), 1247-1258

The World Bank, (1992) ""World Development Report 1992: Development and the Environment", OUP, New York

Thorstenson, D.C. (1970) "Equilibrium Distribution of Small Organic Molecules in Natural Waters", Geochimica et Cosmochimica Acta, 34, 745-770

Tromp, T.K. Van Cappellen, P., & Key, R.M. (1995) "A Global Model for the Early Diagensis of Organic Carbon and Organic Phosphorous in Marine Sediments", Geochimica et Cosmochimica Acta, 59 (7), 1259-1284

Tulkki, P., (1968) "Effects of Pollution on the Benthos of Gothenburg", Helgolander wiss. Meeresunters, 17, 209-215

Tuppen, C., (1996) "Communicating with Customers - Some Environmental Dilemmas", in *Teaching Ethics Vol. 3: Environmental Ethics*, R.M. Thomas (Ed.), Ethics International Press Limited, Cambridge

UK Department of the Environment (1979) "Report of the Standing Committee on the Disposal of Sewage Sludge to Sea, 1975-1978", Standing Technical Committee Report No. 18, Dept of the Environment-National Water Council, London, 65

UK Government (1998) "Select Committee on Environment, Transport and Regional Affairs, Second Report", HMSO

UKWIR (1996) "WW-03 Forecasting the Deposition and Biological Effects of Excess Organic Carbon from Sewage Discharges", Final Report, unpublished report

Ullman, W.J., & Aller, R.C., (1982) " Diffusion Coefficients in Nearshore Marine Sediments", Limnology and Oceanography, 27(3), 552-556

UNCED (1992) "Report of the UN Conference on the Environment and Development", UN, New York

Underwood, A.J., (1992) "Beyond BACI: the Detection of Environmental Impacts on Populations in the Real, but Variable World", Journal of Experimental Marine Biology and Ecology, 161, 145-178

Valiala, I., (1995) "Marine Ecological Processes", Second edition, Springer Verlag, New York

Van Cappellen, P., Gaillard, J.F., & Rabouille, C., (1993) "Biogeochemical Transformation in Sediments: Kinetic Models of Early Diagenesis", in *Interactions of C,N,P and S Biogeochemical Cycles and Global Change*, Wollast, R., Mackenzie, F.T., and Chou, L., (Eds.), NATO ASI Series, V.14, 401-445

Van Cappellen, P., & Wang, Y., (1995) "Metal Cycling in Surface Sediments: Modelling the Interplay Between Transport and Reaction" in *Metal Speciation and Contamination of Aquatic Sediments*, Allen, H.E. (Ed.), Ann Arbor Press, 21-64

Van Cappellen, P., & Gaillard, J.F., (1996) "Biogeochemical Dynamics in Aquatic Sediments", in *Reactive Transport in Porous Media*, P.C. Lichtner, C.I. Steefel & E.H. Oelkers (Eds.), Reviews in Minerology, 34, pp 335-376

Van Cappellen, P., & Wang, Y., (1996) "Cycling of Iron and Manganese in Surface Sediments: A General Theory for the Coupled Transport of Carbon, Oxygen, Nitrogen, Sulfur, Iron, and Manganese", American Journal of Science, 296, 197-243

Vetter, E.W., (1996) "Enrichment Experiments and Infaunal Population Cycles on a Southern California Sand Plain: Response of The Leptostracan Nebalia Daytoni and Other Infauna", Marine Ecology-Progress Series, 137 (1-3), 83-93

Vismann, B., (1991) "Sulfide Tolerance: Physiological Mechanisms and Ecological Implications", Ophelia, 34(1), 1-27

Wang, Y., & Van Cappellen, P., (1996) "A Multicomponent Reactive transport Model of Early Diagenesis: Application to Redox Cycling in Coastal Marine Sediments", Geochimica et Cosmochimica Acta, 60 (16), 2993-3014

Warwick, R.M, (1988) "Effects on Community Structure of Pollutant Gradients - an Introduction", Marine Ecology Progress Series, 46, 149

Weston, D.P., (1990) "Quantitative Examination of Macrobenthic Community Changes Along an Organic Enrichment Gradient", Marine Ecological Progress Series, 61(3), 233-244

Westrich, J.T., & Berner, R.A., (1988) "The Effect of Temperature on Rates of Sulfate Reduction in Marine Sediments", Geomicrobiology Journal, 6, 99-117

Wheatcroft, R.A., Jumars, P.A., Smith, C.R. and Nowell, A.R.M. (1990) "A Mechanistic View of the Particlate Diffusion Coefficient: Step Lengths, Rest Periods and Transport Directions", Journal of Marine Research, 48, 177-207

Wheatcroft, R.A., & Martin, W.R., (1996) "Spatial Variability in Short Term (^{234}Th) Sediment Bioturbation Intensity Along a Gradient of Enrichment", Journal of Marine Research, 54, 763-792

Whitfield, M. (1969) "Eh as an Operational Parameter in Estuarine Studies", Limnology and Oceanography, 14, 547-558

Whitfield, M. (1974) "Thermodynamic Limitations on the Use of Platinum Electrodes in Eh Measurements", Limnology and Oceanography, 19, 857-865

Wood, I.R., Bell, R.G., & Wilkinson, D.L., (1993) "Ocean Disposal of Wastewater", World Scientific Publishing Co., Singapore

Word, J.Q, (1979) "The infaunal Trophic Index", in *Coastal Water Research Project*, Annual Report 1978, El Segundo, California, USA, 19-39

WRc, (1989) "Effects of Sea Outfalls on the Marine Environment", Report No. FR0031, WRc plc, Marlow

WRc, (1990) "Design Guide for Marine Treatment Schemes", Report No. UM1009, WRc plc, Marlow

WRc plc (1992) "Development of a Biotic Index for the Assessment of the Pollution Status of Marine Benthic Communities", Final Report NR3102/1

WRc, (1995) "Wastewater and Sludge Treatment Processes", WRc plc, Marlow

Wu, R.S.S, (1995) "The Environmental Impact of Marine Fish Culture - Towards a Sustainable Future", Marine Pollution Bulletin, 31(4-12), 159-166

Zmarzly, D.L., Stebbins, T.D., Pasko, D., Duggan, R.M., & Barwick, K.L., (1994) "Spatial Patterns and Temporal Succession in Soft-Bottom Macro-invertebrate Assemblages Surrounding an Ocean Outfall on the Southern San-Diego Shelf - Relation to Anthropogenic and Natural Events", Marine Biology, 118 (2), 293-307

Zobell, C.E., (1946) "Studies on the Redox Potential of Marine Sediments", Bulletin of the American Association of Petroleum Geologists, 30(4), 477-513